CATÓLICA

UNIVERSIDADE CATÓLICA PORTUGUESA | PORTO

Escola Superior de Biotecnologia

ASSOCIATION OF MICRO AND NANOCARRIERS WITH THIN FILMS FOR BUCCAL DELIVERY OF BIOACTIVE MOLECULES

Thesis submitted to the Universidade Católica Portuguesa to attain the degree of PhD in Biotechnology – with specialization in Food Science and Engineering

By

Pedro João Neves Miranda de Castro

Under the supervision of professor Maria Manuela Estevez Pintado

Under co-supervision of professors Bruno Sarmento and Raquel Madureira

October 2018

CATÓLICA

UNIVERSIDADE CATÓLICA PORTUGUESA | PORTO

Escola Superior de Biotecnologia

ASSOCIATION OF MICRO AND NANOCARRIERS WITH THIN FILMS FOR BUCCAL DELIVERY OF BIOACTIVE MOLECULES

Thesis submitted to the Universidade Católica Portuguesa to attain the degree of PhD in Biotechnology – with specialization in Food Science and Engineering

By

Pedro João Neves Miranda de Castro

Under the supervision of professor Maria Manuela Estevez Pintado

Under co-supervision of professors Bruno Sarmento and Raquel Madureira

October 2018

Resumo

Visando o aumento da biodisponibilidade dos compostos bioactivos administrados por via oral (com especial ênfase para a absorção bucal), o plano de trabalhos deste programa doutoral visou a optimização de formulações de filmes orais e de micro- e nanopartículas que, conjugados constituam sistemas inovadores com atividade sinérgica. As moléculas bioactivas seleccionadas para estudar o comportamento e eficácia das formulações optimizadas foram a cafeína e dois péptidos presentes na proteína do soro do leite com actividades antihipertensora (sequência: KGYGGVSLPEW) e relaxante (sequência: YLGYLEQLLR). O processo de optimização das formulações foi iniciado pela seriação e comparação preliminar dos excipientes para a produção de filmes e micro/nanopartículas. No primeiro estudo realizado, foram optimizadas e comparadas duas formulações de filmes (usando-se os polímeros carboximetilcelulose sódica e gelatina tipo A) como veículos para libertação oral de cafeína. Verificou-se, através da análise por espectroscopia no infravermelho por transformada de Fourier com reflectância total atenuada (FTIR-ATR), que a estrutura química da cafeína não fora alterada durante o processo de produção dos filmes. Concluiu-se também, através do ensaio de dissolução estabelecido pela Farmacopeia Americana (USP), que os filmes produzidos com gelatina tipo A permitiram uma libertação mais lenta da cafeína ao passo que os filmes de carboximetilcelulose apresentaram um perfil de libertação imediata. Em concordância, o valor de permeabilidade aparente da cafeína, determinada através do ensaio de permeabilidade *ex vivo*, através de excisões de intestino delgado de origem porcina, verificou-se superior quando esta foi veiculada pelos filmes de carboximetilcelulose, comparativamente com os filmes de gelatina tipo A. O tempo de desintegração de ambas as formulações mostrou-se, contudo, demasiado alto para formulações orodispersíveis, não ocorrendo desintegração completa após 30 segundos. Ainda na sequência da escolha do polímero com melhores características para integrar a composição de filmes orais, uma nova formulação contendo goma-guar foi optimizada por desenho factorial. Os filmes de goma-guar apresentaram características mecânicas e físico-químicas superiores às verificadas para os filmes de carboximetilcelulose e gelatina, tomando-se como factores de decisão a capacidade de absorção de água, a erosão em saliva artificial e o tempo de desintegração apresentados pelos filmes de goma-guar. Procedeu-se também à optimização (por desenho fatorial) de uma formulação de micropartículas de alginato que garantissem, em conjunto com os filmes de goma-guar, uma libertação controlada de cafeína, assim como uma maior biodisponibilidade da mesma. A associação de micropartículas de alginato aos filmes de goma-guar – GfB - não induziu alterações das características químicas da cafeína, de acordo com o verificado por FTIR-ATR, nem toxicidade para as linhas celulares usadas para mimetizar as mucosas bucal (TR146) e intestinal (Caco-2/HT29-MTX), de acordo com os resultados obtidos pelo ensaio de viabilidade celular MTT (Brometo de 3-(4,5-Dimethylthiazol-2-yl)-2,5-Diphenyltetrazólio). Adicionalmente, os perfis de libertação e permeabilidade *in vitro* (através das linhas celulares TR146 e Caco-2/HT29-MTX cultivadas em camada) e *ex vivo* (através de epitélio intestinal de origem porcina) mostraram-se mais lentos que os observados para as micropartículas de alginato, filmes de goma-guar ou com a solução controlo de cafeína. A formulação GfB promoveu o aumento do contacto efectivo entre a cafeína e o epitélio bucal, oferecendo uma permeação mais completa ao longo do tempo.

De forma a incrementar também a biodisponibilidade do péptido KGYGGVSLPEW com actividade anti-hipertensora, as micropartículas de alginato foram substituídas por nanopartículas de ácido poli(láctico-co-glicólico) – PLGA - por estas oferecerem uma eficácia de associação

superior, assim como um maior potencial de permeação das membranas biológicas, dado o tamanho de partícula ser significativamente inferior. A formulação de nanopartículas de PLGA foi optimizada por desenho factorial. O sistema compreendido pelas nanopartículas de PLGA associadas aos filmes de goma-guar (GfNp) não comprometeu a viabilidade das linhas celulares TR146 e Caco-2/HT29-MTX às concentrações testadas. O sistema desenvolvido promoveu a libertação e permeabilidade controladas do péptido, através das células TR146 e Caco-2/HT29-MTX cultivadas em camada, comparativamente com os filmes e nanopartículas isoladamente, assim como com a solução de péptido livre (controlo). Contudo, a permeabilidade aparente verificou-se superior para a formulação GfNp, comparativamente com as restantes formulações. Estes resultados deveram-se ao contacto íntimo entre o péptido e o epitélio absorptivo, promovido pela formulação GfNp. Verificou-se ainda, através da realização do ensaio *in vitro* da capacidade de inibição da enzima conversora da angiotensina I, que o péptido transportado por GfNp apresentava a maior actividade anti-hipertensora após ser sujeito à simulação do tracto gastrointestinal, comparativamente com o péptido transportado pelas nanopartículas ou filme, isoladamente, ou com a solução de péptido livre.

O sistema previamente optimizado para a libertação do péptido antihipertensor foi também usado de forma a incrementar a biodisponibilidade do péptido relaxante alfa-casozepina (sequência: YLGYLEQLLR). Através do ensaio MTT, foi possível concluir que nenhuma das formulações comprometeu a viabilidade da linha celular TR146 e da co-cultura Caco-2 /HT29-MTX. Por isso, a permeabilidade do péptido, sujeito às condições do tracto gastrointestinal simulado, através dos modelos *in vitro* bucal e intestinal foi estudada. Verificou-se que a associação de nanopartículas de PLGA com filmes de goma-guar promoveu um aumento da permeabilidade face às nanopartículas e filmes não conjugados, assim como com o péptido em solução (controlo). Estes resultados estão correlacionados com o incremento da mucoadesão conferida pela associação das nanopartículas de PLGA com os filmes de goma-guar, verificada através da análise da adesividade e trabalho de adesão à língua de vaca.

Validada a efectividade das formulações para a libertação e permeabilidade de cafeína e péptidos bioactivos, foram realizados estudos preliminares de modo a verificar a estabilidade da formulação GfB e a compreender a opinião de potenciais futuros consumidores face aos produtos desenvolvidos. As formulações foram sujeitas a condições de degradação acelerada (i.e. 40 ºC e 75% de humidade relativa) de acordo com a *International Conference of Harmonization* (ICH), não se verificando alterações químicas da cafeína em nenhum dos tempos de amostragem (imediatamente após a preparação da formulação e após 3, 6 e 9 meses) através da análise do espectro obtido por ATR-FTIR, assim como dos tempos de retenção em HPLC-UV. Verificou-se ainda um aumento significativo do conteúdo em água de GfB ao longo dos tempos de amostragem. Por fim, um estudo por *focus group* e um estudo de análise sensorial com um painel *naive* permitiram compreender a adequabilidade dos sabores propostos, assim como a tolerância à acidez e amargor por parte do consumidor. Observou-se uma ligeira tendência para a aceitação do sabor a menta e alguma tolerância ao amargor e acidez quando a menta foi usada na formulação.

Os sistemas para libertação oral de compostos bioactivos, desenvolvidos e optimizados no âmbito desta tese, induziram melhorias significativas no comportamento farmacocinético *in vitro* dos compostos veiculados. De facto, a associação de filmes orais com micro- ou nanopartículas pode representar um novo sistema de libertação que ofereça maior efectividade e adesão por parte do consumidor/utente.

Abstract

Aiming for the protection and absorption enhancement of bioactive compounds administered by oral route (with special focus on buccal absorption), this thesis had as goals, the optimization of oral films and micro/nanoparticles which, through conjugation of both, worked as innovative oral delivery systems with synergic activity.

The bioactive molecules selected to study the behaviour and efficacy of the optimized formulations were caffeine and two whey-derived peptides with antihypertensive and relaxing activities (sequences: KGYGGVSLPEW and YLGYLEQLLR, respectively).

The optimization process began with the selection and preliminary comparison of the characteristics of the excipients to be used to prepare films. Indeed, the first study included the optimization and comparison of two film formulations as carriers for the oral release of caffeine, prepared using sodium carobymethylcellullose and type A gelatine as polymers. It was observed by the analysis of the spectra obtained by Fourier-transformed infrared spectroscopy with attenuated total reflectance (FTIR-ATR) that caffeine chemical structure was not altered during the film production process. It was also observed, through the dissolution assay established by the United States Pharmacopoeia (USP), that type A gelatine films offered a slow caffeine release, whereas caroboxymethylcellulose films offered a burst release profile. Accordingly, the apparent permeability of caffeine observed from the *ex vivo* permeability assay, across small intestine tissues from porcine origin, was higher for carboxymethylcellullose films than for type A gelatine films. Nonetheless, disintegration time of both formulations was too high to meet the criteria of orodispersible formulations, taking longer than 30 s to achieve total disintegration.

Still in the process of choosing the best polymer to integrate the composition of oral films, a new formulation containing guar gum as polymer was optimized by factorial design. Guar gum films presented superior mechanical and physico-chemical characteristics than carobxymethylcellullose or type A gelatine films, mainly regarding water-uptake capacity, erosion in artificial saliva and disintegration time. Furthermore, a formulation of alginate microparticles was also optimized by factorial design to associate with guar gum films and guarantee the controlled release of caffeine, as well as an increased bioavailability.

The association of alginate beads to guar gum films – GfB – did not induce alterations in the chemical characteristics of caffeine, as outlined in the data obtained by FTIR-ATR, nor cytotoxicity to the cell lines used to mimic the buccal (TR146) or intestinal (Caco-2/HT29-MTX) mucosa, as determined by MTT ((3-(4,5-Dimethylthiazol-2-yl)-2,5-Diphenyltetrazolium Bromide). Additionally, the release and *in vitro* (through TR146 and Caco-2/HT29-MTX cell lines) and *ex vivo* (through porcine intestinal mucosa) permeability profiles of caffeine from GfB was slower when compared with alginate microparticles, guar gum films or caffeine control solution. GfB also increased the effective contact between caffeine and buccal epithelia, offering a more complete permeation along time.

Further, aiming to increment the bioavailability of the peptide KGYGGVSLPEW with antihypertensive activity, alginate beads were replaced with poly(lactic-co-glycolic) acid (PLGA) nanoparticles, since the last offer a higher association efficiency and a higher permeability of biologic membranes, due to the significantly lower particle size. The formulation of PLGA nanoparticles was optimized by factorial design. The delivery system comprising PLGA nanoparticles into guar gum films (GfNp) did not compromise the viability of the cell lines TR146 and Caco-2/HT29-MTX at tested concentrations. Moreover, GfNp promoted a slower peptide release and *in vitro* permeability across TR146 and Caco-2/HT29-MTX cell layers when

compared with the films and nanoparticles alone or with a free peptide solution (control). However, apparent permeability was higher for GfNp when compared with remaining formulations. Results may be due to the intimate contact between the peptide and the epithelia, promoted by GfNp. It was also possible to observe that the peptide carried by GfNp presented a higher *in vitro* capacity to inhibit the angiotensin-converting enzyme after being subjected to the simulation of gastrointestinal tract, therefore presenting higher antihypertensive potential, when compared with the peptide carried by the nanoparticles or films alone or with the control solution (free peptide).

The previously optimized system as carrier and delivery system for the antihypertensive peptide was also used to enhance the bioavailability of the relaxing peptide alpha-casozepine (sequence: YLGYLEQLLR). It was possible to conclude, through MTT assay, that none of the formulations compromised cell viability of TR146 cell line or Caco-2/HT29-MTX co-culture. Moreover, peptide permeability across *in vitro* buccal and intestinal epithelial models, while being subjected to simulated gastrointestinal tract, was higher and faster (higher apparent permeability) for the association of guar gum films with PLGA nanoparticles, when compared with PLGA nanoparticles or guar gum films alone or with the free peptide solution (control). Obtained results are related with the increased mucoadhesion conferred by the association of PLGA nanoparticles with guar gum films, verified through the analysis of adhesivity and work of adhesion to cow tongue.

After validation of the effectivity of the formulations regarding release and permeability of caffeine and bioactive peptides, preliminary studies were performed to understand the stability of GfB and the opinion of potential future consumers of the developed products.

Formulations were subjected to accelerated degradation conditions according to the *International Conference of Harmonization* (ICH) and it was verified, through analysis of spectra (by FTIR-ATR spectroscopy) and retention times (by HPLC-UV), that no chemical alterations of caffeine molecule carried by GfB were observed in any of the set time points (i.e. immediately after preparation of GfB and 3, 6 and 9 months after preparation, under accelerated degradation conditions – 40 ºC and 75% of relative humidity). Moreover, an increased water content was observed along the three time points. Further, a *focus group* and a sensory analysis study with a *naïve* panel allowed to understand the suitability of the flavours but also the tolerability to acidity and bitterness by the consumer. A slight tendency to the acceptance of mint flavour and some tolerance to bitterness and acidity was verified when mint was used in the formulation.

Developed and optimized oral delivery systems in the scope of the present thesis induced significant improvements on the *in vitro* pharmacokinetic behaviour of carried bioactive molecules. Indeed, the association of oral films with micro- and nanoparticles may represent conceptually new delivery systems that offer higher effectivity and consumer/patient compliance.

Acknowledgements

This thesis, like a living being, was born and raised. To excuse myself from being unfair, the acknowledgements will be made in chronological order.

Thank you to my parents. They taught me everything that defines me, for better or worse. They also paid for all my education and I am totally aware of the sacrifice it represented. I hope to grow as a human being to justify your personal investment. I will never be able to pay you back, I hope you know that! Thank you to my little sister, for being a very patient super-friend that, somehow, forgave all the torture that I, as the older brother, inflicted to her. Thank you to my grandparents, as I still use the WWGD? ("What Would my Grandparents Do?") to jump through the barriers in my life. Thank you to my godfather and to my cousin, both called Pedro, that are two important references for me. Thank you to my family, we are lucky enough to have busy Christmas.

Thank you to my oldest friends – António Pinto de Mesquita, Flávia Sousa, Jorge Jacinto, Mariana Melo e Castro, Pedro Cardoso and Pedro Matos that believed that this project was a good idea. It was!

I would like to thank professor Bruno Sarmento, my co-supervisor. In about seven months, professor Bruno Sarmento allowed me to work in his laboratory, gave a good reference of myself which got me my first (horrible!) first job in pharmaceutical industry, heard my "caffeine, nanoparticles and oral films" idea and literally led me to Escola Superior de Biotecnologia to meet professor Manuela Pintado. He also introduced me to a great friend of mine – professor Pedro Fonte – that wasted his time teaching very laboratory techniques that were of paramount importance to the development of the present work. He also read and corrected the first paper I have co-written.

To professor Manuela Pintado, that I know will be a little angry with me because her name is only appearing here – **this is chronological ok?** Seriously, she deserves to be on the top as she will always represent my scientific mother in all senses! She was patient with me from day zero. Professor Manuela Pintado was the one who said "yes" to this idea, perfected it and gave me all the resources to effectively develop it without even knowing me or my limited skills back then. She motivated, nurtured, taught, heard and believed in me, when I needed the most. That is the definition of a pretty good mother, right? Professor Manuela Pintado is a natural leader, not an employer. She cried when our FCT project was approved, she felt even happier than me when I finally got my PhD scholarship, she trusted me to do many, many things that I would not trust myself to. If only her day had some extra hours… she would work more for us. That says it all.

To Raquel Madureira, my co-supervisor and friend. The patience you had with me and all the kind words that you always gave me were and are priceless. Raquel saw me preparing oral films for the first time in the laboratory and, even after that dreadful experience, she always **believed** in me. All I did then was try to work and perform to live up to her expectations. One day I will be worth of them. I know you think I already am, I still am not, but I will be.

To the initial team: Alejandro Canaza, Ana Amaro, Ana Gomes, Ana Oliveira, Ana Vilas Boas, Anita Pintado, Cristian Torres, Eduardo Costa, Ezequiel Coscueta, Débora Campos, Glenise Voss, Ivone Vaz-Moreira, Joana Costa, Joana Odila, José Soares, Lígia Pimentel, Luís Alcalá, Manuela Amorim, Maria João, Marta Coelho, Miguel Pereira, Ricardo Gómez García, Sara Silva, Sérgio Sousa, Tânia Bragança, Teresa Bonifácio. I came out of nowhere and you accepted me as I have been part of the team since ever. And I learned from you. A lot! You are family to me. Thank you! The team eventually grew a

lot and there are over fifty names that I will not write on paper because it would be unfair to "just" fit them in a giant list. This manuscript does not have enough space to **properly** highlight each and every one of them.

To Patrícia Baptista, that shared this project with me, got into my nerves and I surely replied accordingly. I am sorry to have mocked you in every possible way but, let us be honest: it really worked! Thank you for all the effort you did for this project to move along, all the tough work and true friendship.

To Ana Pilosof, Victor Pizones and all the guys in the "Departamento de Industrias – Universidade de Buenos Aires) and to Coscueta family that treated me like I was one of their own.

To professor Giampaolo Zuccheri, an amazing human being that, with nothing else than a Skype meeting and a couple of exchanged e-mails, accepted me in his laboratory in University of Bologna, taught me how to work with atomic force microscopy, did everything he could for my work to become richer and my staying in Bologna to be as amazing as it was. Professor Giampaolo Zuccheri gained nothing but work, expenses and headaches with my trip to Italy. Well, to be fair, he gained a friend. I hope one day I can pay you back. To Andrea, Carlo, Charlotte, Filomena, Ilker, Lorenzo, Marco, Mariafrancesca, Martina, Nicola, Rocco and Virginia – this manuscript gained form in your company and there is no Italy without you, in my mind.

I acknowledge Miles Davis because he dared to play it *cool*. One day, science will play it *cool* as well.

Keywords

Alginate Beads
Antihypertensive peptide
Buccal delivery
Bioactive molecules
Bioavailability
Caffeine
Carboxymethylcellulose
Drug delivery
Experimental design
Gelatin type A
Guar gum films
Nutritional
Oral delivery
Oral films
PLGA nanoparticles
Relaxing peptide
Slow release
Whey protein

Table of Contents

List of figures

List of tables

List of abbreviations

AFM – Atomic Force Microscopy

ATR-FTIR – Attenuated Total Reflectance Fourier Transform Infrared

CMC - Carboxymethylcellulose

ED - Experimental design

FNp – Guar gum film with α-casozepine-loaded PLGA nanoparticles

GeltA – Gelatin type A

GfNp – Guar gum films with antihypertensive peptide-loaded PLGA nanoparticles

GfB – Guar gum film with caffeine-loaded alginate beads

SEM – Scanning electron microscope

Scope and outline

Chapter I
Literature survey, state-of-the-art and main thesis goals

Section 1: Introduction

Chapter II
Optimization of two biopolymer-based oral films for the delivery of caffeine

Section 2: Optimization of formulations for improved oral delivery of caffeine

Chapter III
Incorporation of beads into oral films for buccal and oral delivery of bioactive molecules

Chapter IV
Combination of PLGA nanoparticles with mucoadhesive guar gum films for buccal delivery of antihypertensive peptide

Section 3: Association of guar gum films with PLGA nanoparticles for improved oral delivery of bioactive peptides

Chapter V
Combination of PLGA nanoparticles with mucoadhesive guar gum films for buccal deliveyr of alpha-casozepine

Chapter VI
Stability of the products and validation of consumer opinion

Section 4: Stability of developed products and validation of consumer acceptance

Chapter VII
Conclusions

Section 5: Conclusions and future perspectives

Chapter VIII
Future perspectives

Section 1

Introduction

Chapter I – Introduction

1.1. Disposition of bioactive molecules and role of delivery systems applied to the oral route on bioavailability enhancement

The disposition of bioactive molecules (i.e. compounds that have a biologic effect on living organisms) is commonly divided in four steps, namely: absorption, distribution, metabolism and excretion (Rang, 2007). However, when bioactive compounds are artificially or naturally entrapped to a system (e.g. to a blend of excipients in pharmaceutics or to biologic membranes with variable complexity in food products) liberation is a critical step that precedes their absorption of bioactive molecules. Therefore, development and optimization of new delivery systems that promote specific liberation, from now on mentioned as release, is of paramount importance due to the influence on the pharmacokinetic profile of carried bioactive molecules.

Oral route refers to the administration of bioactive molecules by mouth and includes buccal, sublingual, gingival and gastrointestinal administration routes. Among the available administration routes, oral route is painless and the most convenient and easy to perform, therefore leading to a higher patient compliance when compared with alternative administration routes (e.g. parenteral, intranasal, intrarectal, intravaginal or pulmonary). Nevertheless, conditions inherent to gastrointestinal tract such as selective permeation across absorptive mucosa, extreme pH values, enzymatic activity and first-pass hepatic metabolism may compromise the overall physico-chemical original

configuration of bioactive molecules, therefore leading to an unpredictable pharmacodynamic profile with risks of toxicity or ineffectiveness. Moreover, gastrointestinal absorption is highly variable, depending on factors as the digestive tract motility, physicochemical characteristics inherent to the bioactive molecule along with variations on the splanchnic blood flow and on the particle size of the bioactive molecule and/or of the carrier.

Effectively, motility along the gastrointestinal tract varies with feeding state, being higher during meal digestion than in the fasted state. Also, for instance, the intake of muscarinic receptor blockers and some clinical conditions such as diabetic neuropathy or migraine can cause gastric stasis (Rang, 2007). On the other hand, some drugs (e.g. metoclopramide), infections, inflammation, or simply the irritation of the gastrointestinal mucosa, may lead to an increment of motility. Moreover, physico-chemical characteristics of bioactive molecules may lead to interactions that hinder or promote gastrointestinal absorption. Tetracycline is a common example due to the inherent calcium-chelating activity, preventing the normal absorption of the cations. A contrasting example is the co-administration of ascorbic acid and Fe^{3+} (ferric oxidation state) that leads to the reduction to Fe^{2+} (ferrous oxidation state) which is more easily absorbed in the intestinal mucosa (Sharp & Srai, 2007). Also, food intake increases splanchnic blood flow, inducing a higher absorption of bioactive molecules taken *per os*. Oppositely, hypovolaemia, that may occur for instance due to dehydration, or cardiac insufficiency, may reduce splanchnic blood flow, resulting in a decrease of the absorption of bioactive molecules. Finally (and with high relevance to this thesis), particle size and the characteristics of the delivery system formulation have major impact on the absorption of carried bioactive molecule. For instance, in 1971, in a New York hospital, it was verified

that different doses of digoxin, a cardiac glycoside, were required to maintain normal heart conditions of the patients, depending on the particle size that occurred in the different tablets provided by different manufacturers (Lundquist & Artursson, 2016; Rang, 2007; Xiong, Bao, Yang, Zhu & Wang, 2014).

Before reaching the systemic circulation, bioactive molecules contact with a wide array of enzymes, either present in the intestinal gut or in the liver, which may result in the partial or total inactivation of the compound, therefore reducing bioavailability. Bioavailability refers to the intact fraction of administered bioactive molecule that reaches the systemic circulation and is only considered to be total by intravenous administration. Hence, there is a constant effort to overcome the need of new delivery systems that combine the convenience of oral administration (to maximize patient/consumer compliance) without compromising the bioavailability of the carried bioactive molecule.

1.1.1. Buccal delivery route

Buccal delivery route presents several advantages over conventional *per os* route that implies swallowing (Pather, Rathbone & Senel, 2008). Human buccal mucosa is multistratified, non-keratinized and allows the permeation of molecules either by transcellular or intercellular route (Patel, Liu & Brown, 2012). Buccal mucosa presents high blood vessel density (with a mean blood flow of 20.3 mL/min per 100 g of tissue) and is more permeable than the skin. Moreover, alternative non-invasive delivery routes present significant disadvantages over buccal administration as aforementioned high enzymatic activity, discomfort, irreproducibility, and misuse of the delivery systems (e.g. rectal, vaginal, ocular, pulmonary and nasal routes). Indeed, absorption of bioactive

molecules directly through buccal mucosa bypasses the gastrointestinal tract and, therefore, the pre-systemic elimination that includes stomach and intestinal extreme pH and enzymatic activity (Patel, Liu & Brown, 2012). Moreover, first-pass hepatic metabolism is avoided, therefore enhancing the bioavailability of the bioactive molecule.

Nonetheless, buccal administration also has disadvantages that need to be overcome (Washington, Washington & Wilson, 2000). Indeed, human oral mucosa presents several chemical and physical barriers to transmucosal absorption to avoid toxicity, due to the intimate contact with internal jugular vein. The relatively small surface area, salivary turnover and premature swallowing may hinder an effective permeation across buccal mucosa. Also, cellular turnover and absorptivity of buccal epithelia is higher than dermal route but significantly lower than the intestinal epithelia that is absorption-specialized.

Buccal administration route is, therefore, especially relevant for molecules that are prone to suffer pre-systemic (within the gastrointestinal tract) and systemic metabolism with consequent loss of bioavailability. But, due to inherent conditions that hinder permeability across buccal mucosa, patients/consumers would benefit from a delivery system that also protects and enhances intestinal permeability of carried bioactive molecule. This thesis proposes conceptually new solutions to improve the bioavailability of bioactive molecules either by overcoming buccal permeability issues and by protecting carried molecules from gastrointestinal digestion. Proposed solutions consist on the development and optimization of conceptually new delivery systems that result from gathering micro/nanoparticles with orodispersible films, aiming buccal and intestinal permeability enhancement and overall increase in bioavailability of carried bioactive molecules.

Thus, since proteins and peptides are examples of molecules with therapeutic interest that may be degraded across gastrointestinal tract, two bioactive peptides were chosen as representative molecules to be carried by developed formulations, aiming to assess advantages over traditional delivery systems. Caffeine, on the other hand, is known to be absorbed in the buccal epithelia by paracellular route and is a relevant model molecule to study and optimize buccal delivery systems.

1.2. Bioactive molecules used as models to optimize developed formulations

1.2.1. Caffeine

Caffeine is the most popular drug consumed worldwide and acts as a stimulant in the central nervous system (Fredholm, Battig, Holmen, Nehlig & Zvartau, 1999; Harland, 2000). Also known as 1,3,7-trimethylxanthine, caffeine molecule comprises a pyrimidinedione and a imidazole ring bound together and is mildly alkaline (Spiller, 1997).

Caffeine improves alertness, vigilance, learning, memory and mood state in humans by antagonizing the adenosine receptor (A_1 and A_{2a}) agonists and, therefore, inhibiting the drowsiness typically induced by adenosine. A_1 adenosine receptors are highly expressed in the cortex (sensory, motor and association functions), cerebellum (functions on motor control and regulation of some behaviors), hypothalamus (neuroendocrine function) and hippocampus (short-term, long-term and space memory functions). A_{2a} adenosine receptors are mainly expressed in regions as the striatum (reward cognition), nucleus accumbens (reward processing) and olfactory tubercle (sensory integration).

There is also some evidence that caffeine can promote an increase on physical performance by inducing calcium release from sarcoplasmic reticulum with concomitant reuptake inhibition. Therefore, athletes, militaries, factory shift workers, transport workers, first responders, among many other professionals resort to repeated administration of caffeine to maintain both physical and cognitive capabilities and achieve optimal performances (McLellan, Caldwell & Lieberman, 2016).

Caffeine is mostly consumed *per os* and peak plasma levels are reached between 15 minutes and 1 hour after intake. The most significant sources of caffeine are coffee, tea and energetic drinks and absorption occurs mostly in the intestine. Indeed, 99% of administered caffeine is reported to be absorbed by intestinal mucosa 45 minutes after intake. Nevertheless, even though unexplored, buccal administration was reported as being more effective and faster than conventional gastrointestinal administration of caffeine. Indeed, in a double-blind study that compared the absorption rate of caffeine after administration of caffeine-loaded chewing-gum and capsules, it was verified that caffeine absorption from chewing-gum was faster than from capsules (even though caffeine release was incomplete), indicating that buccal mucosa is permeable to caffeine, allowing direct absorption to systemic circulation (Kamimori et al., 2002b).

Half-life stands between 3 to 5 hours but is highly variable among individuals, mainly due to smoking habits, liver diseases, dietary choices (absorption of caffeine is significantly slower when consumed with a meal), gender, pregnancy or even the intake of specific drugs (McLellan, Caldwell & Lieberman, 2016). Caffeine is rapidly distributed through all body tissues and poorly binds to plasma albumin. Also, caffeine extensively permeates the blood brain barrier and placenta. First-pass effect, even though not very representative after gut absorption, occurs especially through cytochrome P450

monoxygenase, that converts caffeine into trimethyl uric acid, paraxanthine and theobromine. Being a hepatic inducer, caffeine promotes its own metabolism and elimination. Liver, especially by the action of CYP1A2, plays an important role regarding elimination of caffeine, through biotransformation into other dimethylxanthines, mainly paraxanthine (81.5%), theobromine (10.8%) and theophylline (5.4%) (Gu, Gonzalez, Kalow & Tang, 1992). Formed dimethylxanthines are further metabolized into monomethylxanthines, dimethylurates and uracil derivatives. Finally, monomethylxanthines are metabolized into monomethylurates (Rodopoulos, Hojvall & Norman, 1996; Rodopoulos & Norman, 1996). Other enzymes, such as xanthine oxidase and N-acetyltransferase, play a minor role on the metabolism of caffeine (Mitoma, Lombrozo, LeValley & Dehn, 1969). The excretion of caffeine occurs mainly by hepatobiliary elimination, but also by urine (through transformation into methylated xanthin and uric acid metabolites), sweat and breast milk (Tang-Liu, Williams & Riegelman, 1983).

Caffeine is known to induce withdrawal effect to consumers (headache, fatigue, decreased concentration are some of the most common effects that occur after 20 to 48 hours after removal of caffeine) and *caffeinism* was reported as a serious syndrome that occurs with the ingestion of more than 1 g of caffeine a day, leading to muscle over excitation and consequent tremor, nervousness, headache, irritability, gastrointestinal disturbances, tachypnea, attention impairment and even panic in some cases (1989; Pohler, 2010). Therefore, oral administration of caffeine carried by oral films associated with micro or nanocarriers that promote sustained release can lead to both an increased permeability and a controlled caffeine absorption, therefore avoiding superdosage unwanted effects and decreasing the caffeine intake frequency along the day.

1.2.2. Bioactive peptides

Pharmacologically active proteins and peptides have been extensively studied regarding hormonal, immune, anti-hypertensive, antinociceptive, among other biological properties, with the advantages of great target-specificity and safety comparatively to most conventional drugs (Castro, Fonte, Sousa, Madureira, Sarmento & Pintado, 2015a). Also, therapeutic proteins and peptides demonstrate unique, peerless, pharmacological characteristics such as high specificity to receptors and superior biological mimicking of physiological mechanisms, resulting in a better therapeutic index compared to conventional chemical-derived drugs. Bioactive proteins and derived peptides may be obtained from a broad array of natural resources. For instance, concentrated peptide extract obtained by hydrolysis of concentrated whey proteins with cardosins - enzymes from *Cynara cardunculus* - demonstrated antinociceptive effect, acting in opioid receptors. Also, peptides obtained from enzymatic degradation of β-lactoglobulin and α-lactalbumin exhibited antihypertensive activity by inhibition of angiotensin-converting enzyme) or by chemical synthesis (Madureira, Tavares, Gomes, Pintado & Malcata, 2010).

Nevertheless, some bioactive molecules present inherent drawbacks regarding oral administration, namely low intestinal absorption profile and potential loss of bioactivity due to the harsh pH conditions and enzymatic activity prevailing throughout gastrointestinal tract. Consequently, bioactive proteins and peptides are usually administered by invasive routes in order to assure the expected efficacy (Shaji & Patole, 2008). However, as aforementioned, oral administration is still the preferred one among all administration routes mainly because it is noninvasive, which leads to a better

compliance to treatment (Brayden & O'mahony, 1998; Dixit & Puthli, 2009a). Consequently, numerous attempts to overcome oral administration problems have been performed, by developing new delivery systems that promote an overall higher bioavailability of carried bioactive proteins and peptides.

1.3. Oral films as oral/buccal delivery systems

Oral films are delivery systems that present pleasant flavor and texture, are small-sized (fitting comfortably in the oral cavity) and are easily dissolved in the oral cavity, immediately releasing the active ingredient (disintegration time is ca. 30 seconds). Additionally, the characteristic mucoadhesion of polymeric films is ideal for uncooperative patients since, once in the oral cavity, oral films are very difficult to remove (Castro, Fonte, Sousa, Madureira, Sarmento & Pintado, 2015a). Moreover, oral films do not require water to be administered, and thus are much more practical than tablets, capsules or syrup forms (Nagaraju et al., 2013b). Hence, a delivery system such as oral films can be specifically tailored to represent a good solution regarding the improvement of pharmacokinetic and pharmacodynamic properties of bioactive molecules to be delivered, along with a greatly enhanced compliance to treatment. However, these systems have a limited incorporation capacity of active ingredients (ca. 5%, w/w, to 30%, w/w) implying that bioactive molecules must be potent enough at low doses, which may be considered an important drawback of oral films. Also, when using oral films, it is crucial to acknowledge that buccal epithelia presents a molecular weight (MW) cut-off of ca. 500-1000 Da, above which permeation of bioactive molecules is hindered, requiring a specific formulation optimization to overcome buccal permeability

issues (Merkle & Wolany, 1992). Subsequently, if bioactive molecules carried by oral films are not totally absorbed in the oral cavity, protection from gastrointestinal tract conditions (e.g. extreme pH and enzymatic degradation) must be granted and permeability-enhancing techniques need to be effective. This will allow carried molecules to pass throughout the gastrointestinal tract, without losing activity and the capacity of permeation through intestinal epithelium, reaching the systemic circulation (Choonara, Choonara, Kumar, Bijukumar, du Toit & Pillay, 2014). A list of bioactive molecules that either were already included in oral film matrices or that may represent good candidates to be delivered by oral films, with biopotency increment, is outlined in **Table 1**.

Table 1: Potential candidates of bioactive molecules to be delivered by oral films

Native protein/ peptide	Molecular formula	MW (Da)	Uses	Absorption	Ref.
Linaclotide	$C_{59}H_{79}N_{15}O_{21}S_6$	~1526,7	Treatment of chronic constipation.	Gastrointestinal local action	(Busby et al., 2010)
Ropinirole	$C_{16}H_{24}N_2O$	260.4	Management of Parkinson's disease	Buccal	(Lai et al., 2018)
Plecanatide	$C_{65}H_{104}N_{18}O_{26}S_4$	~1681,8	Treatment of chronic constipation.	Gastrointestinal local action	(Jadallah, Kullab & Sanders, 2014; Shailubhai et al., 2013)
Nystatin	$C_{47}H_{75}NO_{17}$	926.1	Treatment of fungal infections	Gastrointestinal local action	(Gajdošová et al., 2016)
α-lactalbumin (α-LA)	Peptide segment (YGLF)	~499	Antinociceptive activity; Antihypertensive activity; Intestinal motility stimulator	Potential buccal absorption**	(Otte, Shalaby, Zakora & Nielsen, 2007)

Enrofloxacin	$C_{19}H_{22}FN_3O_3$	359.4	Fluoroquinolone antibiotic	Potential buccal absorption	(Kumar et al., 2014a)
α-lactalbumin (α-LA)	Peptide segment (EQLTK)	~618,3	Antibacterial activity	Potential buccal absorption**	(Gulzar, Bouhallab, Jardin, Briard-Bion & Croguennec, 2013; Madureira, Tavares, Gomes, Pintado & Malcata, 2010)
β-LB	Peptide segment (VAGTWY)	~695,3	Antihypertensive activity; Antibacterial activity	Potential buccal absorption	(Català-Clariana, Benavente, Giménez, Barbosa & Sanz-Nebot, 2010; Madureira, Tavares, Gomes, Pintado & Malcata, 2010)
Octreotide	$C_{51}H_{70}N_{10}O_{12}S_2$	~1019,2	Acromegaly and gigantism treatment	Buccal*/intestinal	(Popova, Nikolskaia, Gluzdikov & Trifonov, 2014; Veuillez, Kalia, Jacques, Deshusses & Buri, 2001)
Salmon calcitonin	$C_{145}H_{240}N_{44}O_{48}S_2$	~3431.8	Osteoporosis treatment and/or management	Buccal*/intestinal	(Lee & Sinko, 2000)

Metformin	$C_4H_{11}N_5$	129.2	Diabetes *mellitus* management	Buccal	(Sander, Nielsen & Jacobsen, 2013a)
Insulin (aspart)	$C_{256}H_{387}N_{65}O_{79}S_6$	5831.648	Diabetes *mellitus* management.	Buccal*/intestinal*	(Sousa, Castro, Fonte & Sarmento, 2015a)
Stichodactyla helianthus neurotoxin	*Stichodactyla helianthus* neurotoxin (RSCIDTIPKSR CTAFQ---- CKHSMKYRLS FCRKTCGTC)	~4060.8	Treatment of autoimmune diseases.	Buccal*	(Chi et al., 2012; Jin, Boyd, White, Pennington, Norton & Nicolazzo, 2015)
Buserelin	Buserelin peptide	~1299,4	Fertility pre-treatment; Endometriosis treatment.	Buccal*	(Hoogstraate et al., 1996)

***Formulation must contain permeability enhancers.**

****May require permeability enhancers in the formulation.**

Since oral films are very thin layers usually composed of polymers, plasticizers, saliva stimulating agents, disintegrants (or super-disintegrants), sweetening agents, flavoring agents, coloring agents and stabilizers, special care must be taken in order to avoid active ingredient-excipient interactions. Excipients may yield positive effects, increasing overall bioavailability of carried active ingredients, but may also lead to problems such as precipitation, structure loss and bioavailability modification (Dixit & Puthli, 2009b; García-Arieta, 2014; Kamerzell, Esfandiary, Joshi, Middaugh & Volkin, 2011). Also, some excipients may induce alterations in gastrointestinal tract motility

and/or fluid secretion rate, therefore interfering with the absorption of carried bioactive molecules (Maher & Brayden, 2012).

Thus, despite the inherent advantages, the intimate contact between all excipients and the active ingredients demands that the oral film formulation must be thoroughly idealized regarding functional structure maintenance of carried molecules along with preservation of biological function. Moreover, oral films classic production methods may represent some struggles regarding stability of susceptible bioactive molecules. Among the different methodologies to prepare films, the solvent casting is the most feasible, cost-effective technique and, therefore, the most used one. Briefly, solvent casting is performed by heating the formulation for the solvent to be evaporated and sometimes implies energetic stirring during the homogenization or de-aeration steps, factors that can lead to degradation of carried molecules. Moreover, in order to decrease solvent casting time, organic solvents are frequently used, which can represent a serious problem regarding stability of bioactive molecules, with special regards to protein structure maintenance. Finally, since active ingredients are added to the oral film formulation before the solvent is casted, the possibility of phase separation and precipitation of incorporated bioactive molecules must be considered, which could not only alter activity but also induce texture and flavor modifications.

Hot-melt extrusion, an alternative method for oral films production that avoids organic solvents, is also impracticable for proteins, especially thermolabile bioactive molecules, not only due to heating, but also to the pressure applied during the process.

Flexographic printing technology (FPT) is a gentle process to produce oral films that can be particularly suitable for heat-sensitive molecules such as proteins and peptides, and thus it is a very promising tool to effectively incorporate them into oral

films (Buanz, Belaunde, Soutari, Tuleu, Gul & Gaisford, 2015). Since mixing and drying of the oral films formulation is performed before drug incorporation (drug is posteriorly added by a printing technique), mechanical stress and dehydration are obviated. Among other advantages, FPT allows the incorporation of bioactive molecules with personalized-drug and highly precise dosage. Nevertheless, special care must be taken with drug imprinting process in order to avoid premature disintegration, rupture and/or crumbling of oral films. Thus, drug-containing "ink" must not dissolve the constituting polymers of the oral films. Moreover, FPT presents an inherent risk of contamination. Inkjet-printing is another suitable oral film preparation method that can be applicable for incorporation of proteins or peptides. Like FPT, inkjet-printing add solution drops containing the active substances onto (and not into) the oral film but with a very high precision (5-15 pL/droplet) (Janssen, Schliephacke, Breitenbach & Breitkreutz, 2013). Nevertheless, since some bioactive molecules are very prone to suffer hydrolytic degradation, incorporation into droplets must be performed with care, especially regarding solvent choice.

Both FPT and inkjet-printing allow two or more proteins or peptides to be added to the same oral film in individualized, pre-designed patterns. Thus, different compounds can be printed on different spots of the oral film matrix, avoiding interaction between bioactive molecules during storage time (Genina et al., 2012).

Additionally, matching commonly used excipients to help tailoring the best oral film delivery system and the use of different manufacturing processes to successfully incorporate bioactive molecules without losing bioactivity must be thoroughly performed.

1.4. Tools to enhance the bioavailability of bioactive molecules delivered *per os*

The incorporation of permeability enhancers as part of the formulation of the delivery systems may directly or indirectly increase the permeation of bioactive molecules through absorptive mucosa. A summary of strategies to improve bioavailability of bioactive molecules, namely nano- and microencapsulation, are outlined in **Figure 1.**

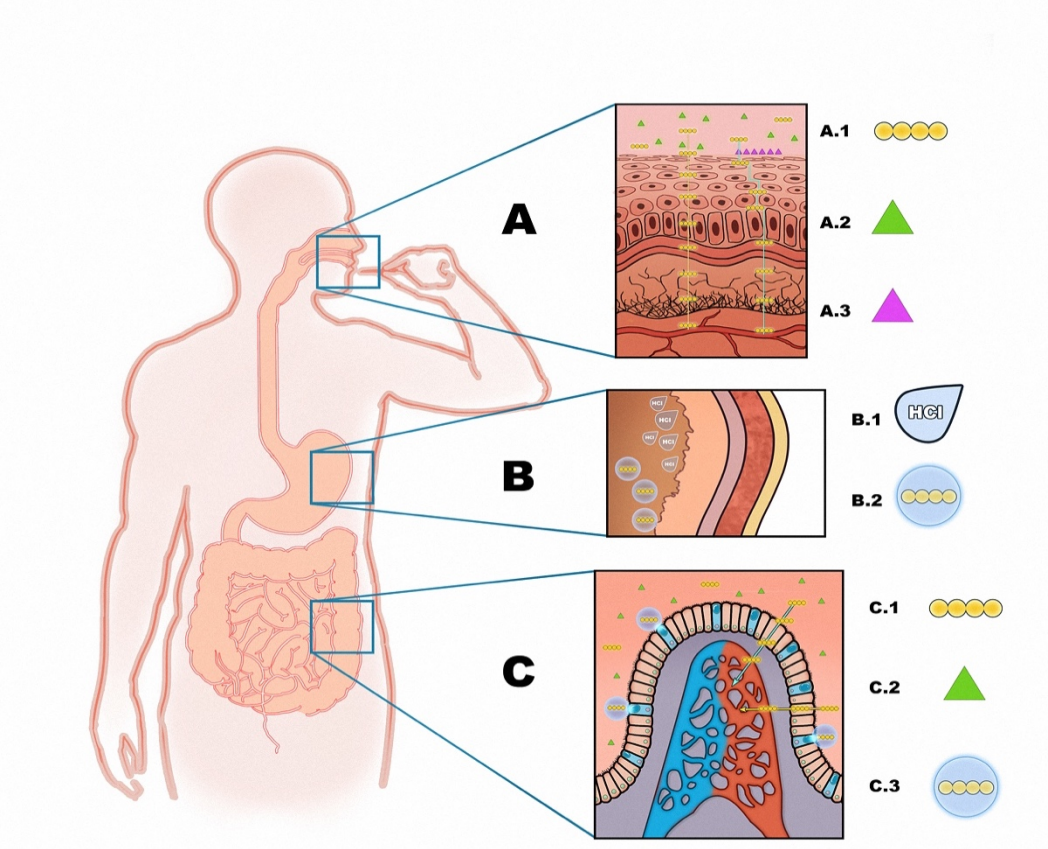

Figure 1: When oral strips are introduced in the oral cavity (A), carried proteins (A.1) cross epithelial barriers by transcellular and paracellular routes, helped by the action of permeability enhancers that facilitate internalization (A.2) and/or adhesion to the mucosa (A.3). Nanoparticles (B.2) may be used to protect proteins from gastrointestinal extreme conditions as low pH (B.1) in the stomach (B). If proteins reach the intestine (C), permeability enhancers (C.2) facilitate transcellular and paracellular protein (C.1) permeation. Nanoparticles with matrices such as PLGA, besides the protection offered, also favour internalization of proteins by interacting with intestinal M-cells (represented in blue) and promote proteins controlled release

1.4.1. Polymers

The inclusion of polymers, especially mucoadhesive polymers, can improve the overall bioavailability of molecules delivered by oral route by reducing the clearance from the local of absorption and attenuating saliva turnover effect. Indeed, most polymers used in oral/buccal delivery formulations are mucoadhesive. Mucoadhesion occurs through interaction processes that culminate in successive entanglements that are explained by several theories as the electronic theory (formation of a double layer of electrical charges from the mucoadhesive polymer and mucus), the adsorption theory (mucoadhesive molecules and mucus are attracted by van der Waals forces and hydrogen bonds), the diffusion theory (physical entanglement between proteins and polyssacharides of the mucus and the mucoadhesive polymer) and the wetting theory (association between the concepts of surface tension and mucoadhesion, indicating that interfacial energy is of paramount importance on mucoadhesion processes) (Dodou, Breedveld & Wieringa, 2005). Also, mucoadhesion has been paradoxically reported as a method to obtain sustained release of carried drugs, which would not be immediately predicted due to the closer, intimate contact between drug and absorptive tissue that would expectedly lead to a faster release and absorption (Hagesaether, Hiorth & Sande, 2009). Indeed, because of mucoadhesion, the contact between bioactive molecules and the oral mucosa is maximized, therefore favoring absorption.

Some polymers may also work as protein stabilizers and assemblers by specific mechanisms, as occurs for charged polymers, and by non-specific mechanisms, as occurs for hydrophilic polymers (Maher & Brayden, 2012). Polymer molecular size demonstrated to be positively related to protection of carried molecules, due to a non-

specific protection mechanism called crowding effect (Minton, 2005). Also, some polymers (e.g. dextran) are specially effective by avoiding protein aggregation during lyophilization and to prevent the difficulty of lyophilizate reconstitution (Costantino, Schwendeman, Langer & Klibanov, 1998).

Gelatin and starch, two polymers commonly used in pharmaceutical and food industries, provide stabilization to carried bioactive molecules. Indeed, charged polymers seem to be better protectors of bioactive molecules due to metal chelating ability (Suh, Cho & Lee, 1991). Chitosan is a good example of mucoadhesive molecule that can promote both buccal and intestinal permeation by prolonged adhesion to the mucosa, disrupting lipid organization of buccal epithelium thereby facilitating paracellular permeation (Senel, Kremer, Kas, Wertz, Hincal & Squier, 2000). Effectively, even though in the format of bilaminated buccal film, chitosan was used as a polymer to deliver insulin through buccal mucosa (Boateng & Okeke, 2014; Cui et al., 2009). A relevant and sustained decrease of blood glucose was verified 5 hours after administration. It was also reported that thiolated polymers (e.g. thiolated chitosan and polyacrylate) are particularly good permeation enhancers, promoting reversible and efficient paracellular permeation of hydrophilic molecules, by inhibition of tyrosine phosphatase, involved in the closing process of tight junctions (Bernkop-Schnurch, Kast & Guggi, 2003a; Borchard, Lueβen, de Boer, Verhoef, Lehr & Junginger, 1996a; Lehr, 1996a). Additionally, thiolated polymers increase mucoadhesivity of the formulation, contributing to an effective liberation and absorption of bioactive molecules (Dixit & Puthli, 2009b). Polymers such as chitosan may also present antibacterial activity, contributing to the elimination of bacteria that are prone to degrade carried bioactive molecules (Castro, Fonte, Sousa,

Madureira, Sarmento & Pintado, 2015a). Some other polymers such as polycarbophil were found to protect proteins from proteolytic enzymes.

A summary of advantages and disadvantages of polymers to be included in oral delivery system formulations, aiming the transport and delivery of bioactive molecules, is shown in **Table 2**.

Table 2: Advantages and disadvantages of polymers used in the production of oral drug delivery systems as carriers for bioactive molecules

Polymer	Advantages	Disadvantages	Ref.
PVP	Nonionic polymer; Good filmogenic properties; Promote stabilization of proteins/peptides from heat-induced aggregation; Bulking agent for peptide formulations.	Possible formation of amide bonds between proteins/peptides and PVP during oral films production process, leading to an alteration of delivery profile.	(D'Souza, Schowen, Borchardt, Salsbury, Munson & Topp, 2003; Gombotz et al., 1994; Izutsu & Kojima, 2000)
Gelatine	Stabilizer of proteins by preventing aggregation	Mitigates protein buccal absorption; Disruption of the three-dimensional functional structure of proteins; Formation of complexes with anionic proteins, altering delivery profile.	(Antonov & Zhuravleva, 2013; Cao, Chen, Cui & Foster, 2003)

PLGA	Mucoadhesive and biodegradable, facilitating oral delivery of molecules;	pH variation, which may compromise proteins/peptides bioactivity; Sensible to degradation from heat treatment in solvent casting process.	(Blanco & Alonso, 1998; Jorgensen, Hostrup, Moeller & Grohganz, 2009)
Chitosan	Mucoadhesive, biodegradable, facilitating oral delivery of molecules; Maintains drugs in the oral activity, compensating the saliva turnover; Protein permeability enhancer; Thiolated chitosan is a reversible paracellular permeation enhancer; Transient opening of tight-junctions, allowing polar drugs to penetrate intestinal barriers (GIT absorption only); Antibacterial effect.	Presents astringency and may be unpleasant when in high concentration; Formation of complexes with anionic proteins, altering delivery profile; Soluble in water at low pH, being unsuitable to carry some proteins.	(Bernkop-Schnurch, Kast & Guggi, 2003b; Borchard, Lueßen, de Boer, Verhoef, Lehr & Junginger, 1996b; Lehr, 1996b)
Guar gum	Nonionic polymer, reducing the possibility of negative interactions with proteins;	Oral films production implies heating to avoid gelation; High viscosity at low temperatures.	(Prabaharan, 2011)

	Guar gum conjugated with alginate and cross-linked with glutaraldehyde allows controlled release of proteins.		
Carrageenan gum	Potential to act as protein/peptide stabilizer by steric stabilization; Suitable for oral delivery systems, promoting sustained release; Leads to water absorption when in contact with proteins/peptides.	Negative charge may destabilize or alter delivery profile of proteins; Protein/peptide stabilizing effects are concentration-dependent.	(de Souza, Ramos, Câmara, Gulão, de Campos & Garcia-Rojas, 2015; Li, Ni, Shao & Mao, 2014)
GIT – gastrointestinal tract **PVP - polyvinylpyrrolidone**			

1.4.2. Amino acids

Some amino acids are also good examples of stabilizing excipients by favouring bioactive molecules to be surrounded by water and, therefore, becoming more stable and reducing the probability of aggregation (Hedoux et al., 2009; Schneider & Trout, 2009). Indeed, as an example, aggregation of proteins and peptides represents a structural problem that leads to immediate disapproval of the formulation. Arginine, although it is not a stabilizing agent, is useful as an excipient in the development of formulations as protein delivery systems. Indeed, arginine binds to some proteins (and is excluded from the surface of others) preventing aggregation, therefore increasing the shelf life of the formulation. Moreover, arginine promotes refolding of some proteins, being an important

additive regarding protein bioactivity maintenance. Also, the mechanisms of stabilizing/destabilizing effects of arginine seem to be protein-specific, which can explain why, at the same concentration, arginine causes stabilization of some proteins and destabilization of others. Nevertheless, it has been claimed that multiple direct interactions with the charged portions of proteins may be the cause of stabilizing effects (Platts & Falconer, 2015). Moreover, arginine stabilizing effects are mostly expressed when proteins are in the dissociated form, apparently due to the existence of more free arginine binding sites (Ohtake, Kita & Arakawa, 2011). Arginine may also increase the solubility of proteins, seemingly by avoiding aggregation effects (Arakawa et al., 2007).

Oligo-arginine and penetratin are able to promote the endocytic pathway and adsorption to glycosaminoglycans present on the surface of mammalian cells and were thus reported as permeability enhancers for hydrophilic molecules, such as some proteins and peptides and caffeine (Khafagy & Morishita, 2012; Maitani & Hattori, 2009; Tseng, Liu & Hong, 2002). Indeed, cell-penetrating peptides (CPP) have been successfully used as absorption enhancers, improving absorption and bioavailability profiles of bioactive molecules with intracellular activity, which were only liable to be administrated by invasive routes (Khafagy, Kamei, Nielsen, Nishio & Takeda-Morishita, 2013). Moreover, inhibitors of enzymes as chymotrypsin, trypsin, carboxy peptidases or aminopeptidase are effective permeability enhancers and are reported as interesting tools regarding bioavailability enhancement of molecules that are prone to suffer enzymatic degradation along gastrointestinal tract (Rekha & Sharma, 2013). Nevertheless, toxicity issues, mainly digestion problems of diet proteins, must be carefully considered and studied.

It is therefore observed that amino acids, if used properly, may be used to stabilize, increase solubility and enhance absorption profile of bioactive substances across physiological barriers, leading to an overall pharmacokinetic improvement.

1.4.3. Ions

Ions have also been extensively reported as useful permeability enhancers. Some ions promote aggregation of proteins in specific binding sites, working as stabilizers, being zinc an important example by inducing the formation of insulin hexamers. Actually, metal ions may contribute to stabilization or destabilization of bioactive molecules, with special relevance to proteins (Wang, 1999). Thus, metallic composition must be thoroughly controlled, since structure alteration caused by a specific metallic element is dependent on the protein or peptide to be carried and delivered.

When preparing formulations regarding oral delivery of bioactive molecules, ions from the Hofmeister series may also be chosen ($CO_3^{2-} > SO_4^{2-} > S_2O_3^{2-} > H_2PO_4^- > F^- > Cl^- > Br^- \sim NO_3^- > I^- > ClO_4^- > SCN^-$) (Zhang & Cremer, 2010). Anions on the left side of the Hofmeister series, or kosmotropic ions, are prone to precipitate proteins and to prevent from unfolding. On the other hand, anions from the right side of the Hofmeister series, or chaotropic ions, tend to increase protein solubility but also to promote denaturation of proteins. Anions are reported to influence proteins stability by selective accumulation on the protein surface (Kamerzell, Esfandiary, Joshi, Middaugh & Volkin, 2011). Chloride is one of the most used anions from the series, being located in the dividing line between Kosmotropic and Chaotropic ions and it has demonstrated, when in the form of guanidinium chloride, to induce a decrease of the thermal destabilization rate and unfolding of proteins by binding to one or more cation binding sites, as verified for

ribonuclease T1 (Mayr & Schmid, 1993). Once again, the choice of ions must be performed considering the behaviour of each protein or peptide might behave differently when in contact with different anions. In addition, some excipients are used in the salt form (e.g. saliva stimulating agents, such as citric acid, malic acid, tartaric acid, lactic acid) and released ions should be accounted.

Some metallic ions are also prone to promote the formation of reactive oxygen substances that may oxidize carried bioactive molecules, potentially compromising bioactivity. Citric acid, a saliva-stimulating agent broadly used in oral delivery formulations, may also act as a chelating agent, binding or reacting with carried bioactive molecules or by capturing destabilizing metal ions. Indeed, caffeine anhydrous reacts with citric acid by an acid-base reaction, leading to the formation of a more hydrosoluble product: caffeine citrate. Moreover, citric acid captures calcium ions leading to disruption of intracellular junctions, increasing permeability of bioactive molecules (Sood & Panchagnula, 2001).

1.4.4. Polyols and sugars

Other important stabilizers, currently used in oral films formulations, are polyols and sugars, such as glycerol, sorbitol (commonly used as plasticizers in formulations for oral delivery) and sucrose, lactose, mannitol and dextrose (used as sweeteners/saliva stimulating agents) (Boctor & Mehta, 1992; Chang et al., 1996). It was verified for some bioactive molecules that, during purification processes, sugars present at high concentrations can prevent loss of bioactivity (De La Cruz & Pollard, 1995; Lee & Timasheff, 1981; Ohtake, Kita & Arakawa, 2011). This bioactivity maintenance offered by sugars seems to be due both to water replacement and vitrification phenomena

(Grasmeijer, Stankovic, de Waard, Frijlink & Hinrichs, 2013). Water replacement occurs, for instance, when proteins are freeze-dried and hydrogen bonds that were previously established between proteins and water are now settled between proteins and sugars (preferentially in the amorphous state, in order to fit the surface of the protein), favouring the maintenance of protein structure. On the other hand, vitrification is explained by retention of the protein or peptide inside the sugar matrix, restricting aggregation.

Potential of polyols to hinder aggregation of proteins correlates to two main factors: polyol size and chemical composition, especially regarding the number of –OH groups. Indeed, polyol size seems to be positively correlated with protection ability of bioactive molecules but, above the molecular weight of sorbitol (182.2 g/mol), this correlation it not observed anymore. Moreover, the number of –OH groups of polyols also seems to be positively related to protection efficacy of carried substances, presumably due to an increased possibility of hydrogen bonds establishment between polyols and carried bioactive molecules. Sorbitol, for instance, is commonly used both as a plasticizer and sweetening agent in the elaboration of oral delivery systems and it was proven to inhibit heat-induced aggregation of some bioactive molecule, such as proteins and peptides, even though the effect decreased for high concentrations (Tsai, van Zanten & Betenbaugh, 1998). Glycerol also induces stabilization of certain bioactive molecules but may potentially destabilize others and, therefore, must be used carefully (Faber-Barata & Sola-Penna, 2005). Nevertheless, the inclusion of sugars with reducing capacity may be harmful due to the possible occurrence of Maillard reactions that may generate toxic compounds (Li, Nguyen, Schoneich & Borchardt, 1995; Li, Schoneich & Borchardt, 1995).

In conclusion, sugars and polyols may offer stability, protection and inhibition of aggregation of proteins and peptides, assuring that carried proteins and peptides successfully reach the local of action and perform the expected bioactivity.

1.4.5. Chemical modification

The chemical modification of bioactive molecules to be delivered is another relevant bioavailability enhancement tool. Desmopressin, for instance, is obtained from deamination of the first amino-acid and inversion of the stereochemical configuration – from levo to dextro – of the arginine at the eighth position of vasopressin, thus offering an exponentially higher permeability across intestinal epithelia and enzymatic stability (Vilhardt & Lundin, 1986).

Another effective way of chemical modification is lipidization, resulting from conjugation of fatty acids with bioactive molecules, leading to an increased lipophilicity and consequently pharmacokinetic improvement (Zhang & Bulaj, 2012). Lipidization is a successful resource regarding *in vivo* oral absorption of calcitonin conjugated with N-palmitoyl cysteinyl 2-pyridyl disulfide, comparatively to unmodified calcitonin, leading to overall bioavailability improvement. Lipidization was also a breakthrough mean to obtain detemir (Levemir®) and degludec insulin modifications. Detemir was obtained by myristoylation of the penultimate lysine residue in position B29 and removal of the terminal threonine resulting in an increased affinity to albumin and consequent increase in half-life and stability (Hackett, Zaro, Shen, Guley & Cho, 2013). Degludec results from an addition of a palmitoyl group to the B29 ε-lysyl amino group using a γ–glutamic acid spacer with an additional removal of terminal threonine, resulting in a more stable insulin analogue, with a longer lasting glycemic control. Also, acyclovir was conjugated with a

lipophilic raft that overcomes low permeability of the drug across cell membranes by increasing docking affinity to membrane transporter (sodium multivitamin transporter for biotin) (Vadlapudi et al., 2012). Consequently, acyclovir is more rapidly translocated across cell membrane, representing an effective bioavailability improvement that can be extrapolated for other bioactive molecules.

Creating prodrugs that are activated by enzymatic or non-enzymatic processes, is also a suitable tool regarding the optimization of bioavailability of bioactive molecules (Jana, Mandlekar & Marathe, 2010). Prodrugs are engineered to obtain improved stability and permeability across gastrointestinal barriers. Even though this tool was unsuccessfully used attempting to modify some proteins, a successful case was obtained for opioid peptides ([Leu5]-enkephalin), achieving a significantly higher permeability profile using Caco-2 cell models, by cyclization technique (Borchardt, 1999; Pauletti, Gangwar, Siahaan, Aube & Borchardt, 1997).

1.4.6. Micro- and nanoparticles as bioavailability enhancers of loaded bioactive molecules

Besides benefits that can be obtained from commonly used excipients in oral delivery system formulations to enhance bioavailability of carried bioactive molecules, other tools may be used to reach similar goals. The encapsulation of bioactive molecules into nanoparticles, for instance, has been used to increase stability and permeability.

Micro and nanoparticles can also be combined with other oral delivery systems (e.g. oral films, capsules, pills, syrups) to enhance overall efficacy of the carried bioactive molecules and functionalized to target specific tissues or organs (Castro, Fonte, Sousa, Madureira, Sarmento & Pintado, 2015c). Mucoadhesive polymers represent an important

example of molecules that can significantly improve characteristics of nanoparticles as buccal delivery systems for bioactive molecules. Indeed, mucus represents an important barrier that hinders the permeability of several drugs, mainly lipophilic drugs (Sigurdsson, Kirch & Lehr, 2013). Polycations (e.g. chitosan and derivatives, poly(L-lysine), poly(amido amine), among others) are well-known examples of mucoadhesive molecules that can be used as nanoparticle-forming polymers or even as coatings for nanoparticle-based formulations (Schulz, Gauthier & Leroux, 2015). Moreover, as mentioned above, the advantages of mucoadhesive molecules for buccal delivery are related with the induced increment of retention time of drugs in intimate contact with buccal epithelia along with other mechanisms (Deacon et al., 2000). Nevertheless, the inclusion of some mucoadhesive molecules may also entangle carried drugs (especially for proteins with high molecular weight) or contribute to an increased rigidity of the drug delivery system, thus leading to a slower release (Takahashi, Takeda, Seto, Kawano & Machida, 2007).

1.4.6.1. Production methods of nanoparticles as oral delivery systems for bioactive molecules

There are two major classes of nanoparticle production methods aiming the incorporation and release of bioactive molecules: chemical and physicochemical methods (Iqbal, Zafar, Fessi & Elaissari, 2015). Chemical methods include emulsion polymerization, mini-emulsion polymerization and interfacial polymerization (Kumari, Yadav & Yadav, 2010; Soppimath, Aminabhavi, Kulkarni & Rudzinski, 2001). On the other hand, physicochemical methods include multiple emulsion techniques, spray drying, layer by layer process and emulsion solvent diffusion. However, the two most

common methods for the preparation of micro and nanoparticles are schemed in **Figure 2.**

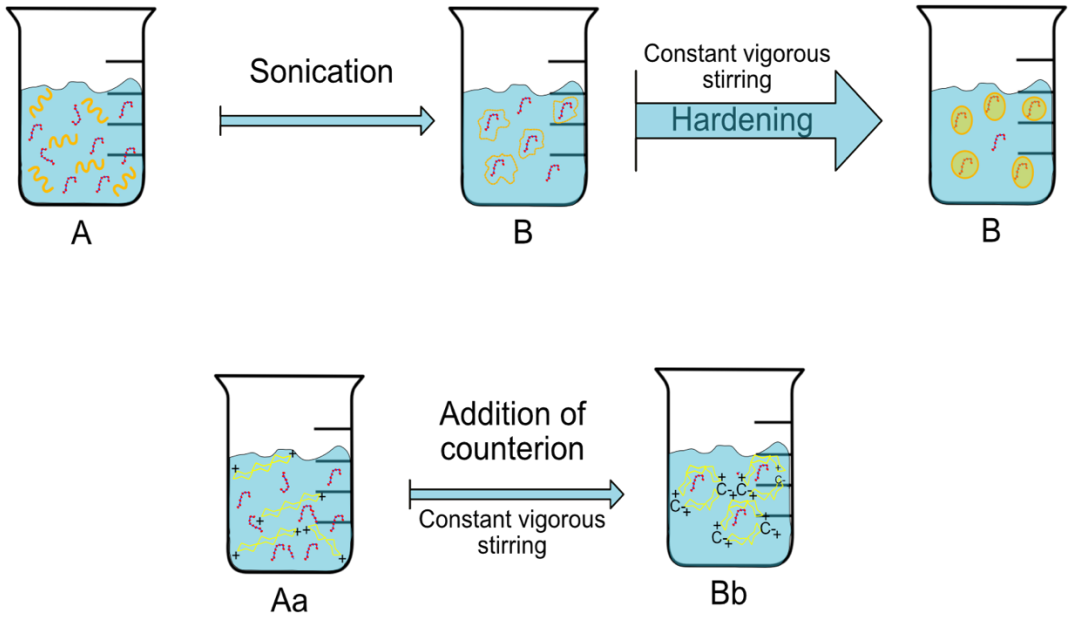

Figure 2: Most common nanoparticle production methods: solvent evaporation and ionic gelation. In solvent evaporation method, the encapsulating polymer and the bioactive molecules to be entrapped are dissolved in an organic solvent (A). After sonication, the polymer surrounds the molecules to be carried (B) and is kept under vigorous stirring until all organic solvent is evaporated (C). In Ionic gelation, a solution of a proper coacervation agent is added dropwise containing a charged polymer and the bioactive molecules to be entrapped (Aa), leading to the formation of the nanoparticles (Bb)

Regarding emulsion polymerization technique, it is a very common and simple nanoparticle preparation method and is subdivided in simple and double-emulsion techniques (Danhier, Ansorena, Silva, Coco, Le Breton & Preat, 2012). In the spontaneous emulsification and solvent diffusion methods, the water miscible solvent along with a small amount of the water immiscible organic solvent is used as an oil phase. Due to the spontaneous diffusion of solvents, an interfacial turbulence is created between the two phases, leading to the formation of small particles. As the concentration of water miscible solvent increases, a decrease in the size of particle can be achieved. Both solvent evaporation and solvent diffusion methods can be used for hydrophobic or hydrophilic

drugs (Mohanraj & Chen, 2006). Simple o/w emulsions, on the other hand, are useful delivery systems for the entrapment of lipophilic molecules. In opposition, association efficiency of hydrophilic molecules is usually low and, therefore, nanoparticles prepared by w/o simple emulsion are not suitable for most proteins and peptides or for caffeine (Chung, Huang & Liu, 2001; Khalil et al., 2013). Mean size of particles produced by simple o/w emulsion was found to be influenced by the type and concentrations of stabilizer, homogenizer speed and polymer concentration (Kwon, Lee, Choi, Jang & Kim, 2001; Mohanraj & Chen, 2006).

Double emulsion are more complex systems than simple emulsions, leading to the presence of nanoparticles that contain one or more smaller particles inside the matrix. Water-in-oil-in-water (w/o/w) double emulsions are useful for the incorporation of both hydrophilic and lipophilic molecules (individually or together) and, therefore, can be used for the entrapment of bioactive proteins and peptides or caffeine (Iqbal, Zafar, Fessi & Elaissari, 2015). Moreover, nanoparticles produced by double emulsion technique are more effective on the protection of carried bioactive molecules. However, formulations of nanoparticles are hard to scale-up, as the production method involves two steps. Moreover, high polydispersity index and the possibility of leakage of entrapped molecules to the external water phase may represent potential storage problems. Particle replication in non-wetting templates have also been described in the literature for production of nanoparticles (Maruthi, Smith & Manavalan, 2011; Mohanraj & Chen, 2006). When organic solvents must be avoided, solid-in oil-in-water (s/o/w) method is a feasible approach (Bilati, Allemann & Doelker, 2005b).

Nanoprecipitation is the ideal method for bioactive molecules prone to suffer hydrolytic degradation since water is avoided. Nanoprecipitation results in small-sized

nanoparticles. Moreover, since nanoprecipitation method does not imply high-shear stress, integrity of bioactive molecules to be encapsulated is not compromised (Bilati, Allemann & Doelker, 2005a).

Ion-pairing is a suitable nanoentrapping method for bioactive molecules that are stable at pH values below isoelectric point. Ion pairing occurs in the presence of a surfactant below the critical micelle concentration and induces an increased hydrophobicity that may lead to a superior association efficiency (Meyer & Manning, 1998; Quintanar-Guerrero, Allemann, Fessi & Doelker, 1997).

1.4.6.2. Critical nanoparticle characteristics for biological interaction and characterization methods

Particle size, polydispersity index and zeta-potential are core characteristics of the nanoparticles as delivery systems and on their behaviour in biologic systems. Indeed, it has been previously reported that nanoparticles with a mean size of 100 nm exhibit increased circulation half-life when compared with particles with superior or inferior dimensions (Barua & Mitragotri, 2014). Moreover, besides from being an indicator of the stability of colloidal dispersions, zeta-potential is also an important factor in the interactions (mainly electrostatic) with the biologic membranes. As an example, positively charged nanoparticles (e.g. chitosan nanoparticles) are capable of strong interaction with the carboxyl and sulphate groups of the oligosaccharide chains of mucus (Bhattacharjee et al., 2017; Cone, 2009).

The main techniques used for the determination of mean size are Scanning Electron Microscopy (SEM), Atomic Force Microscopy (AFM), Transmission Electron Microscopy (TEM) and Dynamic Light Scattering (DLS). Methods used for the

determination of mean size can also be used for observing the presence or formation of agglomerates and, regarding the microscopy techniques, surface morphology and conformational analysis over time can also be assessed. Further qualitative nanoparticle surface characteristics can be determined by techniques as X-ray photoelectron spectroscopy (XPS), energy dispersive spectroscopy (EDS), Fourier-transform infrared (FTIR) and Raman spectroscopy. Zeta-potential, in turn, can be determined by the analysis of the electrophoretic mobility of the particles.

Indeed, the characterization of nanoparticles is of paramount importance and remains unstandardized by the regulatory agencies worldwide (Lin, Lin, Wang & Sridhar, 2014). Nonetheless, the determination of specific physicochemical characteristics as morphology, mean size, size distribution (polydispersity index), aggregation, surface properties, conformational changes, drug content and drug release is commonly performed (Crucho & Barros, 2017). The specifications of a certain nanoparticle formulation depend on the application and, therefore, cannot be strictly standardized, but must be thoroughly understood to predict *in vivo* behaviour and to guarantee effectiveness and lack of toxicity. It is widely reported that nanoparticle shape and size represent a very important factor regarding the intimate contact and interaction with biological interfaces (Banerjee, Qi, Gogoi, Wong & Mitragotri, 2016). Also, the assumption that spherical-shaped nanoparticles are the most suited as drug delivery systems is not necessarily true in all cases. Aiming to study the influence of shape and size of nanoparticles for oral drug delivery, Banerjee et al. prepared polystyrene nanoparticles of different shapes (i.e. sphere-, disc- and rod-shaped) and sizes (i.e. 50, 200, 500 and 1000 nm) and tested the cellular uptake and transport across Caco-2, Caco-2/HT29, Caco-2/Raji-B and Caco-2/HT29/Raji-B triple culture. It was observed that particle uptake by Caco-2 and Caco-

2/HT-29 cells was higher when particle size was smaller, as revealed by confocal microscopy. Similar results were observed regarding transport studies, revealing that particles with sizes of 50 nm and 200 nm were more effectively transported across cell layers than 500 nm or 1000 nm particles. Regarding shape, rods and discs offered a higher uptake on Caco-2 cells when compared with spheres. Uptake of rod-shaped particles was also higher when compared with particles with other shapes in Caco-2/HT-29 co-culture. Transport across Caco-2 cell layer or Caco-2/HT-29 co-culture was not shape dependent. On the other hand, transport across Caco-2/Raji-B co-culture was significantly higher for rods and discs (~20% after 5 h) when compared with spherical particles (~14% after 5 hours) and similar results were obtained for Caco-2/Ht-29/Raji-B co-culture.

Also, understanding the bioactive molecule-nanoparticle interactions, i.e. the composition and organization of this system, and the residence times of the carried molecules on the nanoparticles is of paramount importance regarding delivery-system characterization. Bioactive molecules with high concentrations and high association rate constants will initially occupy the nanoparticles surface. Nonetheless, molecules adsorbed to nanoparticles may also dissociate quickly and be replaced by other molecules with higher affinity to the particle matrix (Lynch & Dawson, 2008). Adsorption of bioactive molecules to various materials has been widely studied and it has been found that factors such as electrostatic interactions, hydrophobic interactions and specific chemical interactions between the carried bioactive molecule and the adsorbent play important roles. For example, studies of adsorption of bioactive molecules prove that some have a strong adsorption to the nanoparticles and a long residence time, while others present shorter residence times and/or lower affinities (Lynch & Dawson, 2008). Polymers, such as poly-(lactic acid) (PLA), poly-(lactide-co-glycolide) (PLGA),

polycaprolactone (PCL), chitosan, alginate, gelatin, starch and amphiphilic copolymer polyethylene glycol (PEG), are commonly used for fabricating nanoparticles due to the excellent biocompatibility and biodegradability (Giovino, Ayensu, Tetteh & Boateng, 2012; Mundargi, Babu, Rangaswamy, Patel & Aminabhavi, 2008; Patel, Cholkar & Mitra, 2014; Rawat, Singh, Saraf & Saraf, 2006).

1.4.6.3. Selection of excipients to produce micro and nanocarriers

The selection of the excipients to produce micro and nanoparticles must be done according to the required size of the particles, zeta potential, drug loading, association efficiency, the inherent properties of the molecule to be incorporated (i.e. solubility and stability), surface characteristics (i.e. charge and shape), the degree of biodegradability, biocompatibility and toxicity, the desired release profile of the bioactive molecule and the antigenicity of the final product (Maruthi, Smith & Manavalan, 2011; Mohanraj & Chen, 2006).

Hence, it was verified that PLGA nanoparticles with a hydrogenated phosphatidylcholine (HSPC) surface coating improved ovalbumin intestinal delivery and absorption (Pawar, Meher, Singh, Chaurasia, Surendar Reddy & Chourasia, 2014). Not only PLGA nanoparticles offered protection from gastrointestinal extreme conditions, but also granted controlled release to the carried proteins along with enhanced affinity to intestinal M-cells, which can be especially interesting regarding intestinal delivery of vaccines. In another approach, poly(ethylene glycol)methyl ether-block-polylactide (PEG-b-PLA) was used as copolymer in a nanoparticle formulation with the purpose of encapsulating insulin and impregnating nanoparticles into chitosan oral films, obtaining a suitable buccal delivery system for insulin (Giovino, Ayensu, Tetteh & Boateng, 2012,

2013). It was concluded that chitosan oral films impregnated with insulin entrapped into PEG-b-PLA nanoparticles represent a buccal delivery system that offers insulin biphasic and sustained release. Indeed PEG-b-PLA nanoparticles erosion was shown to first depend on the swelling of polymeric matrix and then from the nanoparticles. Similarly, another oral film formulation was impregnated with nanoparticles coated with lysozyme attaining sustained release (4 hours) detected in the basolateral side of a Franz diffusion cell, used to mimic buccal epithelia (Morales, Ross & McConville, 2013).

Solid lipid nanoparticles (SLN) are also suitable carriers for bioactive molecules as stated for insulin intestinal delivery and absorption, demonstrating a significant hypoglycemic effect that lasted for 24 hours, after oral administration in mice (Sarmento, Martins, Ferreira & Souto, 2007; Sousa, Castro, Fonte & Sarmento, 2015b). Also, SLN combination with mucoadhesive and absorption enhancing polymers (e.g. chitosan) showed to be very effective calcitonin delivery systems, offering improved bioavailability and continuous release (Garcia-Fuentes, Torres & Alonso, 2005). Moreover, controlled release of bioactive molecules was demonstrated to be possible, by manipulating relative amounts of chitosan, tripolyphosphate (TPP) and carried molecule, as evidenced using bovine serum albumin (BSA) as model (Gan & Wang, 2007). Indeed, an initial burst release (30-70% after 3-6 h) and a posterior protein release were observed, and continued for some days after oral administration. Furthermore, it was demonstrated that SLN can be tailored to obtain controlled release of bioactive molecules (as shown for insulin), also offering protection from hostile gastrointestinal environment and promoting absorption, inducing significant hypoglycemia in diabetic rats (Gan & Wang, 2007; Garcia-Fuentes, Torres & Alonso, 2005; Olbrich & Muller, 1999; Sarmento, Martins, Ferreira & Souto, 2007).

As verified for nanoparticles, good results were also obtained using PLGA microparticles as cholera toxin B carriers administered *per os*, inducing an effective immune response observable *in vivo* (O'Hagan et al., 1993).

Moreover, the encapsulation of bioactive molecules may avoid direct contact with oral films matrix. This approach has been explored for the improvement of several oral delivery formulations regarding the delivery of different molecules with pharmaceutical or nutraceutical interest (Shen et al., 2013; Sievens-Figueroa et al., 2012).

Micro- and nanoencapsulation are also prone to offer increased permeability of carried molecules, either by specific or unspecific pathways. Thus, microparticles and nanoparticles can be tailored in order to favourably enhance pharmacokinetic profile of bioactive molecules and can easily be associated with other delivery systems.

Another interesting tool may be adapting colon-specific delivery approaches, creating microparticles or nanoparticles coated with methacrylic acid copolymers or Eudragit, allowing preferential disintegration and preferential release of proteins at alkaline pH values (Philip & Philip, 2010). Moreover, coating polymers for micro- and nanoparticles (e.g. chitosan, pectin, chondroitin sulphate or inulin) that are preferentially degraded by the colonic microflora are also good candidates to achieve colon-specific delivery of proteins.

1.5. Strategies to assess buccal and intestinal permeability and predict bioavailability of bioactive molecules

Several buccal absorption (e.g., swirl and spit) and perfusion tests have been developed to mimic *in vivo* buccal permeability, but many were inaccurate and did not

reproduce the complexity of human buccal mucosa (Patel, Liu & Brown, 2012). On the other hand, *in vivo* studies are too expensive, impractical, and laborious (Kulkarni, Mahalingam, Pather, Li & Jasti, 2010). Hence, *ex vivo* models appear to be plausible and smart tools because they have a significantly lower cost than *in vivo* studies. In such models, only a small portion of animal buccal mucosa is used for each experiment, buffers are used as samples instead of blood, and it is possible to vary conditions such as temperature, pH, and osmolarity, which allows the study of permeability under different physicochemical conditions and with different mechanisms and interactions (Teubl, Absenger, Frohlich, Leitinger, Zimmer & Roblegg, 2013). However, it is essential that *ex vivo* buccal models have the greatest similarity to human buccal mucosa, especially regarding central factors for permeability such as mucus production and composition (which has been proved to influence drug mobility) and epithelium keratinization (Patel, Liu & Brown, 2012; Teubl, Absenger, Frohlich, Leitinger, Zimmer & Roblegg, 2013). Because the buccal mucosa of rats and hamsters is keratinized, it does not represent a suitable buccal permeability model of human buccal mucosa (Patel, Liu & Brown, 2012). Dog and monkey buccal mucosa is nonkeratinized, but it is also thinner and therefore more permeable than human buccal mucosa. The animal that has a similar buccal mucosa to humans is the pig, and thus it represents the most frequently used model in studies pertaining to permeability of molecules, even though high variability was observed in permeation studies (Kulkarni et al., 2010). Also, porcine buccal mucosa is cheap and does not involve the same ethical considerations as, for instance, dogs or monkeys (Patel, Liu & Brown, 2012).

Other approach to mimic buccal mucosa is to perform *in vitro* permeability assays on human buccal carcinoma TR146 cell layers (Jacobsen, Pedersen & Rassing, 1996;

Jacobsen, van Deurs, Pedersen & Rassing, 1995; Nielsen & Rassing, 1999; Nielsen & Rassing, 2000a; Nielsen & Rassing, 2000b). Models using cell lines are widely used and accepted to perform permeability testing of bioactive molecules. Indeed, when cultured in layers, TR146 cells resemble the characteristic human buccal mucosa epithelium, regarding morphology, stratification ability or barrier properties (Jacobsen et al., 1999). As occurs in normal human buccal epithelium, TR146 cells expressed K4, K10, K13, K16 and K19 keratins (responsible for the formation of filaments between epithelial cells) along with similar involucrin, plasma membrane-associated glutaminase, and epidermal growth factor receptor.

As stated for buccal permeability studies, porcine intestinal mucosa is commonly used to perform *ex vivo* permeability studies of bioactive molecules. Effectively, the fact that both humans and pigs are omnivores and that pig intestine presents high microscopic and macroscopic similarities with human intestine, excised intestinal porcine tissues are therefore useful to predict permeability *in vivo* in humans (Ripken & Hendriks, 2015). Permeability assays using porcine intestinal tissue present some advantages over the homologous *in vitro* assays using cell lines since intestinal segments present multiple cell types other than epithelial cells (e.g. enteroendocrine, goblet cells, enterochromaffin cells, Paneth cells) being useful for the permeation mechanisms that include cell-cell communication. Moreover, tissues from different intestinal regions can be excised and used, with a more reliable approach on *in vivo* intestinal permeation. Nevertheless, tissue excision process requires higher expertise when compared with *in vitro* approaches. Indeed, the operator must know how to distinguish the different portions of porcine small intestine and know how to surgically separate the epithelial section from the basal membrane of the tissue. Furthermore, biological variation between pigs, the source of the

tissue, the occurrence of unreported diseases and the variations in the diet of the animal are important factors that may induce unwanted deviations in the results.

In vitro intestinal permeability assays are commonly accepted by pharmaceutical industry and scientific community, as reliable to mimic *in vivo* behaviour and are performed using Caco-2 cell line, or co-cultures of intestinal cells (Caco-2/HT29-MTX or Caco-2/HT29-MTX/Raji B) (Lozoya-Agullo et al., 2017). Caco-2 human epithelial cell line spontaneously differentiate into monolayers and achieve the morphological (e.g. the brush border layer with microvilli, a distinctive trait of the epithelia of the small intestine) and functional properties of absorptive enterocytes. Caco-2 cell line usually express typical digestive enzymes, as lactase, and aminopeptidase N, sucrase-isomaltase and dipeptidylpeptidase IV, along with active, membrane ionic and non-ionic transport mechanisms, cytokine production and receptors as expressed *in vivo* by the enterocytes. As stated for TR146 cells, cultivation of Caco-2 cells on filter supports is performed for the improvement of morphological and functional differentiation. Nonetheless, Caco-2 cell monoculture is insufficient to represent some features of *in vivo* intestinal mucosa. For instance, the absence of other cell lines or of the production of mucins lead to physical and chemical differences, mainly in the adherence and absorption extension of some molecules. Effectively, the lack of mucus will result in an overestimation of the permeability of some molecules, mainly small compounds with high diffusivity. On the other hand, some permeability underestimation of molecules that cross the intestinal mucosa via paracellular mechanisms is observed due to the high density of tight-junctions present between Caco-2 cells. Thus, aiming to obtain a more representative *in vitro* intestinal model, HT29-MTX goblet cells (producers of mucins) were co-cultivated with Caco-2 cells to form a system comprising the two major epithelial cell types of the

intestine (Kleiveland, 2015). Moreover, the presence of HT29-MTX cells assures the secretion of MUC1 and MUC5 that form a mucus layer on top of the epithelial cells. Also, since HT29-MTX cells do not present tight junctions, the paracellular permeation is more resembling of the *in vivo* reality.

1.6. Oral film-based products in pipeline

Oral films were developed around 1970, so they are not actually new. Nevertheless, many new pharmaceutical products based on oral films as delivery systems are being developed, with a predictable growth in the market in the next few years. All inherent advantages of oral films as delivery systems allows pharmaceutical companies to manage a new life cycle to reference pharmaceutical products that lost or are about to lose patenting protection. Additionally, as oral films are different delivery systems from tablets or capsules, when prescribed, they cannot be replaced in the pharmacy for the conventional oral dosage forms, hence representing a smart alternative strategy to achieve a higher market quote. Moreover, practicality is arguably one of the most important characteristics that any product may present nowadays, which is a key point not only for pharmaceutical but also food industries, to be developing new oral films formulations as drugs and nutraceuticals delivery systems. However, oral films as oral delivery systems are not extensively available yet and this gap might represent a marketing opportunity for pharmaceutical industry. Indeed, a significant amount of oral films-based products is already in pipeline or have already been marketed. **Table 3** enlists some examples of different products based on oral films and similar delivery systems, in different stages of

development, indicating the wide array of utilization of oral films along with industry emerging interest.

Table 3: Examples of products in different stages of development that serve distinct therapeutic purposes

Product	Owner company	Uses	Development stage	Ref.
Listerine® Pocketpacks®	Johnson & Johnson	Breath fresheners	Marketed	(Castro, Fonte, Sousa, Madureira, Sarmento & Pintado, 2015a)
Ondansetron Rapidfilms®	Labtec GmbH	Post-operatory- and chemotherapy-induced nausea and vomiting	Marketed	(Dixit & Puthli, 2009a)
Aripiprazole	Labtec	Schizophrenia management	Recently completed clinical studies	(Castro, Fonte, Sousa, Madureira, Sarmento & Pintado, 2015a)
Apomorphine*	Labtec	Treatment of parkinson's disease and depressive disorders	Currently running phase II experiments	(Giovinazzo, Hedden, de Somer & Bryson, 2011)
Breakyl®**(fentanyl)	BioDelivery Sciences	Chronic pain management	Marketed	(Rauck, North, Gever, Tagarro & Finn, 2010)
*Sublingual film **Buccal film				

Additionally, different oral films systems are being developed. VersaFilm™ and IntelGenX were designed to obtain immediate release of incorporated bioactive molecules. Bio-FX™ (NAL Pharma) promote absorption of bioactive molecules directly in the oral cavity. Also, BEMA® (BioDelivery Sciences) are highly mucoadhesive oral films applied directly in the cheek to obtain maximum buccal absorption.

On the other hand, oral delivery of bioactive molecules that currently are only administered by invasive routes has been pursued for quite some time, ambitioning to avoid painful drug administration and to maximize compliance to treatment. Insulin is a classic case that would deeply benefit from oral delivery, obtaining painless administration without any stigma and, perhaps more importantly, obviate co-morbidities that result from noncompliance to subcutaneous treatment. An effective insulin oral delivery system, for instance, would seriously improve lifestyle of the patients and avoid substantial financial burdens inherent to untreated (or poorly managed) diabetes. Indeed, several companies are currently investing in research and development that regards oral delivery of proteins and peptides.

To meet the proposed goals of the present thesis, the optimization of delivery systems (i.e. the formulations of oral films and micro/nanoparticles) was performed to achieve an improved release profile, to offer protection against pre-systemic and systemic metabolism and to guarantee an enhanced permeability across buccal and intestinal absorptive epithelia. Also, an antihypertensive peptide, a relaxing peptide and caffeine were used as model bioactive molecules. The improved biopotency of both the peptides and caffeine when carried by developed formulations can represent a small (but firm) step forward towards the replacement of invasive delivery routes.

Section 2

Optimization of formulations for improved oral delivery of caffeine

Chapter II: Optimization of two biopolymer-based oral films for the delivery of caffeine

Pedro M. Castro [1,2], Pedro Fonte [2,3], Ana Oliveira [1], Ana Raquel Madureira [1], Bruno Sarmento [2,4,5], Manuela E. Pintado [1]

[1]CBQF – Centro de Biotecnologia e Química Fina – Laboratório Associado, Escola Superior de Biotecnologia, Universidade Católica Portuguesa/Porto, Rua Arquiteto Lobão Vital Apartado 2511, 4202-401 Porto, Portugal

[2]CESPU, Instituto de Investigação e Formação Avançada em Ciências e Tecnologias da Saúde, Rua Central de Gandra 1317, 4585-116 Gandra-PRD, Portugal

[3]REQUIMTE, Department of Chemical Sciences – Applied Chemistry Lab, Faculty of Pharmacy, University of Porto, Rua de Jorge Viterbo Ferreira 228, 4050–313 Porto, Portugal

[4]i3S - Instituto de Investigação e Inovação em Saúde, Universidade do Porto, Portugal

[5]INEB – Instituto de Engenharia Biomédica, University of Porto, Rua do Campo Alegre 823, 4150–180 Porto, Portugal

** Corresponding author: mpintado@porto.ucp.pt*

2.1. Abstract

An experimental design was established in order to optimize the mechanical characteristics of two oral film formulations intended for oral delivery of bioactive compounds. Carboxymethylcellulose and gelatin type A were selected as polymeric matrix, differing in chemical nature and charge, and were tested regarding caffeine

delivery aptness. Caffeine was used either as a nutraceutical *per se* and as model for other bioactive molecules with nutritional/nutraceutical value, to assess the potential of formulations as practical and effective delivery systems of bioactive compounds. Scanning electron microscopy revealed that caffeine crystals were homogeneously dispersed onto oral film matrix. Fourier-transform infrared analysis did not indicate formation of new chemical entities, suggesting that caffeine chemical characteristics were not altered when incorporated into oral films. USP modified dissolution assay revealed that gelatin type A was more effective in controlling caffeine release since maximum release (97.4% ± 0.95) occurred only after 20 min. On the other hand, carboxymethylcellulose is better suited when immediate release is aimed, since maximum caffeine release (81.1% ± 2.14) occurred immediately after 4 min. Data obtained from the simulation of gastrointestinal tract with *ex vivo* permeability assay was in accordance with those obtained from USP dissolution assay (42.0% ± 7.8 and 15.3% ± 4.0 of caffeine released from CMC and GeltA oral films – respectively - permeated porcine intestinal mucosa after 120 min). Carboxymethylcellulose and gelatin type A optimized oral film formulations were obtained and represent two suitable oral delivery systems for immediate and controlled release, respectively.

2.2. Introduction

Oral films represent promising alternatives to conventional oral delivery systems (e.g. tablets, capsules) to carry and deliver bioactive molecules directly into the mouth, especially dietary supplements or other molecules with nutritional or nutraceutical interest (Castro, Fonte, Sousa, Madureira, Sarmento & Pintado, 2015b; Dixit & Puthli,

2009a). Intake of oral films is advantageous, as it does not require water, obviating swallowing difficulty issues inherent to traditional oral delivery systems. Additionally, oral films can be favorable delivery systems for uncooperative users (e.g. children or psychiatric patients) as, once administered, are difficult to remove from the oral cavity (Nagaraju et al., 2013a).

Mechanical characteristics of oral films are of paramount importance for the overall quality and efficacy of the formulation and must be optimized before scale-up. The fact that oral films are intended to be handled and transported without great care (a factor that greatly contributes to enhanced practicality and, therefore, compliance to oral films as delivery systems) implies that formulations must be resistant to mechanical aggressions (Zhao, Quan & Fang, 2015). Moreover, if mechanical characteristics of oral films are inappropriate, issues as inaccurate dosage and handling problems may occur. Also, the production of complex and potentially expensive packaging systems may have to be done. Mechanical stability of oral films depends on the type and relative amount of polymer used in the formulation (Dixit & Puthli, 2009a).

Oral films are usually prepared using hydrophilic polymers, offering toughness and resistance but also rapidly dissolving in the oral cavity (Dixit & Puthli, 2009a; Nagaraju et al., 2013a). Also, physical and chemical characteristics of the polymers are central regarding incorporation efficacy of nutrients in films, and also to delivery profile (Castro, Fonte, Sousa, Madureira, Sarmento & Pintado, 2015b). Gelatine type A (GeltA) and carboxymethylcellulose (CMC) were the chosen polymers for being well-known hydrophilic film forming polymers and included in FDA inactive ingredient guide. Net charge of polymers was also taken into account due to the possible differences regarding delivery of carried nutrients (Adeleke et al., 2013). In acidic conditions, GeltA molecules

present positive charge and CMC presents negative charge (Rowe, Sheskey & Owen, 2006; Zhang, Zhang & Vardhanabhuti, 2014). Also, the fact that GeltA is a protein (whereas CMC is a polysaccharide) may help to understand the consequences of chemical nature in filmogenic capability, film properties and overall delivery profile of carried nutrients or nutraceuticals. Indeed, CMC is not digested by the gastrointestinal tract and is very poorly absorbed (Vaclavik & Christian, 2014). On the other hand, GeltA is highly degraded throughout the passage of gastrointestinal tract, especially in the stomach due to the extreme pH and enzymatic activity. Thus, oral films with CMC or GeltA backbone are expected to offer different release profiles of carried molecules.

Mechanical characteristics of oral films can also be tailored by including plasticizers in the formulation. Plasticizers must act in accordance with the polymer used, enhancing the strength of polymers and preventing brittleness (Castro, Fonte, Sousa, Madureira, Sarmento & Pintado, 2015b; Dixit & Puthli, 2009a). Hence, glycerol and sorbitol were used as plasticizers according to the reported compatibility and good plasticizing effect when used with GeltA or CMC (Dixit & Puthli, 2009a). Citric acid was used for being a potent saliva stimulating agent.

Therefore, in order to obtain oral films with optimal mechanical properties the present work included two experimental designs to evaluate the impact of four varying independent variables (polymer concentration, plasticizer concentration, and film thickness) on dependent variables (tensile strength, folding endurance, elongation at break, strain energy, strain at tensile strength, offset yield stress and disintegration time), to obtain and compare two optimal oral film formulations, regarding delivery potential of compounds with nutraceutical/nutritional value.

Caffeine anhydrous was used as model nutraceutical molecule as this methylxanthine is devoid of charge and is able to readily permeate intestinal mucosa, being suitable for oral films testing (Kamimori et al., 2002a). Also, several health claims have been proposed and scientifically recognized regarding the biological effects of caffeine on general population, especially regarding alertness and attention (Gaspar & Ramos, 2016).

Dissolution assay, simulation of gastrointestinal conditions, an *ex vivo* permeability assay in porcine intestine, water-uptake and erosion assays were performed to assess the potential of developed oral films as oral delivery systems for a wide array of nutrients and nutraceuticals. Moreover, Scanning Electron Microscopy (SEM) and Fourier-Infrared (FTIR) spectroscopy analysis were performed in order to obtain a thorough overview about morphological and physico-chemical properties of optimized formulations.

2.3. Materials ansd Methods

2.3.1. Materials

Caffeine anhydrous crystalline powder (food chemicals codex, 99% purity), carboxymethylcellulose sodium salt (medium viscosity), α-amylase, pepsin, bovine bile salts, pancreatin, gelatin type A (from porcine skin) and D-sorbitol (assay purity ≥98%) were purchased from Sigma-Aldrich (Steinheim, Germany). Citric acid monohydrate, potassium phosphate monobasic anhydrous and sodium phosphate dibasic were purchased from Merck (Darmstadt, Germany). Sodium chloride was purchased from Panreac (Barcelona, Spain). Glycerol (analytical reagent grade) and methanol (HPLC gradient grade) were purchased from Fisher (Loughborough, United Kingdom).

Deionized water was used to prepare all oral films formulations and ultrapure water was used to prepare caffeine standard solutions and eluents used in chromatography procedures. Porcine intestine was obtained from a local slaughterhouse.

2.3.2. Preparation of oral films

Oral films were prepared using the well-established solvent casting method (Dixit & Puthli, 2009a). Briefly, polymer, plasticizers and citric acid were weighted and transferred to a flask and deionized water was added as solvent. Caffeine anhydrous crystalline powder (Sigma) was dissolved in the film formulation. Film formulations were then covered, in order to avoid premature loss of solvent, maintained at constant homogenization (magnetic stirring, 300 rpm) and at room temperature for 120 min. Finally, homogeneous solutions were poured into a wooden mold (15 cm x 15 cm) with a plastic base. Solvent was casted at 37 ºC for 48 h. Formulations were peeled from the mold and divided into individual strips (1.5 cm x 7.5 cm) to perform mechanical tests.

Selected optimized formulations of oral films were prepared and finally cut in 3.5 x 3.5 cm portions to perform water-uptake, erosion, simulated gastrointestinal tract, dissolution assay and *ex vivo* permeability assay.

2.3.3. Experimental design

Design of experience was performed using SAS JMP® 9 software. Each design was performed considering seven dependent variables - folding endurance, tensile strength, strain at tensile strength, young's modulus, offset yield stress, strain energy and disintegration time - and for each polymer tested four independent variables were considered (polymer concentration, plasticizers type and concentration, and film

thickness) and one constant independent variable (citric acid). **Table 4** indicates the range of concentrations of the excipients (independent variables) tested in the experimental design.

Table 4: Experimental design pre-established characteristics

	Parameters					
	Level (code unit)	Polymer concentration (%, w/v)	Sorbitol concentration (%, w/w of dry polymer weight)	Glycerol concentration (%, w/w of dry polymer weight)	Citric acid concentration (%, w/v)	Caffeine concentration (mg/mL)
CMC	-1	1.6	12	0	4	13.5
	0	2.4	15	4	4	13.5
	1	3.2	20	8	4	13.5
GeltA	-1	8	12	0	4	13.5
	0	11.5	15	4	4	13.5
	1	15	20	8	4	13.5
	DPW – dry polymer weight; CMC – caroboxymethylcellulose; GeltA – gelatine type A					

Polymers were selected according to charge and chemical nature. Indeed, CMC presents net negative charge and GeltA presents net positive charge. Moreover, CMC is a polysaccharide whereas GeltA is a mixture of proteins and peptides. Concentrations of both GeltA and CMC were chosen according to previous studies, where GeltA and CMC were used as filmogenic polymers (Cheng, Abd Karim, Norziah & Seow, 2002; Coimbra, Gil & Figueiredo, 2014). Accordingly, 8% (w/v) of GeltA was set as minimum concentration tested in the design of experiment (Coimbra, Gil & Figueiredo, 2014). Also, CMC minimum concentration was initially set to 2.1% (w/v) (Cheng, Abd Karim,

Norziah & Seow, 2002). Nevertheless, since CMC can be used either as disintegrant or binding agent depending on the concentration, a preliminary experiment dictated that CMC minimum concentration for the experimental design could be lowered to 1.6% (w/v) without compromising the stability of the structure of the film (Dixit & Puthli, 2009a).

Since it is accepted that plasticizers act by interposing between the polymer molecules, sorbitol and glycerol concentrations were stipulated according to polymer dry weight (Dixit & Puthli, 2009a). Citric acid was used to induce the production of saliva in order to promote the disintegration of oral films in the oral cavity.

Every response test was performed in triplicate. When responses were determined, a screening design was executed, and the independent variables that influenced the behavior of evaluated dependent variables were selected for the elaboration of the predictive statistic model, according to RSquare and RSquare adjusted values. Finally, optimal formulations for each polymer were obtained by setting desirability values to each response type to obtain maximum desirability.

2.3.4. Texture analysis

Texture analysis was performed using a texturometer (TA.XT plus Texture Analyser, Stable Micro Systems, Cardiff, UK). Force calibration was performed with a weight of 5 Kg and height calibration was performed for Mini Tensile Grips (Stable Micro Systems). The evaluated parameters were young's modulus (Eq. (1)), offset yield stress, tensile strength, strain at tensile strength, and strain energy (Eq. (2)). Offset yield stress (MPa) corresponds to an arbitrary approximation of the elastic limit. Tensile strength

(MPa) stands for the maximum tensile stress that the test sample was capable of carrying. All measurements were performed in three films for each formulation.

$$Young's\ modulus\ (MPa) = \frac{Force\ at\ corresponding\ strain}{Cross\text{-}sectional\ area\ of\ the\ film \times Corresponding\ strain} \quad (1)$$

$$Strain\ Energy\ (MPa) = \frac{1}{2} \times \frac{Volume}{Young's\ modulus} \times Stress^2 \quad (2)$$

2.3.5. Thickness measurement

Thickness of the oral films was measured using a calibrated vernier gauge caliper micrometer. Thickness was measured in five points of each oral film and the average value was determined and accounted for mechanical tests (Kumar et al., 2014b).

2.3.6. Folding endurance

Oral films were repeatedly folded at the same point until break (Kumar et al., 2014b). The number of times the films were folded at the same point was accounted as folding endurance value. Five samples of each optimized oral film were tested.

2.3.7. ATR-FTIR analysis

FTIR analysis were conducted in a FTIR spectrometer, model ABB MB3000 (ABB, Switzerland), equipped with a deuterated triglycine sulphate detector and using a MIRacle^{TM} single reflection horizontal attenuated total reflectance (ATR) accessory (PIKE Technologies, USA) with a diamond/Se crystal plate. All spectra were acquired with 256 scans and 4 cm^{-1} resolution, in the region of 4000-500 cm^{-1}.

2.3.8. SEM analysis

Scanning electron microscopy film analyses were performed on a JEOL-5600 Lv Scanning Electron Microscope (Tokyo, Japan) equipped with SPRITE HR Four Axis Stage controller (Deben Research). Samples were placed on metallic stubs with carbon tape and coated with gold/palladium using a Sputter Coater (Polaron, Bad Schwalbach, Germany). Images were obtained using a spot size of 18-20 and a potential of 10-22 kV. All analyses were performed at room temperature (20 ºC).

2.3.9. Water-uptake, erosion and disintegration time

Water-uptake was determined by placing CMC and GeltA films in contact with 20 mL of artificial saliva, prepared as previously described. Weight changes were registered at 1, 2, 3, 4 and 5 min and water-uptake was calculated according to Eq. (3) (Tang, Guan, Yao & Zhu, 2014a). Afterwards, hydrated samples were introduced in an oven at 60 ºC for 24 h and weight variation of oral films were recorded in order to determine erosion. Erosion (%) was calculated according to Eq. (4).

$$Water - uptake\ (\%) = \frac{(Wt - W1)}{\mathrm{W}t} \times 100 \qquad (3)$$

$$Erosion\ (\%) = \frac{(W1 - W3)}{W1} \times 100 \qquad (4)$$

where, W1 is initial weight of tested oral films, Wt is the weight of the oral films after contact with artificial saliva at determined periods of time and W3 is the weight of dry oral films, after erosion.

Disintegration time of oral films was determined by dipping oral films into Petri dishes containing 20 mL of artificial saliva pre-heated to 37 ºC, until complete disintegration occurs.

2.3.10. Dissolution assay

Dissolution assay was performed according to a modification of the United States Pharmacopoeia (USP) dissolution assay (Adrover, Pedacchia, Petralito & Spera, 2015b). Briefly, 500 mL of artificial saliva were prepared using 8 g/L of NaCl, 0.19 g/L of KH_2PO_4 and 2.38 g/L of Na_2HPO_4 and adjusting pH to 6.8 with phosphoric acid. The basket of the apparatus (Erweka® DT 70) filled with artificial saliva was pre-heated to 37 ºC ± 1 ºC (Adrover, Pedacchia, Petralito & Spera, 2015b; Peh & Wong, 1999). Shafts were equipped with a small basket, where oral film samples rested during the assay and were programed to rotate at 100 rpm. Samples of 10 mL were taken at 1, 2, 3, 4, 5, 10, 15, 20, and 30 min and collected in 15 mL tubes. Withdrawn volume was replaced with artificial saliva. Three oral films of each polymer were tested for caffeine dissolution. Each sample was then filtered using sterile syringe filter units with a 0.22 μm cut-off (Merck, Germany) in order to retain polymers. Dosing was performed by HPLC-UV on a Waters Alliance® instrument (Milford, MA, USA). Water and methanol mixture (60:40) was used as mobile phase and isocratic flow was set to 1 mL/min (Carey & DePalma, 1994b). Samples were run through a Kromasil® C18 column, 5 μm (particle size) × 4.6 mm (internal diameter) × 250 mm (length) (AkzoNobel, Bohus, Sweden). UV detector wavelength was set to 270 nm. The injection volume was set to 50 μL.

2.3.11. Simulation of gastrointestinal conditions

Gastrointestinal tract conditions were simulated according to a modification of the method developed by Madureira et al. (Madureira, Amorim, Gomes, Pintado & Malcata, 2011a). Briefly, mouth digestion was mimicked by introducing caffeinated CMC and GeltA oral films and a solution of caffeine anhydrous (2 mg/mL) into 15 mL of a 1 mM $CaCl_2$ solution of 100 U mL^{-1} α-amylase (Sigma, Germany), under constant stirring (200 rpm) for 2 min, simulating masticatory movements (Gomes de Oliveira et al., 2014; Höld, de Boer, Zuidema & Maes, 1996). A 1 M $NaHCO_3$ solution was used to adjust pH of artificial saliva to 6.9.

Tested oral films were prepared by pouring 1 mL (corresponding to 13.5 mg of caffeine) of each solution into the molds with further solvent casting.

Esophagus-stomach step was performed by sequentially lowering the pH values from 6.9 to 2.0 at pre-defined times (Aura, 2005; Gomes de Oliveira et al., 2014; Madureira, Amorim, Gomes, Pintado & Malcata, 2011a). Finally, intestinal digestion and absorption, was simulated by adjusting pH values to 5 using a $NaHCO_3$ 1M solution, and adding a solution of bile salts (Sigma) and pancreatin (Sigma) to the digest (Laurent, Besancon & Caporiccio, 2007; Madureira, Amorim, Gomes, Pintado & Malcata, 2011a). Final volume of digestive solutions was of 16.19 mL.

Immediately after, 1 mL of the resulting solution was transferred to the donor chamber of a Franz's diffusion cell with a 9 mm orifice diameter, a donor chamber with 1 mL and a receiving chamber with 5 mL (PermeGear, PA, USA) (Provenza, Calpena, Mallandrich, Sánchez, Egea & Clares, 2014; Westerhout et al., 2014). The receiving chamber was previously filled with PBS (pH = 7.4) and temperature was equilibrated at 37 ± 2 ºC. Tissue samples of porcine intestinal mucosa were mounted between the donor

and receiving chamber. Agitation was set to 45 rpm, to simulate intestinal peristaltic movements. 600 μL samples were withdrawn at pre-defined times (5, 10, 15, 20, 30, 45, 60, 75, 90, 105 and 120 min) and volume was replaced with PBS to maintain sink conditions. A solution of caffeine anhydrous (2 mg/mL) was used as positive control and apparent permeability coefficient (P_{app}) was determined, in order to assess the validity of the permeability assay. The fractional amount of caffeine that permeated porcine intestinal mucosa tissues (dQ) was determined over the time intervals (dt) and the flux (*J*) was determined by calculating the slope of the resulting plots, according to Eq. (5) (di Cagno, Bibi & Bauer-Brandl, 2015).

$$J = \frac{dQ}{A \times dt} \qquad (5)$$

Apparent permeability (cm/s) was calculated for positive control, GeltA and CMC oral films by normalizing the flux (J) over the concentration of caffeine in the donor compartment (C_0) according to Eq. (6).

$$Papp = \frac{J}{Co} \qquad (6)$$

where, dQ/dt stands for the amount of permeated caffeine over time, A for the tissue surface area and Co for the initial concentration of permeated caffeine.

Porcine intestinal mucosa was obtained from a local slaughterhouse and transported into refrigerated containers. Tissue samples were harvested from the whole small intestine and basal lamina was surgically removed with a scalpel blade. Only tissue samples with thickness of 500 ± 50 μm were used on the performed assays (Amores, Lauroba, Calpena, Colom, Gimeno & Domenech, 2014). Intestinal epithelium was washed with PBS (pH = 7.4) before being frozen at -20 ºC. Tissue samples were thawed in PBS (pH = 7.4) pre-

heated at 37 ºC, before being mounted on Franz cells. Samples (600 μL) were withdrawn from the sampling port of the receptor chamber of Franz cells at 5, 10, 15, 20, 30, 45, 60, 75, 90, 105, and 120 min. Dosing was performed by HPLC-UV as described above.

2.3.12. Statistical analysis

Statistical analysis regarding dissolution profile data was performed using IBM® SPSS® Statistics version 22.

Average percentage of caffeine released from oral films was calculated for each time point, along with respective standard deviation values.

Shapiro-Wilk test was used to verify if water-uptake values are normally distributed (since n< 50). Independent-samples T test was used to verify the existence of statistically significant differences of water-uptake values between CMC and GeltA oral films.

Prediction formulas that describe statistically significant influence of independent variables on dependent variables were obtained using SAS JMP® software. From the analysis of R-Squared and adjusted R-Squared, best models were chosen and prediction formulas were obtained. From prediction formulas, predictive profilers were obtained and optimal formulations were determined for each formulation of oral films.

2.4. Results

2.4.1. Experimental design

An experimental design (custom design) was performed in order to obtain optimized formulations of GeltA and CMC oral films and to understand how excipients influence the mechanical characteristics of the films.

From the evaluated dependent variables, only tensile strength, young's modulus, offset yield stress and strain energy were significantly affected ($P < 0.05$) by independent variables. Prediction profilers used in the optimization of the formulations of CMC oral films and GeltA oral films are outlined in **Figure 3** and **Figure 4**, respectively.

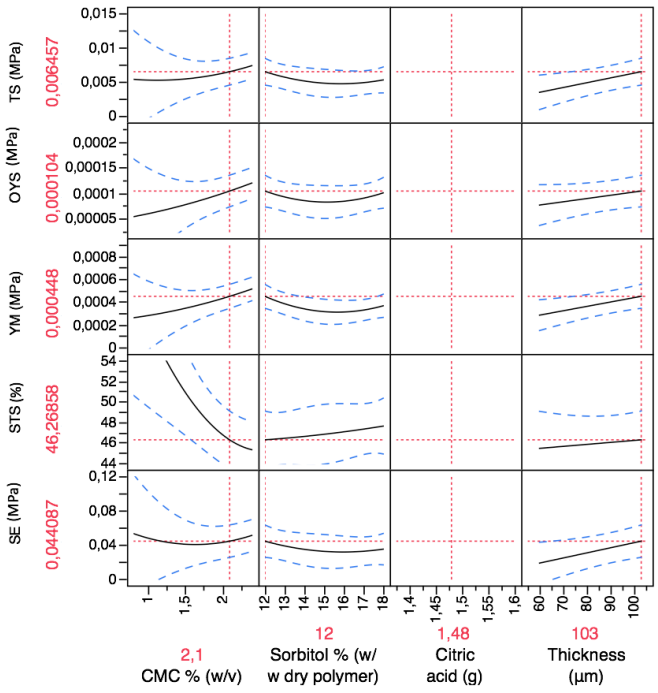

Figure 3: Prediction profiler for CMC oral films. Relative amount of excipients (x axis) and thickness are established according to the aimed mechanical characteristics (y axis). SE – Strain Energy; STS – Strain at tensile strength; YM – Young's modulus

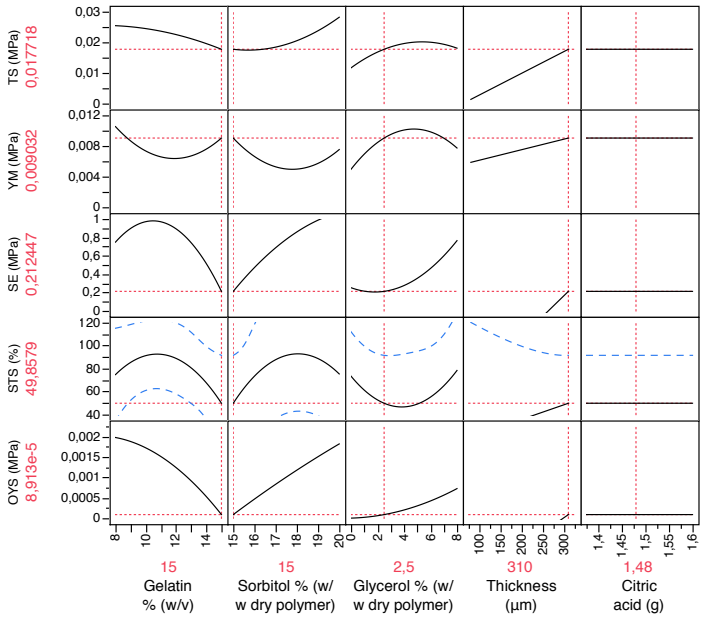

Figure 4: Prediction profiler for GeltA oral films. Relative amount of excipients (x axis) and thickness are established according to the aimed mechanical characteristics (y axis). OYS – Offset yield stress; STS – Strain at tensile strength; SE – Strain energy; YM – Young's modulus; TS – Tensile strength

Influence of independent variables on responses is described by the predictive formulas shown in **Table 5** and **Table 6**. Disintegration time and folding endurance (always folded above 300 times, without breaking) were not significantly affected by variation of independent variables, considering a confidence interval of 95%. Thus, disintegration time and folding endurance were not included in the statistical models.

Table 5: Explanatory prediction expressions of the variability of dependent variables with the variation of independent variables, for GeltA oral films

	GeltA oral films				
	Offset yield stress (MPa)	Strain energy	Young's modulus (MPa)	Strain at tensile strength	Tensile strength (MPa)
Predictive formula	0,00086437138474 -0,0001654112403 + [(Gelatin % (w/v)-11,5)/3,5] 0,00029521815123 + [(Sorbitol % (w/w dry polymer)-17,5)/2,5] 0,00027679637345 + [(Glycerol % (w/w dry polymer)-4)/4] [(Gelatin % (w/v)-11,5)/3,5] + [[(Gelatin % (w/v)-11,5)/3,5] * -0,0003460018808] [(Gelatin % (w/v)-11,5)/3,5] + [[(Sorbitol % (w/w dry polymer)-17,5)/2,5] * 0,000223113128 18] [(Sorbitol % (w/w dry polymer)-17,5)/2,5] + [[(Sorbitol % (w/w dry polymer)-17,5)/2,5] * 0,000320862965 99] [(Gelatin % (w/v)-11,5)/3,5] + [[(Glycerol % (w/w dry polymer)-4)/4] * 0,0000272668126 6] [(Sorbitol % (w/w dry polymer)-17,5)/2,5] + [[(Glycerol % (w/w dry polymer)-4)/4] * -0,0001286179 45] [(Glycerol % (w/w dry polymer)-4)/4] + [[(Glycerol % (w/w dry polymer)-4)/4] * -0,0002595988695]	0,69350513499805 0,03354904799928 + [(Gelatin % (w/v)-11,5)/3,5] 0,23299593850466 + [(Sorbitol % (w/w dry polymer)-17,5)/2,5] 0,09060676418109 + [(Glycerol % (w/w dry polymer)-4)/4] [(Gelatin % (w/v)-11,5)/3,5] + [[(Gelatin % (w/v)-11,5)/3,5] * -0,3887274441292] [(Gelatin % (w/v)-11,5)/3,5] + [[(Sorbitol % (w/w dry polymer)-17,5)/2,5] * 0,013274268517 44] [(Sorbitol % (w/w dry polymer)-17,5)/2,5] + [[(Sorbitol % (w/w dry polymer)-17,5)/2,5] * 0,197274439445 68] [(Gelatin % (w/v)-11,5)/3,5] + [[(Glycerol % (w/w dry polymer)-4)/4] * -0,0141712474078] [(Sorbitol % (w/w dry polymer)-17,5)/2,5] + [[(Glycerol % (w/w dry polymer)-4)/4] * -0,1745621693712] [(Glycerol % (w/w dry polymer)-4)/4] + [[(Glycerol % (w/w dry polymer)-4)/4] * -0,0841840325249]	0,00064687544536 0,00067756048271 + [(Gelatin % (w/v)-11,5)/3,5] -0,0019607804092 + [(Sorbitol % (w/w dry polymer)-17,5)/2,5] 0,00078079836486 + [(Glycerol % (w/w dry polymer)-4)/4] [(Gelatin % (w/v)-11,5)/3,5] + [[(Gelatin % (w/v)-11,5)/3,5] * 0,004044187703 12] [(Gelatin % (w/v)-11,5)/3,5] + [[(Sorbitol % (w/w dry polymer)-17,5)/2,5] * -0,0005637764036] [(Sorbitol % (w/w dry polymer)-17,5)/2,5] + [[(Sorbitol % (w/w dry polymer)-17,5)/2,5] * 0,002865437163 24] [(Gelatin % (w/v)-11,5)/3,5] + [[(Glycerol % (w/w dry polymer)-4)/4] * -0,0002221773362] [(Sorbitol % (w/w dry polymer)-17,5)/2,5] + [[(Glycerol % (w/w dry polymer)-4)/4] * -0,0005416651222] [(Glycerol % (w/w dry polymer)-4)/4] + [[(Glycerol % (w/w dry polymer)-4)/4] * -0,0040812695273]	98,6899445073335 -3,2986271902446 + [(Gelatin % (w/v)-11,5)/3,5] 7,04552782230278 + [(Sorbitol % (w/w dry polymer)-17,5)/2,5] -13,058463647952 + [(Glycerol % (w/w dry polymer)-4)/4] [(Gelatin % (w/v)-11,5)/3,5] + [[(Gelatin % (w/v)-11,5)/3,5] * -27,319126812302] [(Gelatin % (w/v)-11,5)/3,5] + [[(Sorbitol % (w/w dry polymer)-17,5)/2,5] * 1,268618675640 38] [(Sorbitol % (w/w dry polymer)-17,5)/2,5] + [[(Sorbitol % (w/w dry polymer)-17,5)/2,5] * -14,473758299634] [(Gelatin % (w/v)-11,5)/3,5] + [[(Glycerol % (w/w dry polymer)-4)/4] * 2,600321986548 79] [(Sorbitol % (w/w dry polymer)-17,5)/2,5] + [[(Glycerol % (w/w dry polymer)-4)/4] * -1,2460497889422] [(Glycerol % (w/w dry polymer)-4)/4] + [[(Glycerol % (w/w dry polymer)-4)/4] * 20,417234093593 4]	0,0101094453177 0,00175346322289 + [(Gelatin % (w/v)-11,5)/3,5] -0,0018407766677 + [(Sorbitol % (w/w dry polymer)-17,5)/2,5] 0,00037656739548 + [(Glycerol % (w/w dry polymer)-4)/4] [(Gelatin % (w/v)-11,5)/3,5] + [[(Gelatin % (w/v)-11,5)/3,5] * 0,005342285971 95] [(Gelatin % (w/v)-11,5)/3,5] + [[(Sorbitol % (w/w dry polymer)-17,5)/2,5] * 0,001224684777 56] [(Sorbitol % (w/w dry polymer)-17,5)/2,5] + [[(Sorbitol % (w/w dry polymer)-17,5)/2,5] * 0,007526319041 83] [(Gelatin % (w/v)-11,5)/3,5] + [[(Glycerol % (w/w dry polymer)-4)/4] * -0,0016586529187] [(Sorbitol % (w/w dry polymer)-17,5)/2,5] + [[(Glycerol % (w/w dry polymer)-4)/4] * 0,000262678867 52] [(Glycerol % (w/w dry polymer)-4)/4] + [[(Glycerol % (w/w dry polymer)-4)/4] * -0,0076849620875]
RSquare	0.446	0.719	0.824	0.842	0.618
RSquare adjusted	0.361	0.473	0.781	0.785	0.522

Table 6: Explanatory prediction expressions of the variability of dependent variables with the variation of independent variables, for GeltA oral films

	CMC oral films				
	Offset yield stress (MPa)	Strain energy	Young's modulus (MPa)	Strain at tensile strength	Tensile strength (MPa)
Predictive formula	-0,0304720447806 +0,09078528867307*[(CMC % (w/v)-1,6)/0,8] -0,000809519827 +*[(Sorbitol % (w/w dry polymer)-15)/3] -0,0017000710728 +*[(Glycerol % (w/w dry polymer)-4)/4] *[(CMC % (w/v)-1,6)/0,8] +*[[(CMC % (w/v)-1,6)/0,8]*-0,0064169287056] *[(CMC % (w/v)-1,6)/0,8] +*[[(Sorbitol % (w/w dry polymer)-15)/3] *0,00337728678337 *[(Sorbitol % (w/w dry polymer)-15)/3] +*[[(Sorbitol % (w/w dry polymer)-15)/3] *0,00508951040997 *[(CMC % (w/v)-1,6)/0,8] +*[[(Glycerol % (w/w dry polymer)-4)/4] *0,00732020615329 *[Sorbitol % (w/w dry polymer)-15)/3] +*[[(Glycerol % (w/w dry polymer)-4)/4] *0,00625918039281 *[(Glycerol % (w/w dry polymer)-4)/4] +*[[(Glycerol % (w/w dry polymer)-4)/4] *0,01075643411572	-1,5070208369031 +44,8201165219653*[(CMC % (w/v)-1,6)/0,8] -0,7322475214986 +*[(Sorbitol % (w/w dry polymer)-15)/3] -0,6668613821114 +*[(Glycerol % (w/w dry polymer)-4)/4] *[(CMC % (w/v)-1,6)/0,8] +*[[(CMC % (w/v)-1,6)/0,8]*-3,5055955657848] *[(CMC % (w/v)-1,6)/0,8] +*[[(Sorbitol % (w/w dry polymer)-15)/3] *2,35016323284509 *[(Sorbitol % (w/w dry polymer)-15)/3] +*[[(Sorbitol % (w/w dry polymer)-15)/3] *3,33453431740054 *[(CMC % (w/v)-1,6)/0,8] +*[[(Glycerol % (w/w dry polymer)-4)/4] *4,3324418636947 *[Sorbitol % (w/w dry polymer)-15)/3] +*[[(Glycerol % (w/w dry polymer)-4)/4] *3,22876670090378 *[(Glycerol % (w/w dry polymer)-4)/4] +*[[(Glycerol % (w/w dry polymer)-4)/4] *8,00423914096896	0,35798131458451 +-0,0239541663643*[(CMC % (w/v)-1,6)/0,8] -0,0083693074571 +*[(Sorbitol % (w/w dry polymer)-15)/3] 0,0049051611904 +*[(Glycerol % (w/w dry polymer)-4)/4] *[(CMC % (w/v)-1,6)/0,8] +*[[(CMC % (w/v)-1,6)/0,8]*-0,0070024207277] *[(CMC % (w/v)-1,6)/0,8] +*[[(Sorbitol % (w/w dry polymer)-15)/3] *0,0167246577158 *[(Sorbitol % (w/w dry polymer)-15)/3] +*[[(Sorbitol % (w/w dry polymer)-15)/3] *0,0198573367692 *[(CMC % (w/v)-1,6)/0,8] +*[[(Glycerol % (w/w dry polymer)-4)/4] *0,01659378212011 *[Sorbitol % (w/w dry polymer)-15)/3] +*[[(Glycerol % (w/w dry polymer)-4)/4] *0,00190897839613 *[(Glycerol % (w/w dry polymer)-4)/4] +*[[(Glycerol % (w/w dry polymer)-4)/4] *0,06666722831453	1409,37280955359 +1174,50892267056*[(CMC % (w/v)-1,6)/0,8] 8026,06913003458 +*[(Sorbitol % (w/w dry polymer)-15)/3] 3297,86520472513 +*[(Glycerol % (w/w dry polymer)-4)/4] *[(CMC % (w/v)-1,6)/0,8] +*[[(CMC % (w/v)-1,6)/0,8]*-621,25294548332] *[(CMC % (w/v)-1,6)/0,8] +*[[(Sorbitol % (w/w dry polymer)-15)/3] *94,5136275804003 *[(Sorbitol % (w/w dry polymer)-15)/3] +*[[(Sorbitol % (w/w dry polymer)-15)/3] *158,444591439569 *[(CMC % (w/v)-1,6)/0,8] +*[[(Glycerol % (w/w dry polymer)-4)/4] *653,555032807399 *[Sorbitol % (w/w dry polymer)-15)/3] +*[[(Glycerol % (w/w dry polymer)-4)/4] *938,745898942532 *[(Glycerol % (w/w dry polymer)-4)/4] +*[[(Glycerol % (w/w dry polymer)-4)/4] *928,124630424003	1,37906844548521 +4,16433902139976*[(CMC % (w/v)-1,6)/0,8] -0,1052894552237 +*[(Sorbitol % (w/w dry polymer)-15)/3] -0,0426191551922 +*[(Glycerol % (w/w dry polymer)-4)/4] *[(CMC % (w/v)-1,6)/0,8] +*[[(CMC % (w/v)-1,6)/0,8]*-0,3634662169602] *[(CMC % (w/v)-1,6)/0,8] +*[[(Sorbitol % (w/w dry polymer)-15)/3] *0,29482443267849 *[(Sorbitol % (w/w dry polymer)-15)/3] +*[[(Sorbitol % (w/w dry polymer)-15)/3] *0,40184555121271 *[(CMC % (w/v)-1,6)/0,8] +*[[(Glycerol % (w/w dry polymer)-4)/4] *0,48295680492981 *[Sorbitol % (w/w dry polymer)-15)/3] +*[[(Glycerol % (w/w dry polymer)-4)/4] *0,31545688610954 *[(Glycerol % (w/w dry polymer)-4)/4] +*[[(Glycerol % (w/w dry polymer)-4)/4] *1,04539209033
RSquare	0.913	0.800	0.886	0.691	0.855
RSquare adjusted	0.892	0.770	0.868	0.644	0.832

By setting desirability of dependent variables to maximum, it was possible to obtain the best possible formulations for both polymers. Thus, CMC oral film optimized formulation was set as 2.1 % (w/v) of polymer, 4.1 % (w/v) of citric acid, 12.0 % (w/w of dry polymer) of sorbitol and an ideal thickness of 103 μm. GeltA oral film optimized formulation was set as 15 % (w/v) of polymer, 4.3 % (w/v) of citric acid, 2.5 % (w/w of dry polymer) of glycerol, 15 % (w/w of dry polymer) of sorbitol and an ideal thickness of 310 μm.

2.4.2. FTIR analysis

FTIR analysis was performed in order to identify potential physicochemical interactions (with formation of new covalent bonds) between caffeine and oral films.

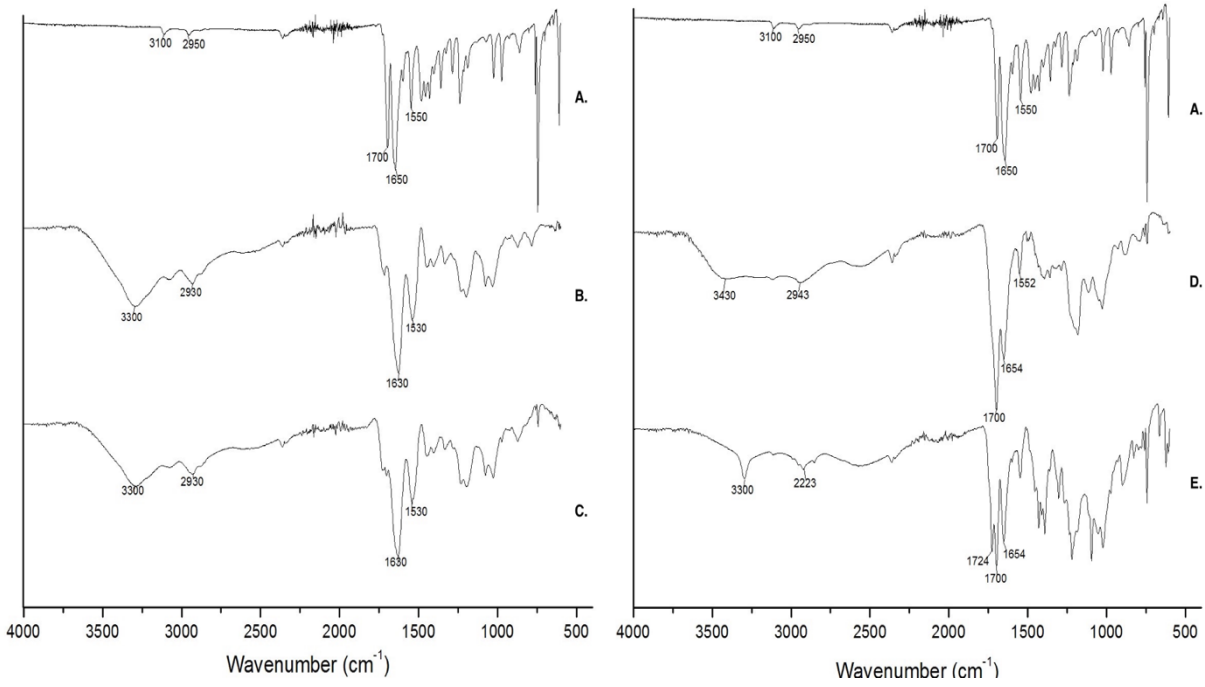

Figure 5: FTIR spectra of caffeine anhydrous (A), placebo GeltA oral films (B), caffeinated GeltA oral films (C), placebo CMC oral films (D) and caffeinated CMC oral films (E)

Figure 5 shows the resulting spectra for placebo oral films, oral films with caffeine and for pure caffeine anhydrous powder. Double-bond region was thoroughly analyzed, since caffeine characteristic peaks are typically found in the 1700-1500 cm^{-1} range (Molinari & Lata, 1962b; Nafisi, Monajemi & Ebrahimi, 2004; Singh, Wechter, Hu & Lafontaine, 1998).

Caffeine spectrum reveals two peaks (3100 cm^{-1} and 2950 cm^{-1}) assigned to the stretching of N-H bonds. Caffeine infrared spectrum presented other characteristic bands in the 1700-1650 cm^{-1} and 1666-1550 cm^{-1} ranges (Molinari & Lata, 1962b; Nafisi, Monajemi & Ebrahimi, 2004; Singh, Wechter, Hu & Lafontaine, 1998). Typical caffeine bands that appear around 1700 cm^{-1} are representative of the stretch of C=O bond (amide III) and can be a good indicative of caffeine presence and structure maintenance when incorporated into oral films (Garrigues, Bouhsain, Garrigues & de la Guardia, 2000). Moreover, the bands showed in the range of 1666-1550 cm^{-1} were assigned to the stretches of C=C bonds (Lázaro Martínez, Leal Denis, Campo Dall'Orto & Buldain, 2008b; Molinari & Lata, 1962b).

GeltA oral films (placebo and with caffeine) spectra are overlapping. Spectra of both caffeinated and placebo GeltA oral films presented a wide bands around 3300 cm^{-1} that is representative of amide A (Vidal, 2014). Also, both spectra showed a broad band at 2930 cm^{-1} that is assigned to the stretch of C-H bonds. Both caffeinated and placebo GeltA oral films exhibited strong bands around 1630 cm^{-1} and 1530 cm^{-1} that may be assigned to stretch of C=C and N-H bonds of secondary amides of gelatin, respectively (Sionkowska, Wisniewski, Skopinska, Kennedy & Wess, 2004; Staroszczyk, Sztuka, Wolska, Wojtasz-Pająk & Kołodziejska, 2014).Carboxymethylcellullose placebo oral films spectra revealed a broad peak at 3430 cm^{-1} that is assigned to O-H stretching.

Other broad peak at 2943 cm^{-1} was assigned to C-H stretch vibration. Moreover, placebo CMC oral films spectra revealed a band at 1700 cm^{-1} and 1654 cm^{-1} that was assigned to C=O stretching in CMC and citric acid molecules (Biswas, Kim, Selling & Cheng, 2014). Weak peak at 1552 cm^{-1} was revealed, that may be assigned with C-O-H bending. Indeed, hydroxyl functional groups are present in sorbitol that was used in CMC oral films formulation. Strong peaks within the fingerprint region (e.g. 1182 cm^{-1} and 1027 cm^{-1}) may be assigned to C-O bond, present in CMC molecules. A small, sharp peak at 3300 cm^{-1} appeared in caffeinated CMC oral films spectra and is assigned to N-H bonds (secondary amines) present in caffeine molecules. Also, besides from the peaks at 1700 cm^{-1} and 1654 cm^{-1} assigned to C=O stretching that also appeared in placebo CMC oral film spectrum, a new band at 1724 cm^{-1} appeared and is assigned to C=O bond of the imidazole ring of the caffeine molecule.

2.4.3. Morphology analysis

Morphology analysis of oral films was performed by SEM. Both placebo and caffeinated oral films were analyzed and resulting images are presented in **Figure 6.**

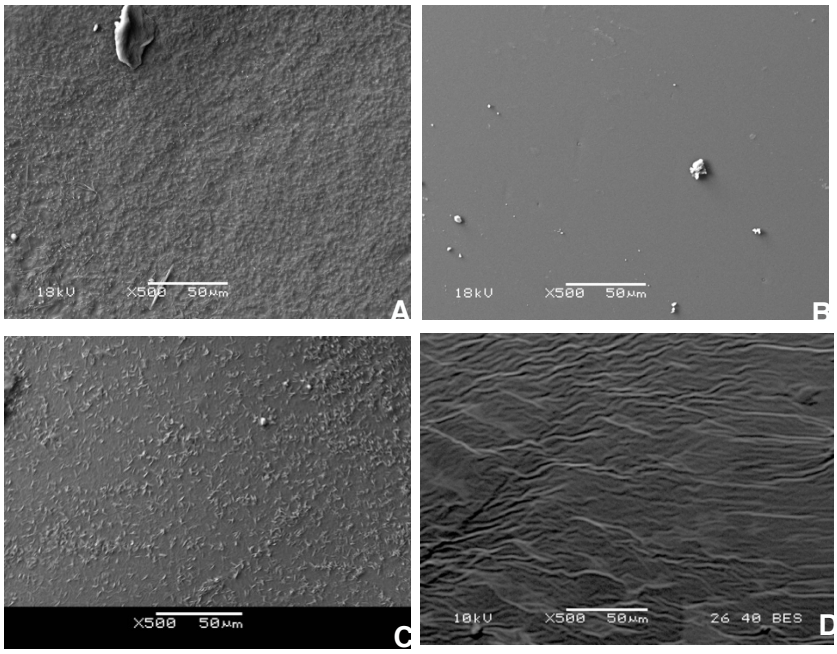

Figure 6: Micrographs of oral films formulations, produced with gelatin type A and CMC, with caffeine (A and C, respectively) and placebo (B and D,

Surface of placebo CMC and GeltA oral films (**Figure 6B. and 6D.**) showed to be smooth, not presenting any trace of crystalline structures. Oppositely, caffeinated oral films (**Figure 6A. and 6C.**) presented a rugged surface, covered by homogeneously dispersed marks of crystalline structures, probably due to caffeine.

Caffeine crystals distribution through oral films was homogeneous for both formulations and caffeine crystals were dispersed (and not dissolved), being perfectly individualized from the matrix. Thus, caffeine delivery was not restricted, which was confirmed by FTIR analysis and dissolution assay.

2.4.4. Water-uptake, erosion and disintegration time

Water-uptake (%) capacity of GeltA and CMC was significantly different as indicated in **Figure 7**. Indeed, even though CMC oral films incorporated more water in the first 3 min, GeltA oral films absorbed significantly more water after 5 min ($P < 0.05$). The superior water-uptake of GeltA was also translated into faster disintegration, in comparison with CMC disintegration time. Erosion revealed to be more pronounced for CMC oral films (67.50 ± 1.09 %) than for GeltA oral films (15.54 ± 12.02 %).

It was also observed that GeltA oral films completely disintegrated after 5 min in artificial saliva at 37 ºC. On the other hand, CMC oral films did not disintegrate completely in contact with artificial saliva solution at 37 ºC for 30 min.

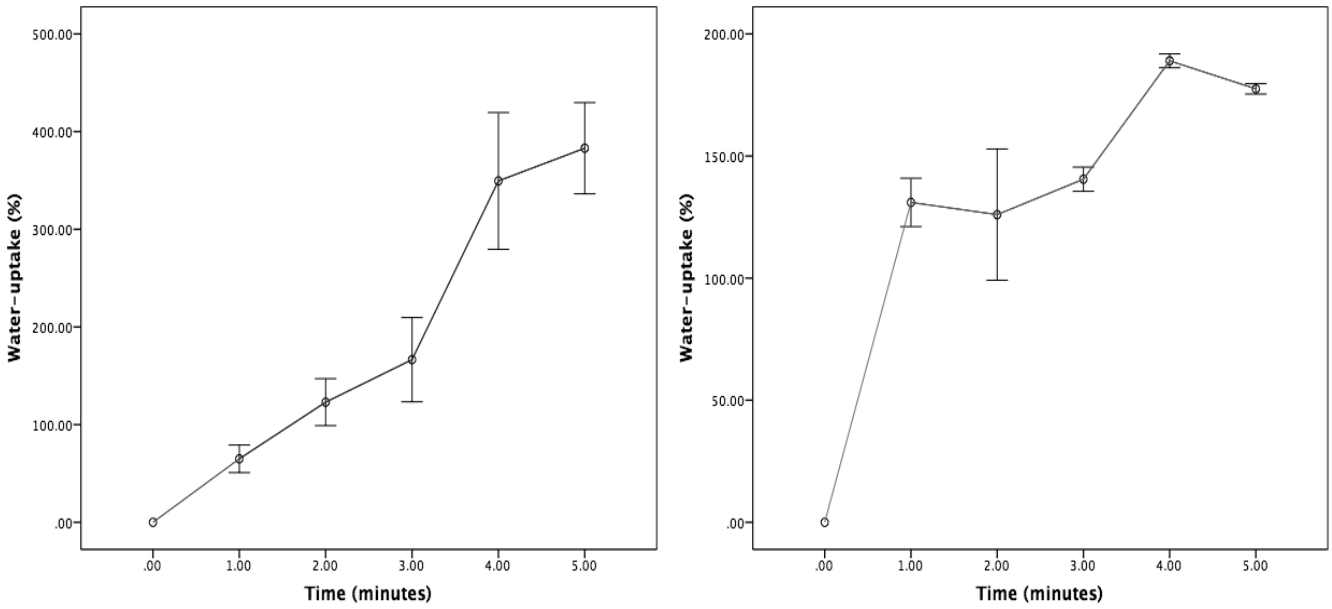

Figure 7: Water-uptake profile of GeltA (A) and CMC (B) oral films throughout time. Results are presented as mean ± SD

2.4.5. Dissolution assay

In vitro dissolution assay was carried according to a modification of the basket method (USP 1) dissolution method (Adrover, Pedacchia, Petralito & Spera, 2015b). As the matter of fact, to our knowledge, literature still does not offer a standardized dissolution study for oral films. Therefore, dissolution assays approved for other solid oral delivery systems are used to test oral films.

Dissolution assay analysis provided a preliminary approach for *in vivo* caffeine delivery from CMC and GeltA oral films, as illustrated in **Figure 8**. Indeed, dissolution assay revealed that CMC and GeltA oral films presented very distinct release profile of caffeine.

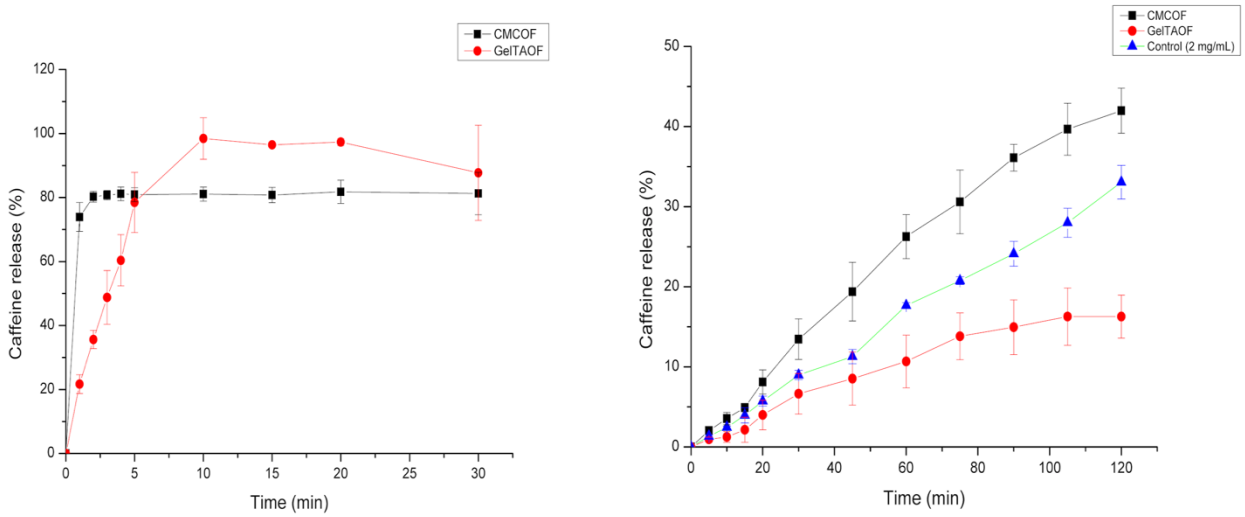

Figure 8: Dissolution and permeation profiles of caffeine delivered from CMC (A and C respectively) and GeltA (B and D respectively). A solution of caffeine anhydrous (E) was used as positive control to assess viability of the *ex vivo* permeability assay

Indeed, CMC oral films allowed a burst release of caffeine (73.9 ± 4.5 %) after 1 minute. Moreover, after the first minute, caffeine release reached a plateau. Gelatine type A oral films, in turn, assured a more delayed release of caffeine (21.7 ± 2.9 %, after 1 min). Moreover, CMC oral films showed to reach a plateau stage after 2 min of dissolution, but caffeine was not totally released after 30 min. On the other hand, GeltA oral films resulted in controlled release of caffeine along 30 min, reaching a plateau state only after 10 min, but with a complete release of caffeine.

Oppositely to CMC films, it was possible to observe that GeltA films were completely disintegrated after 3 min. Disintegration of small fragments, resulting from GeltA oral film disintegration was also observed. Moreover, GeltA oral films presented higher variability of caffeine release throughout time when compared with CMC oral films, as demonstrated by higher standard deviation values for most time points.

2.4.6. Simulation of gastrointestinal tract and ex vivo permeability assay

Gastrointestinal tract simulation with *ex vivo* permeability assay (**Figure 8**) was performed to attain a reasonable approach to *in vivo* fate of oral films along with delivery profile and permeability of caffeine across the intestine. It was possible to observe that, as verified for the dissolution assay, CMC and GeltA oral films offer distinct delivery profile of caffeine. Indeed, *ex vivo* permeability assay helped confirming that CMC oral films offer a burst release of caffeine leading, in turn, to a higher P_{app} when compared to GeltA oral films or to positive control (**Figure 9**).

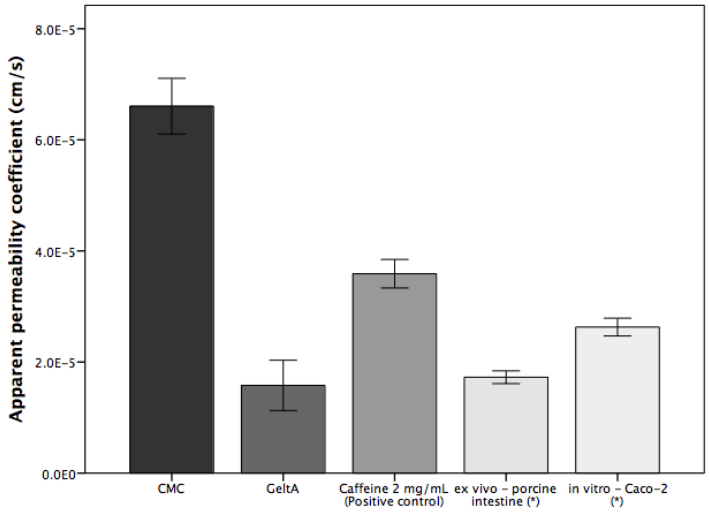

Figure 9: Comparison between permeability coefficients of caffeine delivered from CMC and GeltA oral films, positive control and *ex vivo* (porcine intestinal mucosa) and *in vitro* (Caco-2 cells) permeability coefficients
(*) Values reported by Westerhout et al.

In turn, GeltA oral films offer a more controlled release of caffeine comparing to CMC oral films and positive control. But, since caffeine is slowly released from GeltA oral films, permeability across intestinal mucosa occurs in a lesser extent. Positive control attested the robustness of the developed simulated gastrointestinal system and *ex vivo* permeability assay.

Differences between values obtained for positive control and values reported in the literature were expected, due to high variability inherent to *ex vivo* assays (Castro, Madureira, Sarmento & Pintado, 2016). Moreover, values reported in the literature for caffeine P_{app} determined both *in vivo* and *ex vivo* were not preceded by the simulated gastrointestinal tract. Indeed, bile salts used in the digestion simulation are well-known permeability enhancers regarding transcellular permeation (mechanism of caffeine permeation through intestinal mucosa) (Castro, Fonte, Sousa, Madureira, Sarmento & Pintado, 2015b; Westerhout et al., 2014).

2.5. Discussion

Experimental design allowed to obtain the optimal formulations, regarding mechanical properties of oral films, based on two different polymers used. Effectively, it has been reported that mechanical characteristics do influence release of carried molecules (Boateng, Stevens, Eccleston, Auffret, Humphrey & Matthews, 2009). Indeed, formulation with high values of tensile strength (i.e. with high toughness) is important to avoid damage (and, therefore, premature release of carried molecule) during production, packaging, transporting or even after intake. Also, formulations with higher Young's modulus are reported to offer a sharp burst release of carried molecules.

As optimization of the formulations of oral films was based on mechanical properties that overall express rigidity and elasticity, it is possible to observe that GeltA oral films presented higher toughness (higher offset yield stress, tensile strength and strain energy) and less elasticity (higher young's modulus and lower strain at tensile strength values) when compared with CMC oral films. Thus, release profiles were expected to be

different from those observed. Indeed, dissolution assay analysis allowed to conclude that GeltA is more suitable for oral films intended for controlled release of active substances, due to slower release of caffeine and possibility to achieve delayed release along 30 min. Actually, GeltA has been described as a versatile polymer for the attachment of bioactive molecules due to the great availability of functional groups (Elzoghby, 2013). Also, simulated digestion and *ex vivo* permeability assay also revealed that a slower caffeine release is associated with less permeation through the intestinal mucosa, possibly compromising bioavailability. On the other hand, CMC appears to be a better polymer to integrate immediate release oral films, as demonstrated by the dissolution assay results. Moreover, simulated gastrointestinal tract and *ex vivo* permeability assay allowed to conclude that faster release rate of caffeine also translates into more caffeine effectively permeating the intestinal mucosa. Indeed, CMC polymer seemed to enhance bioavailability of caffeine, in comparison with GeltA oral films or positive control. Nevertheless, disintegration time was excessively high for CMC oral films, which might contribute to discomfort after administration. Caffeine release profile of both oral film formulations might be partially related with disintegration profile. Gelatine Type A oral films disintegrated completely after 5 min resting in a Petri dish with artificial saliva. GeltA oral films disintegrated into smaller fragments soon after contacting with simulated saliva but both dissolution and *ex vivo* permeability assays led to the conclusion that caffeine seemed to be hindered from being released. Results suggest that caffeine remains entrapped into the fragments and does not contact with the intestinal mucosa. Oppositely, CMC oral films did disintegrate into smaller fragments but did not completely dissolve even after 30 min and, thus, caffeine was not totally delivered after 30 min of dissolution assay. Moreover, water-uptake was considerably higher for GeltA oral films than for

CMC oral films. The fact that erosion was higher for CMC oral films may be due to dissolution of some components from the formulation, but polymeric backbone integrity was maintained thus explaining the faster caffeine release in comparison with GeltA oral films. Carboxymethylcellullose oral films could benefit from the inclusion of a disintegrant (or super-disintegrant) in the formulation.

Also, the fact that CMC and GeltA present extremely distinct physico-chemical and also mechanical characteristics could also be implied in the differences in the release profile of caffeine. Effectively, since CMC and GeltA present different filmogenic potential, relative amounts of each polymer were used to produce oral films and this fact can also be of great importance regarding different release profiles from both formulations. Since optimized formulation of GeltA oral films required a substantially higher relative amount of polymer when compared with optimized formulation of CMC oral films, caffeine is much more likely to be hindered in the GeltA matrix, resulting in a delay of delivery.

Moreover, GeltA is a mixture of proteins and peptides, it would be expected that conformational changes occurred when contacting with extreme pH and enzymatic action (e.g. pepsin, pancreatin proteases) in the gastrointestinal tract (Sahoo, Sahoo, Biswas, Guha & Kuotsu, 2015). Conformational changes (for instance, aggregation of proteins and peptides) can also lead to the capture of caffeine, hindering the contact with intestinal mucosa and, therefore, absorption.

A visual explanation of caffeine release profile from CMC and GeltA is outlined in **Figure 10.**

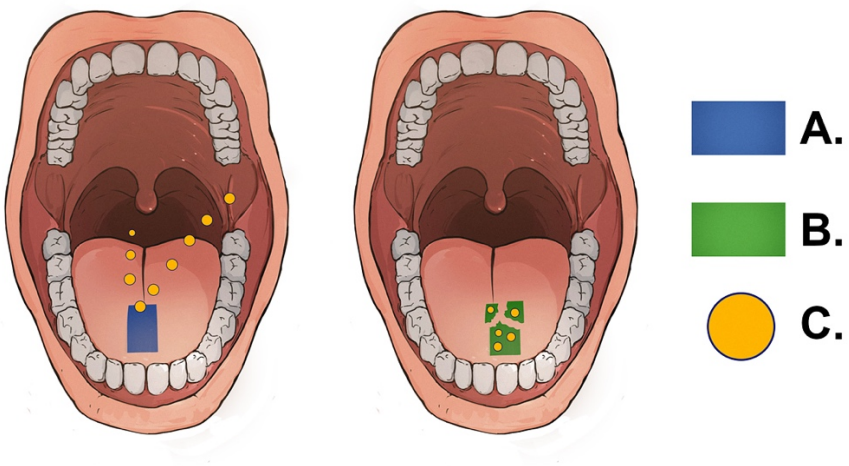

Figure 10: Scheme representing distinct release profiles of caffeine (C) from CMC (A) and GeltA (B) oral films. CMC oral films provide burst release of caffeine, even though disintegration is slow. In contrast, GeltA oral films hindered caffeine delivery, providing slower release but with faster disintegration of the polymeric matrix

FTIR analysis did not indicate the formation of new covalent bonds between oral films and caffeine that could potentially modify caffeine release profile. Thus, caffeine release hindering was potentially due to physical entrapment in the oral films matrix. Scanning electron microscopy images also suggested that caffeine was dispersed but not dissolved in the matrix of oral films, since individualized caffeine crystals could be easily observed, when compared with placebo oral films.

2.6. Conclusions

Two oral films formulations were successfully optimized based on an experimental design, using CMC and GeltA polymers as polymeric matrix, assuring mechanical quality-by-design of developed formulations. FTIR analysis allowed to understand that caffeine structure was not changed during the preparation of oral films.

Developed oral films offered distinct delivery and permeation profiles. Observed differences were related with distinct disintegration times, differences in chemical nature of polymeric backbone (and, therefore, distinct behavior when in contact with gastrointestinal tract conditions).

Besides from oral delivery systems, oral films can potentially be interesting buccal delivery systems. Further research shall be performed to assess the extent of permeation of bioactive molecules across buccal mucosa when carried by CMC and GeltA oral films, using appropriate *in vitro* models to assess human buccal epithelial permeability.

Nutraceuticals and nutrients with well-known roles on prevention and depletion of diseases are gaining relevance regarding life quality and overall human enhancement. Oral films can represent a new paradigm on innovative delivery systems for molecules with nutraceutical or nutritional importance.

Acknowledgments

The authors acknowledge the support granted by national funds from FCT through project PTDC/BBB-NAN/3249/2014 and from the project UID/Multi/50016/2013. The authors also acknowledge the support granted by the funds through the project NORTE-07-0162-FEDER-00010.

Pedro Fonte thanks Fundação para a Ciência e a Tecnologia (FCT), Portugal, for his PhD grant (SFRH/BD/78127/2011).

Chapter III: Incorporation of beads into oral films for buccal and oral delivery of bioactive molecules

*Pedro M. Castro [1,2], Flávia Sousa 2,3,4,5, Rui Magalhães1, Victor Manuel Pizones Ruiz-Henestrosa 6,7, Ana M. R. Pilosof 6,7, Ana Raquel Madureira1, Bruno Sarmento2,4,5, Manuela E. Pintado1**

1CBQF – Centro de Biotecnologia e Química Fina – Laboratório Associado, Escola Superior de Biotecnologia, Universidade Católica Portuguesa/Porto, Rua Arquiteto Lobão Vital, 172, 4200-374 Porto, Portugal

2CESPU, Instituto de Investigação e Formação Avançada em Ciências e Tecnologias da Saúde, Rua Central de Gandra 1317, 4585-116 Gandra-PRD, Portugal

3ICBAS - Instituto Ciências Biomédicas Abel Salazar, Universidade do Porto, 4150-180 Porto, Portugals

4 i3S - Instituto de Investigação e Inovação em Saúde, Universidade do Porto, Rua Alfredo Allen 208, 4200-393 Porto, Portugal

5 INEB - Instituto Nacional de Engenharia Biomédica, Universidade do Porto, Rua Alfredo Allen 208, 4200-393 Porto, Portugal

6 Departamento de Industrias, Facultad de Ciencias Exactas y Naturales, Universidad de Buenos Aires, Ciudad Universitaria, 1428, Buenos Aires, Argentina

7 Consejo Nacional de Investigaciones Científicas y Tecnicas (CONICET), Argentina

3.1. Abstract

The association of alginate beads and guar gum films in a single delivery system was idealized to promote a more effective buccal and oral delivery of bioactive molecules.

A response surface method (experimental design approach) was performed to obtain optimal formulations of alginate beads to be incorporated into guar gum oral films as combined buccal and oral delivery systems for caffeine delivery. The combined formulation was further characterized regarding physicochemical properties, drug release, effect on cell viability and buccal permeability. Beads average size, determined by dynamic light scattering (DLS), was of 3.37 ± 6.36 μm. Film thickness was set to 62 μm. Scanning electron microscopy micrographs revealed that beads were evenly distributed onto the film matrix and beads size was in accordance to data obtained from DLS analysis. Evaluation of Fourier-transform infrared spectra did not indicate the formation of new covalent bonds between the matrix of guar gum films, alginate beads and caffeine. The association of alginate beads to guar gum films improved overall adhesion to cow tongue as indicated by the increased work of adhesion and debonding distance (0.195 ± 0.060 N.sec and 1.773 ± 0.444 mm, respectively) when compared with guar gum films alone (0.118 ± 0.062 N.sec and 1.608 ± 0.679 mm, respectively). *In vitro* release assays by dialysis membrane allowed to understand that the combination of guar gum films and alginate beads assure a slower release of caffeine when compared with the delivery profile of free caffeine from alginate beads or guar gum films alone. MTT assay, performed on human buccal carcinoma TR146 cell line and Caco-2/HT29-MTX co-culture, allowed concluding that neither guar gum film, alginate beads nor alginate beads incorporated into guar gum film significantly compromised cell viability after 12 h of exposure. As demonstrated by *in vitro* permeability assay using TR146 human buccal carcinoma cell lines, combination of guar gum films and alginate beads also promoted a slower release and, thus, lower apparent permeability (1.15E-05 ± 3.50E-06) than for caffeine solution (2.68E-05 ± 7.30E-06), guar gum film (3.12E-05 ± 4.70E-06) or alginate

beads (2.01E-05 ± 3.90E-06). Moreover, GfB also presented a slower permeability than remaining formulations, across both porcine intestinal mucosa and Caco-2/HT29-MTX cell layer. Nonetheless, the amount of caffeine that was found to be absorbed/adsorbed to the buccal and intestinal cell layers and also to intestinal mucosa was superior when compared with remaining formulations, indicating that GfB promoted an intimate contact between caffeine and the epithelia offering a gradual release and permeability of caffeine along time. The conjugation of alginate beads with an orodispersible film matrix represents an effective oral/buccal delivery system that induces a controlled release along with an increased permeation of carried drugs in the buccal mucosa.

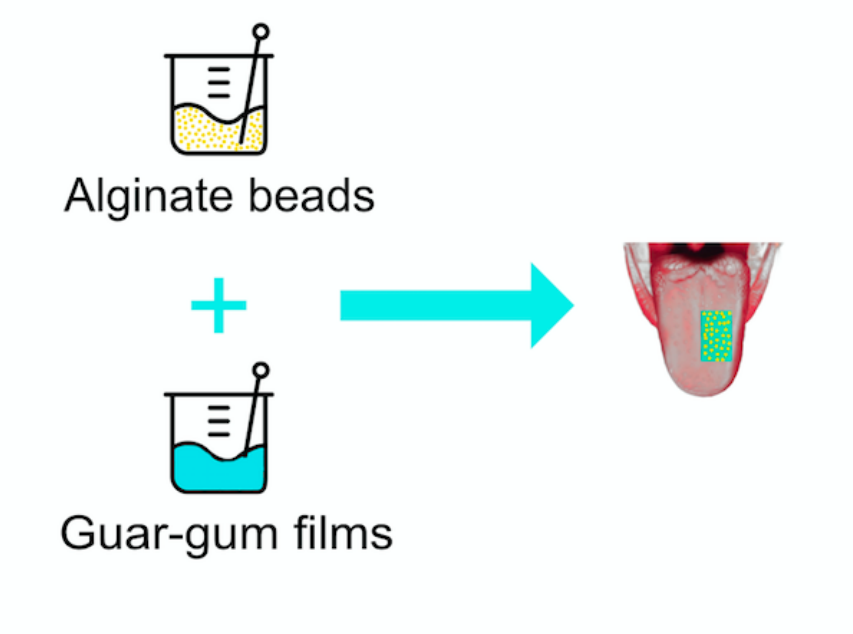

3.2. Introduction

Buccal route is an attractive delivery route especially due to ease of administration and possibility to avoid first-pass metabolism (Castro, Madureira, Sarmento & Pintado, 2016). Transport of drugs across buccal mucosa occurs exclusively by passive diffusion, an undifferentiated, unselective, transport mechanism (Rathbone, Pather & Şenel, 2015).

Lipophilic bioactive molecules may permeate buccal mucosa by transcellular route whereas hydrophilic bioactive molecules are more prone to permeate buccal epithelia by intercellular route. Moreover, buccal epithelium presents a molecular weight cut-off that ranges from 500-1000 Da (Castro, Fonte, Sousa, Madureira, Sarmento & Pintado, 2015c). Hence, molecules with superior molecular weights may be hindered from transposing buccal epithelia and reach systemic circulation. Furthermore, saliva turnover limits the residence time of drugs within buccal mucosa, sometimes leading to premature swallowing (Castro, Madureira, Sarmento & Pintado, 2016).

Aiming to develop more effective buccal delivery systems, alginate beads containing caffeine as model drug were introduced within an orodispersible film matrix. Orodispersible films, or simply oral films are mucoadhesive oral delivery systems that disintegrate in the mouth in less than 30 s (Castro, Fonte, Sousa, Madureira, Sarmento & Pintado, 2015c). Besides from the inherent advantages shared with tablets or capsules (e.g. ease of administration and portability) administration of oral films does not require water. Moreover, oral films are especially useful for uncooperative patients since, once introduced into the mouth, they are very difficult to remove. Also, variables such as colour and taste are easily manipulated according to the preferences of the consumer/patient. Oral films are convenient delivery systems when buccal release is aimed (Khan, Trivedi & Boateng, 2016).

Alginate is a natural anionic copolymer of 1,4-linked-β-D-mannuronic acid and α-L-guluronic acid that is highly biocompatible and can be used to produce beads for buccal delivery of bioactive molecules (Martins, Sarmento, Souto & Ferreira, 2007). Alginate beads can represent suitable delivery systems for the buccal mucosa, featuring mucoadhesion and sustained delivery of carried molecules. Production of alginate beads

is cheap and does not imply using organic solvents, therefore being predictably safe for human consumption. For the entrapment of hydrophilic molecules, emulsification-internal gelation technique to produce alginate beads was used to provide high association efficiency for caffeine.

Alginate beads/microparticles have been used as delivery systems for buccal delivery of drugs but, to our knowledge, were not intended for buccal absorption, only aiming local activity (Cavallari, Brigidi & Fini, 2015; Goncalves et al., 2016; Martin, Calpena, Fernandez, Mallandrich, Galvez & Clares, 2015). Furthermore, alginate has been used for the production of buccal delivery systems (e.g. tablets) but not in the format of beads (Ravi Kumar Reddy, Indira Muzib & Chowdary, 2013). Moreover, incorporation of alginate beads on film matrices represents an unconventional, conceptually new oral/buccal delivery system that conjugates the practicality and user-friendly characteristics of oral films and the slower release of carried bioactive molecules provided by alginate beads.

An experimental design based on response-surface method allows obtaining optimized formulations, assuring quality-by-design, thus avoiding excessive expending of time and resources and allowing to obtain robust and optimal results. In this study, both alginate beads and guar gum films formulations were optimized using an experimental design approach and optimal formulations were prepared, based on characteristics (factors and responses) that are well-known for conditioning overall quality and performance of beads and oral films. Therefore, chosen variables for the optimization of guar gum films were the relative amounts of guar gum (matrix-forming polymer), sorbitol (plasticizer and sweetener) and citric acid (saliva-stimulating agent). Distance at burst and film burst strength were chosen as mechanical responses, being

directly correlated with elasticity and rigidity, respectively. Film erosion (%) and the ratio of water-uptake over time (mg s^{-1}) were set as representative responses of the capacity of the oral films to absorb water and disintegrate, releasing the content (Tang, Guan, Yao & Zhu, 2014b). Film thickness was not controllable at the moment of the production of guar gum films but is known as being an important factor for the variation of mechanical characteristics. Therefore, thickness was considered as a factor (independent variable) even though thickness values were not circumscribed to a pre-defined range at the moment of the experimental design (Dixit & Puthli, 2009b). Concerning the optimization of alginate beads, association efficiency (%), particle size (μm), corresponding polydispersity index and zeta-potential (mV) were set as responses for the variation of alginate and Tween® 80 concentrations.

Authors attempted to gather the controlled release and mucoadhesion offered by alginate beads with the convenience and mucoadhesion of guar gum orodispersible films to obtain a buccal and oral delivery system that enhances buccal absorption and promotes an increased bioavailability of carried bioactive molecule, when compared with alginate beads or orodispersible films alone.

3.3. Materials and Methods

3.3.1. Materials

Caffeine anhydrous (food chemicals codex, 99% purity), alginic acid (sodium salt from brown algae, molecular weight ranging from 80,000 to 120,000, 61% of mannuronic acid and 39% of guluronic acid, as stated by supplier in safety and documentation section), guar gum and D-sorbitol (assay purity ≥98%) were purchased from Sigma-

Aldrich (Steinheim, Germany). Citric acid monohydrate, calcium carbonate, potassium phosphate monobasic anhydrous, sodium phosphate dibasic were purchased from Merck (Darmstadt, Germany). Sodium chloride was purchased from Panreac (Barcelona, Spain). Methanol (HPLC gradient grade) was purchased from Fisher (Loughborough, United Kingdom). Deionized water was used to prepare all oral films formulations and ultrapure water was used to prepare caffeine standard solutions and eluents used in chromatography procedures. TR146, Caco-2 and HT29-MTX cell lines were purchased from Sigma-Aldrich (Stenheim, Germany). Transwell® flasks (12 well) and inserts (collagen-coated, 1.12 cm^2 of culture area, 0.4 μm pore size and 12 mm membrane diameter) were purchased from Corning (New York, USA). 96-well plates were purchased from Thermo Scientific (Denmark). Fetal Bovine Serum (FBS), DMEM and HAMS-F12 culture media and Pen-Strep (10 000 U Penicillin, 10 000 U Streptomycin) were purchased from Lonza® (Verviers, Belgium). TrypLE™ express was purchased from Gibco® (Denmark). Thiazolyl Blue Tetrazolium Bromide (MTT) Ultra Pure was purchased from VWR (Solon, USA). Dimethyl sulfoxide (DMSO) 99.7% was purchased from Fisher Bioreagents™ (EUA). For cell wash, pH of PBS was adjusted to 6.8, using a solution of hydrochloric acid 0.1 M.

3.3.2. Experimental design

Experimental design was performed recurring to SAS JMP® 9 software. Response surface method for the optimization of film formulation was defined using the amounts of guar gum (polymer), sorbitol (plasticizer and sweetener) and citric acid (saliva production inducer) as factors (independent variables). Erosion, water-uptake/time ratio, distance at burst and film burst strength were set as responses (dependent variables).

Alginate beads formulation was optimized by setting the relative amounts of sodium alginate and Tween® 80 as factors and association efficiency, ζετα-potential, mean size and polydispersity index were set as responses.

3.3.3. Production and characterization of oral films

Preparation of oral films was performed using solvent casting technique (Dixit & Puthli, 2009b). Briefly, guar gum, citric acid and sorbitol were dissolved into 100 mL of ultra-pure water. Thereafter, resulting solution was spread onto a glass cast heated to 50 ºC for 1 h. Resulting film was then maintained at room temperature for 12 h. Finally, individual films (2 cm x 3 cm) were cut from the glass cast for further testing. Oral films were collected directly from the glass cast and packaged into thermo-sealed polyethylene sheets.

3.3.4. Texture analysis

Texture analysis was performed on a texturometer equipment (TA.XT plus Texture Analyser, Stable Micro Systems, Cardiff, UK). Force calibration for a 5 kg load cell was performed using a 2 kg weight and height calibration was performed for the film support rig and corresponding probe. Film burst strength (g) and distance at burst (mm) were considered as measures of rigidity and elasticity, respectively.

Mucoadhesion assessment was performed to characterize the contact between the developed formulations and the top of the tongue. Briefly, the formulations were adhered to a testing probe (squared shape, 6.25 cm^2) and a cow tongue (obtained fresh from a local slaughterhouse) was mounted on the texturometer support platform. Following, 3.5 mL of artificial saliva (pre-heated to 37 ºC) were poured dropwise on the top of the tongue.

The probe was set to descend until contact between the formulation and the tongue occurred. Contact force was set to 5 g and contact time was set to 30 s. Thereafter, the probe ascended at a speed rate of 0.1 mm/s and debonding force was registered, allowing to determine adhesiveness (N), work of adhesion (N.s) and debonding distance (mm).

3.3.5. Thickness measurement

Thickness of the oral films was measured using a calibrated vernier gauge caliper micrometer. Thickness was measured in five points of each oral film and the average value was determined (Kumar et al., 2014a).

3.3.6. Water-uptake, erosion and disintegration time

Water-uptake (WU) was determined by placing guar gum films in contact with 1 mL of artificial saliva. Weight changes were registered at 30, 60, 90, and 120 s and WU was calculated according to Eq. (3) (Tang, Guan, Yao & Zhu, 2014b). Afterwards, hydrated samples were introduced in an oven at 60 ºC for 24 h and weight variation of oral films was recorded in order to determine erosion. Erosion (%) represents the amount of film that was lost during the contact with artificial saliva and was calculated according to Eq. (4).

$$Water-uptake\ (\%) = \frac{(Wt - W1)}{Wt} \times 100 \qquad (3)$$

$$Erosion\ (\%) = \frac{(W1-W3)}{W1} \times 100 \qquad (4)$$

where, W1 is initial weight of tested oral films, Wt is the weight of the oral films after contact with artificial saliva at determined periods of time and W3 is the weight of dry oral films, after erosion.

Since, according to United States Food and Drug Administration (FDA), oral films, as orodispersible delivery systems, must disintegrate within 30 s in the oral cavity, the water-uptake/time ratio was determined as an indicator of disintegration speed (Administration, 2008). Water-uptake/time ratio was calculated according to Eq. (3.1).

$$Water - uptake/time = \frac{Water-uptake}{t(\max water-uptake)} \qquad (3.1)$$

where, water-uptake (%) is an indicator of water taken up by the oral film (Eq. 3) and t(max water-uptake) is the time (s) at which water-uptake (%) value was maximum.

3.3.7. Production and characterization of alginate beads

3.3.7.1. Production of alginate beads

Alginate beads were prepared by emulsification/internal gelation (Song, Yu, Gao, Liu & Ma, 2013). Briefly, calcium carbonate and caffeine were dissolved into an alginate solution. In a separate beaker, Tween® 80 was dispersed into 10 mL of liquid paraffin. Both dispersions were stirred for 30 min and then the alginate solution was added drop wise to the paraffin dispersion and the resulting emulsion was kept stirring (600 rpm) for 30 min. Then, glacial acetic acid was added drop wise to the emulsion to liberate calcium ions for gelation. Resulting emulsion was kept stirring (900 rpm) for 1 h. Resulting

emulsion was centrifuged (6,000 rpm, 15 ºC) and the pellet was recovered and washed with PBS. Washing procedure was performed three times for each formulation of beads.

3.3.7.2. Characterization of alginate beads

Caffeine association efficiency (AE), mean size, zeta-potential, scanning electron microscopy (SEM) and delivery profile were the parameters used to characterize alginate beads.

3.3.7.3. Particle size and zeta-potential analysis determination

All alginate bead formulations were diluted (1:100) with ultrapure water before particle size and zeta-potential analysis. Particle size and polydispersity index were determined by dynamic light scattering (DLS). Zeta-potential was determined by phase analysis light scattering. All measurements were performed in triplicate in a Zetasizer Nano ZSP equipment (Malvern Instruments Ltd, Worcestershire, UK).

3.3.7.4. Caffeine association efficiency (AE)

Caffeine association efficiency was determined by dosing (HPLC-UV) the free caffeine content of the supernatant of each bead formulation after being centrifuged (6,000 rpm, 30 min, 16 ºC). Caffeine concentration in the supernatant was determined by HPLC-UV on a Waters Alliance® instrument (Milford, MA, USA). Water and methanol mixture (60:40) was used as mobile phase, column temperature was defined as 35 ºC and isocratic flow was set to 1 mL/min (Carey & DePalma, 1994a). Samples were run through a Kromasil® C18 column, 5 μm (particle size) × 4.6 mm (internal diameter) × 250 mm (length) (AkzoNobel, Bohus, Sweden). UV detector wavelength was set to 270 nm. The

injection volume was set to 50 µl. Finally, caffeine association efficiency was calculated according to the following Eq. (7):

$$\frac{Wtc - Wsc}{Wtc} \times 100 \qquad (7)$$

where, Wtc stands for total weight of caffeine used in the alginate bead formulations and Wsc stands for caffeine collected from the supernatant after centrifugation.

3.3.8. Surface tension analysis

A pendant drop tensiometer (PAT-1, SINTERFACE Technologies, Berlin, Germany) was used to measure dynamic surface tension of developed formulations at the air/water interface. A drop of the delivery systems dissolved in artificial saliva solution is formed at the tip of a capillary (constant volume: 12 µl), which is into a cuvette with water saturated atmosphere to avoid droplet evaporation, covered by a compartment, which is maintained at constant temperature (20 ± 0.2 ºC) by circulating water from a thermostat. It was allowed to stand for 30 min to reach constant temperature and humidity in the compartment. Then, the silhouette of this drop is cast onto a CCD camera and digitized. The digital images of the drop are recorded over time and fit to the Young-Laplace equation to accurately (± 0.1 mN/m) determine surface tension using drop profile analysis tensiometry. All experiments were performed at 20 ºC and at least two measurements have been done for each system. The computer controlled dosing system allows to control a constant volume of the drop during the measurement and also to induce area deformations (Ruiz-Henestrosa, Martinez, Sánchez, Patino & Pilosof, 2014). All the

glass materials were properly cleaned using a mixture of ammonium persulfate and sulphuric acid and further rinsed with ultrapure water to eliminate all the possible surface active contaminants that could interfere in the measurements.

3.3.9. Molecular Interactions analysis

ATR-FTIR analysis was performed for guar gum films and alginate beads (placebo and with caffeine) to assess eventual chemical interactions with caffeine. Analysis was conducted in a FTIR spectrometer, model ABB MB3000 (ABB, Switzerland), equipped with a deuterated triglycine sulphate detector and using a MIRacle^{TM} single reflection horizontal attenuated total reflectance (ATR) accessory (PIKE Technologies, USA) with a diamond/Se crystal plate. Obtained spectra were baseline corrected using a 3-4 point adjustment. Area of obtained spectra was normalized to a 0-1 range. Spectra treatment was performed using the OriginPro® (version 9.0) software. Spectra of caffeinated guar gum films, alginate beads, association of guar gum films with alginate beads (GfB) and physical mixture of GfB formulation were subtracted from spectra of placebo guar gum films, alginate beads and GfB, respectively (Soares et al., 2013). Resulting spectra were compared with the spectra of pure caffeine anhydrous powder.

3.3.10. Morphological analysis

Morphological analysis was performed on a JEOL-5600 Lv Scanning Electron Microscope (Tokyo, Japan) equipped with SPRITE HR Four Axis Stagecontroller (Deben Research). Samples were placed on metallic stubs with carbon tape and coated with gold/palladium using a Sputter Coater (Polaron, Bad Schwalbach, Germany). Images

were obtained for guar gum films, alginate beads and GfB. using a spot size of 18-20 and a potential of 15-22 kV. All analyses were performed at room temperature (20 ºC).

3.3.11. Tongue adhesion

Adhesion to tongue assessment was performed for FNp and guar gum films on a texturometer (TA.XT plus Texture Analyser, Stable Micro Systems, United Kingdom). Mounted load cell presented a 5 kg capacity and force was calibrated with a 2 kg weight. Briefly, the formulations were adhered to the testing probe (squared shape, 6.25 cm^2) and a cow tongue (obtained fresh from a local slaughterhouse) was mounted on the texturometer support platform. Following, 3.5 mL of artificial saliva (pre-heated to 37 ºC) were poured dropwise on the top of the tongue. The probe was set to descend until contact between the formulation and the tongue occurred. Contact force was set to 5 g and contact time was set to 30 s. Thereafter, the probe ascended at a speed rate of 0.1 mm/s and debonding force was registered, allowing to determine adhesiveness (N), work of adhesion (N.s) and debonding distance (mm).

3.3.12. Caffeine release profile

In vitro release assays were performed in order to assess and compare release profiles of guar gum films, alginate beads and GfB. Briefly, *in vitro* dialysis delivery assay was performed according to Wang, Liu, Sun, Wang, Wang and Zhu (2014). Briefly, the formulations (alginate beads, guar gum films and GfB) and a caffeine control solution (2 mg/mL) were introduced into a 500 Da dialysis membrane. Dialysis membrane with a pore size of 500 Da was chosen to mimic the pore size of buccal mucosa (Castro, Fonte, Sousa, Madureira, Sarmento & Pintado, 2015c). Immediately, the dialysis membrane was

filled with the formulations and 35 mL of artificial saliva (pH = 6.8), clumped and dipped into 50 mL of phosphate buffered saline - PBS - solution (release media) pre-heated to 37 ºC. The system was kept on continuous shaking (100 rpm). Aliquots of 5 mL were withdrawn from release media at 15, 30, 60, 120, 180, 240, 300, 360, 420, 480, 540, 600, 660 and 720 min. Withdrawn volume was immediately replaced with 5 mL of PBS and pre-heated to 37 ºC to preserve sink conditions.

3.3.13. Simulation of gastrointestinal tract and *ex vivo* caffeine permeability across porcine intestinal tissue

Gastrointestinal tract conditions were simulated according to a modification of the method developed by Madureira et al. (Madureira, Amorim, Gomes, Pintado & Malcata, 2011a). Briefly, mouth digestion was mimicked by introducing caffeine-loaded GfB, guar gum films, alginate beads and a solution of caffeine anhydrous (16.7 mg/mL) into 15 mL of a 1 mM $CaCl_2$ solution of 100 U mL^{-1} α-amylase (Sigma, Germany), under constant stirring (200 rpm) for 2 min, simulating masticatory movements (Gomes de Oliveira et al., 2014; Höld, de Boer, Zuidema & Maes, 1996). A 1 M $NaHCO_3$ solution was used to adjust pH of artificial saliva to 6.9.

Tested oral films were prepared by pouring 1 mL (corresponding to 16.7 mg of caffeine) of each solution into the molds with further solvent casting.

Esophagus-stomach step was performed by sequentially lowering the pH values from 6.9 to 2.0 at pre-defined times (Aura, 2005; Gomes de Oliveira et al., 2014; Madureira, Amorim, Gomes, Pintado & Malcata, 2011a). Finally, intestinal digestion and absorption, was simulated by adjusting pH values to 5 using a $NaHCO_3$ 1M solution, and adding a solution of bile salts (Sigma) and pancreatin (Sigma) to the digest (Laurent,

Besancon & Caporiccio, 2007; Madureira, Amorim, Gomes, Pintado & Malcata, 2011a). Final volume of digestive solutions was of 16.19 mL.

Immediately after, 1 mL of the resulting solution was transferred to the donor chamber of a Franz's diffusion cell with a 9 mm orifice diameter, a donor chamber with 1 mL and a receiving chamber with 5 mL (PermeGear, PA, USA) (Provenza, Calpena, Mallandrich, Sánchez, Egea & Clares, 2014; Westerhout et al., 2014). The receiving chamber was previously filled with PBS (pH = 7.4) and temperature was equilibrated at 37 ± 2 ºC. Tissue samples of porcine intestinal mucosa were mounted between the donor and receiving chamber. Agitation was set to 45 rpm, to simulate intestinal peristaltic movements. 600 µL samples were withdrawn at pre-defined times (5, 10, 15, 20, 30, 45, 60, 75, 90, 105 and 120 min) and volume was replaced with PBS to maintain sink conditions. A solution of caffeine anhydrous (16.7 mg/mL) was used as positive control.

3.3.14. *In vitro* buccal and intestinal cell models

3.3.14.1. Human buccal epithelium cell line

Cell viability after contact with produced formulations and transepithelial permeability assay were performed using TR146 human buccal epithelium cell line. TR146 cell line was chosen due to great resemblance of normal human buccal mucosa namely regarding undifferentiated, non-keratinized stratified epithelium, morphological and functional characteristics as activity of carboxypeptidase, esterase and aminopeptidase (Morck Nielsen & Romer Rassing, 2000). Also, expression of K4, K10, K13, K16 and K19 keratins, membrane-associated receptors for involucrin and epidermal growth factors also reflect other common characteristics to normal human buccal epithelium cells (Jacobsen et al., 1999; Jacobsen, van Deurs, Pedersen & Rassing, 1995).

TR146 cell line was purchased from Sigma-Aldrich (USA) and passage 9 was used. The culture medium consisted of HAMS F-12 medium enriched with 2 mM Glutamine (Lonza), 10% (v/v) fetal bovine serum (FBS) and 1% (v/v) of penicillin-streptomycin antibiotic blend. TR146 cells were seeded and maintained in 75 cm^2 T-flasks (T-75) and incubated in a 5% CO_2, 95% air and 98% relative humidity atmosphere. The culture medium was replaced every two days. When 70-80% of cell confluence was reached, cells were detached from T-75 flasks using 2 mL of TrypLE™ Express. Detached cells were then prepared and seeded either in other T-75 flasks, 96-well culture plates (Nunc®) or in Transwell® inserts 12-well culture plates purchased from Corning® (Germany).

3.3.14.2. Co-culture of Caco-2/HT29-MTX intestinal cells

Caco-2 (Caucasian colon adenocarcinoma) cell line is widely used for the study of intestinal permeation of bioactive molecules (Araujo & Sarmento, 2013). Nevertheless, Caco-2 monoculture was not significantly representative of duodenum epithelia due to the formation of tight junctions that typically occur in the colon but not in the small intestine, leading to a hindrance of the absorption of hydrophilic molecules. Also, Caco-2 monoculture is exclusively composed of enterocytes and overexpress efflux transporters, typical of an excretory rather than absorptive epithelia. Therefore, HT29-MTX (Caucasian colon adenocarcinoma grade II) cell line is used in co-culture with Caco-2 cells. HT29-MTX were chosen due to mucus producing ability, as occurs in the duodenum mucosa.

Thus Caco-2/HT29-MTX co-culture was used to better mimic the *in vivo* conditions that occur in the duodenum. HT29-MTX and Caco-2 cell lines were grown separately in Dulbecco's Modified Eagle Medium (DMEM) supplemented with 10% (v/v) fetal bovine

serum, 1% (v/v) L-glutamine, 1% (v/v) penicillin and streptomycin and 1% (v/v) of non-essential aminoacids, at 37 ºC under a 5% CO_2 water-saturated atmosphere. Upon 70-80% confluence, cells were detached as described before. Co-culture seeding in Transwells® was performed in a 9:1 ratio of Caco-2 (3 x 10^5 cells/well) and HT29 (3 x 10^5 cells/well) cells, respectively (Antunes, Andrade, Araujo, Ferreira & Sarmento, 2013).

3.3.14.3. Cell mitochondrial activity assessment

Cell-viability studies were carried out on proliferating cells, chosen when cells were 70-80% confluent in T-75 flasks and properly detached as described above. After detachment, cells were re-suspended in medium and seeded in 96-well plates at density of 1 x 10^4 cells/mL, 200 μL per well. The same cell concentration was adopted in the 12-well plates but using 500 μL of cell suspension, after *in vitro* permeability assay, to assess the cell viability after being in contact with developed formulations. Cell-viability studies were performed after 24 h of culture, with previous supervision by light microscopy of the morphology and confluence of the cells in the plate wells. MTT assay allows to assess mitochondrial viability and, therefore, cell viability after 12 h contact with prepared drug delivery systems (da Silva, Ferreira, Pintado & Sarmento, 2016b). If cells were viable, succinic dehydrogenase was able to transform the tetrazolium salt into insoluble, purple-coloured, crystals of formazan (Mosmann, 1983b). Medium with 1% (V/V) Triton X-100 solution was added as lysis buffer and served as positive control. Negative control consisted of cells in contact with medium only. After treatment with produced drug delivery formulations, 100 μL of the MTT reagent (0.5 mg/mL prepared in culture medium) was added to each well and the plates were incubated for 4 h at 37 ºC and in a

5% CO_2 atmosphere. After incubation time has passed, reagent was carefully removed, allowing the insoluble formazan crystals to remain in the bottom of the wells. 100 μL of DMSO per well was used to solubilize the formazan crystals in a dark room and, after 15 min of agitation on an orbital shaker, the absorbance at 570 nm and 630 nm was read on a FLUOstar OPTIMA microplate reader (United Kingdom), in triplicate. Absorbance values for all readings at 630 nm were subtracted from the absorbance values read at 570 nm. Cell viability (%, n = 5 different, independent wells for the same experiment) was calculated according to Eq. (8):

$$Cell\ viability\ (\%) = \frac{Experimental\ value - negative\ control}{Positive\ control - negative\ control} \times 100 \qquad (8)$$

Concentration of the formulations tested for potential commitment of TR146 and Caco-2/HT29-MTX cell viability were chosen according to the average amount of saliva produced in the human mouth when in contact with food products (Watanabe & Dawes, 1988a).

3.3.14.4. Drug transepithelial diffusion study

Permeability assay was assessed in Corning® Transwell® inserts, using 12-well plates. TR146 buccal cells and Caco-2/HT29-MTX cell co-culture were seeded onto the inserts to mimic stratified epithelium of human buccal mucosa and intestinal epithelia, respectively, as reported previously (Jacobsen, van Deurs, Pedersen & Rassing, 1995; Silva, Almeida, Prezotti, Cury, Campana-Filho & Sarmento, 2017; Zeng et al., 2015a). Briefly, TR146 cell line was used due to the reported similarities between keratinization

profile and metabolic activity with physiologic human buccal mucosa cells and Caco-2/HT29-MTX co-culture was used to mimic the duodenum absorptive epithelia. TR146 cells and Caco-2/HT29-MTX cell co-culture were seeded on the inserts. The medium was changed every two days, during 21 days for buccal cells and 28 days for Caco-2/HT29-MTX cell co-culture. For medium replacement, medium was removed from the wells and 0.5 and 1.5 mL of fresh culture medium was added to the apical and basolateral sides, respectively. On the day of the study, culture medium was totally removed. Medium in the basolateral side (receptor part) was replaced with 1.5 mL of PBS, pH 6.8. Medium in the apical side (donor part) was replaced with fresh medium and drug delivery formulations were introduced afterwards. Guar gum films, alginate beads, GfB and free caffeine were tested for permeability (n = 5). Samples of 600 μL were withdrawn from receptor part at 0, 15, 30, 60, 120, 180, 240, 300, 360, 420, 480, 540, 600, 660 and 720 min. Withdrawn volume was immediately replaced with fresh PBS, pre-heated to 37 ºC, to maintain sink conditions. The amount of permeated caffeine was quantified by HPLC-UV, as described previously.

The amount of caffeine that permeated Transwell® inserts with the stratified epithelium formed by confluent TR146 or Caco-2/HT29-MTX cells (dQ) was determined over the time intervals (dt) and the flux (J) was determined by calculating the slope of the resulting plots, according to Eq. (6) (di Cagno, Bibi & Bauer-Brandl, 2015).

Apparent permeability ($cm.s^{-1}$) was calculated for free caffeine, guar gum films, alginate beads and GfB, by normalizing the flux (J) – calculated according to Eq. (5) - over the concentration of caffeine in the donor compartment (C_0), according to Eq. (6).

$$J = \frac{dQ}{A \times dt} \qquad (5)$$

$$Papp = \frac{J}{C0} \qquad (6)$$

where, dQ/dt stands for the amount of permeated caffeine over time, A for the tissue surface area and C_0 for the initial concentration of caffeine. All tested formulations presented the same initial concentration of caffeine (2 mg/mL) at the beginning of the drug trans-epithelial study.

Caffeine remaining entrapped by the TR146 cell layer and caco-2/HT29-MTX co-culture was obtained by disruption of the monolayer with 1 mL of DMSO. Resulting solution was centrifuged (14,000 rpm, 15 min, 4 ºC) and caffeine concentration in the supernatant was determined by HPLC-UV.

At the end of the drug trans-epithelial diffusion study, MTT mitochondrial viability assay was performed in order to verify the viability of the cell layers (De Caro, Giandalia, Siragusa, Paderni, Campisi & Giannola, 2008). Inserts incubated with culture medium only, during the caffeine trans-epithelial study (n = 5) were considered as positive control (i.e. total cell viability). Inserts incubated with Triton-X lysis solution (n = 3) were considered as negative control (i.e. reference for total cell death). MTT assay was performed as previously described.

3.3.15. Statistical analysis

Statistical analysis regarding dissolution profile data was performed using IBM® SPSS® Statistics version 22.

Shapiro-Wilk (n< 50) test was used to verify if the values obtained for the responses in the experimental design were normally distributed. One sample T test was used to

verify the existence of statistically significant differences between predictive models and experimental values. Experimental values were obtained from three samples selected from three new batches, for both alginate beads and guar gum films. Mean values for each batch were compared with the values predicted in the model.

3.4. Results and discussion

An experimental design was performed to optimize two formulations as delivery systems that can be used alone or combined for an enhanced buccal delivery of bioactive molecules. A physico-chemical characterization (analysis of molecular interactions and morphological analysis), a release assay, TR146 cells and caco-2/HT29-MTX viability tests and permeability assays were performed for developed formulations.

3.4.1. Optimization of the formulation of guar gum oral films and validation of results

Factorial design (response surface method) performed for optimization of the guar gum films is briefly described in **Table 7**.

Table 7: Factorial design parameters established for the optimization of the formulation of guar gum oral films

Factorial design parameters (guar gum films)				
Level (code unit)	Guar gum concentration (%, w/v)	Sorbitol concentration (%, w/v)	Citric acid concentration (%, w/v)	Caffeine concentration (mg/mL)
-1	2.5	3.75	0.75	16.7
0	3.75	5.69	1.0	16.7
1	5.0	7.50	1.25	16.7

Prediction profiler (**Figure 11**) obtained from the experimental design allowed elaborating an optimized guar gum films formulation with desired values of erosion (%), distance at burst (mm), film burst (g) and water-uptake/time (%, w/w.s^{-1}) ratio.

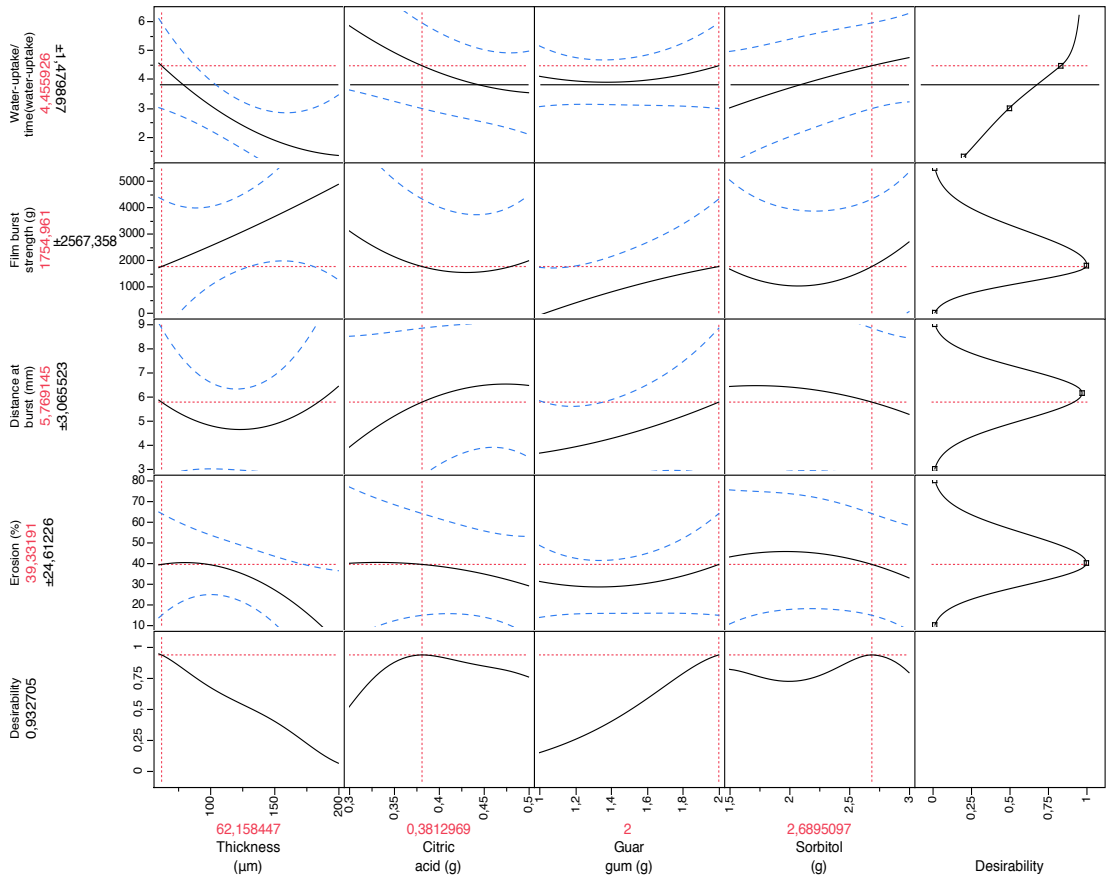

Figure 11: Prediction profiler for guar gum oral films. Quantities of citric acid, guar gum and sorbitol are set considering a final volume of 100 mL of ultra-pure water

Since very wide standard-deviation values were obtained for responses (dependent variables), three batches of the guar gum films formula predicted by the statistical model as being optimal were prepared and erosion (%), distance at burst (mm), film burst strength (g) and water-uptake/time (mg/s) ratio were determined (n = 6) and compared with theoretically predicted values. Oral films were prepared according to the prediction

profiler, by dissolving 2.7 g of sorbitol, 2.0 g of guar gum and 0.380 g of citric acid in 100 mL of ultrapure water. Only oral films with 0.06 mm were selected for validation purposes. Predicted and experimental values for the optimized formulation of guar gum films are outlined in **Table 8.**

Table 8: Predicted and experimental values obtained for the optimized formulation of guar gum film

Parameter	Predicted value (mean ± SD)	Experimental value (mean ± SD; n = 6)
Erosion (%)	39.33 ± 24.61	41.78 ± 3.97
WU/time(max WU) (mg/s)	4.46 ± 1.48	4.28 ± 0.33
Distance at burst (mm)	5.77 ± 3.07	5.39 ± 0.65
Film burst strength (g)	1754.96 ± 2567.36	1595.42 ± 300.13

No statistical differences ($p > 0.05$) were observed between mean predicted values and mean experimental values (**Figure 12**).

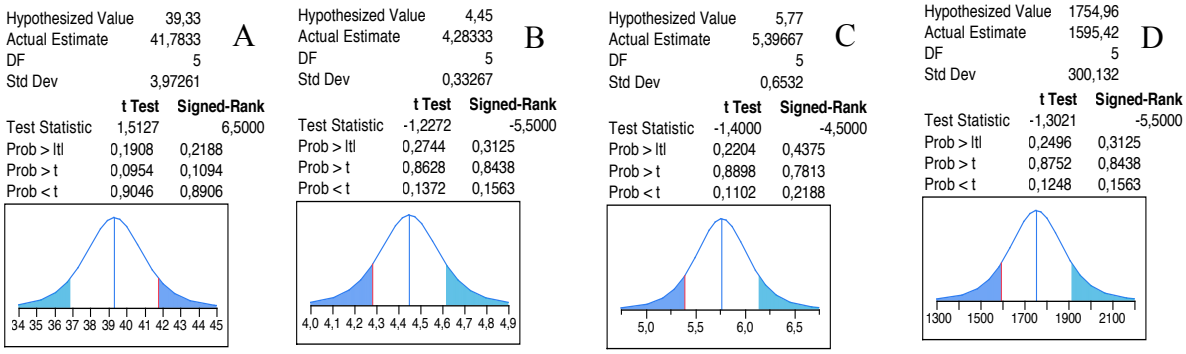

Figure 12: One sample T-test for comparison of experimental values of erosion (A), water-uptake/time ratio (B), distance at burst (C) and film burst strength (D) with values predicted in the model

Many other polymers have been previously reported as having film-forming properties at similar concentrations as observed for guar gum films (Dixit & Puthli, 2009b). Indeed, chitosan and sodium carboxymethylcellulose oral films were previously

optimised by our group but disintegration times were much higher and drug release was very distinct from developed guar gum films (Castro, Fonte, Oliveira, Madureira, Sarmento & Pintado, 2017). Moreover, chitosan oral films are reported as being astringent and, therefore, potentially unpleasant, compromising patient/consumer compliance. On the other hand, guar gum is commonly used in food products as thickener in a wide array of products and consumers already accept the flavour and used to find guar gum referred on packaging labels (Lv, Kong, Mou & Fu, 2017).

Also, in comparison to mucoadhesive oral films recently developed, guar gum films presented superior mechanical characteristics either regarding film burst strength (average of 1754.96 g for guar gum films against 546.57 g for sodium carboxymethylcellulose films) or distance at burst (average of 5.77 mm for guar gum films against 0.74 mm for sodium carboxymethylcellulose films) (Gajdošová et al., 2016). Distance at burst was similar to vaginal films (blend of 72% of hydroxypropylmethylcellulose, 18% polyvinyl alcohol and 10% glycerine) containing nanoparticles developed by our group (average of 5.77 mm for guar gum films against 5.34 mm for vaginal films) indicating good elasticity characteristics (Cunha-Reis et al., 2016).

Indeed, mechanical characteristics are very important either to assure stability during transport, accurate dosage of carried bioactive molecules or to avoid handling and administration issues (Zhao, Quan & Fang, 2015).

Unfortunately, there is still a great lack of information regarding standardized technological characteristics (e.g. mechanical characterization, dissolution and disintegration assays, shelf-life assessment and appropriate storing and packaging conditions) making the optimization of oral films formulations a task requiring further

studies (Adrover & Nobili, 2015; Adrover, Pedacchia, Petralito & Spera, 2015a; Dixit & Puthli, 2009b; Preis, Woertz, Kleinebudde & Breitkreutz, 2013).

3.4.2. Optimization of the formulation of alginate beads and validation of results

Alginate beads formulation was optimized with the purpose of obtaining high stability and enhancement of residence time of caffeine in contact with buccal mucosa.

The summary of the factorial design (response surface method) performed for the optimization of the formulation of alginate beads is outlined in **Table 9**. Relative amounts of sodium alginate (particle-forming polymer) and Tween® 80 (polysorbate, surfactant) were chosen as factors for the optimization of alginate beads. Association efficiency, mean particle size, polydispersity index and zeta-potential were selected as responses, being considered of main importance for the characterization of beads. Caffeine anhydrous was the model drug carried by alginate beads, attending to achieve sustained release.

Table 9: Factorial design parameters established for the optimization of the formulation of alginate beads

Factorial design parameters (Alginate beads)			
Level (code unit)	**Alginate solution concentration (%, w/v)**	**Tween 80 (%, w/v)**	**Caffeine concentration (mg/mL)**
-1	2	2	16.7
0	3	3	16.7
1	4	4	16.7

Prediction profiler (**Figure 13**) allowed elaborating an optimized alginate beads formulation to achieve desired values of association efficiency (AE, %), mean particle size, polydispersity index (PdI) and zeta-potential (mV).

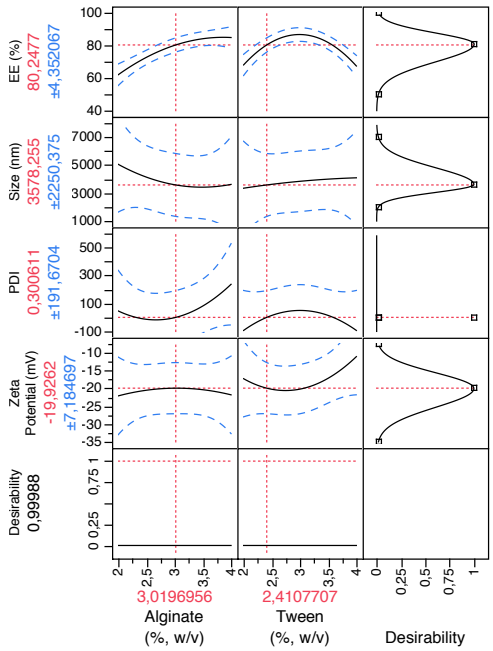

Figure 13: Prediction profiler for the formulation of alginate beads

As observed for guar gum films, since very wide standard deviation values were obtained for responses (dependent variables), three batches of alginate beads were prepared and mean values of AE (%), size (µm), PdI and zeta-potential (mV) were determined and compared with the average values predicted by the statistical model. Alginate beads were prepared using 3.0% (%, w/v) of alginate and 2.4% (%, w/v) of Tween® 80. Predicted and experimental values for the optimized formulation of alginate beads films are outlined in **Table 10**.

Table 10: Predicted and experimental values obtained for the optimized formulation of alginate beads

	Predicted value (mean ± SD)	**Experimental value (mean ± SD; n = 6)**
Association efficiency (%)	80.25 ± 4.35	81.57 ± 6.59
Particle size (µm)	3.57 ± 2.25	3.37 ± 0.64
Polydispersity index	0.300 ± 0.192	0.348 ± 0.060
Zeta-potential (mV)	-19.93 ± 7.18	-25.27 ± 1.50

No statistical differences ($p > 0.05$) were observed between mean predicted values and mean experimental values, except for zeta-potential. Indeed, experimental values for zeta-potential were significantly inferior, i.e. more negative, than values predicted in the statistical model.

A graphical analysis of one sample T-tests performed for validation of the prediction profiler is provided in **Figure 14**.

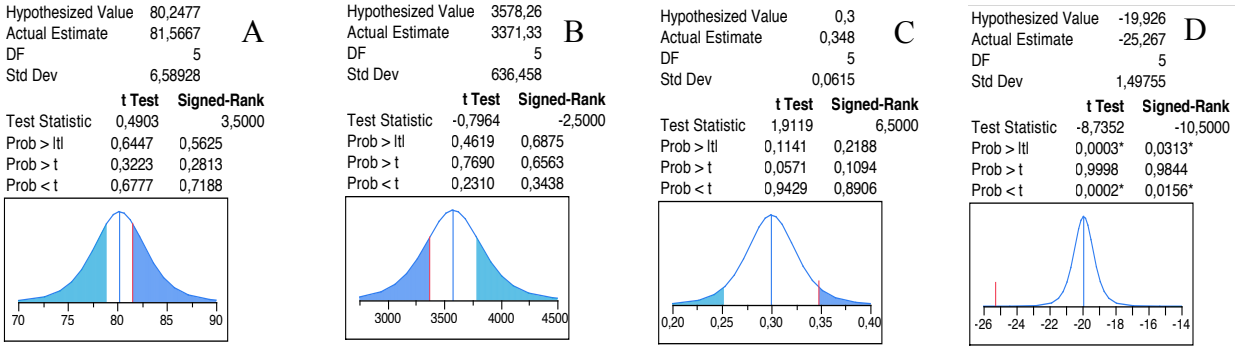

Figure 14: one sample T-test for comparison of experimental values of association efficiency (A), average particle size (B), polydispersity index (C) and zeta-potential (D) with values predicted in the model

There is still a gap in the literature concerning microparticles as buccal delivery systems, albeit it has been reported by some researchers (Sudhakar, Kuotsu & Bandyopadhyay, 2006). Nevertheless, most researchers are using nanoparticles aiming to increase apparent permeability of carried drugs and not to achieve a slower release of carried molecules. For instance, it has been reported that poly(lactide-co-glycolide) (PLGA) nanoparticles carrying acyclovir were incorporated into mucoadhesive buccal films and succeeded on increasing *ex vivo* permeability of the drug across rabbit buccal mucosa (Al-Dhubiab, Nair, Kumria, Attimarad & Harsha, 2015). Nevertheless, most works concerning the development of microparticles for buccal delivery are aiming local administration and not permeation across buccal mucosa to reach systemic circulation

(Giunchedi, Juliano, Gavini, Cossu & Sorrenti, 2002; Sosnik, das Neves & Sarmento, 2014). Alginate was previously used to produce mucoadhesive microparticles by ionic gelation aiming to an increased residence time of drugs in the buccal mucosa. Effectively, alginate microparticles guaranteed an increased residence time of flurbiprofen and delmopinol when compared to reference solutions, decreasing the administration frequency (Cilurzo, Gennari, Selmin, Musazzi, Rumio & Minghetti, 2013).

3.4.3. Dynamic surface tension analysis

Analysis of water/air interfacial tension is outlined in **Figure 15**. The lower water/air surface tension was associated with higher possibility of the formulation to adhere to other solutions or surfaces (e.g. digestive juices or enteric tissues) (Ahuja, Khar & Ali, 2008). Indeed, surface tension is a way of measuring the work of adhesion. The smaller the work of internal adhesion within the drop, the greater the possibility of interaction with external environment.

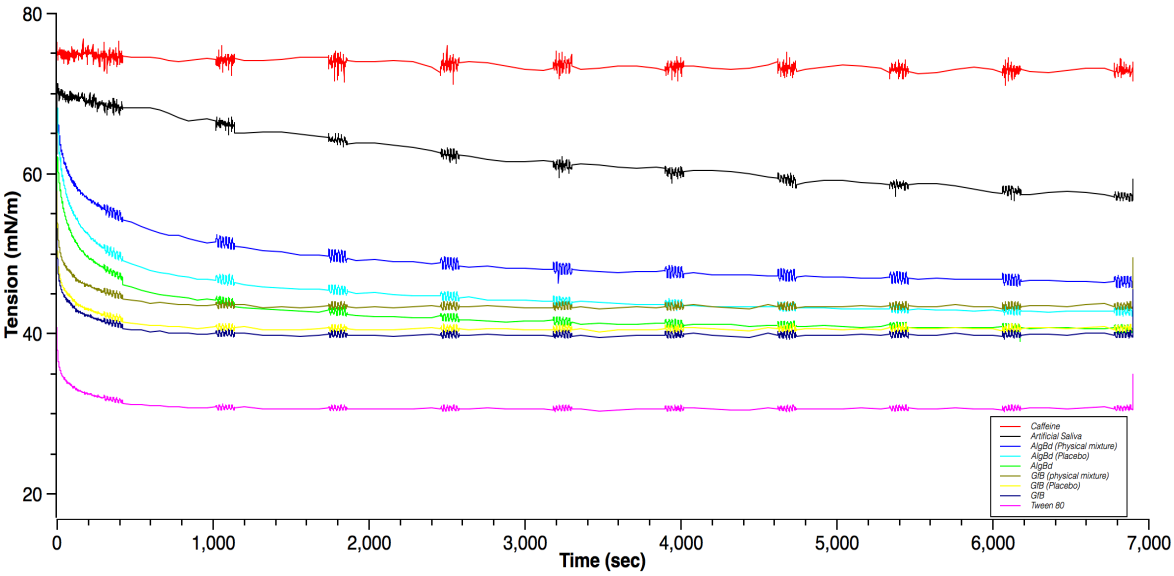

Figure 15: Time evolution of water/air superficial tension for the alginate beads containing caffeine along with respective physical mixture and isolated formulation components

The interfacial behaviour of developed formulations along with individualized components of the beads (i.e. sodium alginate and Tween 80) reflected significant differences that can be translated into distinct mucoadhesion profiles. Indeed, it was observed that caffeine did not present interfacial activity.

Artificial saliva solution presented a small variation of superficial tension along time as well, even though slightly more pronounced when compared to caffeine.

On the other hand, sodium alginate presented tensioactive activity with a variation of 24 mN/m during the 7,000 s of the assay, indicating a potentially favourable interaction with gastrointestinal mucosa. Tween 80 (polysorbate) induced the most extensive reduction of surface tension with time (Shah, Bharatiya, Shukla, Mukherjee & Shah, 2016). Effectively, Tween 80 is well-known to present very expressive tensioactive activity and a high drop stability was expected.

Caffeine-loaded alginate beads and GfB presented the higher stabilization (i.e. the lower the surface tension, the higher the possibility of interacting with external media as the buccal mucosa or absorptive epithelia along the gastrointestinal tract) capacity of all formulations, indicating that the association of caffeine with alginate beads is expected to offer a greater interaction with gastrointestinal tract mucosa when compared with caffeine or excipients alone.

Moreover, the incorporation of caffeine-loaded alginate beads within the guar gum film matrix led to the greatest decrease in the surface tension of the drop (Tween 80 is not being considered due to intrinsic tensioactive activity) indicating that the guar gum film-alginate beads synergism may potentially offer a higher mucoadhesion along gastrointestinal tract when compared to the remaining formulations (Ahuja, Khar & Ali, 2008).

3.4.4. Molecular interaction analysis

Attenuated total reflectance-Fourier-transform infrared (ATR-FTIR) analysis was performed to perceive the onset of new bonds between caffeine and developed formulations during production steps.

Resulting infrared spectra achieved from the subtraction of alginate beads, guar gum films, GfB and for the physical mixture of all excipients of GfB and caffeine from corresponding placebo formulations is outlined in **Figure 16**. Spectra of caffeine anhydrous powder was used for comparison with obtained subtracted spectra.

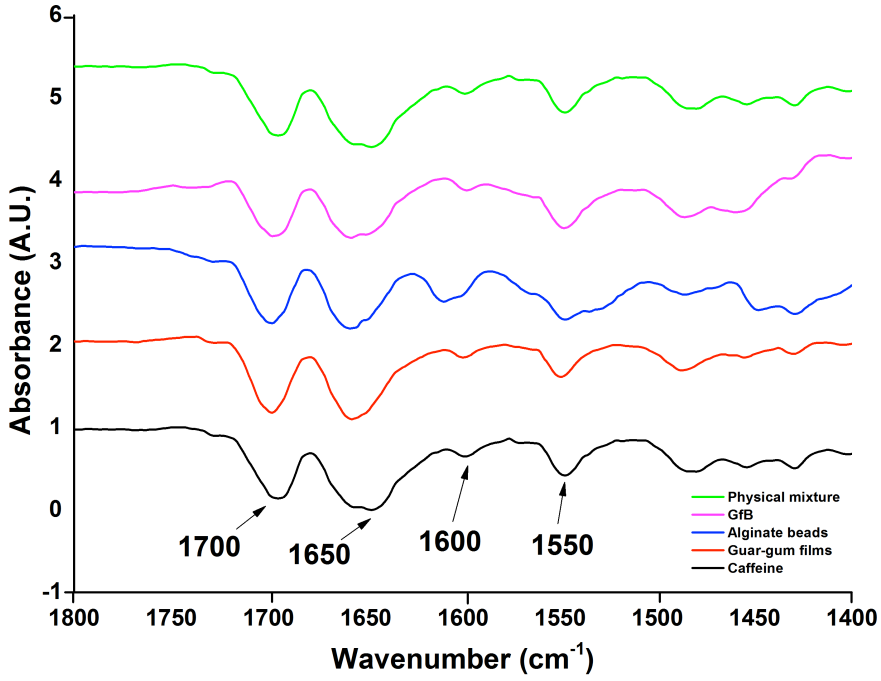

Figure 16: Subtracted FTIR spectra corresponding to the caffeine present on alginate beads, GfB, guar gum films caffeine anhydrous powder and the physical mixture of all excipients of GfB

Typical caffeine bands that appear at 1700-1600 cm^{-1} are representative of the C=O stretch of amide I (Bourbon, Cerqueira & Vicente, 2016). C-N stretch coupled with N-H

bending of the amide II present in the caffeine molecule are represented by the bands at 1600-1500 cm^{-1}. The bands showed in the range of 1666-1550 cm^{-1} are addressed to the stretches of C=C, C=O and C=N bonds of caffeine molecules (Lázaro Martínez, Leal Denis, Campo Dall'Orto & Buldain, 2008a; Molinari & Lata, 1962a). Subtracted spectra for alginate beads, guar gum films, GfB and physical mixture of all excipients of GfB represented in **Figure 16**, showed the same characteristic infrared bands as caffeine anhydrous infrared spectra. Thus, there is no indication of the formation of new chemical bonds between caffeine and the excipients of alginate beads or guar gum oral films during formulations processes. Also, there are no significant differences between caffeine spectra and the subtracted spectra for the physical mixture, revealing that the excipients do not induce alterations in the chemical structure of caffeine. Spectral analysis indicates that the formation of new chemical bonds that may hinder caffeine release from developed delivery systems is not observed. Instead, caffeine release from guar gum films, alginate beads or GfB may be affected mainly by physical shielding and/or electrostatic bonds (Castro, Fonte, Oliveira, Madureira, Sarmento & Pintado, 2017).

3.4.5. Morphology analysis

Scanning electron microscopy (SEM) was used to perform a visual recognition of the matrix structure of oral films and alginate beads, in order to obtain further information regarding caffeine delivery profile.

Morphology analysis of alginate beads, guar gum films and alginate beads dispersed on oral films was performed by SEM (**Figure 17**).

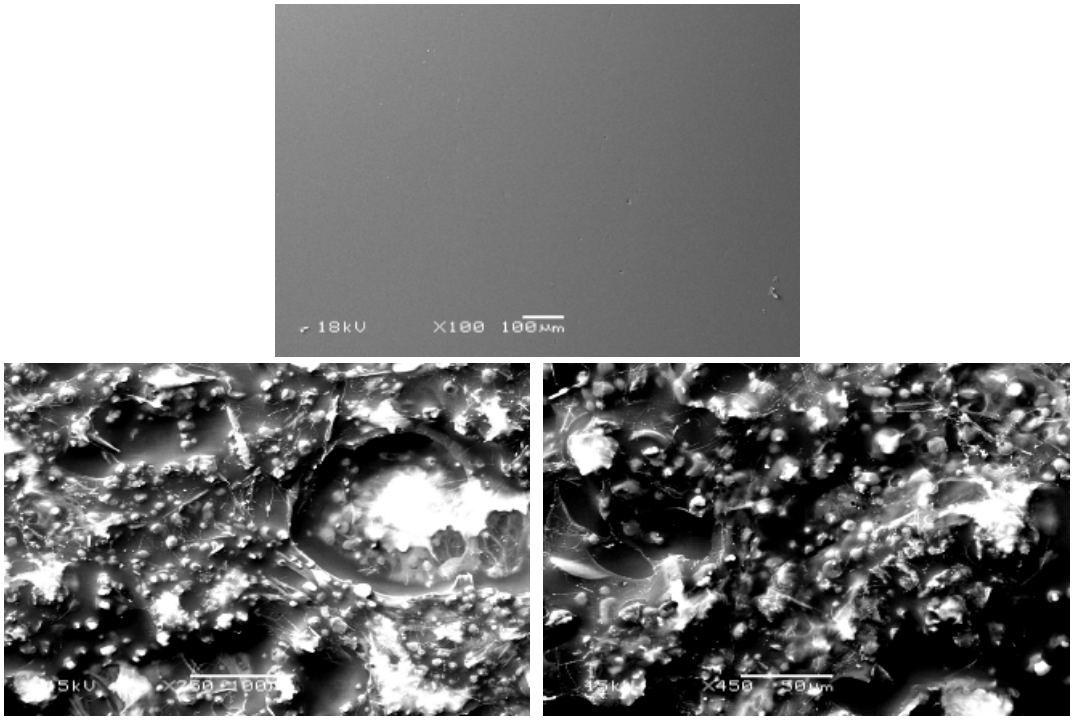

Figure 17: SEM Micrographs of guar gum films (A), alginate beads (B) and alginate beads incorporated in the guar gum films matrix (C)

Alginate beads were added to guar gum films formulation before solvent casting for the blend to be as homogeneous as possible. The fact that alginate beads are hydrophilic could represent a stability problem since it would be very likely that alginate would be dissolved in the guar gum films matrix during solvent casting procedure. However, it is noticeable that alginate beads are homogeneously spread on the film matrix, indicating good stability of alginate beads. Also, bead size and morphology observed in the microphotographs are coherent with the size predicted by the statistical model and corroborated by DLS analysis that indicated that mean particle size is around 3.58 µm. Both size and shape of alginate beads were homogeneous. Also, some particle agglomeration seems to occur. Nevertheless, homogeneous dispersion of alginate beads into/onto the guar gum films matrix indicates that caffeine dosage in each film is very

similar and, thus, caffeine release profile is likely to be similar when testing different batches. Therefore, the chances of a successful future scale-up are promising.

3.4.6. Tongue adhesion

Orodispersible films are intended to be placed on the top of the tongue where disintegration occurs after contact with saliva. Indeed, adhesion to tongue is an important first step regarding a homogeneous disintegration of the films so that resulting fragments are evenly dispersed within the oral cavity. Results regarding adhesiveness, work of adhesion and debonding distance are outlined in **Table 11.**

Table 11: Characterization of developed formulations regarding adhesion to the tongue

Formulation	Adhesiveness (N)	Work of adhesion (N·s)	Debonding distance (mm)
Guar gum film	0.026 ± 0.003	0.118 ± 0.062	1.608 ± 0.679
GfB	0.020 ± 0.004	0.195 ± 0.060	1.773 ± 0.444

Even though no significant statistic differences ($P > 0.05$) regarding adhesion to the tongue were found between the guar gum film formulation and GfB, the addition of GfB seemed to offer higher work of adhesion when compared with adhesiveness. Indeed, the increased roughness of the surface of guar gum films due to the presence of alginate beads led to an apparent decrease of adhesiveness value, meaning that GfB is does not attach to the tongue as strongly as guar gum film alone. Nonetheless, GfB offered an apparently higher debonding distance and, therefore, higher work of adhesion, indicating that the higher surface area induced by the presence of alginate beads results in the occurrence of more points of attachment. An increase of the number of intimate contact areas is usually correlated with an increased intimate contact with buccal absorptive epithelia and,

therefore, improved permeability of carried bioactive molecules (Banerjee, Qi, Gogoi, Wong & Mitragotri, 2016; Castro, Baptista, Madureira, Sarmento & Pintado, 2018; Tan, Shah, Thomas, Ou-Yang & Liu, 2013).

3.4.7. In vitro caffeine release assay

The release assay using dialysis membranes was performed to characterize the delivery profile of caffeine from alginate beads, guar gum films and the combination of both delivery systems (GfB) aiming to test a conceptually new oral delivery system. Pore size of dialysis membrane (500 Da) was chosen according to the intercellular space between epithelial cells of buccal mucosa (Castro, Fonte, Sousa, Madureira, Sarmento & Pintado, 2015c; Merkle & Wolany, 1992).

For the assessment of release profile of caffeine from developed delivery systems, guar gum films and alginate beads alone and in combination were tested. **Figure 18** represents delivery profile from guar gum films, alginate beads and GfB compared with a control solution of free caffeine (2 mg/mL).

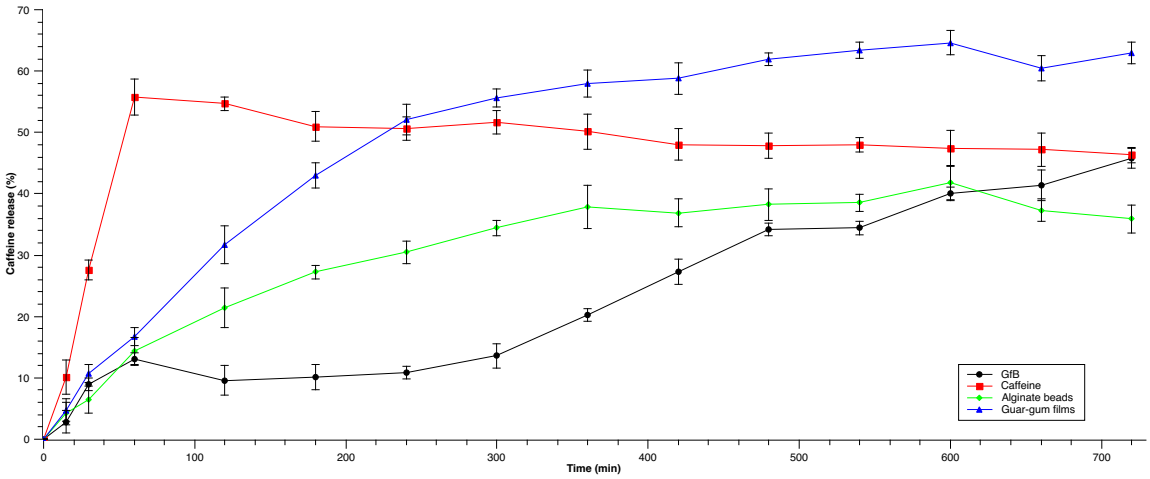

Figure 18: Caffeine cumulative release (mean ± S.D., n = 5) across a 500 Da dialysis membrane

The higher flux of caffeine from control solution crossed the dialysis membrane occurred in the first 15 min, indicating that caffeine flux easily occurred from the inside of the dialysis membrane to the outside, following Fick's first law. Caffeine is a small (194.194 $g.mol^{-1}$), highly hydrophilic (2.16E04 mg/L) molecule and a fast efflux from the dialysis membrane was predictable (Santos, Teijeiro, Ribeiro, Rodrigues, Romero & Esteso, 2016; Yalkowski, He & Jain, 2010). Release profile of caffeine content in control solution was almost linear in the first 60 min, approaching a zero-order release kinetics and reaching a plateau from 60 min till the end of the release study. Indeed, caffeine is expected to permeate buccal mucosa according to the simplified version of Fick's first law (Eq. (9)) by paracellular path (Brodin, Steffansen & Nielsen, 2010; Nicolazzo, Reed & Finnin, 2004).

$$J = P(Cdonor - Creceiver) \qquad (9)$$

where, P is the permeability coefficient, *Cdonor* and *Creceiver* are the concentrations of caffeine inside the dialysis membrane and on the receiver compartment, respectively, and J is the flux from the dialysis membrane (donor compartment) to the receiver compartment (Brodin, Steffansen & Nielsen, 2010). Caffeine release from guar gum films was significantly slower than the control caffeine solution but fast disintegration of the film led, yet, to a significantly fast caffeine release to the outside of the dialysis membrane. Effectively, the same noticeable burst release of bioactive molecules loaded in a thin film was observed in other studies, indicating a clear trend regarding delivery of bioactive molecules from thin films (Akil et al., 2015; Machado et al., 2016). The differences observed between guar gum films release profile and control

may be due to physical and/or electrostatic hindrance of caffeine release from guar gum films matrix. Caffeine release from alginate beads across dialysis membrane was significantly slower when compared with guar gum films or control. The fact that caffeine molecules are associated (either inside or at the surface) to the alginate beads may delay the release of caffeine, therefore preventing a sooner passage across dialysis membrane pores. Indeed, alginate beads, may have to disintegrate for the entrapped caffeine to be free and able to cross the membrane. The combination of guar gum films and alginate beads to form one delivery system offers the highest impedance of caffeine release over time. Indeed, the conjugation of guar gum film and alginate matrices implies that caffeine must be released from a double barrier before contacting with the absorptive epithelium. Both film and bead matrices must disintegrate and dissolve to allow the complete release of caffeine. Nevertheless, caffeine release in the first 60 min was very similar for GfB and alginate beads. The initial burst release may be due to some premature release of caffeine from alginate beads shortly after the production of the formulations, as verified in other studies (Cunha-Reis et al., 2016; Machado et al., 2016).

3.4.8. TR146 cell viability studies

TR146 cells were used to evaluate potential toxicity caused by different concentrations of caffeine-loaded alginate beads, guar gum films and GfB. Placebo formulations with the same mass as caffeine-loaded delivery systems were used as controls. Cell viability was assessed by MTT reduction assay.

Results of cell viability *in vitro* assay for placebo and caffeine-loaded alginate beads, guar gum films and alginate beads incorporated into guar gum films are shown in **Figure 19**.

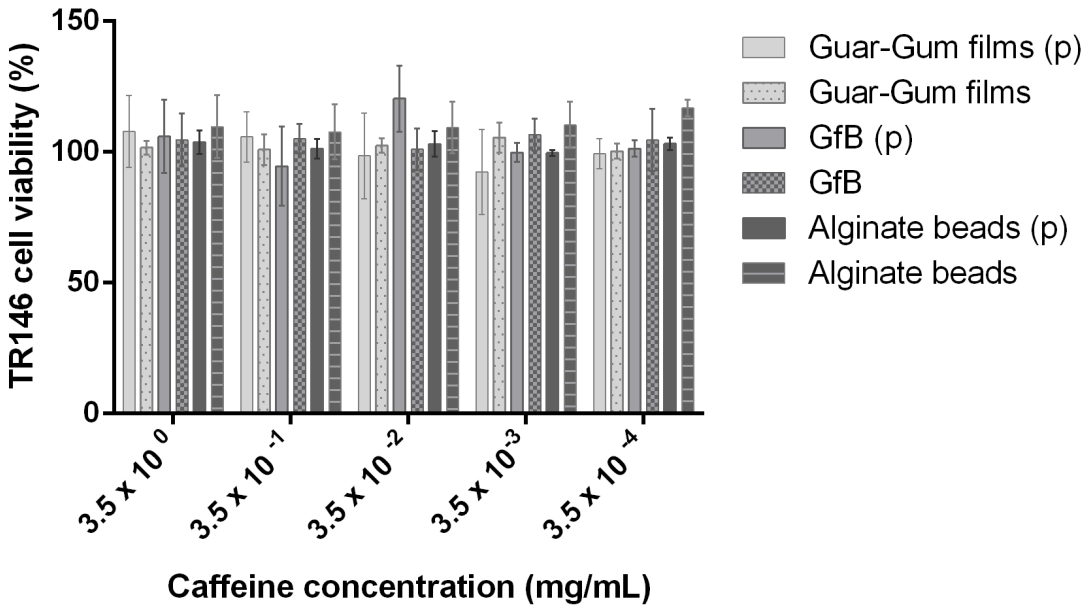

Figure 19: Cytotoxicity assessment of different concentrations of caffeinated (alginate beads, guar gum films and GfB), placebo (alginate beads(p), guar gum films(p) and GfB(p)) formulations

None of the tested concentrations of caffeine alone or incorporated into alginate beads, guar gum films or GfB did significantly compromise cellular viability of TR146 cells, after 12 h of exposure. Total TR146 cell viability indicates that, when administered *per os* there was no evidence that suggests that some of the drug delivery systems (either alone or combined) are hazardous for the buccal epithelium.

3.4.9. Permeability assay on TR146 monolayers

TR146 human buccal carcinoma cells were used to determine buccal permeability of caffeine from developed formulations.

The permeation profiles through TR146 cells grown on Transwell® inserts were distinct according to the formulation (**Figure 20**).

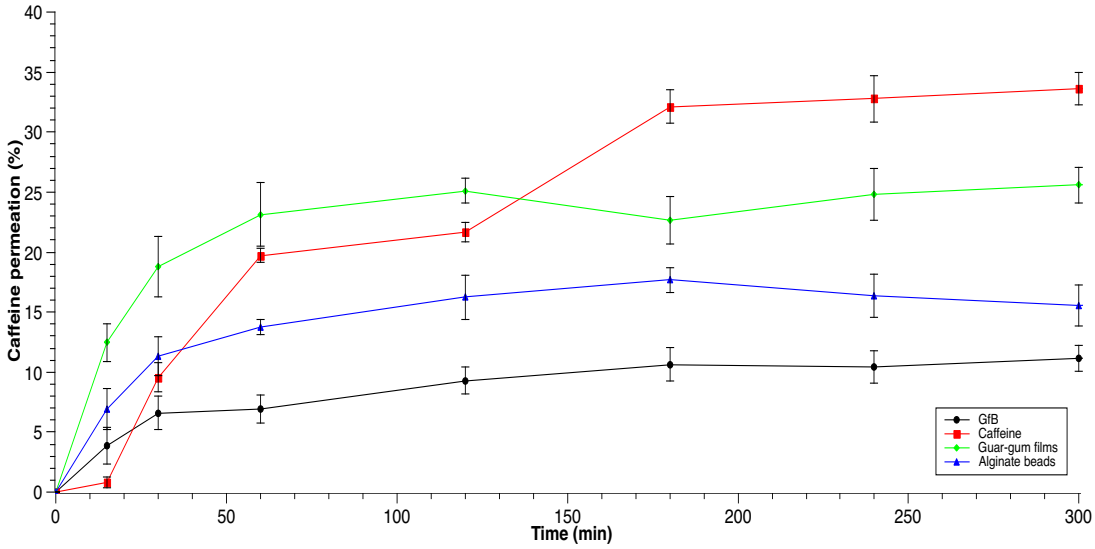

Figure 20: Cumulative permeability of caffeine (mean ± S.D., n = 3) across TR146 cells seeded in Transwell®

Values of the apparent permeability ($cm.s^{-1}$) for all the formulations are outlined in **Table 12**.

Table 12: Apparent permeability of GfB, guar gum films, alginate beads and caffeine solution (control) across transwell® seeded with confluent TR146 cells

Formulation	**Papp $cm.s^{-1}$ (mean ± S.D., n = 5)**
GfB	1.15E-05 ± 3.50E-06
Guar gum films	3.12E-05 ± 4.70E-06
Alginate beads	2.01E-05 ± 3.90E-06
Free caffeine	2.68E-05 ± 7.30E-06
Free caffeine[1]	8.14E-06 ± 7.30E-07

[1] Data from Kulkarni et al. using porcine buccal mucosa mounted on Franz diffusion cells (Kulkarni, Mahalingam, Li, Pather & Jasti, 2011)

Results obtained for caffeine control solution (2 mg/mL) are in accordance with previously reported caffeine buccal apparent permeability (Kulkarni, Mahalingam, Pather, Li & Jasti, 2009; Kulkarni, Mahalingam, Li, Pather & Jasti, 2011). Also, caffeine control solution presented a permeability profile that strongly correlates with diffusion

from dialysis membrane (**Figure 20**). Indeed, caffeine permeation also occurred according to Fick's first law following a zero-order kinetics. Caffeine released from guar gum films permeated TR146 cell layer faster than the control caffeine solution for 100 min. After being inserted into the Transwell® inserts, guar gum films began disintegrating. Then, fragments resulting from disintegration of guar gum films deposited and adhered to the apical layer of TR146 cells. Immediate adhesion of guar gum films fragments offered a higher contact surface area with the cell layer and thus, more effective caffeine permeation. Effectively, mucoadhesive delivery systems were reported, by peer researchers, to increase permeation of carried molecules across TR146 cell layer (Sander, Nielsen & Jacobsen, 2013a). Both alginate beads and GfB offered slower caffeine permeation when compared with guar gum films or caffeine control solution. Lower permeation of caffeine across TR146 cell layer may be at least partially due to the slower caffeine release, as observed in the caffeine release assay (**Figure 18**). In fact, as previously observed for the release assay using dialysis membranes, GfB promoted a slower release of caffeine when compared with control, alginate beads or guar gum films alone. The cross-analysis of dialysis release assay and *in vitro* permeability assay on TR146 buccal mucosa cells indicated a strong correlation between caffeine release profile and permeability effectiveness. When caffeine-loaded alginate beads are combined with guar gum films, caffeine is doubly hindered from being released since both alginate and guar gum matrices must be disintegrated and dissolved before caffeine contacts with buccal cells. Moreover, since alginate beads present high mean particle size, permeation of the whole beads is not likely to happen unless the integrity of buccal epithelium is somehow compromised. Also, since transepithelial permeation study was performed using a static model, swallowing, salivation, masticatory movements or even phonation

were not considered. Indeed, it is predictable that a caffeine solution is almost immediately swallowed after being introduced in the oral cavity in *in vivo* conditions.

Moreover, after cellular disruption of the TR146 monolayer, it was possible to observe (**Figure 21**) that most caffeine was present either within or retained by the cell layer. The fact that guar gum films, alginate beads and GfB were capable to maintain caffeine in intimate contact with the monolayer may enhance permeability of caffeine over time, especially in *in vivo* conditions.

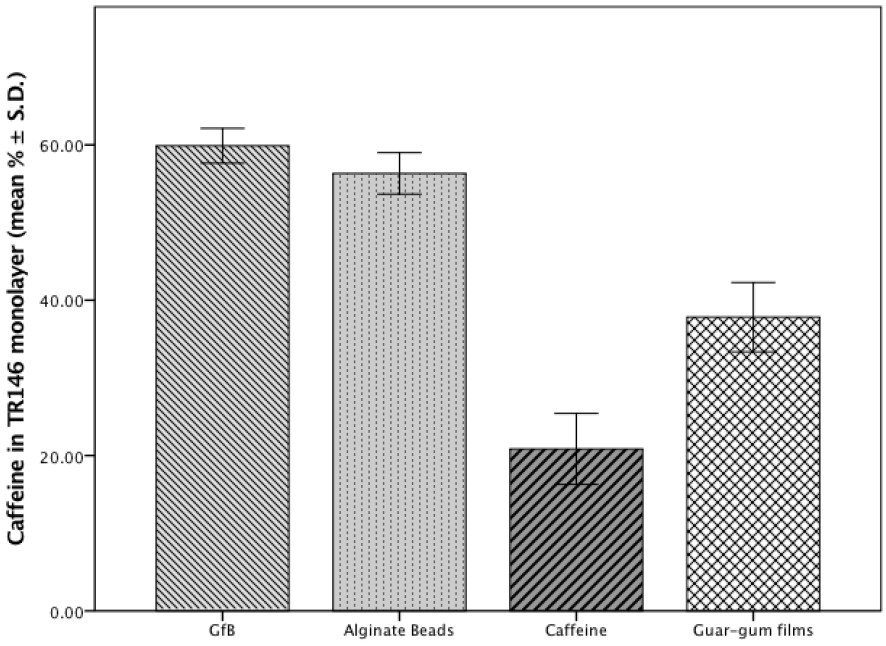

Figure 21: Caffeine (mean ± S.D.) collected from TR146 cell monolayer (by delivery system)

3.4.10. Simulation of gastrointestinal tract and caffeine permeability across porcine intestinal mucosa

Simulation of gastrointestinal tract was performed to assess the differences on the fate of caffeine, namely regarding intestinal permeation, when carried by developed formulations in comparison with free caffeine. Caffeine permeability across porcine

intestinal mucosa and across Caco-2/HT29-MTX co-culture cell layer were performed as a model to resemble *in vivo* fate of caffeine when delivered by developed formulations.

3.4.10.1. *Ex vivo* intestinal permeability of caffeine

The profile of *ex vivo* permeability of caffeine across porcine intestinal tissue is outlined in **Figure 22**.

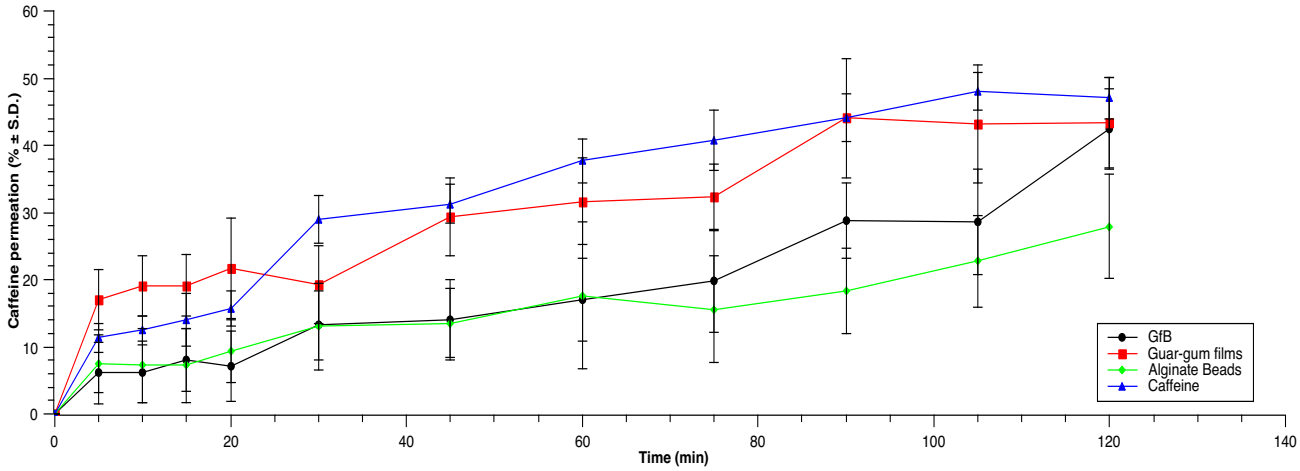

Figure 22: Caffeine cumulative permeation (% ± S.D.) across porcine intestinal mucosa

Both alginate beads and GfB promoted an overall slower permeability of caffeine across intestinal tissue when compared with caffeinated guar gum films or the solution of free caffeine. Indeed, caffeine permeation for GfB and alginate beads was almost overlapping in the first 60 min. Even though the pattern of intestinal permeability of caffeine was similar to release profile observed in the *in vitro* release assay, differences between cumulative caffeine permeation from GfB, alginate beads and guar gum films and free caffeine were less appreciable in comparison with *in vitro* release assay. Results indicated that GfB system and alginate beads were successively disintegrated along the simulated gastrointestinal tract and the amount of free caffeine that was present in the

intestinal phase was responsible for the faster permeation through intestinal tissue in comparison with *in vitro* release assay.

Despite the slower permeation of caffeine across porcine intestinal mucosa when carried by GfB, apparent permeability (Papp) coefficient is higher in comparison with remaining formulations or even free caffeine. Indeed, Papp values are in accordance with the amount of caffeine that remained in the apical side, dissolved in the digestive juice, and the caffeine found intimately associated with intestinal tissue that was homogenized by ultrasounds to extract and quantify the caffeine that was intimately associated either by tissue-absorption or adsorption. Results are outlined in **Table 13**.

Table 13: Apparent permeability across porcine intestinal mucosa and relative amounts of caffeine in the apical side (post-digestion) and in intimate contact – adsorbed or absorbed to the tissue – referring to caffeine-loaded GfB, guar gum films, alginate beads

Formulation	Papp $cm.s^{-1}$ (mean ± S.D.)	Apical (mean % ± S.D.)	Absorbed/adsorbed to the tissue (mean % ± S.D.)
GfB	8.21E-05 ± 3.29E-06	14.67 ± 8.13	29.37 ± 5.32
Guar gum films	5.96E-05 ± 4.95E-06	13.98 ± 6.23	22.53 ± 7.59
Alginate beads	4.62E-05 ± 7.81E-06	28.73 ± 9.78	27.89 ± 4.94
Free caffeine (control)	8.09E-05 ± 1.92E-06	42.13 ± 5.67	7.33 ± 3.12

GfB promoted a more intimate contact between caffeine and intestinal tissue, with the highest rate of absorbed/adsorbed caffeine and results are corroborated by the low amount of caffeine that remained dissolved in the digest of the apical side. Alginate beads and guar gum films also lead to high amounts of caffeine intimately contacting with intestinal tissue, especially when compared with control solution that enabled a high

apparent permeability but low intimate contact with intestinal mucosa, being predictable that permeation would be lower in a dynamic system, rather than a static system as tested.

3.4.10.2. Caco-2/HT29-MTX co-culture cell viability

Cell viability of Caco-2/HT29-MTX co-culture was determined by MTT assay. It was verified that none of the formulations compromised the cell viability of the co-culture, as outlined in **Figure 23**.

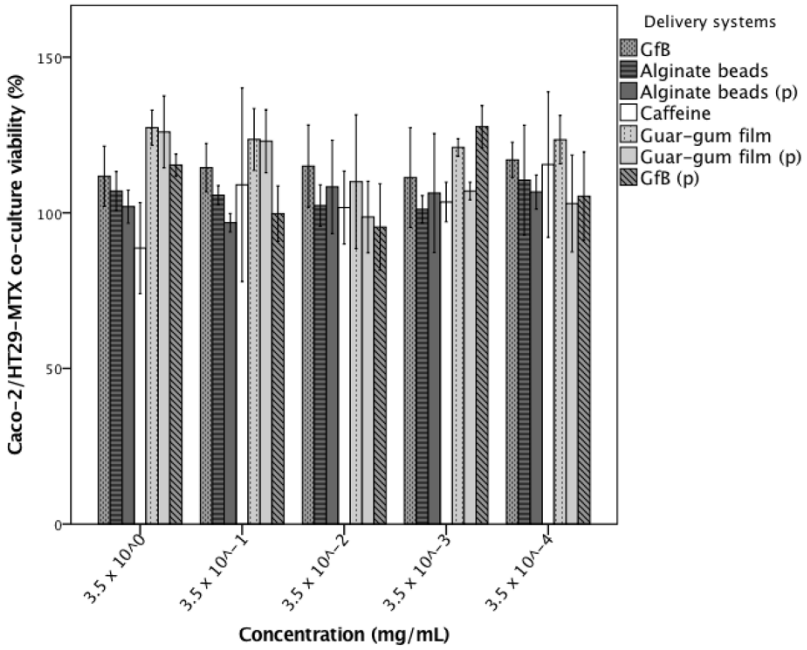

Figure 23: Cytotoxicity assessment of different concentrations of caffeinated (alginate beads, guar gum films and GfB), placebo (alginate beads(p), guar gum films(p) and GfB(p)) formulations

Since no formulation has compromised cell viability below 70%, no significant toxicity was identified according to the International Organization for Standardization (Almeida, Silva, Goncalves & Sarmento, 2018). Also, the fact that no cytotoxicity was observed was a good indicative that developed formulations would not present toxicity *in vivo* as Caco-2/HT29-MTX co-culture represents a robust model to mimic the physiologic characteristics of human intestinal mucosa.

3.4.10.3. *In vitro* intestinal permeability of caffeine

As outlined in **Figure 24**, permeability of caffeine across the layer of Caco-2/HT29-MTX co-culture presented a similar profile as observed for *ex vivo* permeability assay.

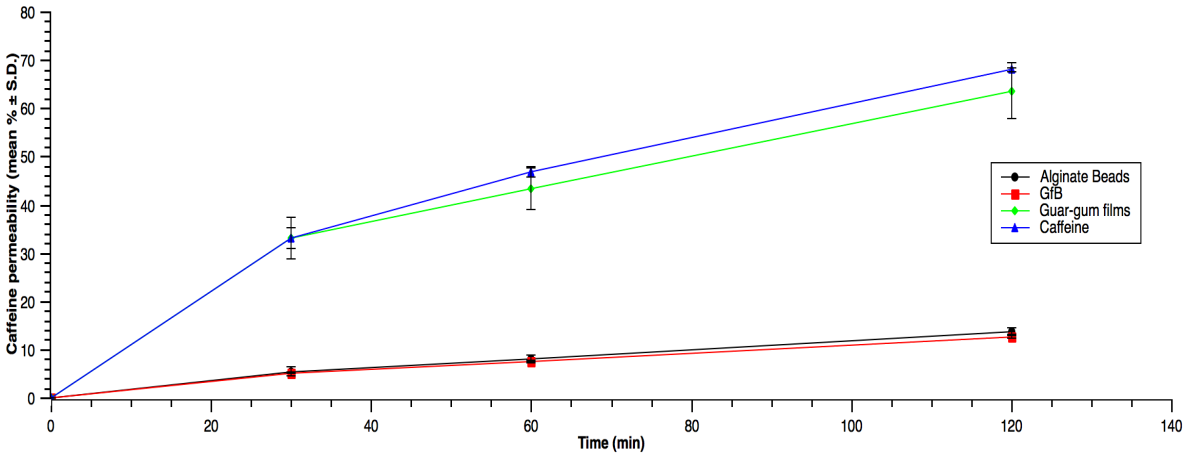

Figure 24: Permeation of caffeine across Caco-2/HT29-MTX co-culture layer

In fact, similarities in permeability for free caffeine solution and guar gum films and for alginate beads and GfB, respectively, were even more evident than for *ex vivo* permeability profile. Moreover, the differences between clusters (i.e. between the group of caffeine and guar gum films and the group of alginate beads and GfB) were also higher. Results suggest that, as mentioned before both alginate beads and GfB promoted a slower release of caffeine when compared with guar gum films or caffeine control solution. Also, after disruption of Caco-2/HT29-MTX cell layer, it was possible to confirm that GfB and alginate beads promoted a closer contact with the epithelia, thus retaining a higher concentration of caffeine in the absorptive area (**Table 14**).

Table 14: Apparent permeability across Caco-2/HT29-MTX co-culture cell layer, and relative amounts of caffeine in the apical side (after permeability assay) and in intimate contact – adsorbed or absorbed to the tissue – referring to caffeine-loaded GfB, guar gum films, alginate beads and caffeine solution (control)

Formulation	Papp $cm.s^{-1}$ (mean ± S.D.)	Apical (mean % ± S.D.)	Absorbed/adsorbed to the cell layer (mean % ± S.D.)
GfB	1.25E-05 ± 1.98E-06	5.30 ± 3.41	73.94 ± 2.46
Guar gum films	5.05E-05 ± 4.82E-06	14.42 ± 5.53	34.15 ± 7.71
Alginate beads	1.36E-05 ± 1.52E-06	9.66 ± 4.19	59.39 ± 9.82
Free caffeine (control)	5.77E-05 ± 1.12E-06	39.71 ± 2.90	9.43 ± 6.31

Even though apparent permeability is higher for caffeine solution and guar gum films, caffeine concentration absorbed by or adsorbed to the cell layer is significantly higher for alginate beads and GfB when compared to guar gum films or caffeine solution. The fact that GfB offered the higher caffeine content in/on the cell layer is in accordance with results described either for permeability across TR146 layer but also across porcine intestinal mucosa. On the other hand, both guar gum films and caffeine solution promoted the presence of high concentration of caffeine in the apical side but without close contact with the epithelia, therefore inducing immediate permeation of the epithelia according to Fick's first law of diffusion, i.e. directly depending on the differences of concentration between the absorptive membrane. On the other hand, since both alginate beads and GfB promote a gradual release of caffeine content, the equilibrium of concentrations in both sides of the membrane is constantly being disrupted, favouring the flux from the apical side of cell layer to the basolateral.

3.5. Conclusions

Two new oral/buccal delivery formulations, consisting on a guar gum based film and caffeine-loaded alginate beads, were optimized by experimental design. Robustness of developed predictive profilers was successfully validated, except for zeta-potential of alginate beads (experimental values for zeta-potential of alginate beads were more negative than predicted values). Nevertheless, more extreme zeta-potential values are beneficial to the stability of alginate beads and less prone to induce toxicity due to disruption of cellular membranes. Thus, attempting to achieve a conceptually new delivery system aiming buccal and oral delivery of bioactive compounds, alginate beads were dispersed in the matrix of guar gum films. Surface tension analysis allowed to conclude that the synergism between alginate beads and guar gum films offered a higher water-air stability when compared with isolated formulations. Therefore, it is predicted that GfB present good capacity to intimately interact with buccal mucosa. ATR-FTIR analysis did not indicate the occurrence of new chemical bonds between caffeine and guar gum films or alginate beads. Indeed, subtracted spectra (placebo formulations subtracted from caffeinated formulations) for guar gum films, alginate beads and GfB present the same characteristic bands as caffeine anhydrous, demonstrating that chemical structure of caffeine was not altered during or after inclusion into guar gum films, alginate beads or in the combination, GfB. Morphological characterization by SEM demonstrated a homogeneous dispersion of alginate beads on the guar gum films matrix, indicating that caffeine content is very likely to be homogeneous in each film unit, a good indicator if scale-up production is intended. Alginate beads, guar gum films and GfB did not compromise cell viability when tested on TR146 cells, by MTT assay. *In vitro* release profile of caffeine (dialysis membrane) and drug trans-epithelial assay (TR146 buccal

cells grown on Transwells®) allowed to conclude that the combination of guar gum films with alginate beads represent a suitable delivery system when a slower release of carried bioactive molecule into oral cavity is intended, when compared with guar gum films and alginate beads alone and with a control (caffeine solution). Also, the highest concentration of caffeine was found absorbed/adsorbed to TR146 cell layer when compared with alginate beads, guar gum films or caffeine alone. Results indicate that there is a synergistic effect between alginate beads and guar gum films that promotes an intimate contact with buccal epithelia, leading to a more extensive absorption over time, corroborating the hypothesis stated by the authors.

Similar results were observed regarding the permeation across intestinal mucosa and the Caco-2/HT29-MTX co-culture cell layer, with a higher adsorption/absorption of caffeine when carried by GfB when compared with alginate beads, guar gum films and caffeine control solution. Also, a higher Papp through porcine intestinal mucosa was observed for the combined formulation that could be related with the intimate tissue-caffeine contact promoted by GfB when compared with remaining formulations or free caffeine.

There are not yet similar delivery systems combining beads and films for oral and buccal delivery of bioactive molecules reported in the literature even though nanoparticles have already been incorporated into films for delivery of anti-HIV microbicidal drugs (Cunha-Reis et al., 2016; Machado et al., 2016). GfB may represent an innovative approach on the buccal delivery of hydrophilic bioactive molecules such as caffeine to assure controlled effects, being also especially suitable for paediatric or psychiatric patients that may be uncooperative to therapy.

Acknowledgments

This article is a result of the project NORTE-01-0145-FEDER-000012 , supported by Norte Portugal Regional Operational Programme (NORTE 2020), under the PORTUGAL 2020 Partnership Agreement, through the European Regional Development Fund (ERDF).

Pedro M. Castro would like to thank Comissão de Coordenação e Desenvolvimento Regional do Norte (CCDR-N), Portugal, for his PhD grant (NORTE-08-5369-FSE-000007).

Flávia Sousa would like to thank Fundação para a Ciência e a Tecnologia (FCT), Portugal for her PhD grant (Grant SFRH/BD/112201/2015).

The authors acknowledge the support granted by national founds from FCT through project PTDC/BBB-NAN/3249/2014.

This work was also financed by FEDER - Fundo Europeu de Desenvolvimento Regional funds through the COMPETE 2020 - Operacional Programme for Competitiveness and Internationalisation (POCI), Portugal 2020, and by Portuguese funds through FCT - Fundação para a Ciência e a Tecnologia/ Ministério da Ciência, Tecnologia e Ensino Superior in the framework of the project "Institute for Research and Innovation in Health Sciences" (POCI-01-0145-FEDER-007274)

Section 3

Association of guar gum films with PLGA nanoparticles for improved oral delivery of bioactive peptides

Chapter IV: Combination of PLGA nanoparticles with mucoadhesive guar gum films for buccal delivery of antihypertensive peptide

Pedro M. Castro 1,2, Patrícia Baptista* 1, Ana Raquel Madureira 1, Bruno Sarmento 2,3,4, Manuela E. Pintado 1***

1 CBQF – Centro de Biotecnologia e Química Fina – Laboratório Associado, Escola Superior de Biotecnologia, Universidade Católica Portuguesa/Porto, Rua Arquiteto Lobão Vital, 172, 4200-374 Porto, Portugal

2CESPU, Instituto de Investigação e Formação Avançada em Ciências e Tecnologias da Saúde, Rua Central de Gandra 1317, 4585-116 Gandra-PRD, Portugal

3 i3S - Instituto de Investigação e Inovação em Saúde, Universidade do Porto, Rua Alfredo Allen 208, 4200-393 Porto, Portugal

4 INEB - Instituto Nacional de Engenharia Biomédica, Universidade do Porto, Rua Alfredo Allen 208, 4200-393 Porto, Portugal

4.1. Abstract

Oral administration of proteins and peptides still is a challenging task, due to low permeability through absorptive epithelia, degradation and metabolism that lead to poor bioavailability. Attempting to overcome such limitations, an antihypertensive peptide derived from whey protein, with KGYGGVSLPEW sequence, was incorporated for the first time into polymeric nanoparticles. An experimental design was followed in order to optimize drug-loading, association efficiency, mean particle size, zeta-potential and polydispersity index of a formulation of poly(lactic-co-glycolic acid) (PLGA)

nanoparticles as carriers for bioactive peptides. In sequence, peptide-loaded PLGA nanoparticles were incorporated in a guar gum film matrix, resulting in a combined delivery system aiming to promote slow release and permeation across buccal epithelium. The association of PLGA nanoparticles with guar gum films resulted in a formulation with higher adhesiveness, work of adhesion and debonding distance when compared with guar gum films alone which contributed to a more intimate contact with epithelia and thus promoting permeability to reach systemic circulation. Neither PLGA nanoparticles, guar gum films, nor the conjugation of PLGA nanoparticles and guar gum films (GfNp) significantly compromised *in vitro* TR146 human buccal carcinoma cell line or Caco-2/HT29-MTX co-culture viability after 12 h contact, as assessed by 3-(4,5-Dimethylthiazol-2-yl)-2,5-Diphenyltetrazolium Bromide reduction assay (MTT). *In vitro* release assay for developed formulations allowed to conclude that the combination of orodispersible film and nanoparticles granted a slower release of AhP when compared with PLGA or guar gum films alone or with control. GfNp offered more effective, synergistic, *in vitro* permeation of TR146 and Caco-2/HT29-MTX cell layers in comparison with guar gum films or PLGA nanoparticles alone. The combination of PLGA nanoparticles with guar gum films represent a suitable alternative to conventional *per os* delivery systems, leading to an increased buccal permeability of carried antihypertensive peptide.

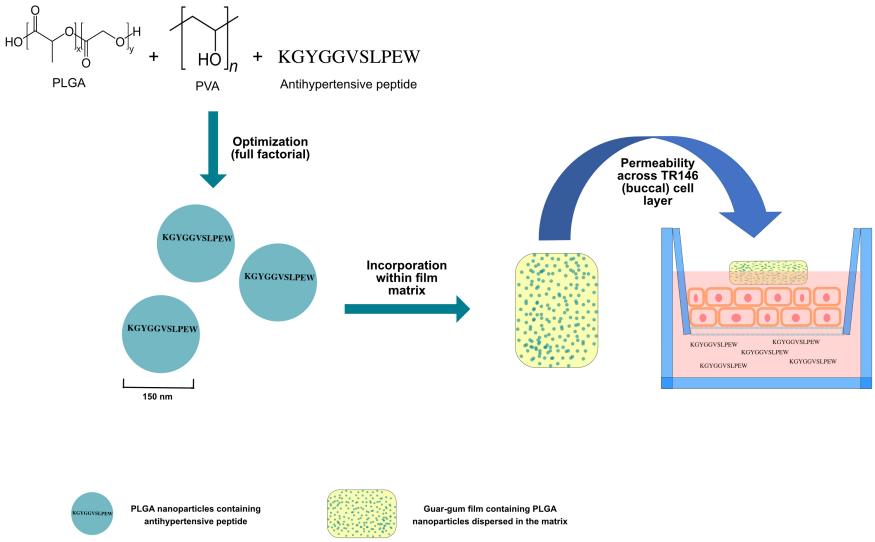

4.2. Introduction

Bioactive whey-derived peptides can be used in the elaboration of products with therapeutic interest, namely in the management and treatment of diseases of the immune, gastrointestinal, cardiovascular and nervous systems (Dullius, Goettert & de Souza, 2018; Tavares, Contreras Mdel, Amorim, Pintado, Recio & Malcata, 2011). Nevertheless, some bioactive peptides are prone to lose biological activity due to enzyme-mediated degradation and extreme pH conditions that occur during passage through the gastrointestinal tract (GIT). Also, proteins and peptides administered *per os* enter the hepatic portal system being metabolized in the liver, greatly reducing the concentration of bioactive proteins/peptides that reach the systemic circulation. The buccal administration route allows to avoid extreme gastrointestinal conditions (i.e. pH,

digestive mechanical action and enzymatic activity) along with first-pass effect, therefore increasing the bioavailability of carried bioactive molecules. Small-sized nanoparticles with proper zeta-potential can be interesting delivery systems with potential to promote adherence to buccal epithelium along with absorption of entrapped molecules, offering a more extensive permeation of carried bioactive molecules across buccal mucosa and a slow release (Al-Dhubiab, Nair, Kumria, Attimarad & Harsha, 2015). Thus, mucoadhesion (or association with mucoadhesive carriers) must be granted for nanoparticles to act as effective buccal delivery systems (Mansuri, Kesharwani, Jain, Tekade & Jain, 2016). Furthermore, due to saliva turnover, tongue movements and swallowing reflexes, a part of the formulation follows through the gastrointestinal tract and nanoparticles should be effective at protecting the peptide from the enzymatic activity and extreme pH values.

The antihypertensive peptide (AhP) was first obtained from the hydrolysis of whey protein concentrate, using a commercial aqueous extract of *C. cardunculus*, that presents cardosins – aspartic proteinases (Tavares, Contreras Mdel, Amorim, Pintado, Recio & Malcata, 2011). After isolation and identification, peptides were tested *in vitro* for ACEI effect. The most potent angiotensin converting enzyme inhibitor (ACEI) peptide that originates from whey protein hydrolysate has the sequence KGYGGVSLPEW (IC_{50} of 0.7 ± 0.05 μM). Aiming for a bioavailability increase of a whey-derived antihypertensive peptide, a buccal delivery system comprising a mucoadhesive oral film associated with poly(lactic-co-glycolic acid) (PLGA) nanoparticles was developed. PLGA polymer was selected due to reported biodegradability and biocompatibility, allowing to produce safe nanocarriers that offer a controlled release of carried molecules (Batista, Castro,

Madureira, Sarmento & Pintado, 2018; Ding & Zhu, 2018; Mir, Ahmed & Rehman, 2017). Guar gum films formulation, previously optimized by the group, are mucoadhesive formulations that are suitable as carriers for peptide-loaded nanoparticles (Castro et al., 2018c). Guar gum films grant an intimate contact with buccal epithelium, enhancing contact time between the peptide-loaded nanoparticles and the mucosa, therefore improving the permeation extension of the antihypertensive peptide (Castro et al., 2018c; Mansuri, Kesharwani, Jain, Tekade & Jain, 2016). Thus, the formulation of PLGA nanoparticles was optimized by factorial design (2^3), aiming to obtain the formulation that grants simultaneously the best association efficiency along with suitable mean size for buccal permeation and zeta-potential values that grant stability of the formulation. Cytotoxicity induced by developed formulations was evaluated by MTT using TR146 human buccal carcinoma cells as model to simulate the buccal epithelium. Finally, *in vitro* release profile was assessed by determining the cumulative AhP release from a dialysis bag and permeability through a TR146 cell multilayer.

4.3. Materials and methods

4.3.1. Materials

The antihypertensive peptide with the sequence KGYGGVSLPEW (99.7%) was purchased from GenScript (China). Poly (lactic-co-glycolic acid) (50:50) was kindly offered by Purac. Ethyl acetate 99.5%, poly(vinyl alcohol) and D-sorbitol (assay purity ≥98%) were purchased from Sigma-Aldrich (Steinheim, Germany). Citric acid monohydrate, potassium phosphate monobasic anhydrous and sodium phosphate dibasic were purchased from Merck (Darmstadt, Germany). Sodium chloride was purchased

from Panreac (Barcelona, Spain). Deionized water was used to prepare all oral films formulations and Milli-Q water was used to prepare peptide standard solutions and eluents used in chromatography procedures. TR146, Caco-2 and HT29-MTX cell lines were purchased from Sigma-Aldrich (Stenheim, Germany). Transwell® flasks (12 well) and inserts (collagen-coated, 1.12 cm^2 of culture area, 0.4 μm pore size and 12 mm membrane diameter) were purchased from Corning (New York, USA). 96-well plates were purchased from Thermo Scientific (Denmark). Fetal Bovine Serum (FBS), HAMS-F12 culture medium and Pen-Strep (10 000 U Penicillin, 10 000 U Streptomycin) were purchased from Lonza® (Verviers, Belgium). TrypLE™ express was purchased from Gibco® (Denmark). Thiazolyl Blue Tetrazolium Bromide (MTT) Ultra-Pure was purchased from VWR (Solon, USA). Dimethyl sulphoxide (DMSO) 99.7% was purchased from Fisher Bioreagents™ (EUA). Phosphate buffer saline (PBS) solution was prepared by dissolving 8.0 g of sodium chloride, 0.2 g of potassium chloride, 1.44 g of monobasic sodium phosphate and 0.24 g of dibasic potassium phosphate to 1 L of ultrapure water and by adjusting pH to 7.4 using a solution of sodium hydroxide 0.1M. For cell wash, pH of PBS was adjusted to 6.8, using a solution of hydrochloric acid 0.1 M.

4.3.2. Experimental design

The experimental design was performed recurring to a full factorial design (n = 11, 2^3) through SAS JMP® 9 software. The concentration of PLGA and PVA were chosen as independent variables due to the well-known significant influence on responses to optimize (i.e. mean particle size, polydispersity index, zeta-potential, association

efficiency and drug loading) (Abdelkader, El-Gizawy, Faheem, McCarron & Osman, 2018). For each factor (independent variable) there a minimum, an intermediate and a maximum values (-1, 0 and 1, respectively) were selected. Formulation of PLGA nanoparticles was optimized by setting the relative amounts of PLGA (0.5%, 1.5% and 2.5%, w/v) and PVA (5%, 7% and 9%, w/v) as factors. Relative amounts of PLGA and PVA to be tested were selected according to the literature (Santos et al., 2017).

4.3.3. Production and characterization of PLGA nanoparticles

Nanoparticles of PLGA were prepared by double emulsion technique, as described by Araújo et al. with slight modifications (Araujo et al., 2014). Briefly, a solution of the bioactive peptides was added dropwise to a solution of PLGA dissolved in 2 mL of ethyl acetate and sonicated for 30 s at 70% amplitude with a ultrasonicator (SONICS VibraCell EUA), resulting in a W/O emulsion. A solution of PVA was simultaneously prepared in separate and added to the sonicated PLGA solution. Immediately, the resulting simple emulsion was sonicated for 30 s and 70% amplitude, resulting in a w/o/w double emulsion. The double emulsion was kept stirring (600 rpm) for 3 h for the complete evaporation of ethyl acetate to occur, leading to the hardening of the nanoparticles.

4.3.4. Characterization of PLGA nanoparticles

PLGA nanoparticles were diluted (1:50) with Milli-Q water before particle size and zeta-potential analysis. Particle size and polydispersity index were determined by dynamic light scattering (DLS). Zeta-potential was determined by phase analysis light

scattering. All measurements were performed in triplicate in a Zetasizer Nano ZSP equipment (Malvern Instruments Ltd, Worcestershire, UK).

4.3.4.1. Peptide association efficiency (AE)

The association efficiency of AhP in PLGA nanoparticles were determined by quantifying the free peptides content (HPLC-UV) of the filtrate of each nanoparticle formulation after being filtered through Amicon® 50,000 Da filters during 45 min at 13 ºC and 4000 rpm. Peptides concentration in the filtrate or supernatant was determined by HPLC-UV on a Waters Alliance® instrument (Milford, MA, USA). Water and trifluoroacetic acid (99.9:0.1) – Phase A - and acetonitrile and trifluoroaceteic acid (99.9:0.1) – Phase B – were used as mobile phases. A gradient was set as follows: 80% of phase A and 20% of phase B for 10 min, 50% of phase A and 50% of phase B for 5 min and 80% of phase A and 20% of phase B for 5 min. Flow was set to 0.8 mL/min. Samples were run through a Kromasil® C18 column, 5 μm (particle size) × 4.6 mm (internal diameter) × 250 mm (length) (AkzoNobel, Bohus, Sweden). UV detector wavelength was set to 280 nm. The injection volume was set to 20 μL.

AhP association efficiency was calculated according to the following Eq. (7):

$$\frac{Wtc - Wsc}{Wtc} \times 100 \qquad (7)$$

where, Wtc stands for total weight of AhP used in the formulations and Wsc stands for AhP collected from the supernatant after centrifugation.

4.3.4.2. Preparation of guar gum films and assembling process with PLGA nanoparticles

Guar gum films were previously optimized by our group and were prepared by the solvent casting technique (Castro, Fonte, Oliveira, Madureira, Sarmento & Pintado, 2017). Briefly, 54 mg of sorbitol, 40 mg of guar gum and 7.6 mg of citric acid were added to 2 mL of distilled water and stirred until complete dissolution. Resulting solution was poured in a Petri dish (90 mm diameter) and heated to 37 ºC for 1 h and kept at room temperature for the following 12 h. For the incorporation of PLGA nanoparticles within the film matrix, sorbitol, guar gum and citric acid were dissolved in 2 mL of a previously prepared nanoparticle dispersion instead of the distilled water.

4.3.5. *In vitro* release assay

In vitro release assays for buccal mucosa were performed to compare the release profile of AhP from guar gum films, PLGA nanoparticles and GfNp. *In vitro* dialysis delivery assay was performed according to Wang, et al. [17]. Formulations were introduced into a 500 Da dialysis membrane. Dialysis membrane with a pore size of 500 Da was chosen to mimic the pore size of buccal mucosa [2]. Dialysis membrane was filled with 5 mL of artificial saliva (pH = 6.8), clumped and dipped into 50 mL of PBS solution (release media) pre-heated to 37 ºC. The system was kept on continuous shaking (100 rpm). Aliquots of 1 mL were withdrawn from release media at 15, 30, 60, 120, 180 and 240 min. Withdrawn volume was immediately replaced with 1 mL of PBS and pre-heated to 37 ºC to preserve sink conditions.

Release kinetics of AhP from tested formulations were tested using zero-order, first-order, Higuchi and Korsmeyer-Peppas functions and best fit was determined by calculating determination coefficient values (R^2) (Jain & Jain, 2016).

4.3.6. Human buccal epithelium cell line culture

Trans-epithelial permeability assay and cell viability after contact with produced formulations were performed using TR146 human buccal epithelium cell line culture. TR146 cell line was chosen due to great resemblance of normal human buccal mucosa, namely regarding undifferentiated, non-keratinized stratified epithelium, morphological and functional characteristics as activity of carboxypeptidase, esterase and aminopeptidase (Morck Nielsen & Romer Rassing, 2000). Also, expression of K4, K10, K13, K16 and K19 keratins, membrane-associated receptors for involucrin and epidermal growth factors also reflect other common characteristics to normal human buccal epithelium cells (Jacobsen et al., 1999; Jacobsen, van Deurs, Pedersen & Rassing, 1995).

TR146 cell line was purchased from Sigma-Aldrich (USA) and passages 9 to 14 were used. The culture medium consisted of HAMS F-12 medium enriched with 2 mM Glutamine (Lonza), 10% (v/v) fetal bovine serum (FBS) and 1% (v/v) of penicillin-streptomycin antibiotic blend. TR146 cells were seeded and maintained in 75 cm^2 T-flasks (T-75) and incubated in a 5% CO_2/95% air and 98% relative humidity atmosphere. The culture medium was replaced every two days. When 70-80% of cell confluence was reached, cells were detached from T-75 flasks using 2 mL of TrypLE^{TM} Express. Detached cells were then prepared and seeded either in other T-75 flasks, 96-well culture

plates (Nunc®) or in Transwell® inserts 12-well culture plates purchased from Corning® (Germany).

4.3.7. Co-culture of Caco-2/HT29-MTX intestinal cells

Caco-2 (Caucasian colon adenocarcinoma) cell line is widely used for the study of intestinal permeation of bioactive molecules (Araujo & Sarmento, 2013). Nevertheless, Caco-2 monoculture was not significantly representative of duodenum epithelia due to the formation of tight junctions that typically occur in the colon but not in the small intestine, leading to a hindrance of the absorption of hydrophilic molecules. Also, Caco-2 monoculture is exclusively composed of enterocytes and overexpress efflux transporters, typical of an excretory rather than absorptive epithelia. Therefore, HT29-MTX (Caucasian colon adenocarcinoma grade II) cell line is used in co-culture with Caco-2 cells. HT29-MTX were chosen due to mucus producing ability, as occurs in the duodenum mucosa.

Thus Caco-2/HT29-MTX co-culture was used to better mimic the *in vivo* conditions that occur in the duodenum. HT29-MTX and Caco-2 cell lines were grown separately in Dulbecco's Modified Eagle Medium (DMEM) supplemented with 10% (v/v) fetal bovine serum, 1% (v/v) L-glutamine, 1% (v/v) penicillin and streptomycin and 1% (v/v) of non-essential aminoacids, at 37 ºC under a 5% CO_2 water-saturated atmosphere. Upon 70-80% confluence, cells were detached as described before. Co-culture seeding in Transwells® was performed in a 9:1 ratio of Caco-2 (3 x 10^5 cells/well) and HT29 (3 x 10^5 cells/well) cells, respectively (Antunes, Andrade, Araujo, Ferreira & Sarmento, 2013).

4.3.8. Peptide integrity analysis

Chemical and structural integrity of AhP was determined by attenuated total reflectance Fourier-transform infrared (ATR-FTIR) spectroscopy. Analysis was performed on the peptide alone and incorporated in PLGA nanoparticles, guar gum films and FNps. ATR-FTIR analysis were conducted in a FTIR spectrometer, model ABB MB3000 (ABB, Switzerland), equipped with a deuterated triglycine sulphate detector and using a MIRacleTM single reflection horizontal attenuated total reflectance (ATR) accessory (PIKE Technologies, USA) with a diamond/Se crystal plate. All spectra were acquired with 256 scans and 4 cm-1 resolution, in the region of 4000-500 cm-1.

4.3.9. Tongue adhesion

Adhesion to tongue assessment was performed for FNp and guar gum films on a texturometer (TA.XT plus Texture Analyser, Stable Micro Systems, United Kingdom). Mounted load cell presented a 5 kg capacity and force was calibrated with a 2 kg weight. Briefly, the formulations were adhered to the testing probe (squared shape, 6.25 cm^2) and a cow tongue (obtained fresh from a local slaughterhouse) was mounted on the texturometer support platform. Following, 3.5 mL of artificial saliva (pre-heated to 37 ºC) were poured dropwise on the top of the tongue. The probe was set to descend until contact between the formulation and the tongue occurred. Contact force was set to 5 g and contact time was set to 30 s. Thereafter, the probe ascended at a speed rate of 0.1 mm/s and debonding force was registered, allowing to determine adhesiveness (N), work of adhesion (N.s) and debonding distance (mm).

4.3.10. Cell mitochondrial activity assessment

Cell-viability studies were carried out on proliferating cells, chosen when TR146 cells were 70-80% confluent in T-75 flasks and properly detached as described above. After detachment, cells were re-suspended in medium and seeded in 96-well plates with a concentration of 1 x 10^4 cells/mL, 200 μL per well. The same cell concentration was adopted in the 12-well plates but using 500 μL of cell suspension, after *in vitro* permeability assay. Cell-viability studies were performed after 24 h of culture, with previous supervision by optical microscopy of the morphology and confluence of the cells in the plate wells. MTT assay allows to assess mitochondrial viability and, therefore, cell viability after 12 h contact with prepared delivery systems (da Silva, Ferreira, Pintado & Sarmento, 2016a). If TR146 cells were viable, succinic dehydrogenase was able to transform the tetrazolium salt into insoluble, purple-coloured, crystals of formazan (Mosmann, 1983a). Medium with 1% (v/v) Triton X-100 solution was added as lysis buffer and served as positive control. Negative control consisted of cells in contact with medium only. After treatment with produced formulations, 100 μL of the MTT reagent (0.5 mg/mL prepared in culture medium) was added to each well and the plates were incubated for 4 h. After incubation time has passed, reagent was carefully removed, allowing the insoluble formazan crystals to remain in the bottom of the wells. 100 μL of DMSO per well was used to solubilize the formazan crystals in a dark room and, after 15 min of agitation on an orbital shaker, the absorbance at 570 nm and 630 nm was read on a FLUOstar OPTIMA microplate reader (United Kingdom), in triplicate. Absorbance values for all readings at 630 nm were subtracted from the absorbance values read at 570

nm. Cell viability (%, n = 6 different, independent wells for the same experiment) was calculated according to Eq. (8):

$$\textbf{\textit{Cell viability}}\ (\%) = \frac{\textit{Experimental value} - \textit{negative control}}{\textit{Positive control} - \textit{negative control}} \times \mathbf{100} \qquad (8)$$

Concentration of the formulations tested for potential commitment of TR146 cell viability were chosen according to the average amount of saliva produced in the human mouth when in contact with food products (Watanabe & Dawes, 1988b).

4.3.11. Peptide trans-epithelial diffusion study across buccal (TR146) and intestinal (Caco-2/HT29-MTX) cell layers

Permeability assay was assessed in Corning® Transwell inserts, using 12-well plates. TR146 cells and Caco-2/HT29-MTX co-culture were seeded into the inserts to mimic stratified epithelium of human buccal mucosa and the intestinal absorptive epithelia, respectively , as reported previously (Jacobsen, van Deurs, Pedersen & Rassing, 1995; Zeng et al., 2015b). TR146 cells and Caco-2/HT29-MTX were seeded on the inserts and the medium was changed every two days for 21 and 28 days, respectively.

For medium replacement, medium was removed from the wells and 0.5 and 1.5 mL of fresh culture medium was added to the apical and basolateral sides, respectively. On the day of the study, culture medium was totally removed. Medium in the basolateral side (receptor part) was replaced with 1.5 mL of PBS, pH 6.8. Medium in the apical side (donor part) was replaced with fresh medium and peptide delivery formulations were

introduced afterwards. Guar gum films, PLGA nanoparticles, GfNp and free AhP (n = 5) were tested. Samples of 600 μL were withdrawn from receptor part at 0, 15, 30, 60, 120, 180 and 240 min. Withdrawn volume was immediately replaced with fresh PBS, pre-heated to 37 ºC, to maintain sink conditions. The permeation experiments were carried out in 5 wells per peptide delivery system sample. After the final samples were drawn from the basolateral side, apical side content was fully aspirated and 1.0 mL of DMSO was used to destroy the cells in each well for the quantification of AhP adsorbed to the cell surface or present within the cells or in the transepithelial space. An aliquot of the aspirated portion from the apical side was also collected to quantify the peptide concentration that was dissolved or suspended. For PLGA nanoparticles and GfNp, 100 μL of ethyl acetate were added to the aliquot obtained from the apical solution to dissolve remaining polymer, inducing the release of the peptide. The concentration of AhP was determined by HPLC-UV, using the same method as previously described.

The fractional amounts of AhP that permeated the layer of TR146 buccal epithelia cells and the co-culture of Caco-2/HT29-MTX cells (dQ) were determined over the time intervals (dt) and the flux (*J*) was determined by calculating the slope of the resulting plots, according to Eq. (5) (di Cagno, Bibi & Bauer-Brandl, 2015).

$$J = \frac{dQ}{A \times dt} \qquad (5)$$

Apparent permeability (P_{app}, cm/s) was calculated for a control solution (500 μg/mL), for peptide-loaded PLGA nanoparticles, guar gum films and GfNp, by

normalizing the flux (J) over the concentration of peptide in the apical side (C_0) according to Eq. (6).

$$Papp = \frac{J}{Co} \quad (6)$$

where, dQ/dt stands for the rate of permeated peptide over time, A for the cell layer surface area and Co for the initial concentration of peptide.

4.3.12. Determination of angiotensin-converting enzyme inhibition capacity

The fractions of the basolateral sides of both TR146 and Caco-2/HT29-MTX cell layers were withdrawn, after the last time point of the permeability assays of each tested formulation, gathered and used to determine the antihypertensive activity, as a representation of the fraction of the peptide absorbed to the systemic circulation. Before permeability across Caco-2/HT29-MTX co-culture layer was determined, the solution remaining in the apical side in the end of the permeability assay across TR146 cell layer was subjected to a simulated gastric and intestinal simulation. Briefly, samples were added to a 0.1 M HCl (pH 5.5) solution with previously dissolved pepsin (25 mg/mL) and maintained stirring (130 rpm) at 37 ºC. Further, after 10, 20 30, 40 and 50 min, pH of the solution was successively lowered (with HCl 1 M) to 4.6, 3.8, 2.8, 2.3 and 2.0, respectively. Finally, the pH of the digest was adjusted to 5.0, using $NaHCO_3$ 1M, and adding a solution of bile salts and pancreatin (final concentrations of 2 mg/mL and 12 mg/mL, respectively) to the digest. Resulting solution was immediately transferred to the apical side of Transwells seeded with Caco-2/HT29-MTX co-culture cell layers (Laurent, Besancon & Caporiccio, 2007; Madureira, Amorim, Gomes, Pintado & Malcata, 2011b).

Following, the determination of the angiotensin-converting enzyme inhibition capacity of AhP was performed on the solutions resulting from the basolateral contents of TR146 and Caco-2/HT29-MTX wells, for each sample. Angiotensin-converting enzyme inhibition capacity was then measured by fluorescence according to the method stated by Quirós et al. with slight modifications (Quirós, del Mar Contreras, Ramos, Amigo & Recio, 2009). Briefly, angiotensin converting enzyme from rabbit lung (Sigma, USA) was diluted with 0.15 M Tris buffer (pH 8.3) containing 0.1 μM $ZnCl_2$ for a final enzyme concentration of 0.04 U/mL. A total of 40 μL of the enzyme solution were added to each well of a black 96-well microplate (ThermoFisher Scientific, USA). Further 40 μL of the samples were added to the wells (40 μL of ultrapure water were added instead for blank and control). The enzyme reaction was started by adding 160 μL of the substrate (0.45 mM o-Abz-Gly-p-Phe(NO_2)-Pro-OH) (Bachem Feinchemikalien, Bubendorf, Switzerland) previously dissolved in 150 mM Tris-base buffer (pH 8.3), containing 1.125 M NaCl. The microplates were then incubated at 37 ºC. Fluorescence was determined every 10 min for a total time of 60 min using a multiscan microplate fluorimeter (FLUOstar optima, BMG Labtech, Effeuburg, Germany). Excitation and emission wavelengths were set to 350 and 420 nm, respectively.

The activity of each sample was tested in triplicate. Inhibitory activity was expressed as the percentage of inhibition of the angiotensin converting enzyme by each fraction corresponding to the developed formulations (i.e. PLGA nanoparticles, guar gum films and FNp) and to free AhP and results were adjusted according to the percentage of peptide that permeated cell layers for each formulation.

4.3.13. Statistical analysis

Statistical analysis regarding dissolution profile data was performed using IBM® SPSS® Statistics version 22.

Shapiro-Wilk ($n < 50$) test was used to verify if the values obtained for the responses in the experimental design were normally distributed. One sample T test was used to verify the existence of statistically significant differences between predictive models and experimental values. Experimental values were obtained from three samples selected from three new batches, for PLGA nanoparticles. Mean values for each batch were compared with the values predicted in the model.

4.4. Results and discussion

4.4.1. Experimental design

Formulation of PLGA nanoparticles was optimized by factorial design ($n = 2^3$). The experimental design was augmented to $n = 11$ to assure robustness of the factorial design. Mean particle size, zeta-potential and association efficiency were selected as responses with equal importance in the optimization of the formulation of PLGA nanoparticles.

4.4.1.1. PLGA nanoparticles characteristics

Peptide-loaded nanoparticles, prepared in the scope of a factorial design, were tested in triplicate. Average results were considered for the determination of both the relative influence of each factor on the responses, but also to obtain the formulation composition that leads to the best combination of nanoparticle characteristics as peptide delivery systems. Characteristics of each nanoparticle formulation prepared are outlined in **Table 15.**

Table 15: Results of experimental design for the optimization of PLGA nanoparticles

PLGA (mg)	PVA (%, w/v)	Association Efficiency (%)	Size (nm)	Polydispersity index	Zeta-potential (mV)
100	9	16.69	199.9	0.217	-7.7
100	7	41.89	200.7	0.188	-8.9
100	5	43.41	222	0.158	-11.2
60	9	41.46	205.8	0.229	-8.9
60*	7*	58.64	160.1	0.095	-9
60*	7*	42.4	158.2	0.07	-10.6
60*	7*	51.53	218.2	0.229	-9.3
60	5	35.85	204.4	0.216	-10
20	9	61.06	125.1	0.146	-6
20	5	48.76	126.6	0.057	-8.9
20	7	37.68	120.9	0.187	-15

*** Centre points added to the experimental design**

Only the factors with statistically significant effects on factorial design responses (i.e. r^2 and r^2 adjusted ≥ 0.9) were chosen to integrate the prediction profiler. From the obtained data regarding each formulation of the factorial design, it was possible to observe that both PLGA amount and PVA solution concentration induced significant influence on responses as outlined in the prediction profiler (**Figure 25)**. After theoretical optimization, to validate the results, formulations of PLGA nanoparticles (n = 3) prepared using 42.6 mg of PLGA and 2 mL of a solution of PVA 7.6% (w/v) were further assessed for mean size, polydispersity index, zeta-potential and association efficiency. The obtained results were individually compared with theoretical (predicted) values by T-student tests. No statistically differences ($P > 0.05$) were found between predicted and experimental values, as outlined in **Figure 26**, supporting the robustness of the optimized nanoparticle formulation obtained by factorial design.

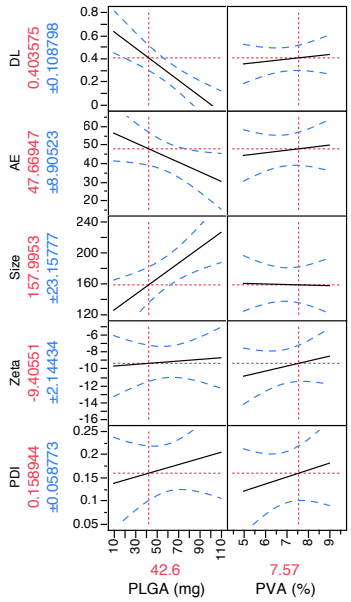

Figure 25: Prediction profiler of the effects of excipients on the responses (DL= drug loading; AE= Association Efficiency, Size= mean particle size; Zeta= zeta-potential; PDI= Polydispersity Index) along with definition of optimal formulation composition

A B C D E

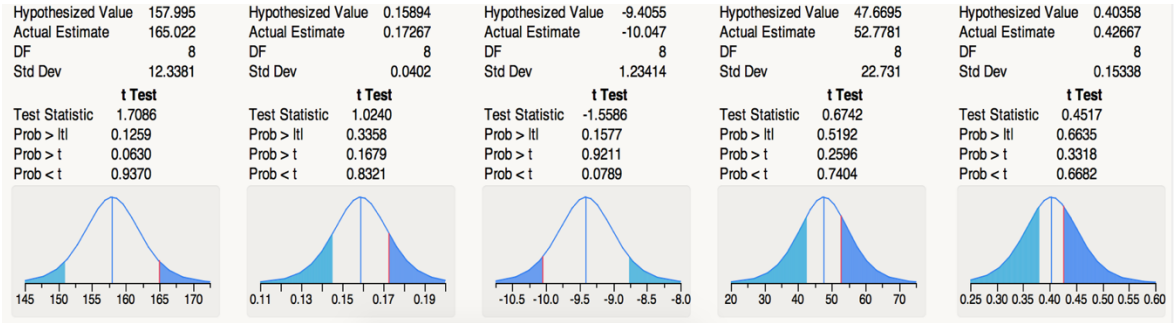

Figure 26: T-student tests indicated that there are not statistically significant differences ($P > 0.05$) between predicted and experimental data, regarding mean particle size (A), polydispersity index (B), zeta-potential (C), association efficiency (D) and drug-loading (E)

Both drug-loading and association efficiency were comparable to other PLGA nanoparticle formulations described in the literature even though, to our knowledge, no attempts to use nanoparticles as carriers for KGYGGVSLPEW peptide were performed (Araujo et al., 2014). Most authors use 100 mg of PLGA dissolved in 2 mL of an aqueous

dispersant as standard amount of polymer (Cerqueira, Lasham, Shelling & Al-Kassas, 2017; Santos et al., 2018; Santos et al., 2017; Shi, Xue, Jia, Du, Niu & Zhang, 2018). In contrast, by the analysis of prediction profiler, an increase of PLGA amount above 42.6 mg would lead to unwanted consequences as decrease of both drug-loading and association efficiency and an increase of particle size, polydispersity index and zeta potential.

Defined optimized formulation of PLGA nanoparticles (i.e. 42.6 mg of PLGA and 2 mL of aqueous PVA solution 7.6% (w/v)) was further used for determination of TR146 cell viability assay, *in vitro* peptide release and peptide transepithelial diffusion studies.

4.4.2. *In vitro* peptide release

In vitro peptide release assay allowed to compare the release profile of AhP provided by each developed delivery system, using a solution of free peptide as control. It was possible to observe that release of free peptide to the external phase was significantly faster and more extensive when compared with AhP-loaded nanoparticles, guar gum films or GfNp along 240 min (**Figure 27)**. Dissolution similarity and difference factors (calculated through the determination of f_2 and f_1 statistic, according to Eq. (10) and Eq. (11) respectively) confirmed the differences in dissolution between the solution of free peptide and developed formulations.

$$f2 = 50.log\{[1 + \frac{1}{n}\sum_{t=1}^{n}(Rt - Tt^2)\,]^{-0.5} \times 100\} \quad (10)$$

$$f1 = 50.log\left\{\frac{\sum_{t=1}^{n}|Rt-Tt|}{\sum_{t=1}^{n}Rt}\right\} \quad (11)$$

where, Rt and Tt are the cumulative percentage dissolved at each of the selected n time points of the reference and test product respectively.

Calculated values of f_2 and f_1 between free AhP solution and developed formulations are outlined in **Table 16**. Indeed, according to the guidelines of European Medicine Agency regarding the investigation of bioequivalence, values of f_2 lower than 50 indicate the absence of bioequivalence (Agency, 2010). Also, f_1 values closer to 50 confirm that the free peptide solution has a significantly higher dissolution rate than developed formulations.

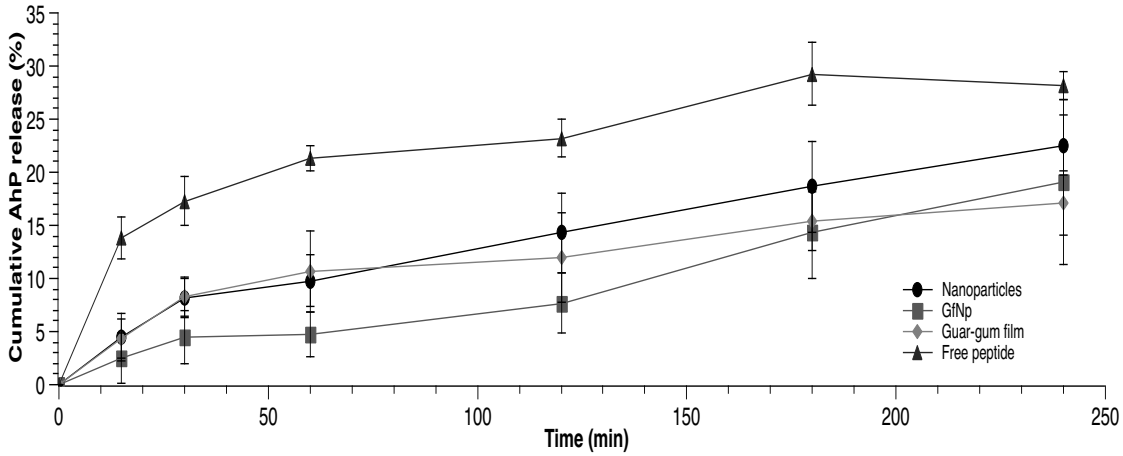

Figure 27: Cumulative release (% ± S.D.) of antihypertensive peptide from developed delivery systems

Table 16: Similarity and difference factors between developed formulations

	Solution of free AhP	**PLGA nanoparticles**	**GfNp**
Guar gum films	$f_2 = 48$ $f_1 = 49$	$f_2 = 76$ $f_1 = 18$	$f_2 = 71$ $f_1 = 28$
GfNp	$f_2 = 43$ $f_1 = 60$	$f_2 = 70$ $f_1 = 29$	x
PLGA nanoparticles	$f_2 = 51$ $f_1 = 41$	x	x

On the other hand, AhP release profile from guar gum films and PLGA nanoparticles were very similar along 240 min of study, also indicating that both formulations offered a slower release of carried peptide when compared to free AhP. Both nanoparticles and films provided a similar burst release in the first 30 min (Dalpiaz et al., 2016). Release profile of AhP from both PLGA nanoparticles and guar gum films followed the Higuchi model (**Table 17**) (Gunday Tureli et al., 2017).

Burst release provided from guar gum films in the first 30 min probably resulted from the dissolution of AhP adsorbed to the surface of the polymeric matrix. On the other hand, from 30 min to 240 min, peptide release occurred as the film disintegrated leading to a gradual dissolution of the carried peptide.

Further, peptide release from PLGA nanoparticles also occurred in two phases. Indeed, PLGA nanoparticles are reported to offer an initial burst release of adsorbed molecules to the particle surface and a second, slower release, as the nanoparticle erodes in contact with media (Cerqueira, Lasham, Shelling & Al-Kassas, 2017).

Even though no significant differences were found between the dissolution profile of guar gum films, PLGA nanoparticles and GfNp (f_2 was always above 50 between formulations), results suggested that GfNp could provide the slowest release of AhP, especially in the first 120 min (Agency, 2010). Indeed, the incorporation of nanoparticles within a film matrix has been reported as a method to reduce initial burst release of carried molecules (dos Santos et al., 2017; Satarkar & Hilt, 2008). Release profile of the peptide carried by GfNp also followed the Higuchi model (**Table 17**). Nevertheless, the continuous peptide release from GfNp after 240 min was also overlapping with both guar gum films and PLGA nanoparticles.

Higuchi kinetics model is commonly used to explain release from polymeric delivery systems and was firstly developed for planar systems as orodispersible films (Petropoulos, Papadokostaki & Sanopoulou, 2012). Indeed, besides from solubility, Higuchi models takes diffusivity of carried molecules from the matrix into account for the characterization of molecule release. Diffusion, along with erosion, are main parameters that define release of carried bioactive molecules from PLGA nanoparticles (Ding & Zhu, 2018; Fredenberg, Wahlgren, Reslow & Axelsson, 2011).

The fact that peptide release was incomplete for all tested formulations is explained by the bidirectional flow of AhP between the inside of the dialysis bag and the external media, according to the Fick's first law of diffusion but also due to the incomplete release of AhP by PLGA nanoparticles. In fact, after an initial burst release, it is widely reported that polymers as PLGA promote a slow or even incomplete release of carried molecules. The release of bioactive molecules from PLGA nanoparticles is reported to occur according to two distinct phases. In phase I, the dissolution medium induces the release of the bioactive molecule contained on the surface of the particle and leads to a random break of the polymeric structure with loss of molecular weight of the polymer (Sharma, Parmar, Kori & Sandhir, 2016). In phase II, the erosion of a thicker polymer layer must occur to allow the diffusion of remaining carried bioactive molecule, leading to a much slower release. Effectively, release of molecules carried from polymeric structures as PLGA nanoparticles is reported to be complete only after several days, especially when impregnated within films (Giovino, Ayensu, Tetteh & Boateng, 2012; Morales & Brayden, 2017). The fact that PLGA nanoparticles were retained in the guar gum polymeric matrix may have also delayed the release of the peptide.

Table 17: Suitability of kinetic models to release profile of developed formulations

Formulation	Zero-order	First-order	Higuchi	Korsmeyer-Peppas
Free peptide	r^2= 0.691	r^2= 0.735	r^2= 0.899	r^2= 0.986*
PLGA nanoparticles	r^2= 0.947	r^2= 0.961	r^2= 0.991*	r^2= 0.855
Guar gum films	r^2= 0.840	r^2= 0.859	r^2= 0.970*	r^2= 0.934
GfNp	r^2= 0.915	r^2= 0.928	r^2= 0.981*	r^2= 0.861

*highest r^2 value, indicating most suitable kinetic release model corresponding to the formulation
GfNp – association of guar gum films with PLGA nanoparticles

4.4.3. Peptide integrity analysis

The infrared spectra of AhP alone or loaded in developed formulations was obtained by ATR-FTIR, aiming to understand if any alteration of the chemical structure of the peptide occurred after inclusion in guar gum films, PLGA nanoparticles or FNps. The spectra are outlined in **Figure 28**.

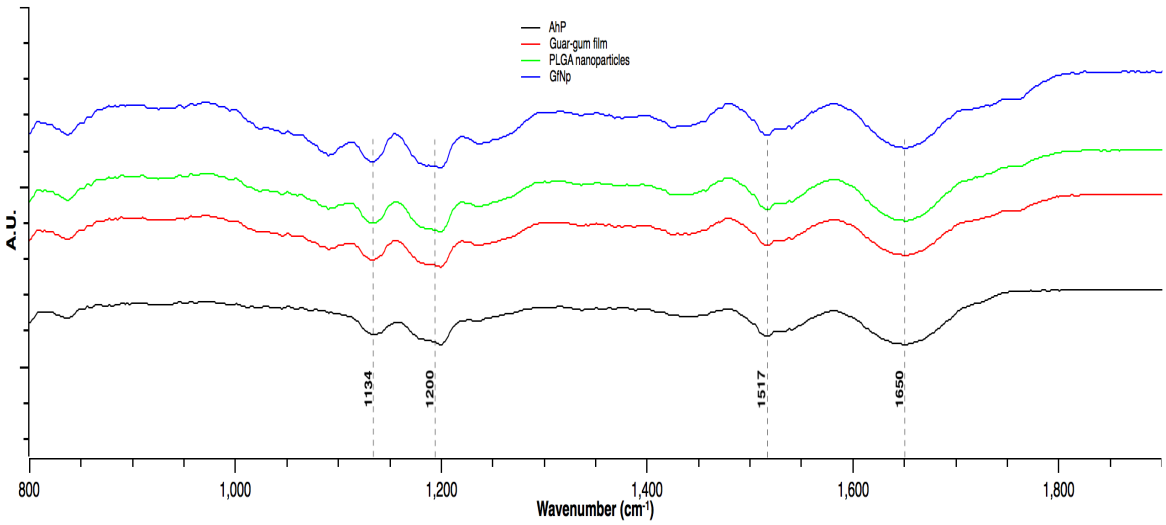

Figure 28: Infrared spectra of AhP and AhP-loaded guar gum films, PLGA nanoparticles and FNps

Bands between 1100 cm^{-1} and 1250 cm^{-1} (within fingerprint region) indicated the presence of C-C-O and C-OH bonds that are present either in the peptide molecules and

in the chemical composition of developed formulations. Peptide bond characteristic bands resulting from the bending motions of the N-H groups and from the stretching of the C-N bonds were observed between 1490 cm^{-1} and 1580 cm^{-1} (amide II band) (Nixon, 2014). Moreover, a band between 1740 cm^{-1} and 1580 cm^{-1}, corresponding to amide I band was observed and indicated the occurrence of C=O stretching vibrations and of C-N stretching.

The fact that the regions of both amide I and amide II of AhP and AhP-loaded formulations are overlapping is an indicator that there was no modification of the chemical structure of carried peptide during incorporation or production of delivery systems (Castro et al., 2018b).

4.4.4. Tongue adhesion

Orodispersible films are intended to be placed on the top of the tongue where disintegration occurs after contact with saliva. Indeed, adhesion to tongue is an important first step regarding a homogeneous disintegration of the films so that resulting fragments are evenly dispersed within the oral cavity. Results regarding adhesiveness, work of adhesion and debonding distance are outlined in **Table 18.**

Table 18: Characterization of the adhesion properties to the tongue, from developed formulations

Formulation	Adhesiveness (N)	Work of adhesion (N·s)	Debonding distance (mm)
Guar gum film	0.026 ± 0.003	0.118 ± 0.062	1.608 ± 0.679
GfNp	0.037 ± 0.007	1.548 ± 0.138	2.023 ± 0.750

As observed, the inclusion of PLGA nanoparticles within the matrix of guar gum oral films led to an increase of adhesiveness, work of adhesion and debonding distance. The fact that nanoparticles present high surface areas may have increased adhesion to cow tongue due to a higher availability of functional groups of GfNp to interact with tongue surface. Moreover, PLGA presents high density of –OH and C=O groups and is, therefore, prone to establish hydrogen bonds with artificial saliva and to the glycoproteins present on the surface of the cow tongue (Shtenberg et al., 2018).

4.4.5. TR146 cell viability profile

Cell viability of TR146 cell lines was not compromised by the tested concentrations of peptide and delivery systems (peptide-loaded or placebo) and, therefore, the highest concentrations (500 μg/mL) could be used in the peptide transepithelial diffusion study across cell multilayer. Cell viability results are outlined in **Figure 29**.

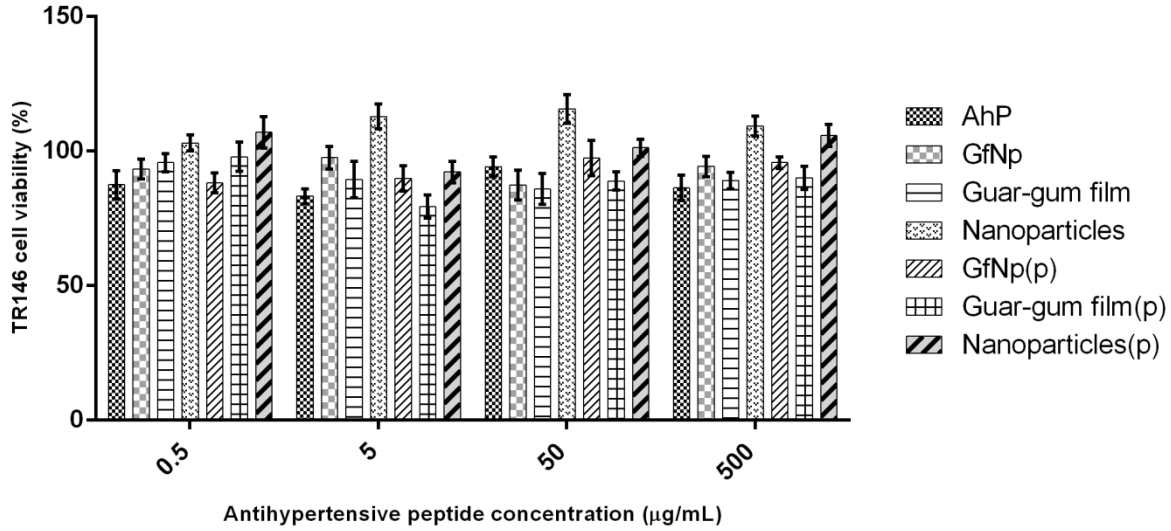

Figure 29: Cytotoxicity assessment of different concentrations of free AhP, AhP-loaded (GfNp, guar gum film, nanoparticles) and placebo (GfNp(p), guar gum film(p) and nanoparticles(p)) formulations

Guar gum is a polysaccharide with widely reported biocompatibility and commonly used in the pharmaceutical industry (Dodi et al., 2016; Thakur & Thakur, 2016). Moreover, guar gum, citric acid and sorbitol are all categorized as generally recognized as safe (GRAS) by United States Food and Drug Administration ((FDA), 2017a, b, c). Therefore, it was previously expected that guar gum films, PLGA nanoparticles of GfNp did not present cytotoxicity to TR146 cells as it was further verified. Moreover, AhP is a relatively small peptide from whey and *in vitro* biocompatibility with TR146 cells was also verified, as expected.

4.4.6. Peptide transepithelial diffusion across buccal cell layer

Transepithelial study was performed on TR146 buccal cells multilayer to mimic buccal *in vivo* diffusion of the peptide. Transepithelial electrical resistance (TEER) was assessed before every sample drawing. No significant drop below 390 $\Omega.cm^2$ on TEER values was observed along the diffusion study (240 min).

Similarly to what occurred in the *in vitro* release assay, permeation of the TR146 multilayer by the free AhP was significantly faster when compared with developed buccal delivery systems, along 240 min **(Figure 30)**. Also, AhP-loaded guar gum films and PLGA nanoparticles induced a similar, overlapping, permeability profile of carried peptide across cell multilayer. Release of AhP from PLGA nanoparticles occurred in two steps, with an initial burst release followed by a *plateau* stage, as extensively reported in the literature. Indeed, the initial burst release is explained by the leakage of AhP adsorbed to the surface of nanoparticles (Brazel & Peppas, 1999; Rodrigues de Azevedo et al., 2017). Remaining peptide release is paced by the erosion of the nanoparticle structure.

However, GfNp dictated a depot delivery of AhP that was not detectable by HPLC-UV for the first 60 min of permeability assay. Indeed, the inclusion of AhP-loaded PLGA nanoparticles within the guar gum films results in a double release impediment that must undergo erosion before dissolution and subsequent permeation of AhP can occur (Castro, Fonte, Oliveira, Madureira, Sarmento & Pintado, 2017). As occurred for *in vitro* release assay, AhP permeability across TR146 multilayer was also overlapping when carried by guar gum films, PLGA nanoparticles and GfNp, from 120 min to 240 min.

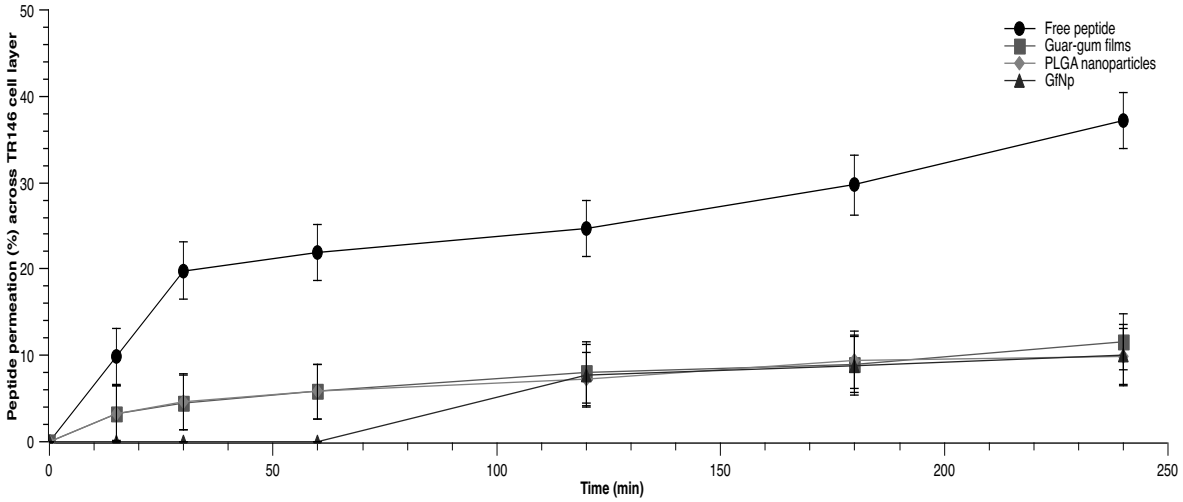

Figure 30: Peptide cumulative permeability (% ± S.D.) across TR146 cell multilayer

Moreover, free peptide has a higher apparent permeability when compared with developed formulations, indicating that the permeation of the peptide across TR146 cell layer was faster and more extensive for the control solution, as outlined in **Table 19.**

Table 19: Apparent permeability of developed formulations

Apparent permeability ($cm.s^{-1}$)			
Free peptide	**Guar gum films**	**PLGA nanoparticles**	**GFNp**
3.57E-06 ± 4.89E-07	1.10E-06 ± 2.29E-07	8.64E-07 ± 4.98E-08	1.31E-06 ± 3.74E-07

Faster and more effective permeation of TR146 cell multilayer by the free AhP was expected for a static *in vitro* permeability assay. Indeed, permeability of free peptide is consistent with AhP passive transport via intercellular route and in accordance with Fick's first law of diffusion. Slower, less extensive permeation of AhP-loaded nanoparticles, films and GfNp across TR146 multilayer was also expected, since the peptide is slowly released from delivery systems, as previously observed, and only then can permeate the epithelia.

The fact that free AhP was faster to permeate the cell multilayer than tested delivery systems does not mean that developed formulations are less effective as buccal delivery systems than a simple solution of free peptide since the model used for the study of permeability is static, not taking salivation, mucus production, tongue movements and consequent swallowing into consideration. Indeed, after disruption of the multilayer, it was possible to observe that a significantly higher amount of AhP was associated (bound to or within) to the cell multilayer especially when carried by GfNp, but also from guar gum films or PLGA nanoparticles, when compared with free peptide. It is predictable that developed mucoadhesive formulations are more competent keeping the carried peptide in intimate contact with absorptive buccal epithelia, leading to a superior permeability along time, also providing slower release than the free peptide solution (**Figure 31**) (Mansuri, Kesharwani, Jain, Tekade & Jain, 2016; Sosnik, das Neves & Sarmento, 2014). Remaining peptide could be found in the apical side of the TR146 cell layer as outlined in **Figure 31.** Guar gum films and PLGA nanoparticles were almost equally effective maintaining an intimate contact between TR146 cell multilayer and carried AhP. It was also possible to observe that GfNp, resulting from the synergism between PLGA

nanoparticles and guar gum films, was responsible for a higher concentration of AhP in intimate and long-lasting contact with absorptive buccal epithelia, being more likely to provide an effective permeation of carried peptide in a dynamic system as occurs *in vivo*. Moreover, according to the data in the literature that indicate that angiotensin-converting enzyme inhibitory activity (IC_{50}) of KGYGGVSLPEW was estimated to be 0.8 ± 0.1 μg/mL being a more potent antihypertensive molecule than, for instance, captopril (IC_{50} = 3.56 μg/mL) (Ding & Zhu, 2018; Ibrahim, Ahmed & Miyata, 2017). Thus, even though AhP permeability across buccal mucosa reaches a *plateau* state after 30 min, the high potency of the peptide and increased permeability indicated that GfNp may represent a suitable delivery system when controlled release is aimed, with potential reducing of intake frequency (Sharma, Parmar, Kori & Sandhir, 2016).

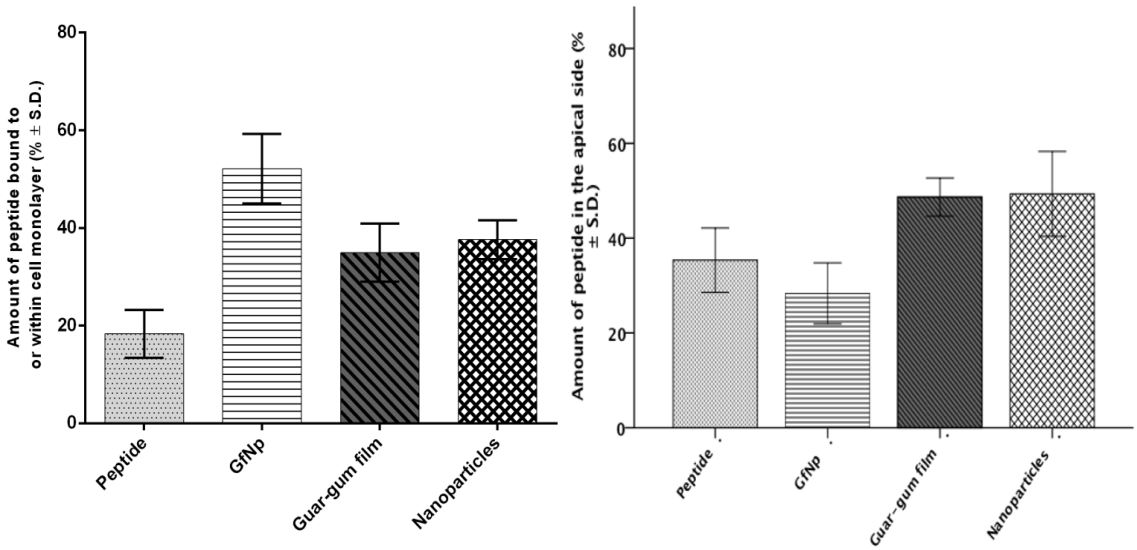

Figure 31: Relative amount of antihypertensive peptide collected from TR146 cell multilayer (A) and from apical side (B), according to delivery system

4.4.7. Caco-2/HT29-MTX co-culture cell viability profile

As previously verified for TR146 cell lines, the viability of Caco-2/HT29-MTX co-culture cells was not compromised, at tested concentrations of peptide and delivery systems (peptide-loaded or placebo). Thus, the highest concentrations (500 μg/mL) could be used in the peptide transepithelial diffusion study across *in vitro* intestinal cell model. Cell viability results are outlined in **Figure 32**.

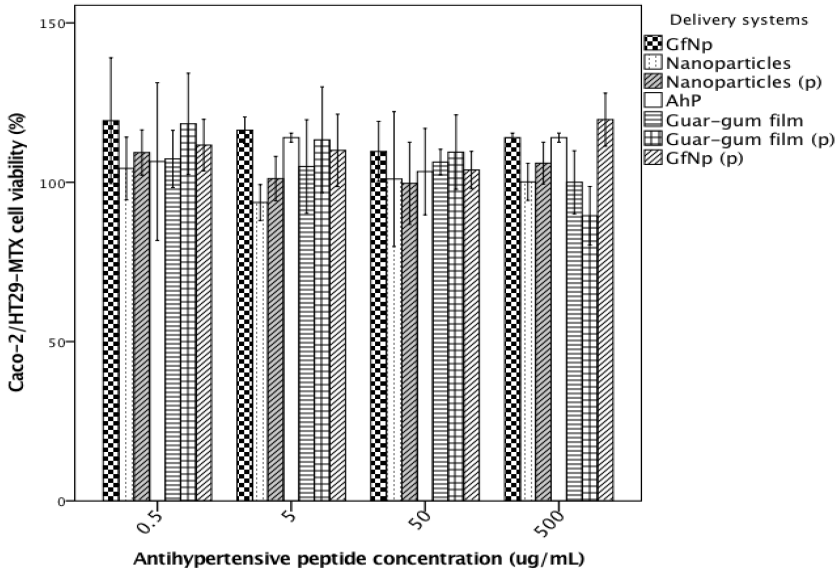

Figure 32: Cytotoxicity assessment of different concentrations of free AhP, AhP-loaded (GfNp, guar gum film, nanoparticles) and placebo (GfNp(p), guar gum film(p) and nanoparticles(p)) formulations

The fact that the viability of the co-culture cells was not compromised at tested concentrations (cell viability was always above 70%) indicated that tested formulations are safe as indicated by the International Organization for Standardization (Almeida, Silva, Goncalves & Sarmento, 2018). Moreover, used antihypertensive peptide was already tested *in vivo* elsewhere, according to the European Union Guidelines, and

toxicity effects were not reported for the tested animals (Tavares, Sevilla, Montero, Carrón & Malcata, 2012).

4.4.8. Peptide transepithelial diffusion across Caco-2/HT29-MTX co-culture

After simulation of buccal permeability, the remaining content in the apical side after permeability studies was transferred to other wells where confluent Caco-2/HT29-MTX cell co-culture were previously grown to confluence in a porous membrane (collagen-coated, 1.12 cm^2 of culture area, 0.4 μm pore size and 12 mm membrane diameter - Transwell® Corning, Germany) to assess *in vitro* intestinal permeability of formulations. This assay was performed to assess if developed formulations were also significantly improving the overall bioavailability of carried peptide even after swallowing and contacting with stomach and intestinal juices.

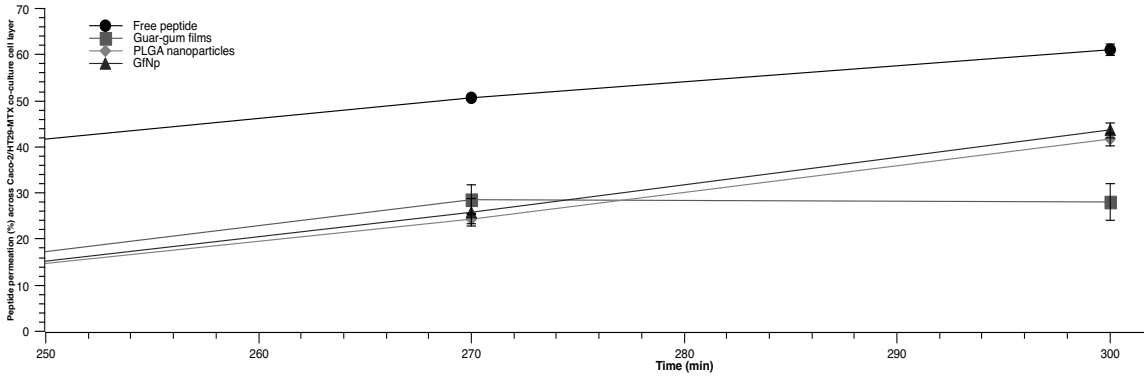

Figure 33: Peptide cumulative permeability (% ± S.D.) across Caco-2/HT29-MTX co-culture cell layer after simulated gastrointestinal tract and in vitro buccal permeability assay

Figure 33 outlines the cumulative permeability of AhP that results from the summed concentration of the peptide that previously crossed the buccal cell layer and the portion that permeated intestinal co-culture cell layer. Cumulative intestinal permeation

of the free peptide was significantly ($P < 0.05$) more extensive than for developed formulations. Nevertheless, apparent permeability of AhP when carried either by GfNp or PLGA nanoparticles was higher when compared with free peptide (**Figure 34**), indicating that both formulations contributed to a faster intestinal permeation when compared with the control.

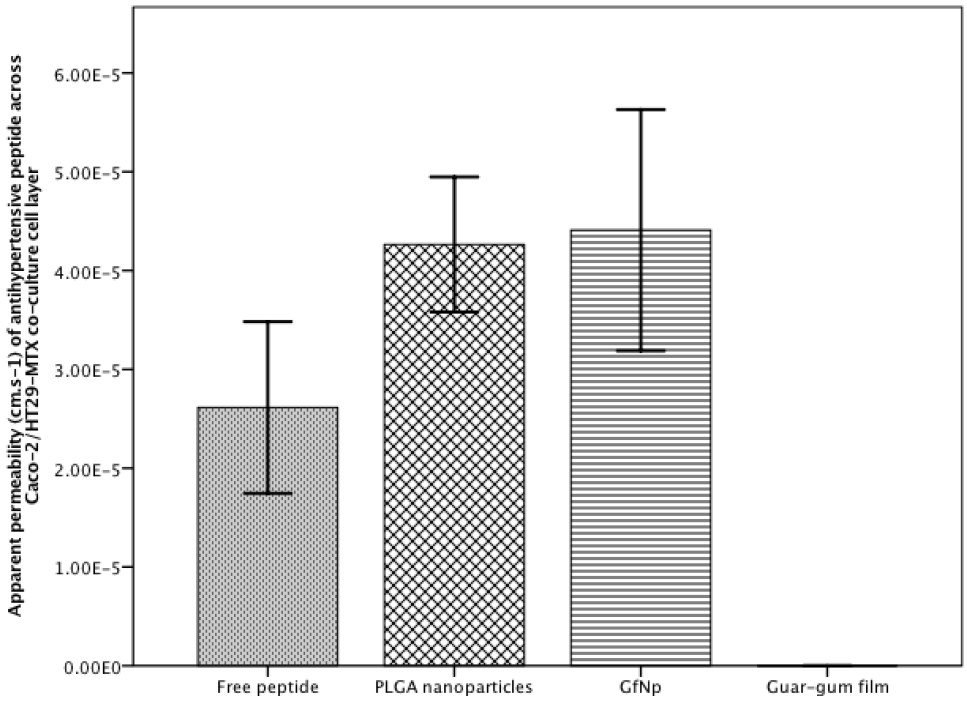

Figure 34: Apparent permeability ($cm.s^{-1}$) of antihypertensive peptide across Caco-2/HT29-MTX co-culture cell layer

*** Negligible apparent permeability**

Effectively, it has been previously reported that PLGA nanoparticles enhance the permeability of carried bioactive molecules across enterocytes (Gang, Dong-Hai, Xin-Xin, Li-Fang, Jun-Teng & Ke, 2013). In fact, it is stated in the literature that particles within the size range of 100-200 nm are internalized by the enterocytes by receptor-mediated endocytosis which could facilitate the permeation of the loaded peptide

(Couvreur & Puisieux, 1993; Win & Feng, 2005). In fact, previous studies reported the presence of intracellular (and even intranuclear, in some cases) PLGA nanoparticles in Caco-2 cells (Gaumet, Gurny & Delie, 2010; He et al., 2013; Reix et al., 2012).

4.4.9. Effects of digestion on antihypertensive activity

The effects of simulated digestion on the antihypertensive activity of AhP were tested *in vitro*, by determining the extent of the capacity to inhibit the angiontesin I converting enzyme and results are outlined in **Figure 35.**

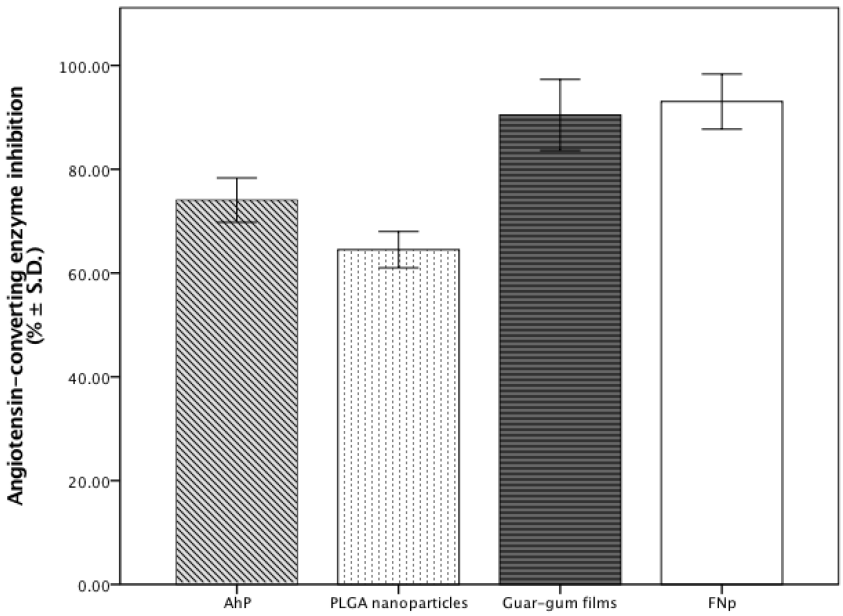

Figure 35: Angiotensin-converting enzyme inhibition capacity of AhP carried by developed formulations, after simulation of gastrointestinal tract

The fact that the angiotensin-converting enzyme inhibition capacity was significantly higher ($P < 0.05$) for AhP carried by guar gum films and FNp, when compared with peptide-loaded PLGA nanoparticles or the particle alone, indicates that

peptide structure was more effectively maintained by the films and by the association of films with PLGA nanoparticles. Indeed, the addition of polysaccharides, as guar gum, to formulations and using nanoparticles as vehicles were previously reported to improve the stability of bioactive proteins and peptides, contributing to the preservation of bioactivity (Sarmento, Ribeiro, Veiga, Ferreira & Neufeld, 2007). The lower *in vitro* bioactivity of the peptide when carried by PLGA nanoparticles could be related with the inherent slower or even incomplete release of carried peptide from the nanoparticles (Shi, Cui, Yamamoto & Kawashima, 2008).

4.5. Conclusions

A buccal delivery system based on the combination of previously optimized guar gum films and PLGA nanoparticles was developed for the first time for the antihypertensive peptide (KGYGGVSLPEW) (Castro et al., 2018c). GfNp did not induce toxicity to TR146 buccal cells after 12 h of contact and cell multilayer integrity was maintained during the whole duration (4 h) of the permeability assay as indicated by the constant transepithelial electrical resistance along time. Also, GfNp did assure a slower release of carried peptide and a more intimate and long-lasting contact with buccal absorptive epithelia when compared with PLGA nanoparticles, guar gum films or free peptide. On the other hand, a faster permeation of antihypertensive peptide across Caco-2/HT29-MTX cell line was observed when carried by GfNp or PLGA nanoparticles, in comparison with guar gum films or free peptide solution. A case of synergism is verified for GfNp and is a promising candidate to be tested *in vivo* as buccal delivery system.

Acknowledgments

This article is a result of the project NORTE-01-0145-FEDER-000012 , supported by Norte Portugal Regional Operational Programme (NORTE 2020), under the PORTUGAL 2020 Partnership Agreement, through the European Regional Development Fund (ERDF).

Pedro M. Castro would like to thank Comissão de Coordenação e Desenvolvimento Regional do Norte (CCDR-N), Portugal, for his PhD grant (NORTE-08-5369-FSE-000007).

The authors acknowledge the support granted by national founds from FCT through project PTDC/BBB-NAN/3249/2014.

This work was also financed by FEDER - Fundo Europeu de Desenvolvimento Regional funds through the COMPETE 2020 - Operacional Programme for Competitiveness and Internationalisation (POCI), Portugal 2020, and by Portuguese funds through FCT - Fundação para a Ciência e a Tecnologia/ Ministério da Ciência, Tecnologia e Ensino Superior in the framework of the project "Institute for Research and Innovation in Health Sciences" (POCI-01-0145-FEDER-007274)

Chapter V: Combination of PLGA nanoparticles with mucoadhesive guar gum films for buccal delivery of alpha-casozepine

Pedro M. Castro 1,2 Patrícia Baptista* 1, Giampaolo Zuccheri 2, Ana Raquel Madureira 1, Bruno Sarmento 3,4,5, Manuela E. Pintado 1***

1 CBQF – Centro de Biotecnologia e Química Fina – Laboratório Associado, Escola Superior de Biotecnologia, Universidade Católica Portuguesa/Porto, Rua Arquiteto Lobão Vital, 172, 4200-374 Porto, Portugal

2 Department of Pharmacy and Biotechnology, Alma Mater Studiorum, University of Bologna INSTM, Centro S3 of CNR-Istituto Nanoscienze, Via Irnerio 48, 40126 Bologna, Italy

3 INEB - Instituto Nacional de Engenharia Biomédica, Universidade do Porto, Rua Alfredo Allen 208, 4200-393 Porto, Portugal

4 i3S - Instituto de Investigação e Inovação em Saúde, Universidade do Porto, Rua Alfredo Allen 208, 4200-393 Porto, Portugal

5 CESPU, Instituto de Investigação e Formação Avançada em Ciências e Tecnologias da Saúde, Rua Central de Gandra 1317, 4585-116 Gandra-PRD, Portugal

** Both authors contributed equally to the paper*

*** Corresponding author: mpintado@porto.ucp.pt*

5.1. Abstract

Whey-derived alpha-casozepine bioactive peptide (YLGYLEQLLR) was associated with previously optimized guar gum film-PLGA nanoparticles, aiming to

increase both stability across gastrointestinal tract and permeability across absorptive epithelia. Oral films associated with nanoparticles (FNp) enhance buccal absorption along with protection of carried bioactive molecules that are swallowed, with inherent increase of bioavailability. None of developed formulations induced significant loss of cell viability. Permeability across both buccal and intestinal cell barriers was enhanced when alpha-casozepine was carried by FNp system, when compared with film and nanoparticles alone, in a simulated gastrointestinal tract environment. Moreover, differences in permeability profile across buccal and intestinal epithelia were in accordance with the slower erosion of PLGA nanoparticles in a media of neutral pH, resembling oral cavity conditions, and a faster erosion in acidic conditions, as occurs in stomach, as observed by a continuous analysis of nanoparticle morphology over 980 min by atomic force microscopy. Additionally, apparent permeability of alpha-casozepine across TR146 human buccal carcinoma cells and Caco-2/HT29-MTX co-culture, carried by FNp was indeed superior when compared with peptide loaded in PLGA nanoparticles and in films alone or with free peptide control solution. Both FNp and PLGA nanoparticles alone enhanced the permeability of relaxing peptide compared with guar gum films alone. An increased tongue adhesion when PLGA nanoparticles were added to the guar gum films was also observed. Developed formulations improved both buccal an intestinal absorption of carried bioactive molecules without compromising cell viability.

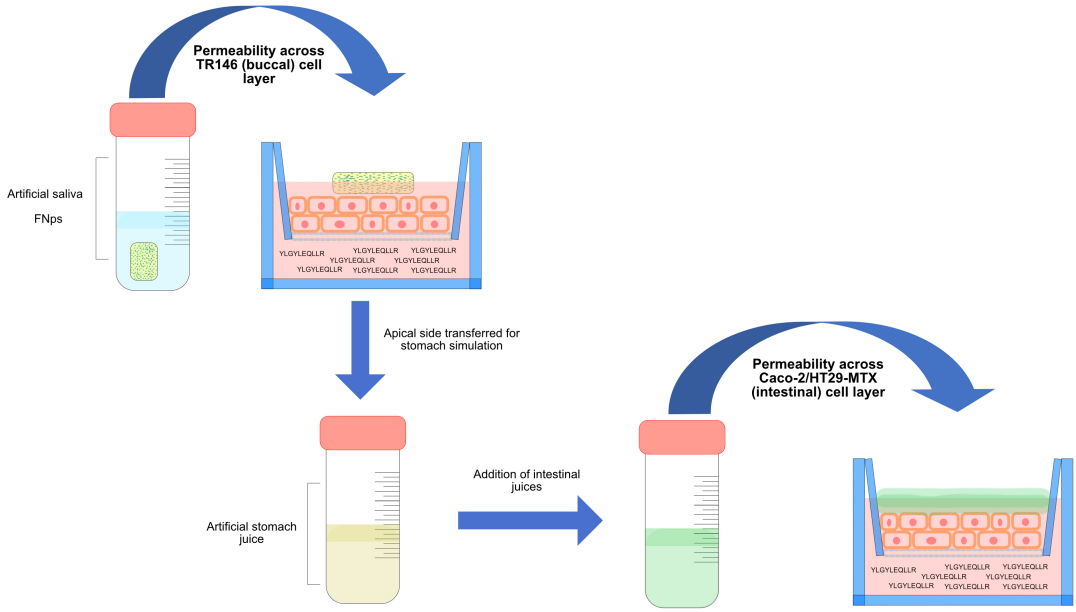

5.2. Introduction

Whey protein is thoroughly studied as an important source of bioactive proteins and peptides. Peptides with antihypertensive, neuroactive, relaxing, immune and balancing of the gastrointestinal tract have been obtained from the hydrolysis of whey protein (Dullius, Goettert & de Souza, 2018). The alpha-casozepine is a decapeptide obtained from the hydrolysis of whey protein, that presents anxiolytic activity by exerting benzodiazepine-like activity with high homology with the diazepam binding inhibitor (Yoshikawa, 2015). Moreover, alpha-casozepine does not seem to present the side effects of benzodiazepines in animals, as incoordination and disinhibition of aggression (Beata et al., 2007b; Landsberg, Milgram, Mougeot, Kelly & de Rivera, 2017; Palestrini et al., 2010). Effectively, the relaxing peptide was classified as food and given the status of Generally Recognized as Safe (GRAS) by the Food and Drug Administration agency (FDA) (Beata et al., 2007a). Nevertheless, the oral administration of alpha-casozepine leads to a lower

bioavailability of about four times when compared with intraperitoneal administration (Benoit, Chaumontet, Schwarz, Cakir-Kiefer, Tomé & Miclo, 2017). Limited activity following oral administration of alpha-casozepine is due to the acidic stomach conditions and enzymatic activity prevailing in the gastrointestinal tract (Batista, Castro, Madureira, Sarmento & Pintado, 2018). Moreover, low permeability across intestinal mucosa and hepatic first-pass (or pre-systemic) effect, also lead to a decrease in the bioavailability of bioactive molecules administered *per os* (Bakhru, Furtado, Morello & Mathiowitz, 2013; Batista, Castro, Madureira, Sarmento & Pintado, 2018; Rehmani & Dixon, 2018; Tyagi, Pechenov & Anand Subramony, 2018).

In opposition to conventional oral route of administration (that usually includes swallowing the dosage form carriyng bioactive molecule, digested across the gastrointestinal tract) buccal delivery aims the local absorption, within the buccal cavity, of payload content across buccal mucosa (Rossi, Sandri & Caramella, 2005). Indeed, buccal administration route was widely reported as a suitable alternative to conventional oral administration, but being equally convenient minimizes crossing gastrointestinal tract and hepatic first-pass effect (Morales & Brayden, 2017). Nevertheless, buccal mucosa is not as absorptive as the small intestine. Moreover, buccal epithelia does not present specific molecule transporting systems. Also, saliva production and stimulation of the receptors in the palate and pharynx inevitably lead to swallowing of a small portion of the formulation, with potential loss of function of the carried bioactive molecules. Therefore, besides from enhancing buccal absorption, bioactive molecules that are swallowed must be protected from the gastrointestinal tract extreme conditions to guarantee that a higher concentration in the systemic circulation is achieved.

Thus, aiming an overall increase of bioavailability by enhancement of buccal and intestinal permeability and protection from extreme pH and enzymatic activity in the gastrointestinal tract, alpha-casozepine was loaded in a buccal/oral delivery system comprised of poly(lactic-co-glycolic acid) – PLGA - nanoparticles and guar gum films (FNp) that was previously optimized as carrier for an antihypertensive peptide (Castro, Baptista, Madureira, Sarmento & Pintado, 2018). Indeed, it was the first time that, to the knowledge of the authors, alpha-casozepine was incorporated within PLGA nanoparticles and guar gum films, aiming protection and overall enhanced bioavailability of the peptide.

Guar gum films were previously developed aiming a burst disintegration within 30 s, thus releasing the PLGA nanoparticles within the buccal mucosa and promoting buccal absorption of the content. Due to limited absorptivity of buccal epithelia, PLGA nanoparticles were previously optimized by the group to present a small size (~160 nm) aiming to enhance permeability of carried bioactive molecules across buccal epithelia (Castro, Baptista, Madureira, Sarmento & Pintado, 2018). When swallowing of the formulation occurs, PLGA nanoparticles were reported to provide protection of carried bioactive molecules across stomach and intestinal extreme pH and enzymatic activity. It has also been reported that PLGA nanoparticles enhance intestinal uptake of carried molecules, with special affinity to M-cells (Fievez et al., 2009; Garinot et al., 2007).

5.3. Materials and methods

5.3.1. Materials

The relaxing peptide with the sequence YLGYLEQLLR (99.7%) was purchased from GenScript (China). Poly (lactic-co-glycolic acid) acid terminated (51:49 mol% of DL-lactide and Glycolide, respectively) was kindly offered by Corbion (Gorinchem, Netherlands). Ethyl acetate 99.5%, poly(vinyl alcohol) and D-sorbitol (assay purity ≥98%) were purchased from Sigma-Aldrich (Steinheim, Germany). Citric acid monohydrate, potassium phosphate monobasic anhydrous and sodium phosphate dibasic were purchased from Merck (Darmstadt, Germany). Sodium chloride was purchased from Panreac (Barcelona, Spain). Deionized water was used to prepare all oral films formulations and ultrapure water was used to prepare peptide standard solutions and eluents used in chromatography procedures. TR146, Caco-2 and HT29-MTX cell lines were purchased from Sigma-Aldrich. Transwell® flasks (12 well) and inserts (collagen-coated, 1.12 cm^2 of culture area, 0.4 μm pore size and 12 mm membrane diameter) were purchased from Corning (New York, USA). 96-well plates were purchased from Thermo Scientific (Denmark). Fetal Bovine Serum (FBS), DMEM and HAMS-F12 culture media and Pen-Strep (10 000 U Penicillin, 10 000 U Streptomycin) were purchased from Lonza® (Verviers, Belgium). TrypLE™ express was purchased from Gibco® (Denmark). Thiazolyl Blue Tetrazolium Bromide (MTT) Ultra-Pure was purchased from VWR (Solon, USA). Dimethyl sulphoxide (DMSO) 99.7% was purchased from Fisher Bioreagents™ (EUA). Phosphate buffer saline (PBS) solution was prepared by dissolving 8.0 g of sodium chloride, 0.2 g of potassium chloride, 1.44 g of monobasic sodium phosphate and 0.24 g of dibasic potassium phosphate to 1 L of ultrapure water and by

adjusting pH to 7.4 using a solution of sodium hydroxide 0.1M. For cell wash, pH of PBS was adjusted to 6.8, using a solution of hydrochloric acid 0.1 M. Artificial saliva was prepared using 8.0 g/L of sodium chloride, 0.19 g/L of monobasic potassium phosphate and 2.38 g/L of dibasic sodium phosphate and pH was set to 6.8 using phosphoric acid. Finally, α-amylase (Sigma) was added to obtain a solution with the final concentration of 100 U/mL.

5.3.2. Production and characterization of PLGA nanoparticles

The formulation of PLGA nanoparticles was previously optimized as described by (Araujo et al., 2014). Briefly, an aqueous solution of the bioactive peptide (125 μg/mL) was added dropwise to a solution of PLGA dissolved in 2 mL of ethyl acetate and sonicated for 30 s at 70% amplitude with a ultrasonicator (SONICS VibraCell EUA), resulting in a W/O emulsion. An aqueous solution of PVA (7% w/v) was simultaneously prepared individually and added to the previously sonicated PLGA solution. Immediately, this simple emulsion was sonicated for 30 s and 70% amplitude, resulting in a w/o/w double emulsion. The double emulsion was kept stirring (600 rpm) for 3 h for the complete evaporation of ethyl acetate to occur, leading to the hardening of the nanoparticles.

5.3.2.1. Characterization of PLGA nanoparticles

PLGA nanoparticles were characterized regarding mean particle size, surface charge, peptide association efficiency and morphology. Moreover, aiming to study the

correlation between nanoparticle erosion with the release of carried peptide, the variation of height along time and in contact with neutral and acidic solutions were also assessed.

5.3.2.1.1. Particle size and zeta-potential analysis

PLGA nanoparticles were diluted (1:50) with Milli-Q water before particle size and zeta-potential analysis. Particle size and polydispersity index were determined by dynamic light scattering (DLS). Zeta-potential was determined by phase analysis light scattering. All measurements were performed in triplicate in a Zetasizer Nano ZSP equipment (Malvern Instruments Ltd, Worcestershire, UK).

5.3.2.2. Peptide association efficiency (AE)

The association efficiency of alpha-casozepine to PLGA nanoparticles was determined by quantifying the free peptides content of the filtrate of each nanoparticle formulation after filtered through Amicon® 50,000 Da filters during 45 min at 13 ºC and 1,640 g. Peptides concentration in the filtrate or supernatant was determined by LC-ESI-UHR-QqTOF-MS.

The LC-ESI-UHR-QqTOF-MS analysis was performed on a UltiMate 3000 Dionex UHPLC (Thermo Scientific), coupled to a Ultra-High Resolution Qq-Time-Of-Flight (UHR-QqTOF) mass spectrometer with 50,000 Full-Sensitivity Resolution (FSR) (Impact II, Bruker Daltonics, Bremen, Germany). Separation of metabolites was performed using an Acclaim RSLC 120 C18 column (100 mm x 2.1 mm, 2.2 um) (Dionex) a 60 ºC. The mobile phases were 0.1% aqueous formic acid (solvent A) and acetonitrile with 0.1 % formic acid (solvent B). The gradient started with 5%, increased

to 95% in 7 min, kept constant for 2 min, returned to 5% B in 1 min and maintained at 5% B for an additional 5 min at a flow rate of 0.25 mL/min. The injection volume was 3 µL. Parameters for MS analysis were set using positive ionization mode with spectra acquired over a mass range m/z 150 to 2500. The parameters were as follow: capillary voltage of 4.5 kV, drying gas temperature of 180 ºC, drying gas flow of 8.0 L/min; nebulizing gas pressure of 1.6 bar, collision RF of 1500 Vpp, transfer time of 100 us and prepulse storage of 10 us. Post-acquisition internal mass calibration used ESI-L Low/concentration tuning mix solution delivered by a syringe pump at the start of each chromatographic analysis.

Relaxing peptide association efficiency was calculated according to the following Eq. (7):

$$\frac{Wtc - Wsc}{Wtc} \times 100 \qquad (7)$$

where, Wtc stands for total weight of relaxing peptide used in the formulation and Wsc stands for relaxing peptide collected from the supernatant after centrifugation.

5.3.3. Morphological characterization and erosion of PLGA nanoparticles

The analysis of morphological characteristics and respective alterations of peptide-loaded PLGA nanoparticles over time was performed by atomic force microscopy (Nanoscope 8 Multimode AFM equipped with an E-type scanner – Bruker, U.S.A.). Regarding the morphological characterization of peptide-loaded PLGA nanoparticles,

freshly prepared according to the method reported in section 5.3.2., the sample was diluted (1:1000 proportion), spread on a mica discand dried by spinning for 5 min. Imaging was performed with ScanAsyst air probes.

To assess the stability of PLGA nanoparticles, samples were analysed in liquid, aiming to understand if the peptide release is related with erosion of the carrier particle. Time-lapse imaging of hydrated specimens was obtained by adsorbing the nanoparticles on freshly-cleaved mica and imaging with the fluidic cell filled with the desired buffer. Imaging was performed with ScanAsyst fluid+ probes. The extension of erosion extension was evaluated by determining particle height along time. The morphology of the borders of the particle was also observed. Briefly, sequential imaging of the same PLGA nanoparticle was performed every 10 min, for 490 min, using a pH 7.4 PBS buffer as dispersant. After 490 min, the buffer in the AFM fluidic cell was totally replaced with a pH 2.0 HCl solution and height and morphology of the nanoparticle were also determined every 10 min.

5.3.4. Preparation of guar gum films and assembling process with PLGA nanoparticles

Guar gum films were previously optimized by our research group and prepared by the solvent casting technique (Castro, Fonte, Oliveira, Madureira, Sarmento & Pintado, 2017; Castro et al., 2018b). Briefly, 54 mg of sorbitol, 40 mg of guar gum and 7.6 mg of citric acid were added to 2 mL of distilled water and stirred until complete dissolution. Resulting solution was poured in a Petri dish and heated to 37 ºC for 1 h and kept at room temperature for the following 12 h. For the incorporation of PLGA nanoparticles within

the film matrix, sorbitol, guar gum and citric acid were dissolved in 2 mL of a previously prepared nanoparticle dispersion instead of the distilled water.

5.3.5. Tongue adhesion of developed formulations

Mucoadhesion assessment to tongue was performed for alpha-casozepine-loaded FNp and guar gum films using a texturometer (TA.XT plus Texture Analyser, Stable Micro Systems, United Kingdom). For calibration purposes, the mounted load cell presented a 5 kg capacity and force was calibrated with a 2 kg weight. Briefly, the formulations were adhered to the testing probe (squared shape, 6.25 cm^2) and a cow tongue (obtained fresh from a local slaughterhouse) was mounted on the texturometer support platform. Then, 3.5 mL of artificial saliva (pre-heated to 37 ºC) were poured dropwise on the top of the tongue. The probe was set to descend until contact between the formulation and the tongue. The contact force was set to 5 g and contact time to 30 s. Thereafter, the probe ascended at a speed rate of 0.1 mm/s and debonding force was registered, allowing to determine adhesiveness (N), work of adhesion (N.s) and debonding distance (mm).

5.3.6. Human buccal epithelium cell line culture

Trans-epithelial permeability assay and cell viability after contact with produced formulations were performed using TR146 human buccal epithelium cell line culture. TR146 cell line was chosen due to great resemblance of normal human buccal mucosa, namely regarding undifferentiated, non-keratinized stratified epithelium, morphological and functional characteristics as activity of carboxypeptidase, esterase and

aminopeptidase (Morck Nielsen & Romer Rassing, 2000). Also, expression of K4, K10, K13, K16 and K19 keratins, membrane-associated receptors for involucrin and epidermal growth factors also reflect other common characteristics to normal human buccal epithelium cells (Jacobsen et al., 1999; Jacobsen, van Deurs, Pedersen & Rassing, 1995).

TR146 cell line was purchased from Sigma-Aldrich (USA) and passages 9 to 14 were used. The culture medium consisted of HAMS F-12 medium enriched with 2 mM Glutamine (Lonza), 10% (v/v) fetal bovine serum (FBS) and 1% (v/v) of penicillin-streptomycin antibiotic blend. TR146 cells were seeded and maintained in 75 cm^2 T-flasks (T-75) and incubated in a 5% CO_2/95% air and 98% relative humidity atmosphere. The culture medium was replaced every two days. When 70-80% of cell confluence was reached, cells were detached from T-75 flasks using 2 mL of TrypLE™ Express. Detached cells were then prepared and seeded either in other T-75 flasks, 96-well culture plates (Nunc®) or in Transwell® inserts 12-well culture plates purchased from Corning® (Germany).

5.3.7. Human intestinal epithelium Caco-2/HT29-MTX cell lines co-culture

Caco-2 (Caucasian colon adenocarcinoma) cell line is widely used for the study of intestinal permeation of bioactive molecules (Araujo & Sarmento, 2013). Nevertheless, Caco-2 monoculture was not significantly representative of duodenum epithelia due to the formation of tight junctions that typically occur in the colon but not in the small intestine, leading to a hindrance of the absorption of hydrophilic molecules. Also, Caco-2 monoculture is exclusively composed of enterocytes and overexpress efflux transporters, typical of an excretory rather than absorptive epithelia. Therefore, HT29-

MTX (Caucasian colon adenocarcinoma grade II) cell line is used in co-culture with Caco-2 cells. HT29-MTX were chosen due to mucus producing ability, as occurs in the duodenum mucosa.

Thus Caco-2/HT29-MTX co-culture was used to better mimic the *in vivo* conditions that occur in the duodenum. HT29-MTX and Caco-2 cell lines were grown separately in Dulbecco's Modified Eagle Medium (DMEM) supplemented with 10% (v/v) fetal bovine serum, 1% (v/v) L-glutamine, 1% (v/v) penicillin and streptomycin and 1% (v/v) of non-essential aminoacids, at 37 ºC under a 5% CO_2 water-saturated atmosphere. Upon 70-80% confluence, cells were detached as described in before. Co-culture seeding in Transwells® was performed in a 9:1 ratio of Caco-2 (3 x 10^5 cells/well) and HT29 (3 x 10^5 cells/well) cells, respectively (Antunes, Andrade, Araujo, Ferreira & Sarmento, 2013).

5.3.8. Cell mitochondrial activity assessment

Cell-viability studies were carried out on proliferating cells, chosen when TR146 cells and Caco-2/HT29-MTX co-culture were 70-80% confluent in T-75 flasks and properly detached as described above. After detachment, cells were re-suspended in medium and seeded in 96-well plates with a concentration of 1 x 10^4 cells/mL, 200 μL per well. The same cell concentration was adopted in the 12-well plates but using 500 μL of cell suspension, after *in vitro* permeability assay. Cell-viability studies were performed after 24 h of culture, with previous supervision by optical microscopy of the morphology and confluence of the cells in the plate wells. MTT assay allows to assess mitochondrial viability and, therefore, cell viability after 12 h contact with prepared delivery systems

(da Silva, Ferreira, Pintado & Sarmento, 2016a). If cells were viable, succinic dehydrogenase was able to transform the tetrazolium salt into insoluble, purple-coloured, crystals of formazan (Mosmann, 1983a). Medium with 1% (v/v) Triton X-100 solution was added as lysis buffer and served as positive control. Negative control consisted of cells in contact with medium only. After treatment with produced formulations, 100 μL of the MTT reagent (0.5 mg/mL prepared in culture medium) was added to each well and the plates were incubated for 4 h. After incubation time has passed, reagent was carefully removed, allowing the insoluble formazan crystals to remain in the bottom of the wells. 100 μL of DMSO per well was used to solubilize the formazan crystals in a dark room and, after 15 min of agitation on an orbital shaker, the absorbance at 570 nm and 630 nm was read on a FLUOstar OPTIMA microplate reader (United Kingdom), in triplicate. Absorbance values for all readings at 630 nm were subtracted from the absorbance values read at 570 nm. Cell viability (%, n = 6 different, independent wells for the same experiment) was calculated according to Eq. (8):

$$\boldsymbol{Cell\ viability}\ (\%) = \frac{\boldsymbol{Experimental\ value - negative\ control}}{\boldsymbol{Positive\ control - negative\ control}} \times \mathbf{100} \qquad (8)$$

Concentration of the formulations tested for potential commitment of cell viability were chosen according to the average amount of saliva produced in the human mouth when in contact with food products (Watanabe & Dawes, 1988b).

5.3.9. Peptide simulated digestion and transepithelial diffusion across buccal (TR146) and intestinal (Caco-2/HT29-MTX) cell layers

Permeability assay was assessed in Corning® Transwell inserts, using 12-well plates. TR146 cells and Caco-2/HT29-MTX co-culture were seeded into the inserts to mimic stratified epithelium of human buccal mucosa and absorptive epithelia of the human intestine, as reported previously (Jacobsen, van Deurs, Pedersen & Rassing, 1995; Zeng et al., 2015b).

For medium replacement, medium was removed from the wells and 0.5 and 1.5 mL of fresh culture medium was added to the apical and basolateral sides, respectively. On the day of the study, culture medium was totally removed. Medium in the basolateral side (receptor part) was replaced with 1.5 mL of PBS, pH 6.8. Medium in the apical side (donor part) was replaced with artificial saliva (containing $CaCl_2$ 1 mM and alpha-amylase 100 U/mL) prepared in HAMS-F12 medium and peptide delivery formulations were introduced afterwards (Castro, Baptista, Madureira, Sarmento & Pintado, 2018). Guar gum films, PLGA nanoparticles, FNp and free alpha-casozepine (n = 5) were tested. Samples of 600 μL were withdrawn from receptor part at 10, 20 and 30 min. Withdrawn volume was immediately replaced with fresh PBS, pre-heated to 37 ºC, to maintain sink conditions. The permeation experiments were carried out in 5 wells per peptide delivery system sample. After the final samples were drawn from the basolateral side, apical side content was collected and added to the simulated stomachal conditions. Briefly, samples were added to a 0.1 M HCl (pH 5.5) solution with previously dissolved pepsin (25 mg/mL) and maintained stirring (130 rpm) at 37 ºC. Further, after 10, 20 30, 40 and 50 min, pH of the solution was successively lowered (with HCl 1 M) to 4.6, 3.8, 2.8, 2.3 and

2.0, respectively. Finally, the pH of the digest was adjusted to 5.0, using $NaHCO_3$ 1M, and adding a solution of bile salts and pancreatin (final concentrations of 2 mg/mL and 12 mg/mL, respectively) to the digest and resulting solution was immediately transferred to the apical side of Transwells seeded with Caco-2/HT29-MTX co-culture cell layers (Laurent, Besancon & Caporiccio, 2007; Madureira, Amorim, Gomes, Pintado & Malcata, 2011b). Samples were withdrawn from the basolateral side at 30, 60 and 120 min. The concentration of alpha-casozepine was determined by LC-ESI-UHR-QqTOF-MS, using the same method as described previously.

The fractional amount of alpha-casozepine that permeated the layer of TR146 buccal epithelia cells and the co-culture of Caco-2/HT29-MTX cells (dQ) was determined over the time intervals (dt) and the flux (*J*) was determined by calculating the slope of the resulting plots, according to Eq. (5) (di Cagno, Bibi & Bauer-Brandl, 2015).

$$J = \frac{dQ}{A \times dt} \qquad (5)$$

Apparent permeability (P_{app}, cm/s) was calculated for a control solution (500 μg/mL), for peptide-loaded PLGA nanoparticles, guar gum films and FNp, by normalizing the flux (J) over the concentration of peptide in the apical side (C_0) according to Eq. (6).

$$Papp = \frac{J}{Co} \qquad (6)$$

where, dQ/dt stands for the amount of permeated peptide over time, A for the cell layer surface area and Co for the initial concentration of peptide.

5.3.10. Cell layer integrity

Transepithelial electrical resistance (TEER) of TR146 monoculture and Caco-2/HT29 co-culture was measured every two days along cell growth and after every sample collection, when the permeability assay was performed, to assess the cell growth rate and cell viability after contacting with tested formulations, using a Millicell® ERS-2 Voltohmmeter (Merck, Germany) (Araujo & Sarmento, 2013; Sander, Nielsen & Jacobsen, 2013b). During permeability experiments, TEER values for TR146 cell culture and for Caco-2/HT29-MTX were always above 130 $\Omega.cm^2$ and 250 $\Omega.cm^2$, respectively, indicating that cell cultures were viable along the assay (Jacobsen, van Deurs, Pedersen & Rassing, 1995; Pan, Han, Zhang, Yu & Liu, 2015).

5.3.10.1. Statistical analysis

Statistical analysis regarding dissolution profile data was performed using IBM® SPSS® Statistics version 22.

Shapiro-Wilk ($n< 50$) test was used to verify if the values obtained for the responses in the experimental design were normally distributed. One sample T test was used to verify the existence of statistically significant differences between predictive models and experimental values. Experimental values were obtained from three samples selected from three new batches, for PLGA nanoparticles. Mean values for each batch were compared with the values predicted in the model.

5.4. Results and discussion

Herein, the impact of using a new delivery system, comprising PLGA nanoparticles embedded in guar gum films, as carrier of a relaxing peptide (alpha-casozepine) aiming the increase of permeability across buccal and intestinal epithelia along with protection of carried peptide along gastrointestinal tract was studied. The characterization of the nanoparticles, either regarding size and zeta-potential but also morphology and degradation was performed and associated with permeability profile of the carried peptide.

5.4.1. Characterization of α-casozepine-loaded PLGA nanoparticles

Developed nanoparticles were characterized regarding their mean sizes, polydispersity index, zeta-pontential and peptide association efficiency and results are outlined in **Table 20**.

Table 20: Physical-chemical characteristics of PLGA nanoparticles

Formulation	Mean size (nm)	Association Efficiency (%)	Polydispersity Index	Zeta-potential (mV)
PLGA nanoparticles (Placebo)	120.4 ± 18.2	N/A	0.201 ± 0.034	-9.8 ± 1.6
Peptide-loaded PLGA nanoparticles	163 ± 11.2	82.0 ± 2.3	0.254 ± 0.032	-11.0 ± 1.9

The inclusion of the peptide in the PLGA nanoparticle formulation induced a statistically significant ($P < 0.05$) increase of mean size of the particles. Indeed, an increase in size of loaded particles, compared to unloaded particles, has been reported in

the literature (Lozoya-Agullo et al., 2018). Also, an increase on polydispersity index was also reported for peptide-loaded PLGA nanoparticles when compared with placebo nanoparticles. Moreover, a high association efficiency of the peptide to the PLGA nanoparticles was obtained, indicating that a high portion of alpha-casozepine added to the formulation is either adsorbed to the surface or incorporated within the polymeric matrix of the nanoparticles. Finally, no statistically differences ($P > 0.05$) between formulations regarding zeta-potential were observed. Indeed, alpha-casozepine presents a neutral net charge at physiological pH values. Moreover, the concentration of the peptide was not enough to shield the surface charge of PLGA nanoparticles.

5.4.1.1. Morphology and stability characterization of PLGA nanoparticles

The images obtained from the AFM analysis of PLGA nanoparticles, outlined in **Figure 36**, allowed to conclude that, despite the observable polydispersity, the observed mean size of the particles is in accordance to the previously reported data obtained by dynamic light scattering (Castro, Baptista, Madureira, Sarmento & Pintado, 2018).

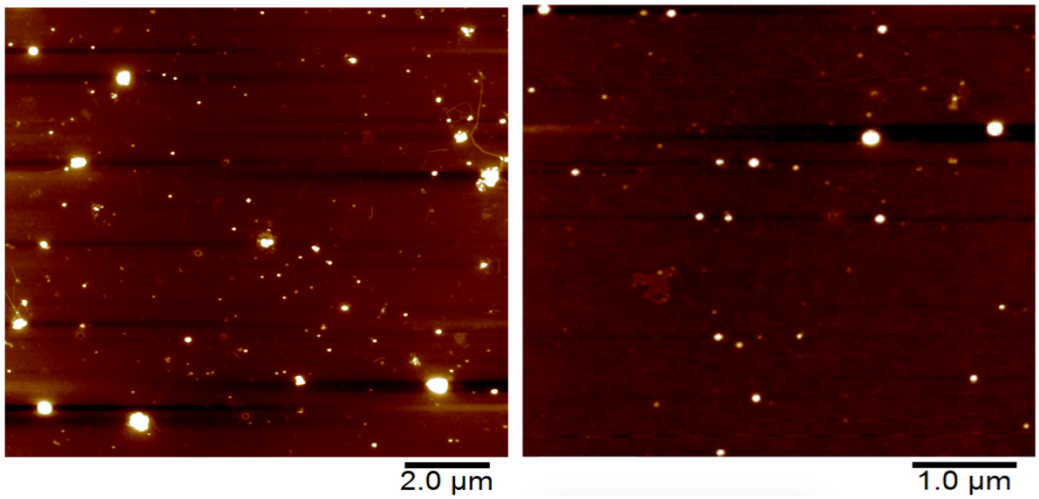

Figure 36: Atomic Force Microscopy images of peptide-loaded PLGA nanoparticles

Besides the observed reproducible size, PLGA nanoparticles are widely reported as promoting long-lasting release of the carried bioactive molecule mainly due to the slow erosion along time (Dinarvand et al., 2011; Hines and Kaplan, 2013). While sequentially in contact with a pH 7.4 PBS buffer (480 min) and a pH 2.0 HCl solution (480 min), the height of one PLGA nanoparticle tracked by the AFM decreased as outlined in **Figure 37**.

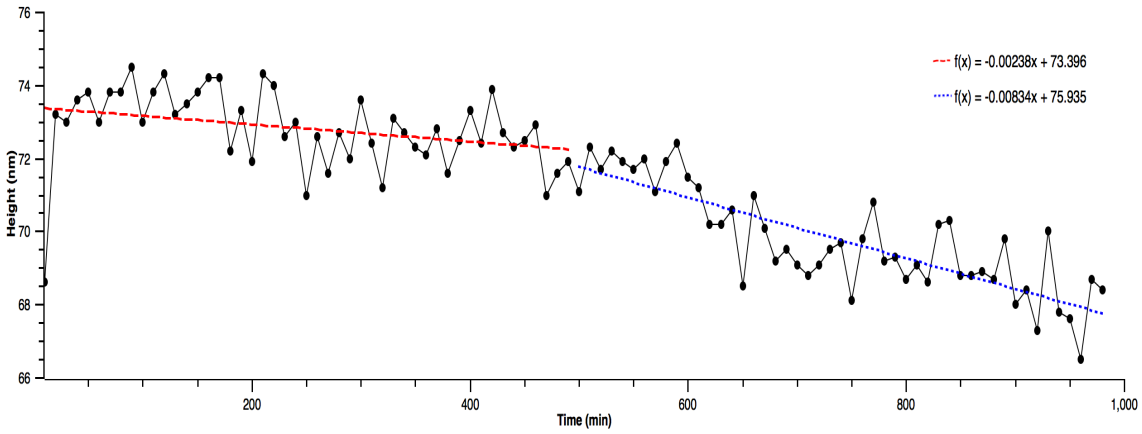

Figure 37: Height variation of PLGA nanoparticles when exposed to pH 7.4 PBS buffer, from 10-490 min (red line), and then to pH 2.0 HCl solution, from 500-980 min (blue dots)

Even though a decrease on the height of the particle was observed, the erosion of the particle was slow over the 980 min. Indeed, the decrease of the height of the particle was of ~5 nm in 980 min, representing only 6.7% of the initial height of the particle or about 19% of its volume (assuming a spherical shape). Moreover, the height decrease tendency was significantly altered by changing the pH value of the external solution as can be verified by the different slopes of the tendency lines (-0.00238 and -0.00834 for 10 – 490 min and 500 – 980 min, respectively. The faster height decrease of the particle

while in acidic media indicates that a faster erosion of the particle occurs when in contact with stomach juices. Therefore, the release of alpha-casozepine while in the oral cavity is expected to be slower when carried by PLGA nanoparticles, offering and extended release of carried peptide. On the other hand, a higher amount of free alpha-casozepine is expected to reach the intestine to be absorbed. Indeed, the faster erosion of PLGA nanoparticles in acidic media, when compared with degradation rate in media with pH close to neutral was already reported elsewhere (Li, Jiang & Ding, 2008). Also, PLGA particles go through an "inside-out" degradation at pH value of 7.4 and "outside-in" degradation at pH value of 2.4, indicating that carried content included within the particles is released faster at neutral pH values, while molecules adsorbed or entrapped in the outer layers of the particle are preferably released at acidic pH values (Zolnik & Burgess, 2007).

5.4.1.2. Tongue adhesion of developed formulations

Tongue adhesion was performed for FNp formulation, aiming to assess whether the addition of peptide-loaded PLGA nanoparticles to the film formulation would change the adhesion-to-tongue properties. As outlined in **Table 21**, the inclusion of PLGA nanoparticles in the guar gum film matrix significantly increased adhesiveness and work of adhesion of the formulation when compared with guar gum film alone. Indeed, it has been reported that polymers with a high number of available polar groups (i.e. –COOH or –OH groups) such as PLGA are strongly mucoadhesive, therefore justify the increased tongue adhesion when nanoparticles were added to the guar gum matrix (Longer, Ch'Ng

& Robinson, 1985; Mathiowitz, 1999; Peppas & Sahlin, 1996; Ponchel & Irache, 1998; Reineke et al., 2013).

Table 21: Tongue adhesion properties of peptide-loaded guar gum films and FNp

Formulation	Adhesiveness (N)	Work of adhesion (N.sec)
Guar gum film	0.026 ± 0.003	0.118 ± 0.062
FNps	0.041 ± 0.002	1.715 ± 0.084

Indeed, the administration of oral films is intended to occur by placing the film on the top of the tongue, where disintegration and spreading of the film fragments will occur through the oral cavity (Castro, Fonte, Sousa, Madureira, Sarmento & Pintado, 2015a). Moreover, improved tongue adhesiveness and work of adhesion by adding PLGA nanoparticles to guar gum films iduces a prolongued and intimate contact between the formulation and the mucosa, therefore enhancing the permeability of carried content through the mucosa (Castro, Baptista, Madureira, Sarmento & Pintado, 2018).

5.4.1.3. TR146 and Caco-2/HT29 cell viability

Cell viability was determined by MTT for both for TR146 human buccal cell line and co-culture of Caco-2/HT29-MTX intestinal cells. Tested concentrations of formulations did not significantly compromise cell viability of both buccal and intestinal cell layers, as outlined in **Figure 38** and **Figure 39.**

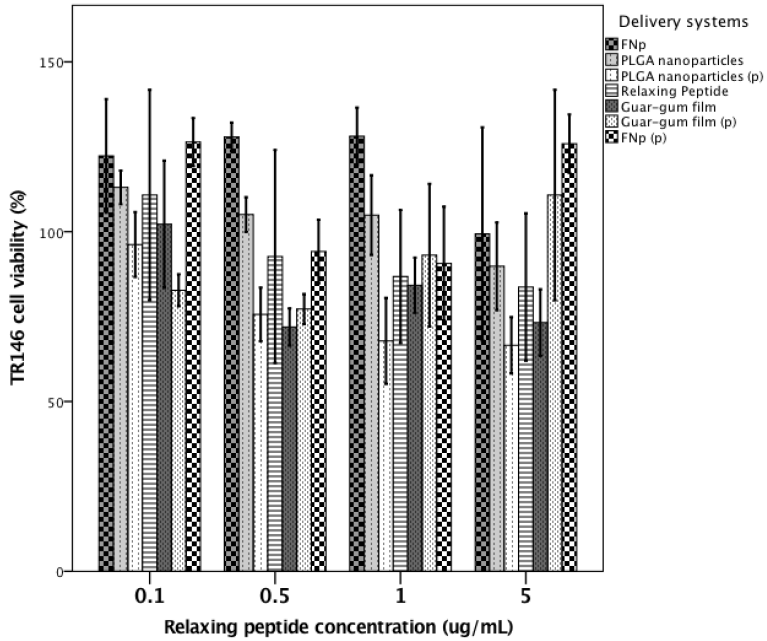

Figure 38: Mitochondrial viability of TR146 cells after contact with developed formulations for 12 h

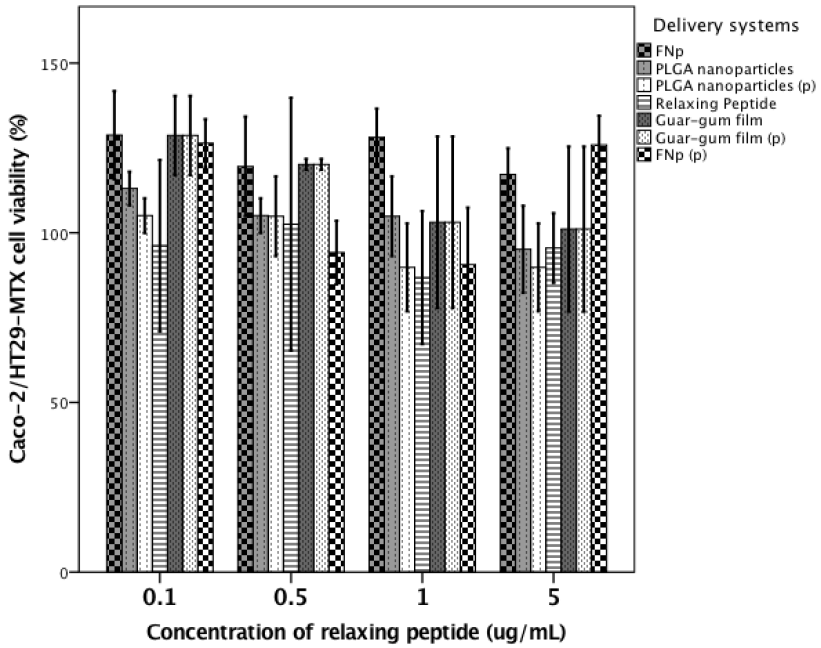

Figure 39: Mitochondrial viability of Caco-2/HT29-MTX cells co-culture after contact with developed formulations for 12 h

Effectively, since no formulation has compromised cell viability below 70%, no significant toxicity was identified according to the International Organization for Standardization (Almeida, Silva, Goncalves & Sarmento, 2018). Moreover, observed results are in accordance with the Food and Drug Administration designation of *generally recognised as safe* (GRAS) at tested concentrations ((FDA), 2017a, b, c). Additionally, placebo formulations were not cytotoxic at tested concentrations, therefore proving the *in vitro* safety of the developed delivery systems. Also, the inclusion of alpha-casozepine within developed formulations did not induce cytotoxicity neither to TR146 cells nor to Caco-2/HT29-MTX co-culture. Finally, alpha-casozepine is a product of whey protein hydrolysis and was not, therefore, expected to compromise cell viability.

5.4.1.4. Peptide transepithelial diffusion and protection across gastrointestinal tract

Developed formulations were intended to enhance permeation of carried peptide across absorptive membranes, but also to offer protection along the gastrointestinal tract. It was verified (as outlined in **Figure 40 A**) that FNp system guaranteed higher peptide permeation across buccal mucosa when compared to PLGA nanoparticles and guar gum films alone or peptide solution (control) mainly after 30 min in contact with TR146 cell layers. Since pH value set for the simulated oral digestion was of 6.8 (close to neutrality), the peptide released from PLGA nanoparticles occurred slowly preferably “inside-out”, according to the slow degradation profile of the particles mentioned in section 5.4.1.1. Thus, released peptide from FNp was mainly due to the migration from the particles to

the film matrix in the mixing process and peptide content in the core of the particle (Zolnik & Burgess, 2007).

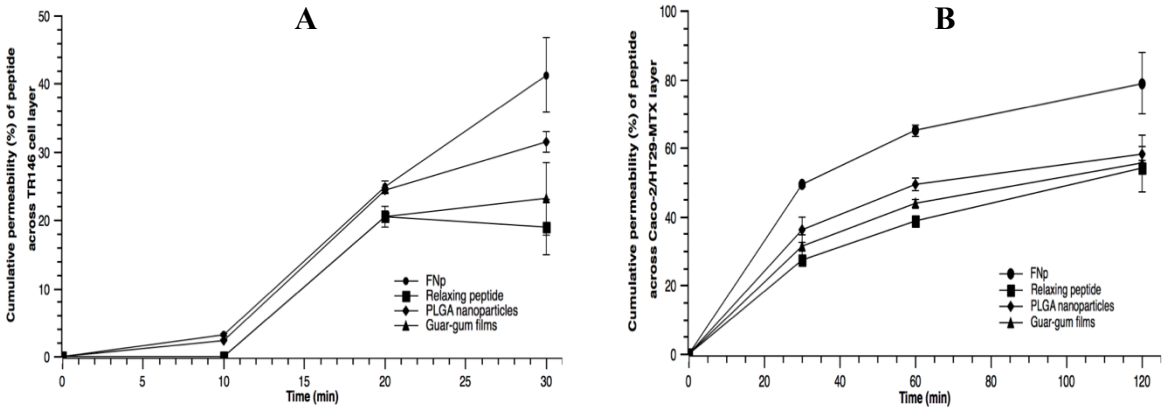

Figure 40: Cumulative permeation (%) of alpha-casozepine across TR146 (buccal) - A - and Caco-2/HT29 (intestinal) cell layers - B

In accordance, apparent permeability of relaxing peptide carried by FNp was significantly higher ($P < 0.05$) across TR146 cell layers, when compared with remaining formulations and control solution, as outlined in **Table 22**.

The higher cumulative permeability of alpha-casozepine across Caco-2/HT29-MTX was also observed for FNp, as outlined in **Figure 40 B**. Results also suggest that the conditions prevailing in each step of gastrointestinal tract simulation contributed to the complete disintegration of tested formulations, therefore leading to the establishment of a *plateau* stage, mainly after 60 min of intestinal *in vitro* permeability (Castro, Baptista, Madureira, Sarmento & Pintado, 2018). Moreover, the uptake of PLGA nanoparticles by Caco-2 intestinal cells was previously reported and can explain the extensive permeation of the peptide carried by FNp across Caco-2/HT29-MTX co-culture, especially in the first 60 min (Joshi, Kumar & Sawant, 2016; Reix et al., 2012). Also, it has been previously

reported that, for Caco-2 cell layers seeded in permeable supports, the endocytosis of PLGA nanoparticles is followed by a quick exocytosis (50% in 1 h) to the basolateral side (Reix et al., 2012). Therefore, the transcytosis of the peptide carried by PLGA nanoparticles could explain the faster permeation when compared with control. The occurrence of the equilibrium stage, mainly after 60 min, led to a decrease of apparent permeability (**Table 22**) of formulations across Caco-2/HT29-MTX cell layers when compared with values for TR146 cell layers. Also, it was reported that degradation of PLGA nanoparticles (mainly "outside-in" degradation) occurs faster while in acidic pH, as occurred in stomach simulation, leading to the release of the peptide adsorbed or incorporated in the outer layer of the particles, thus increasing the concentration available for further intestinal absorption. Besides PLGA nanoparticles, the guar gum fragments remaining from the initial formulation contributed to the adhesion to the epithelia, thus providing an intimate contact between the peptide and cell layer. Thus, intercellular permeability was promoted therefore enhancing the permeation of the peptide either carried by FNp or guar gum films alone (Mansuri, Kesharwani, Jain, Tekade & Jain, 2016).

Observed results are promising regarding the overall bioavailability enhancement of carried peptide, either due to increased permeability across absorptive epithelia and regarding protection of the peptide along gastrointestinal tract.

Table 22: Apparent permeability (Papp) of alpha-casozepine across TR146 and Caco-2/HT29 cell layers

Formulation	Papp ($cm.s^{-1}$) across TR146 cell layers	Papp ($cm.s^{-1}$) across Caco-2/HT29 cell layers
FNp	1.77E-04 ± 2.48E-05	1.37E-04 ± 4.27E-05
PLGA nanoparticles	1.34E-04 ± 6.98E-06	1.01E-04 ± 1.03E-05
Guar gum films	1.07E-04 ± 2.47E-05	1.11E-04 ± 4.83E-05
Peptide solution	8.79E-05 ± 1.88E-05	1.24E-04 ± 8.96E-06

5.4.2. Conclusions

Research regarding oral delivery of bioactive molecules as proteins and peptides has been focusing thoroughly in the permeability enhancement across intestinal mucosa. Nonetheless, buccal route presents several advantages as bypassing hepatic first-pass effect and avoiding contact with extreme pH values and enzymes either in stomach or in the intestine. A conceptually new formulation was successfully developed from the association of guar gum films and PLGA nanoparticles as carriers for alpha-casozepine. Tongue adhesion properties were significantly increased after adding PLGA nanoparticles to guar gum film formulation. Moreover, the delivery system developed from the combination of PLGA nanoparticles and guar gum orodispersible films was not cytotoxic for TR146 buccal carcinoma cells or Caco-2/HT29-MTX co-culture and demonstrated effectiveness regarding the enhancement of both buccal and intestinal permeation of carried relaxing peptide along with protection of the molecule across gastrointestinal tract. Results indicated that developed delivery system are good candidates to be tested *in vivo* for effectiveness.

Acknowledgments

The research work that is exposed in this manuscript support granted by national founds from FCT through project PTDC/BBB-NAN/3249/2014. Pedro M. Castro would like to thank Comissão de Coordenação e Desenvolvimento Regional do Norte (CCDR-N), Portugal, for his PhD grant (NORTE-08-5369-FSE-000007).

This work was also s supported by the project NORTE-01-0145-FEDER-000012, supported by Norte Portugal Regional Operational Programme (NORTE 2020), under the PORTUGAL 2020 Partnership Agreement, through the European Regional Development Fund (ERDF).

Section 4

Stability of developed products and validation of consumer acceptance

Chapter VI – Stability of the products and validation of consumer opinion

*Pedro M. Castro** [1,2], *Patrícia Baptista** [1], *Ana Raquel Madureira* [1], *Bruno Sarmento* [2,3,4], *Manuela E. Pintado* [1**]

[1] *CBQF – Centro de Biotecnologia e Química Fina – Laboratório Associado, Escola Superior de Biotecnologia, Universidade Católica Portuguesa/Porto, Rua Arquiteto Lobão Vital, 172, 4200-374 Porto, Portugal*

[2] *CESPU, Instituto de Investigação e Formação Avançada em Ciências e Tecnologias da Saúde, Rua Central de Gandra 1317, 4585-116 Gandra-PRD, Portugal*

[3] *i3S - Instituto de Investigação e Inovação em Saúde, Universidade do Porto, Rua Alfredo Allen 208, 4200-393 Porto, Portugal*

[4] *INEB - Instituto Nacional de Engenharia Biomédica, Universidade do Porto, Rua Alfredo Allen 208, 4200-393 Porto, Portugal*

**Both authors contributed equally to the paper*

***mpintado@porto.ucp.pt*

6.1. Abstract

After optimization of the formulation comprising guar gum films associated with caffeine-loaded alginate beads (GfB) and overall effectiveness validation, stability of the final product along with acceptability by potential consumers were assessed. Stability characterization of GfB was performed according to the accelerated degradation conditions described in the quality guideline Q1A by the International Conference of Harmonization (ICH). The chemical composition of caffeine molecule was not altered after 3, 6 or 9 months under accelerated degradation conditions (i.e. 40 ± 2 ºC and 75 ±

5% RH), as it was possible to conclude by the analysis of FTIR-ATR spectra of formulations. Moreover, the retention time and recovery rate of caffeine obtained by HPLC-UV were also not altered after subjecting the formulations to temperature and humidity stress conditions, confirming the chemical stability of caffeine molecule. Moisture content of the formulation slightly increased at every time point and indicated that stability may decrease over time due to a higher water activity, formulation stability problems and potential growth of microorganisms. Consumer opinion regarding developed product was initially addressed in a focus group and participants indicated that a product with caffeine (as GfB) should be prepared with mint over fruit-like flavours but that coffee and strawberry could represent other flavor choices. Moreover, for maximum convenience, participants indicated that the formulation should be comfortable within the oral cavity, choosing 3.0 cm x 2.0 m dimensions as the best fitting and indicated a suitable price for a package of 5 units (2 €). Data obtained from the sensory analysis panel regarding most appropriate type of flavor, bitterness, acidity and overall sensory acceptance of the product did indicate a slight preference for mint flavor to mask bitterness and acidity of the product. Important steps were taken through characterization of stability and shelf-life of GfB but sensory optimization must be thoroughly performed to obtain high consumer compliance to the product.

6.2. Introduction

Food and drug association (FDA) established, since 1979, that all prescription drugs must have an associated shelf-life (Capen et al., 2012). Further, International Conference of Harmonization (ICH) defined a series of technical requirements of pharmaceutics for

human use, accorded by Europe, Japan and United States of America. To comply with defined requirements, ICH created guidelines respecting to Quality (regards guidelines on stability studies, definition of thresholds on the amount of impurities, etc), Safety (guidelines to define carcinogenicity, genotoxicity and reprotoxicity of drug products) and Efficacy (concerns to the design, conduct, safety and reporting of clinical trials along with surveillance of novel drug products manufactured by biotechnological processes or pharmacogenetic/pharmacogenomics drug products) of drug products along with a Multidisciplinary section (Harmonization, 2018).

Aiming to test the quality along time of developed formulations comprising micro/nanoparticles included in guar gum films as carriers for caffeine (GfB), ICH guideline Q1A regarding stability testing of new drug substances and products was followed (Guideline, 2003).

In addition to the stability assessment, the formulation containing guar gum films, alginate beads and caffeine was subjected to sensory analysis, regarding acidity, bitterness, flavors and overall sensory acceptance by the consumers. Moreover, the correlation between the amount of malic acid and the bitterness perception was also assessed as malic acid had been previously reported has offering bitterness-masking properties (Brittain, 2001).

6.3. Materials and methods

6.3.1. Materials

Caffeine anhydrous (food chemicals codex, 99% purity), alginic acid (sodium salt from brown algae, molecular weight ranging from 80,000 to 120,000, 61% of mannuronic

acid and 39% of guluronic acid, as stated by supplier in safety and documentation section), menthol 99%, guar gum and D-sorbitol (assay purity ≥98%) were purchased from Sigma-Aldrich (Steinheim, Germany). Citric acid monohydrate, potassium phosphate monobasic anhydrous and sodium phosphate dibasic were purchased from Merck (Darmstadt, Germany). Coffee and strawberry flavors (GLOBO® food grade aromas) were purchased from a local supermarket. Deionized water was used to prepare all oral films formulations.

6.3.2. Production of guar gum films

Guar gum films were previously optimized by our group and were prepared by the solvent casting technique (Castro, Fonte, Oliveira, Madureira, Sarmento & Pintado, 2017). Briefly, 54 mg of sorbitol, 40 mg of guar gum and 7.6 mg of citric acid were added to 2 mL of distilled water and stirred until complete dissolution. Resulting solution was poured in a Petri dish and heated to 37 ºC for 1 h and kept at room temperature for the following 12 h. For the incorporation of alginate beads within the film matrix, sorbitol, guar gum and citric acid were dissolved in 2 mL of a previously prepared micro/nanoparticle dispersion instead of the distilled water.

6.3.3. Production of caffeine-loaded alginate beads

Alginate beads were prepared by emulsification/internal gelation (Song, Yu, Gao, Liu & Ma, 2013). Briefly, calcium carbonate and caffeine were dissolved into an alginate solution. In a separate beaker, Tween® 80 was dispersed into 10 mL of liquid paraffin. Both dispersions were stirred for 30 min and then the alginate solution was added drop

wise to the paraffin dispersion and the resulting emulsion was kept stirring (600 rpm) for 30 min. Then, glacial acetic acid was added drop wise to the emulsion to liberate calcium ions for gelation. Resulting emulsion was kept stirring (900 rpm) for 1 h. Resulting emulsion was centrifuged (6,000 rpm, 15 ºC) and the pellet was recovered and washed with PBS. Washing procedure was performed three times for each formulation of beads.

6.3.4. Stability assessment of optimized formulations

Stability of the optimized formulations comprising guar gum films with caffeine-loaded alginate beads (GfB) was assessed according to the quality guidelines Q1A established by the ICH. Quality guidelines define the accelerated degradation conditions as 40 ± 2ºC/75 ± 5% RH.

6.3.5. Accelerated degradation conditions

Stability tests of the formulations were performed according to Q1A guidelines, as previously mentioned, that stipulate the characteristics of accelerated, intermediate and long term studies. Assays were performed in triplicate, by comparing the chemical integrity characteristics every three months, along nine months (Guideline, 2003). Briefly, formulations were stored at 40 ± 2ºC/75 ± 5% RH (conditioned chamber Climacell from MMM Medcenter Einrichtungen GmbH, Planegg, Germany) protected from light sources, for a period of nine months. Samples were tested at four time points, right after production (t0) and after three (t3), six (t6) and nine (t9) months of storage.

Further, formulations were also analyzed regarding humidity content for all time points, using an A&D MX-50 moisture analyzer from A&D Company Ltd. (Tokyo, Japan).

6.3.6. Chemical stability of caffeine

Chemical stability of caffeine was assessed by HPLC-UV, through the analysis of retention time variation, appearance of new peaks in the chromatogram, caffeine recovery (according to the quality guideline of ICH – Q2(R1) Validation of Analytical procedures: text and methodology) and by the interpretation of spectra obtained by FTIR-ATR regarding to each time point (Guideline, 2005).

6.3.6.1. Caffeine spectra analysis by ATR-FTIR

ATR-FTIR analysis were conducted for GfB in a FTIR spectrometer, model ABB MB3000 (ABB, Switzerland), equipped with a deuterated triglycine sulphate detector and using a MIRacle^{TM} single reflection horizontal attenuated total reflectance (ATR) accessory (PIKE Technologies, USA) with a diamond/Se crystal plate. All spectra were acquired with 256 scans and 4 cm^{-1} resolution, in the region of 4000-500 cm^{-1}.

6.3.6.2. Caffeine analysis by HPLC-UV

Dosing and retention time analysis was performed by HPLC-UV on a Waters Alliance® instrument (Milford, MA, USA). Water and methanol mixture (60:40) was used as mobile phase and isocratic flow was set to 1 mL/min (Carey & DePalma, 1994b). Samples were run through a Kromasil® C18 column, 5 μm (particle size) × 4.6 mm

(internal diameter) × 250 mm (length) (AkzoNobel, Bohus, Sweden). UV detector wavelength was set to 270 nm. The injection volume was set to 50 μL.

6.3.7. Focus group

A focus group composed of five students, female, with ages between 21 and 24, was organized to discuss the most suitable film sizes, appropriate flavors along with potential uses and prices that the group would be willing to pay for the developed formulations. The focus group occurred according to a previously planned script. The participants in the focus group were previously informed regarding the time, place, location and estimated duration of the focus group. The whole session was voice-recorded. Detailed characteristics of the focus group are listed in **Table 23**.

Table 23: Important characteristics of the alignment of the focus group

Previous statements about the session	1. Presentation of the conductors of the focus group 2. Previous statement focusing on the importance of completely honest answers that must be spoken for the group and not only for the conductors 3. Refer that the focus group will last for, approximately, 45 min.
Information regarding the product	1. Show the usual appearance of oral films 2. Explain the advantages (e.g. practicality, ease of administration) and applications (e.g. for drugs or other bioactive molecules) of oral films and the intake procedure 3. Present three different dimensions (i.e. 2.0 cm x 1.5 cm; 3.0 cm x 2.0 cm; 3.5 cm x 2.5 cm)* and ask the preferences, by visual analysis, of the participants

	4. Indicate that three different flavors are being tested (i.e. mint, strawberry and coffee)
Oral questions (Part A: formulation and acceptance analysis)	1. *Do you know what oral films are?* – the conductors must explain the concept of oral films, stressing the most important factors as the fast disintegration (within 30 s), the flavors that can be applied and portability. 2. Do you think that used flavors (i.e. mint, strawberry and coffee) are good options to include in a formulation of this kind? – in this question, every participant must ask by himself. 3. Which of the presented film sizes would suit you best?
Oral questions (Part B: consumer validation)	1. Are you a consumer of caffeine? In which forms (e.g. coffee, tea, energetic beverages, food supplements, etc.). How often? 2. Why do you consume products with caffeine? 3. Would you consume this kind of product? Why/why not? 4. Under which circumstances would you consume this type of product? 5. How much money would you be willing to pay for a pack of 5 oral films, knowing each is the equivalent of one cup of coffee?
*** Dimensions range was chosen according the dimensions of three different marketed oral films**	

6.3.8. Sensory analysis

Sensory analysis of the oral films was performed to deepen the information obtained in the focus group, aiming for the subjective evaluation of acidity (malic acid

concentrations of 0.1, 0.2 and 0.3% w/v were tested) bitterness, suitability of the flavors (i.e. mint, coffee and strawberry) and overall evaluation of the product. Sixteen naïve volunteers participated in the sensory analysis and subjectively evaluated three formulations (with code names) of each flavor in a previously randomized order as outlined in **Table 24**.

Table 24: Outline of the overall characteristics of tested formulations by the sensory analysis panel

Flavor	Concentration of malic acid (% w/v)	Code name*	Testing order (previously randomized)**
Mint	0.1	J87	1st
Mint	0.2	S27	4th
Mint	0.3	E83	5th
Strawberry	0.1	C65	6th
Strawberry	0.2	Q61	7th
Strawberry	0.3	T48	3rd
Coffee	0.1	V33	8th
Coffee	0.2	G97	2nd
Coffee	0.3	R35	9th

* the code names were obtained using a code generator and selecting a "L-NN" pattern
** randomized order was set in Microsoft Excel® 2016

The survey used to register the opinions of the panel was built in Qualtrics® platform software. A summary of the survey is outlined in **Figure 41**.

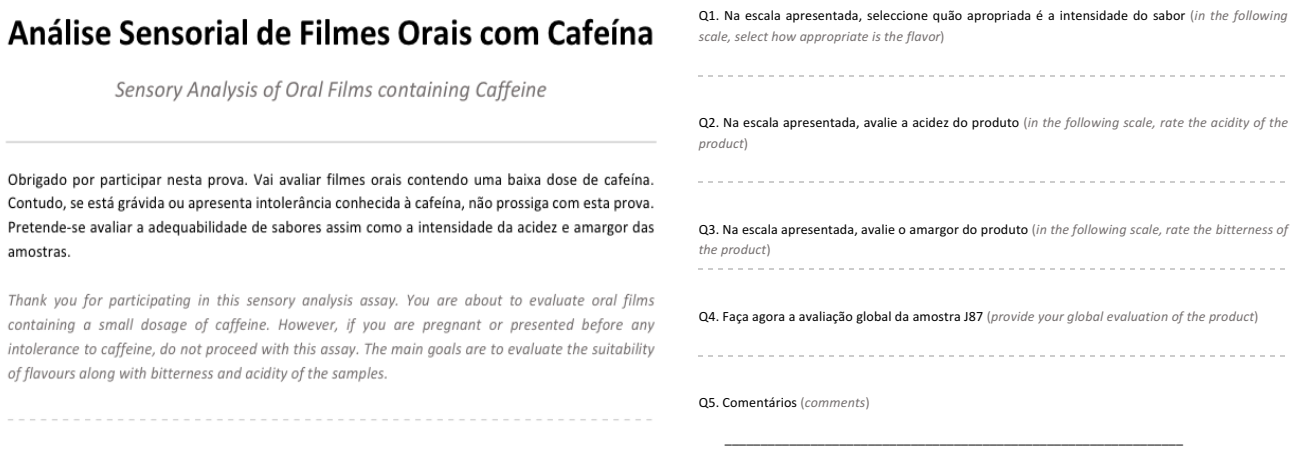

Figure 41: Survey used to register the opinion of participants regarding flavor, acidity, bitterness and global evaluation of the oral films containing caffeine. The scale range was set from 0 to 10

6.3.9. Statistical analysis

Statistical analysis regarding dissolution profile data was performed using IBM® SPSS® Statistics version 22.

Shapiro-Wilk ($n < 50$) test was used to verify if the values obtained for the responses in the experimental design were normally distributed. One-way ANOVA test was performed to compare results regarding the flavour type, acidity, bitterness and global acceptance of the tested samples.

6.4. Results and discussion

6.4.1. Stability of formulations and carried bioactive molecules

Stability was assessed after subjecting the formulations to accelerated degradation conditions as stated by the quality guidelines of international conference of harmonization (Guideline, 2005). Chemical stability and moisture content were assessed.

6.4.1.1. Stability of caffeine-loaded formulation

The occurrence of chemical alterations on caffeine-loaded GfB was controlled by the analysis of the spectra (**Figure 42**) obtained by ATR-FTIR.

Spectra of the formulation was obtained immediately after production (t0) and after thee (t3), six (t6) and nine (t9) months.

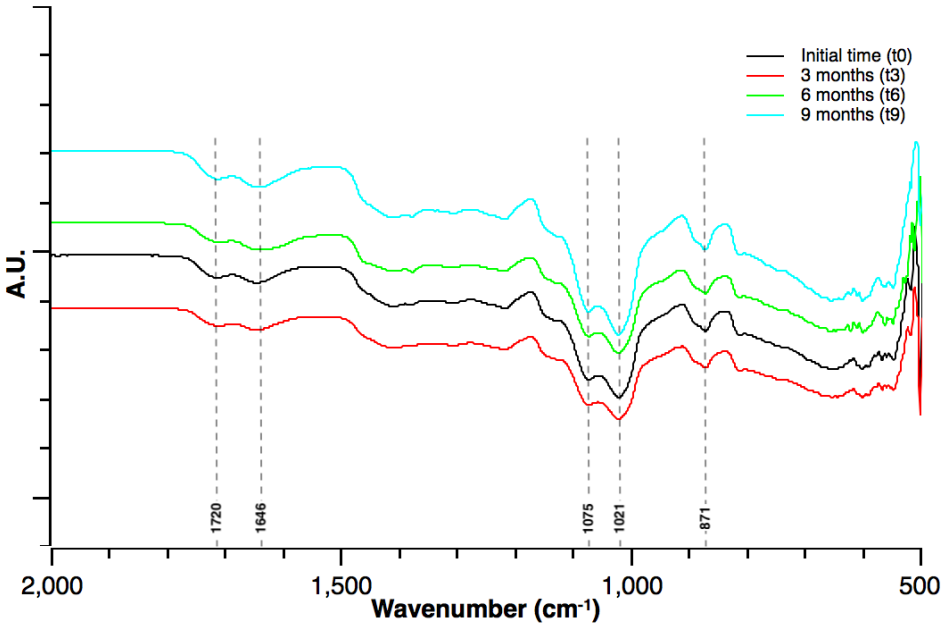

Figure 42: Comparison of spectra of caffeine-loaded GfB before (t0) and after three (t3), six (t6) and nine (t9) months under accelerated degradation conditions (40 ± 2ºC and 75 ± 5% RH)

Spectra obtained by ATR-FTIR did not indicate the formation of new covalent bonds nor the alteration of functional groups at any time point when compared with the

spectra obtained for t0. Typical caffeine bands, representative of the stretching of C=O bonds of amide I bending (1700-1600 cm^{-1}) were not altered in any time point (Castro et al., 2018a). Moreover, the fingerprint region, particularly the bands with peaks at 1075, 1021 and 871 cm^{-1} were overlapping for all the time points, therefore indicating that chemical stability was not compromised under accelerated degradation conditions stated by ICH quality guidelines.

Further information regarding the stability of caffeine molecule carried by GfB was obtained by the analysis of retention time and caffeine recovery by HPLC-UV (**Table 25**).

Table 25: Caffeine retention time and recovery by HPLC-UV immediately after production (t0) and after 3 (t3), 6 (t6) and 9 (t9) months under accelerated degradation conditions

	Retention time (min ± S.D.)	**Caffeine recovery (% ± S.D.)**
T0	3.617 ± 5.439E-16	92.08 ± 1.13
T3	3.639 ± 9.814E-03	89.73 ± 0.92
T6	3.617 ± 5.439E-16	93.42 ± 1.20
T9	3.644 ± 7.113E-07	93.77 ± 1.72

In accordance with data obtained by infrared spectra analysis of the formulations over time, results indicated that the variation in caffeine retention time was not significantly high to be associated with an alteration of the chemical composition of caffeine molecule. Moreover, the appearance of new peaks on the chromatogram was not observed, indicating that the formation of degradation products did not occur. Finally,

caffeine recovery was very similar (i.e. variations were always inferior to 5% of the expected caffeine amount) between tested samples as values are in accordance with ICH quality guideline Q2 (Analytical Validation), therefore attesting caffeine content uniformity on the dosage forms and discarding caffeine loss along time (Guideline, 2005).

However, statistically significant differences were obtained for the moisture content of formulations along time under accelerated degradation conditions, as outlined in **Figure 43.**

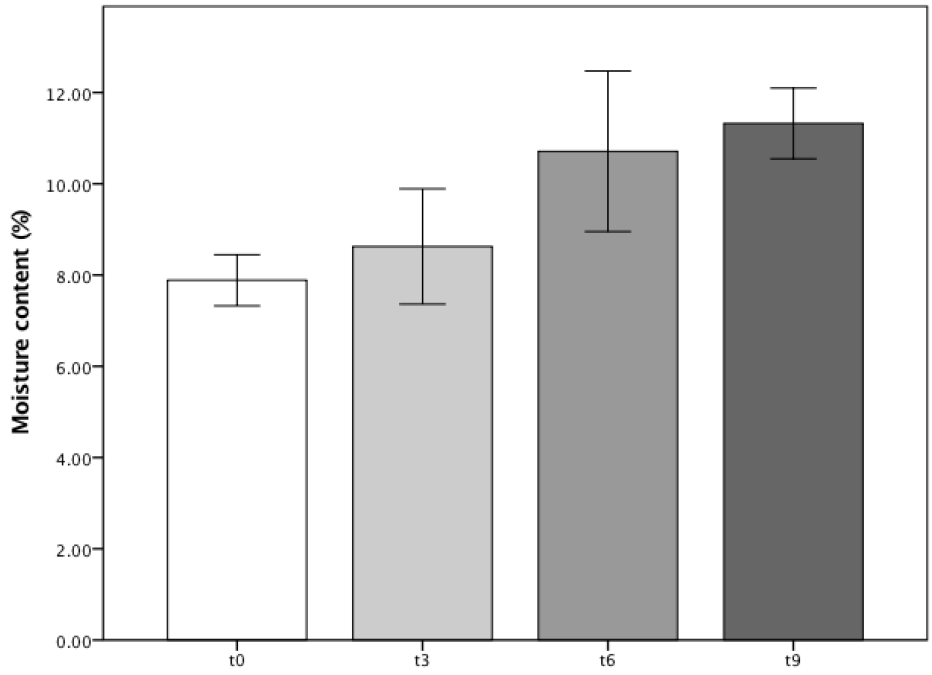

Figure 43: Moisture content of GfBd after production and after 3 (t3), 6 (t6) and 9 (t9) months under accelerated degradation conditions

The moisture content in GfB formulation increased over time under accelerated degradation conditions. Indeed, high relative humidity inside the climatic chamber (75 ± 5%) along with high water-uptake profile of guar gum films induced the increased the overall moisture content (Castro et al., 2018a). It is generally recognized that water

content to a certain extent promotes plasticity and improved sensory characteristics while dried films are friable and less appealing to the consumer (Zhang, Kim, Yokoyama & Kim, 2018). Nonetheless, chemical stability of solid delivery systems is mainly modulated by moisture content and carried bioactive molecules are prone to suffer hydrolysis (Qiu, Chen, Zhang, Yu & Mantri, 2016). Also, high moisture content may induce the creation of proper conditions of microorganism growth, therefore compromising the shelf-life of the product. Moreover, high water content may promote migration of bioactive molecules and excipients within the delivery system, leading to a heterogeneous formulation with potentially different behaviour after administration. Finally, micro and nanoparticles may undergo premature erosion (and, hence, to unwanted release of carried bioactive molecules) and aggregation, compromising the pharmacokinetic function of the formulation (Fonte, Reis & Sarmento, 2016).

6.4.2. Focus group

The focus group meeting was helpful to clarify general issues either regarding the flavors and sizes of GfB, but also the perception of potential consumers regarding the conceptually new delivery system.

None of the participants in the focus group had an immediate perception about what oral films are nor regarding potential uses of the delivery systems. Moreover, three of the participants (60%) affirmed that mint flavor would be the most appropriate to this kind of product due to inherent freshness, whether remaining participants would prefer a sweeter, fruit-like flavor as strawberry, cherry, mango or pineapple. All participants

recognized the advantages of GfB, for both convenience and slower release of caffeine, in comparison with existing products containing caffeine.

Regarding the size choices, after observing and holding three prototypes (with 2.0 cm x 1.5 cm; 3.0 cm x 2.0 cm and 3.5 cm x 2.5 cm, respectively), the participants consensually chose the intermediate dimensions. The comfort within the mouth, the potential uses (surgeons on long procedures, professional drivers, athletes and students were some of the examples given by the participants) and portability were the main reasons highlighted to justify the choice of the dimensions.

Finally, the participants in the focus group recognized that the price would be an important factor and would be willing to spend 2€ for a pack of 5 units of GfB.

6.4.3. Sensory analysis

Sensory analysis was performed by naïve panelists (n = 16) aiming to define the type of flavors that the general consumer would prefer for GfB but also to assess the preferences regarding acidity and tolerance to bitterness (inherent to the caffeine molecule). Moreover, an attempt was made to assess the possibility of masking the bitter taste by increasing the concentration of malic acid, as stated in the literature (Brittain, 2001). Results were collected and compiled in **Figure 44.**

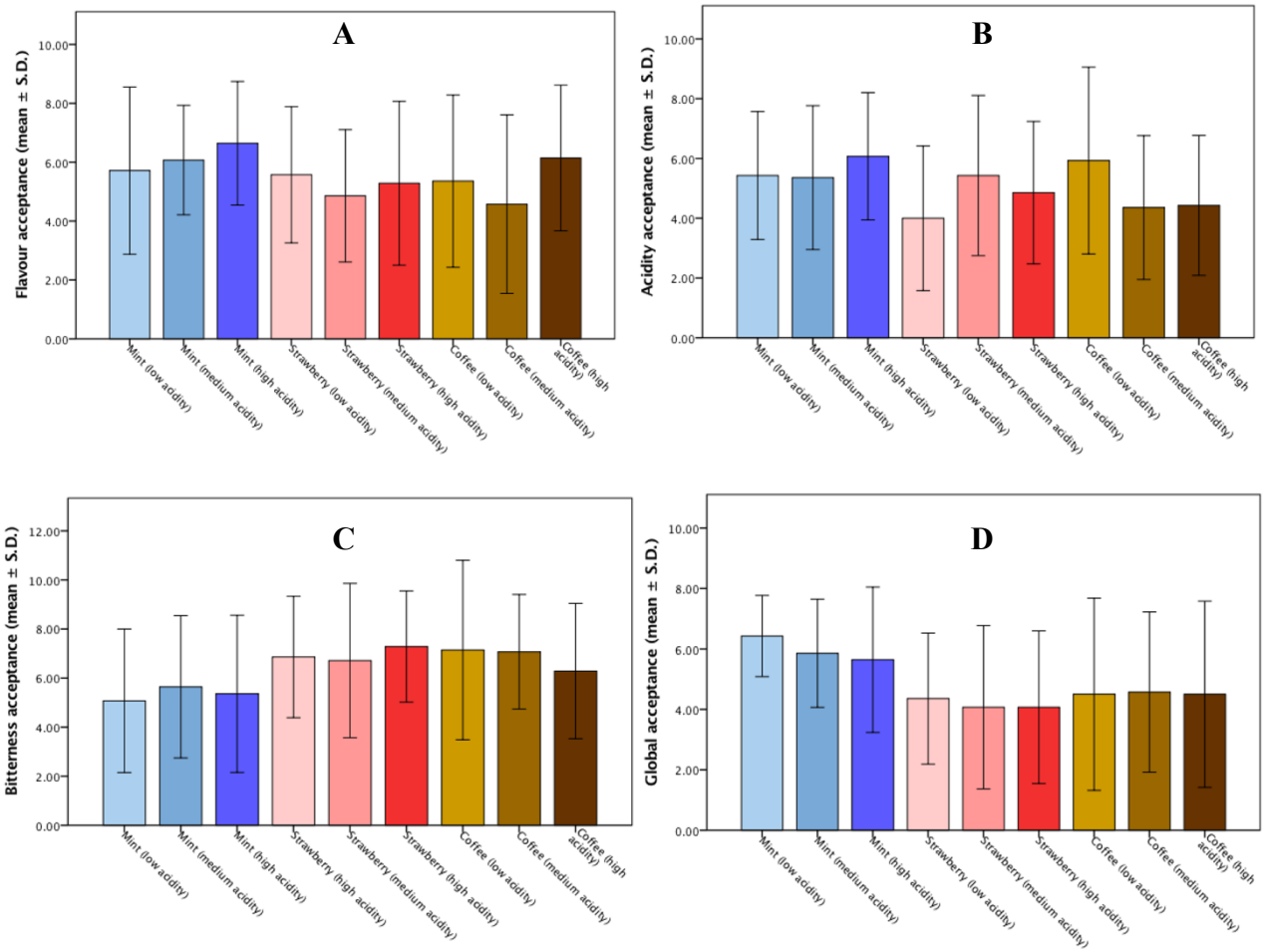

Figure 44: Compilation of survey answers regarding sensory analysis of GfB regarding type of flavor (A), acidity (B), bitterness (C) and global sensory acceptance of the product (D)

No statistically significant differences ($P > 0.05$) were found between tested samples regarding flavor, acidity acceptance, bitterness acceptance or global acceptance of the sensory characteristics of GfB. Lack of significant differences resulted mainly due to the high dispersity of the opinions of the panel. Therefore, an increase of the number of panelists along with training of a panel especially regarding the identification of bitterness and acidity can potentially lead to a decrease of dispersity in the results.

Nevertheless, some conclusions can be obtained from the data collected from the surveys. Indeed, as stated in the focus group, mint flavor (especially with the highest concentration of malic acid) was favorite as can be observed in graph A (**Figure 44**).

Moreover, the acidity acceptance was dependent on the type of flavor. Results suggested that the perception of acidity is more associated with the flavor of the formulation than with the variation of malic acid concentration, even though more data and a specialized panel are required to offer more evidences.

With regards to bitterness, higher values of acceptance were obtained for coffee or strawberry as can be seen in graph C. Indeed, both coffee and strawberry flavors are inherently bitter. Moreover, similar flavors as lemon, cherry, orange or simply the addition of citric acid are well-known taste masking agents (Anaebonam, Clemente & Fawzy, 1998; Brideau, 1995; Sohi, Sultana & Khar, 2004; Wehling, Schuehle & Madamala, 1993). Nevertheless, the global acceptance of the GfB is higher when mint flavor was used as outlined in graph D and stated in the focus group.

6.5. Conclusions

After being tested according to the ICH guidelines of stability after 3, 6 and 9 months, it was possible to conclude that the caffeine content in GfB was stable even after 9 months of accelerated degradation conditions, indicating that the shelf-life of the formulation is long. Moreover, the concept of a product that consists of caffeine-loaded alginate beads embedded onto guar gum oral films was perceived as an interesting solution for the overall improvement of life quality as stated by the focus group. Also, data obtained either from the focus group and from the sensory analysis indicated that mint flavour is more indicated to mask the off-flavours of GfB that could compromise the acceptance of the product by the consumer. Nonetheless, due to inherent bitterness of

caffeine, further studies must be performed, aiming to improve the flavour of the product without compromising the effectiveness and stability.

Section 5

Conclusions and future perspectives

Chapter VII - Conclusions

Formulations of delivery systems, namely oral films and micro/nanoparticles were successfully developed, optimized and tested, always aiming an improved oral bioavailability of carried bioactive molecules, namely caffeine, and two peptides originated from the hydrolysis of whey protein and presenting antihypertensive (sequence: KGYGGVSLPEW) and benzodiazepine-like activity (sequence: YLGYLEQLLR), respectively.

Experimental design methodology was successfully used to optimize the developed formulations, of either oral films, alginate beads and PLGA nanoparticles. Indeed, using a quality-by-design approach, the optimization process was achieved with a lower amount of experiments when compared with trial-to-error approach. It was also possible to obtain formulations tailor-made for caffeine and the peptides, with the specific aim of buccal and intestinal absorption along with effective protection against gastrointestinal tract. The incorporation of either alginate beads or PLGA nanoparticles within the matrix of guar gum films resulted in a very significant alteration of release of the carried bioactive molecules, but also on the permeability across both buccal and intestinal epithelia and stability of carried bioactive molecules.

With regards to GfB, there were no chemical modifications of caffeine molecule either during incorporation in oral films and alginate beads nor during simulation of gastrointestinal tract. Moreover, *in vitro* and *ex vivo* assays allowed to conclude that GfB did not compromise cell viability at tested concentrations. Also, GfB offered the controlled release of caffeine and a more intimate contact between the bioactive molecule and buccal and intestinal cells. Developed model can be adapted to other molecules,

mainly small hydrophilic bioactive molecules that are prone to suffer fast, extensive pre-systemic metabolism (mainly due to the contact with gastrointestinal juices) but also systemic metabolism (e.g. hepatic first-pass effect). In fact, the slower release and more intimate contact with absorptive epithelia granted by GfB can yield either a higher biological effect using the same dosage of bioactive molecule or make it possible to reduce the dosage, thus avoiding waste and overdosage-related side effects.

Similar delivery profiles were obtained for GfNp carrying the antihypertensive peptide as a slower release was observed along with a more intimate contact with the apical side of buccal and intestinal cell layers, without compromising cell viability. Additionally, it was possible to observe that GfNp granted a very effective protection of the peptide across gastrointestinal tract, totally preserving the *in vitro* inhibitory effect of the angiotensin converting enzyme.

With regards to relaxing peptide, apparent permeability was significantly increased across either TR146 buccal cell layer and Caco-2/HT29-MTX co-culture cell layer when using FNp as delivery system, without compromising cell viability. Moreover, the fate of peptide-loaded PLGA nanoparticles was further understood, granting a better insight regarding the possible process through which release of the peptide occurred.

Due to all the advantages demonstrated, the optimized and developed formulations are therefore good candidates for *in vivo* testing of effectiveness and toxicity, especially after chronical exposure. Nonetheless, acceptability by the potential consumers regarding sensory analysis must also be considered. In fact, the optimization of the effectiveness of the products as delivery systems must be followed by a thorough work regarding the sensory characteristics, since further improvement on specific parameters as bitterness, acidity and flavour must be attained.

In sum, the work reported in this thesis resulted into a conceptually new type of delivery system with high scale-up potential and marketing appeal, either for food or pharmaceutical industry.

Chapter VIII - Future perspectives

The association of oral films with micro/nanoparticles for oral delivery of bioactive molecules, with special focus on buccal administration and absorption, may represent a good candidate as a carrier for a wide array of bioactive molecules. Indeed, both buccal and intestinal permeation of caffeine and bioactive peptides was increased when carried by the association of guar gum films and alginate beads and PLGA nanoparticles, respectively.

Products aiming oral delivery via buccal route still represent a potential innovation either due to the lack of effectiveness (especially when compared with conventional delivery systems) and/or marketing appeal. Using mucoadhesive oral strips with incorporated micro and nanoparticles could become a preferential delivery method for therapies requiring rapid nutraceutical/pharmaceutical ingredient absorption, with special emphasis to those used to manage acute health issues as pain, allergies, sleeping impairment, hypertension or central nervous system disorders.

Further, oral film production techniques other than solvent casting such as inkjet printing or FPT offer greater dosage accuracy, stability for thermally labile drugs (e.g. proteins and peptides), enables individualized dosage and are liable to be automated, which are very important factors to consider if production scale-up is pursued (Genina, Janssen, Breitenbach, Breitkreutz & Sandler, 2013). Added to all advantages of oral films mentioned in this manuscript, both for the patients and industry, developed formulations have the potential to offer a breakthrough on oral delivery, with special emphasis on buccal delivery and overall acceptance, improving the every-day life of

patients/consumers. Moreover, oral films production costs are not as high as for tablets or capsules and offer the possibility of a broader therapeutic customization simply by cutting larger or smaller films, which represent important industrial advantages.

Nevertheless, oral films present inherent drawbacks as only being able to carry a maximum of about 30%, w/w, of active ingredient, thus being restricted either to potent drugs or to molecules that play both excipient and active pharmaceutical/nutritional ingredient roles, as observed for Gas-X® (in which Simeticone plays both polymer and active ingredient roles and, thus, the bioactive molecule incorporation rate is ca. 50%, w/w). Moreover, extensive acute and chronical toxicity assessment will be required by regulation entities, when industries plan using oral films as carriers for nutraceutical/pharmaceutical ingredients and penetration enhancers as excipients. Hence, future formulations must be tailored according to a quality-by-design approach and with rigorous toxicity assessment in all development phases.

Also, the inclusion of nanoparticles in food or pharmaceutical products is still not consensual, mainly due to toxicity concerns. Additionally, legislation still lacks information and proper regulation regarding the characterization and usage of nanoparticles in food or pharmaceutical products. The fact that consumers are still fearful of products functionalized with nanoparticles allied to the lack of sufficient legislation that, for instance, properly defines the term *nanomaterials* or any specific steps for the elaboration of a food product containing nanoparticles (from production to labelling) are factors that are strongly contributing to the hindrance of industries from stepping forward into the production of such products (Amenta et al., 2015). Also, the prevailing idea that potential toxicity of micro and nanoparticles is directly related with the toxicity of the excipients used to produce them is an outdated notion and must be questioned (Arts et al.,

2014). Indeed, the claim by the Organization for Economic Co-operation and Development (OECD) that compounds can be grouped in chemical categories aiming the categorization of such compounds as safe or non-safe is rather simplistic (OECD, 2014). Indeed, OECD defends that, once a compound is attributed to a chemical category, hazard estimation would be the one attributed to the overall category and not to the single compound itself. This approach does not seem entirely suitable for the risk assessment of nanoparticles as food or pharmaceutical ingredients. Indeed, besides the potential creation of new chemical entities during production of nanoparticles, particle size represents a characteristic of paramount importance that is not necessarily related with their chemical composition. Effectively, size is a main characteristic to consider when toxicity issues are regarded, since crossing of biological barriers along with tissue and cellular distribution are highly dependent on the dimensions of the particle (Arts et al., 2014). Also, the number of particles along with charge, shape and surface area are considered to contribute to different toxicity profiles on nanoparticles, when compared with larger particles formulated with the same components (Hagens, Oomen, de Jong, Cassee & Sips, 2007). With effect, the European parliament and the Council of the European Union regulated that consumers must be informed of the presence of engineered nanomaterials, suggesting that labels must include this information (Parliament, 2011). But, even though engineered nanomaterials are defined by the EU regulation, no clear boundaries on the size of particles are defined. Thus, grouping compounds into chemical categories is rather insufficient for the risk assessment of nanoparticles to be incorporated within food and pharmaceutical products.

Finally, regarding the products described in this thesis, further evaluation of *in vivo* effectiveness and toxicity along with optimization of texture, flavour, bitterness masking, acidity control, among others, must be thoroughly performed before proceeding to the commercialization of developed formulations. Nonetheless, a substantial advance was performed that should not be wasted.

References: .

(1989). CAFFEINISM. *The Lancet, 333*(8644), 972.

(FDA), F. a. D. A. (2017a). SCOGS (Select Committee on GRAS Substances) - citric acid. (Vol. 2017).

(FDA), F. a. D. A. (2017b). SCOGS (Select Committee on GRAS Substances) - guar gum. (Vol. 2017).

(FDA), F. a. D. A. (2017c). SCOGS (Select Committee on GRAS Substances) - sorbitol. (Vol. 2017).

Abdelkader, D. H., El-Gizawy, S. A., Faheem, A. M., McCarron, P. A., & Osman, M. A. (2018). Effect of process variables on formulation, in-vitro characterisation and subcutaneous delivery of insulin PLGA nanoparticles: An optimisation study. *Journal of Drug Delivery Science and Technology, 43*, 160-171.

Adeleke, O. A., Choonara, Y. E., Kumar, P., du Toit, L. C., Tomar, L. K., Tyagi, C., & Pillay, V. (2013). Evaluation of the impacts of formulation variables and excipients on the drug release dynamics of a polyamide 6,10-based monolithic matrix using mathematical tools. *AAPS PharmSciTech, 14*(4), 1349-1359.

Administration, F. a. D. (2008). Guidance for Industry: Orally Disintegrating Tablets. *Center for Drug Evaluation and Research (CDER)*.

Adrover, A., & Nobili, M. (2015). Release kinetics from oral thin films: Theory and experiments. *Chemical Engineering Research & Design, 98*, 188-201.

Adrover, A., Pedacchia, A., Petralito, S., & Spera, R. (2015a). In vitro dissolution testing of oral thin films: A comparison between USP 1, USP 2 apparatuses and a new millifluidic flow-through device. *Chemical Engineering Research & Design, 95*, 173-178.

Adrover, A., Pedacchia, A., Petralito, S., & Spera, R. (2015b). In vitro dissolution testing of oral thin films: A comparison between USP 1, USP 2 apparatuses and a new millifluidic flow-through device. *Chem. Eng. Res. Des., 95*(0), 173-178.

Agency, E. M. (2010). Guideline on the investigation of bioequivalence. European Medicines Agency, CHMP London, UK.

Ahuja, A., Khar, R. K., & Ali, J. (2008). Mucoadhesive Drug Delivery Systems. *Drug Dev Ind Pharm, 23*(5), 489-515.

Akil, A., Agashe, H., Dezzutti, C. S., Moncla, B. J., Hillier, S. L., Devlin, B., Shi, Y., Uranker, K., & Rohan, L. C. (2015). Formulation and characterization of polymeric films

containing combinations of antiretrovirals (ARVs) for HIV prevention. *Pharm Res, 32*(2), 458-468.

Al-Dhubiab, B. E., Nair, A. B., Kumria, R., Attimarad, M., & Harsha, S. (2015). Formulation and evaluation of nano based drug delivery system for the buccal delivery of acyclovir. *Colloids Surf B Biointerfaces, 136*, 878-884.

Almeida, A., Silva, D., Goncalves, V., & Sarmento, B. (2018). Synthesis and characterization of chitosan-grafted-polycaprolactone micelles for modulate intestinal paclitaxel delivery. *Drug Deliv Transl Res, 8*(2), 387-397.

Amenta, V., Aschberger, K., Arena, M., Bouwmeester, H., Botelho Moniz, F., Brandhoff, P., Gottardo, S., Marvin, H. J., Mech, A., Quiros Pesudo, L., Rauscher, H., Schoonjans, R., Vettori, M. V., Weigel, S., & Peters, R. J. (2015). Regulatory aspects of nanotechnology in the agri/feed/food sector in EU and non-EU countries. *Regul Toxicol Pharmacol, 73*(1), 463-476.

Amores, S., Lauroba, J., Calpena, A., Colom, H., Gimeno, A., & Domenech, J. (2014). A comparative ex vivo drug permeation study of beta-blockers through porcine buccal mucosa. *Int. J. Pharm., 468*(1–2), 50-54.

Anaebonam, A. O., Clemente, E., & Fawzy, A. A. (1998). Pleasant-tasting aqueous liquid composition of a bitter-tasting drug. Google Patents.

Antonov, Y. A., & Zhuravleva, I. L. (2013). Effect of protein thermo aggregation on the binding of BSA to gelatin type A. *Int. J. Biol. Macromol., 53*(0), 160-167.

Antunes, F., Andrade, F., Araujo, F., Ferreira, D., & Sarmento, B. (2013). Establishment of a triple co-culture in vitro cell models to study intestinal absorption of peptide drugs. *Eur J Pharm Biopharm, 83*(3), 427-435.

Arakawa, T., Ejima, D., Tsumoto, K., Obeyama, N., Tanaka, Y., Kita, Y., & Timasheff, S. N. (2007). Suppression of protein interactions by arginine: a proposed mechanism of the arginine effects. *Biophys Chem, 127*(1-2), 1-8.

Araujo, F., & Sarmento, B. (2013). Towards the characterization of an in vitro triple co-culture intestine cell model for permeability studies. *Int J Pharm, 458*(1), 128-134.

Araujo, F., Shrestha, N., Shahbazi, M. A., Fonte, P., Makila, E. M., Salonen, J. J., Hirvonen, J. T., Granja, P. L., Santos, H. A., & Sarmento, B. (2014). The impact of nanoparticles on the mucosal translocation and transport of GLP-1 across the intestinal epithelium. *Biomaterials, 35*(33), 9199-9207.

Arts, J. H., Hadi, M., Keene, A. M., Kreiling, R., Lyon, D., Maier, M., Michel, K., Petry, T., Sauer, U. G., Warheit, D., Wiench, K., & Landsiedel, R. (2014). A critical appraisal of existing concepts for the grouping of nanomaterials. *Regul Toxicol Pharmacol, 70*(2), 492-506.

Aura, A.-M. (2005). *In vitro digestion models for dietary phenolic compounds*. VTT Technical Research Centre of Finland.

Bakhru, S. H., Furtado, S., Morello, A. P., & Mathiowitz, E. (2013). Oral delivery of proteins by biodegradable nanoparticles. *Adv Drug Deliv Rev, 65*(6), 811-821.

Banerjee, A., Qi, J., Gogoi, R., Wong, J., & Mitragotri, S. (2016). Role of nanoparticle size, shape and surface chemistry in oral drug delivery. *J Control Release, 238*, 176-185.

Barua, S., & Mitragotri, S. (2014). Challenges associated with Penetration of Nanoparticles across Cell and Tissue Barriers: A Review of Current Status and Future Prospects. *Nano today, 9*(2), 223-243.

Batista, P., Castro, P. M., Madureira, A. R., Sarmento, B., & Pintado, M. (2018). Recent insights in the use of nanocarriers for the oral delivery of bioactive proteins and peptides. *Peptides, 101*, 112-123.

Beata, C., Beaumont, E., Diaz, C., Marion, M., Marlois, N., Massal, N., Muller, G., Tauzin, J., & Lefranc, C. (2007a). 9: Comparison of the effect of alpha-casozepine (tryptic hydrolysate of alpha s1-casein) and selegiline chlorhydrate in the treatment of anxiety disorders in dogs. *Journal of Veterinary Behavior: Clinical Applications and Research, 2*(3), 86-87.

Beata, C., Beaumont-Graff, E., Coll, V., Cordel, J., Marion, M., Massal, N., Marlois, N., & Tauzin, J. (2007b). Effect of alpha-casozepine (Zylkene) on anxiety in cats. *Journal of Veterinary Behavior-Clinical Applications and Research, 2*(2), 40-46.

Benoit, S., Chaumontet, C., Schwarz, J., Cakir-Kiefer, C., Tomé, D., & Miclo, L. (2017). Mapping in mice the brain regions involved in the anxiolytic-like properties of α-casozepine, a tryptic peptide derived from bovine α s1-casein. *Journal of Functional Foods, 38*, 464-473.

Bernkop-Schnurch, A., Kast, C. E., & Guggi, D. (2003a). Permeation enhancing polymers in oral delivery of hydrophilic macromolecules: thiomer/GSH systems. *J Control Release, 93*(2), 95-103.

Bernkop-Schnurch, A., Kast, C. E., & Guggi, D. (2003b). Permeation enhancing polymers in oral delivery of hydrophilic macromolecules: thiomer/GSH systems. *J. Control. Release., 93*(2), 95-103.

Bhattacharjee, S., Mahon, E., Harrison, S. M., McGetrick, J., Muniyappa, M., Carrington, S. D., & Brayden, D. J. (2017). Nanoparticle passage through porcine jejunal mucus: Microfluidics and rheology. *Nanomedicine, 13*(3), 863-873.

Bilati, U., Allemann, E., & Doelker, E. (2005a). Development of a nanoprecipitation method intended for the entrapment of hydrophilic drugs into nanoparticles. *Eur J Pharm Sci, 24*(1), 67-75.

Bilati, U., Allemann, E., & Doelker, E. (2005b). Nanoprecipitation versus emulsion-based techniques for the encapsulation of proteins into biodegradable nanoparticles and process-related stability issues. *Aaps Pharmscitech, 6*(4), E594-E604.

Biswas, A., Kim, S., Selling, G. W., & Cheng, H. N. (2014). Conversion of agricultural residues to carboxymethylcellulose and carboxymethylcellulose acetate. *Ind. Crop. Prod., 60*(0), 259-265.

Blanco, D., & Alonso, M. J. (1998). Protein encapsulation and release from poly(lactide-co-glycolide) microspheres: effect of the protein and polymer properties and of the co-encapsulation of surfactants. *Eur. J. Pharm. Biopharm., 45*(3), 285-294.

Boateng, J. S., & Okeke, O. (2014). Chitosan-based films for the sustained release of peptides: a new era in buccal delivery? *Ther Deliv, 5*(5), 497-500.

Boateng, J. S., Stevens, H. N., Eccleston, G. M., Auffret, A. D., Humphrey, M. J., & Matthews, K. H. (2009). Development and mechanical characterization of solvent-cast polymeric films as potential drug delivery systems to mucosal surfaces. *Drug Dev Ind Pharm, 35*(8), 986-996.

Boctor, A. M., & Mehta, S. C. (1992). Enhancement of the stability of thrombin by polyols: microcalorimetric studies. *J Pharm Pharmacol, 44*(7), 600-603.

Borchard, G., Lueβen, H. L., de Boer, A. G., Verhoef, J. C., Lehr, C.-M., & Junginger, H. E. (1996a). The potential of mucoadhesive polymers in enhancing intestinal peptide drug absorption. III: Effects of chitosan-glutamate and carbomer on epithelial tight junctions in vitro. *Journal of Controlled Release, 39*(2-3), 131-138.

Borchard, G., Lueβen, H. L., de Boer, A. G., Verhoef, J. C., Lehr, C.-M., & Junginger, H. E. (1996b). The potential of mucoadhesive polymers in enhancing intestinal peptide drug absorption. III: Effects of chitosan-glutamate and carbomer on epithelial tight junctions in vitro. *J. Control. Release, 39*(2-3), 131-138.

Borchardt, R. T. (1999). Optimizing oral absorption of peptides using prodrug strategies. *Journal of Controlled Release, 62*(1-2), 231-238.

Bourbon, A. I., Cerqueira, M. A., & Vicente, A. A. (2016). Encapsulation and controlled release of bioactive compounds in lactoferrin-glycomacropeptide nanohydrogels: Curcumin and caffeine as model compounds. *Journal of Food Engineering, 180*, 110-119.

Brayden, D. J., & O'mahony, D. J. (1998). Novel oral drug delivery gateways for biotechnology products: polypeptides and vaccines. *Pharm. Sci. Technol. To, 1*(7), 291-299.

Brazel, C. S., & Peppas, N. A. (1999). Mechanisms of solute and drug transport in relaxing, swellable, hydrophilic glassy polymers. *Polymer, 40*(12), 3383-3398.

Brideau, M. (1995). Fast dissolving dosage forms. *PCT Int. Appl. WO9533446*.

Brittain, H. G. (2001). Malic Acid. In H. G. Brittain (Ed.). *Analytical Profiles of Drug Substances and Excipients* (Vol. 28, pp. 153-195): Academic Press.

Brodin, B., Steffansen, B., & Nielsen, C. U. (2010). Passive diffusion of drug substances: the concepts of flux and permeability. *Molecular biopharmaceutics: Aspects of drug characterisation, drug delivery and dosage form evaluation* (Vol. 3, pp. 135-151). London: Pharmaceutical Press.

Buanz, A. B. M., Belaunde, C. C., Soutari, N., Tuleu, C., Gul, M. O., & Gaisford, S. (2015). Ink-jet printing versus solvent casting to prepare oral films: Effect on mechanical properties and physical stability. *Int J Pharm, 494*(2), 611-618.

Busby, R. W., Bryant, A. P., Bartolini, W. P., Cordero, E. A., Hannig, G., Kessler, M. M., Mahajan-Miklos, S., Pierce, C. M., Solinga, R. M., Sun, L. J., Tobin, J. V., Kurtz, C. B., & Currie, M. G. (2010). Linaclotide, through activation of guanylate cyclase C, acts locally in the gastrointestinal tract to elicit enhanced intestinal secretion and transit. *Eur. J. Pharmacol., 649*(1–3), 328-335.

Cao, E., Chen, Y., Cui, Z., & Foster, P. R. (2003). Effect of freezing and thawing rates on denaturation of proteins in aqueous solutions. *Biotechnol. Bioeng., 82*(6), 684-690.

Capen, R., Christopher, D., Forenzo, P., Ireland, C., Liu, O., Lyapustina, S., O'Neill, J., Patterson, N., Quinlan, M., Sandell, D., Schwenke, J., Stroup, W., & Tougas, T. (2012). On the shelf life of pharmaceutical products. *AAPS PharmSciTech, 13*(3), 911-918.

Carey, R. J., & DePalma, G. (1994a). A simplified method for the measurement of caffeine in plasma and brain: evidence for a cortical-subcortical caffeine concentration differential in brain. *J Neurosci Methods, 53*(1), 19-22.

Carey, R. J., & DePalma, G. (1994b). A simplified method for the measurement of caffeine in plasma and brain: evidence for a cortical-subcortical caffeine concentration differential in brain. *J. Neurosci. Meth., 53*(1), 19-22.

Castro, P., Madureira, R., Sarmento, B., & Pintado, M. (2016). 4.1 - Tissue-based in vitro and ex vivo models for buccal permeability studies. *Concepts and Models for Drug Permeability Studies* (pp. 189-202): Woodhead Publishing.

Castro, P. M., Baptista, P., Madureira, A. R., Sarmento, B., & Pintado, M. E. (2018). Combination of PLGA nanoparticles with mucoadhesive guar-gum films for buccal delivery of antihypertensive peptide. *Int J Pharm, 547*(1-2), 593-601.

Castro, P. M., Fonte, P., Oliveira, A., Madureira, A. R., Sarmento, B., & Pintado, M. E. (2017). Optimization of two biopolymer-based oral films for the delivery of bioactive molecules. *Mater Sci Eng C Mater Biol Appl, 76*, 171-180.

Castro, P. M., Fonte, P., Sousa, F., Madureira, A. R., Sarmento, B., & Pintado, M. E. (2015a). Oral films as breakthrough tools for oral delivery of proteins/peptides. *J Control Release, 211*(0), 63-73.

Castro, P. M., Fonte, P., Sousa, F., Madureira, A. R., Sarmento, B., & Pintado, M. E. (2015b). Oral films as breakthrough tools for oral delivery of proteins/peptides. *J. Control. Release, 211*(0), 63-73.

Castro, P. M., Fonte, P., Sousa, F., Madureira, A. R., Sarmento, B., & Pintado, M. E. (2015c). Oral films as breakthrough tools for oral delivery of proteins/peptides. *J Control Release, 211*, 63-73.

Castro, P. M., Sousa, F., Magalhaes, R., Ruiz-Henestrosa, V. M. P., Pilosof, A. M. R., Madureira, A. R., Sarmento, B., & Pintado, M. E. (2018a). Incorporation of beads into oral films for buccal and oral delivery of bioactive molecules. *Carbohydrate Polymers, 194*, 411-421.

Castro, P. M., Sousa, F., Magalhaes, R., Ruiz-Henestrosa, V. M. P., Pilosof, A. M. R., Madureira, A. R., Sarmento, B., & Pintado, M. E. (2018b). Incorporation of beads into oral films for buccal and oral delivery of bioactive molecules. *Carbohydr Polym, 194*, 411-421.

Castro, P. M., Sousa, F., Magalhães, R., Ruiz-Henestrosa, V. M. P., Pilosof, A. M. R., Madureira, A. R., Sarmento, B., & Pintado, M. E. (2018c). Incorporation of beads into oral films for buccal and oral delivery of bioactive molecules. *Carbohydrate Polymers*.

Català-Clariana, S., Benavente, F., Giménez, E., Barbosa, J., & Sanz-Nebot, V. (2010). Identification of bioactive peptides in hypoallergenic infant milk formulas by capillary electrophoresis–mass spectrometry. *Anal. Chim. Acta., 683*(1), 119-125.

Cavallari, C., Brigidi, P., & Fini, A. (2015). Ex-vivoand in-vitro assessment of mucoadhesive patches containing the gel-forming polysaccharide psyllium for buccal delivery of chlorhexidine base. *Int J Pharm, 496*(2), 593-600.

Cerqueira, B. B. S., Lasham, A., Shelling, A. N., & Al-Kassas, R. (2017). Development of biodegradable PLGA nanoparticles surface engineered with hyaluronic acid for targeted delivery of paclitaxel to triple negative breast cancer cells. *Mater Sci Eng C Mater Biol Appl, 76*, 593-600.

Chang, B. S., Beauvais, R. M., Arakawa, T., Narhi, L. O., Dong, A., Aparisio, D. I., & Carpenter, J. F. (1996). Formation of an active dimer during storage of interleukin-1 receptor antagonist in aqueous solution. *Biophys J, 71*(6), 3399-3406.

Cheng, L. H., Abd Karim, A., Norziah, M. H., & Seow, C. C. (2002). Modification of the microstructural and physical properties of konjac glucomannan-based films by alkali and sodium carboxymethylcellulose. *Food Res. Int., 35*(9), 829-836.

Chi, V., Pennington, M. W., Norton, R. S., Tarcha, E. J., Londono, L. M., Sims-Fahey, B., Upadhyay, S. K., Lakey, J. T., Iadonato, S., Wulff, H., Beeton, C., & Chandy, K. G. (2012).

Development of a sea anemone toxin as an immunomodulator for therapy of autoimmune diseases. *Toxicon, 59*(4), 529-546.

Choonara, B. F., Choonara, Y. E., Kumar, P., Bijukumar, D., du Toit, L. C., & Pillay, V. (2014). A review of advanced oral drug delivery technologies facilitating the protection and absorption of protein and peptide molecules. *Biotechnol Adv, 32*(7), 1269-1282.

Chung, T. W., Huang, Y. Y., & Liu, Y. Z. (2001). Effects of the rate of solvent evaporation on the characteristics of drug loaded PLLA and PDLLA microspheres. *Int J Pharm, 212*(2), 161-169.

Cilurzo, F., Gennari, C. G., Selmin, F., Musazzi, U. M., Rumio, C., & Minghetti, P. (2013). A novel oromucosal prolonged release mucoadhesive suspension by one step spray coagulation method. *Curr Drug Deliv, 10*(3), 251-260.

Coimbra, P., Gil, M. H., & Figueiredo, M. (2014). Tailoring the properties of gelatin films for drug delivery applications: Influence of the chemical cross-linking method. *Int. J. Biol. Macromolec., 70*(0), 10-19.

Cone, R. A. (2009). Barrier properties of mucus. *Adv Drug Deliv Rev, 61*(2), 75-85.

Costantino, H. R., Schwendeman, S. P., Langer, R., & Klibanov, A. M. (1998). Deterioration of lyophilized pharmaceutical proteins. *Biochemistry (Mosc), 63*(3), 357-363.

Couvreur, P., & Puisieux, F. (1993). Nano-and microparticles for the delivery of polypeptides and proteins. *Advanced Drug Delivery Reviews, 10*(2-3), 141-162.

Crucho, C. I. C., & Barros, M. T. (2017). Polymeric nanoparticles: A study on the preparation variables and characterization methods. *Mater Sci Eng C Mater Biol Appl, 80*, 771-784.

Cui, F., He, C., He, M., Tang, C., Yin, L., Qian, F., & Yin, C. (2009). Preparation and evaluation of chitosan-ethylenediaminetetraacetic acid hydrogel films for the mucoadhesive transbuccal delivery of insulin. *J Biomed Mater Res A, 89*(4), 1063-1071.

Cunha-Reis, C., Machado, A., Barreiros, L., Araujo, F., Nunes, R., Seabra, V., Ferreira, D., Segundo, M. A., Sarmento, B., & das Neves, J. (2016). Nanoparticles-in-film for the combined vaginal delivery of anti-HIV microbicide drugs. *J Control Release, 243*, 43-53.

D'Souza, A. J., Schowen, R. L., Borchardt, R. T., Salsbury, J. S., Munson, E. J., & Topp, E. M. (2003). Reaction of a peptide with polyvinylpyrrolidone in the solid state. *J. Pharm. Sci., 92*(3), 585-593.

da Silva, S. B., Ferreira, D., Pintado, M., & Sarmento, B. (2016a). Chitosan-based nanoparticles for rosmarinic acid ocular delivery--In vitro tests. *International Journal of Biological Macromolecules, 84*, 112-120.

da Silva, S. B., Ferreira, D., Pintado, M., & Sarmento, B. (2016b). Chitosan-based nanoparticles for rosmarinic acid ocular delivery--In vitro tests. *Int J Biol Macromol, 84*, 112-120.

Dalpiaz, A., Sacchetti, F., Baldisserotto, A., Pavan, B., Maretti, E., Iannuccelli, V., & Leo, E. (2016). Application of the "in-oil nanoprecipitation" method in the encapsulation of hydrophilic drugs in PLGA nanoparticles. *Journal of Drug Delivery Science and Technology, 32*, 283-290.

Danhier, F., Ansorena, E., Silva, J. M., Coco, R., Le Breton, A., & Preat, V. (2012). PLGA-based nanoparticles: an overview of biomedical applications. *J Control Release, 161*(2), 505-522.

De Caro, V., Giandalia, G., Siragusa, M. G., Paderni, C., Campisi, G., & Giannola, L. I. (2008). Evaluation of galantamine transbuccal absorption by reconstituted human oral epithelium and porcine tissue as buccal mucosa models: part I. *Eur J Pharm Biopharm, 70*(3), 869-873.

De La Cruz, E. M., & Pollard, T. D. (1995). Nucleotide-free actin: stabilization by sucrose and nucleotide binding kinetics. *Biochemistry, 34*(16), 5452-5461.

de Souza, C. J. F., Ramos, A. V., Câmara, P. B. S., Gulão, E. S., de Campos, M. F., & Garcia-Rojas, E. E. (2015). Polymeric complexes obtained from the interaction of bovine serum albumin and κ-carrageenan. *Food Hydrocolloid., 45*(0), 286-290.

Deacon, M. P., McGurk, S., Roberts, C. J., Williams, P. M., Tendler, S. J., Davies, M. C., Davis, S. S., & Harding, S. E. (2000). Atomic force microscopy of gastric mucin and chitosan mucoadhesive systems. *Biochem J, 348 Pt 3*(3), 557-563.

di Cagno, M., Bibi, H. A., & Bauer-Brandl, A. (2015). New biomimetic barrier Permeapad for efficient investigation of passive permeability of drugs. *Eur J Pharm Sci, 73*, 29-34.

Ding, D., & Zhu, Q. (2018). Recent advances of PLGA micro/nanoparticles for the delivery of biomacromolecular therapeutics. *Mater Sci Eng C Mater Biol Appl, 92*, 1041-1060.

Dixit, R. P., & Puthli, S. P. (2009a). Oral strip technology: overview and future potential. *J. Control. Release, 139*(2), 94-107.

Dixit, R. P., & Puthli, S. P. (2009b). Oral strip technology: overview and future potential. *J Control Release, 139*(2), 94-107.

Dodi, G., Pala, A., Barbu, E., Peptanariu, D., Hritcu, D., Popa, M. I., & Tamba, B. I. (2016). Carboxymethyl guar gum nanoparticles for drug delivery applications: Preparation and preliminary in-vitro investigations. *Mater Sci Eng C Mater Biol Appl, 63*, 628-636.

Dodou, D., Breedveld, P., & Wieringa, P. A. (2005). Mucoadhesives in the gastrointestinal tract: revisiting the literature for novel applications. *Eur J Pharm Biopharm, 60*(1), 1-16.

dos Santos, T. C., Rescignano, N., Boff, L., Reginatto, F. H., Simões, C. M. O., de Campos, A. M., & Mijangos, C. U. (2017). Manufacture and characterization of chitosan/PLGA nanoparticles nanocomposite buccal films. *Carbohydrate Polymers, 173*, 638-644.

Dullius, A., Goettert, M. I., & de Souza, C. F. V. (2018). Whey protein hydrolysates as a source of bioactive peptides for functional foods - Biotechnological facilitation of industrial scale-up. *Journal of Functional Foods, 42*, 58-74.

Elzoghby, A. O. (2013). Gelatin-based nanoparticles as drug and gene delivery systems: Reviewing three decades of research. *J. Control. Release, 172*(3), 1075-1091.

Faber-Barata, J., & Sola-Penna, M. (2005). Opposing effects of two osmolytes - trehalose and glycerol - on thermal inactivation of rabbit muscle 6-phosphofructo-1-kinase. *Molecular and cellular biochemistry, 269*(1-2), 203-207.

Fievez, V., Plapied, L., des Rieux, A., Pourcelle, V., Freichels, H., Wascotte, V., Vanderhaeghen, M. L., Jerome, C., Vanderplasschen, A., Marchand-Brynaert, J., Schneider, Y. J., & Preat, V. (2009). Targeting nanoparticles to M cells with non-peptidic ligands for oral vaccination. *Eur J Pharm Biopharm, 73*(1), 16-24.

Fonte, P., Reis, S., & Sarmento, B. (2016). Facts and evidences on the lyophilization of polymeric nanoparticles for drug delivery. *J Control Release, 225*, 75-86.

Fredenberg, S., Wahlgren, M., Reslow, M., & Axelsson, A. (2011). The mechanisms of drug release in poly(lactic-co-glycolic acid)-based drug delivery systems--a review. *Int J Pharm, 415*(1-2), 34-52.

Fredholm, B. B., Battig, K., Holmen, J., Nehlig, A., & Zvartau, E. E. (1999). Actions of caffeine in the brain with special reference to factors that contribute to its widespread use. *Pharmacol Rev, 51*(1), 83-133.

Gajdošová, M., Vetchý, D., Doležel, P., Gajdziok, J., Landová, H., Muselík, J., Zeman, J., Knotek, Z., Hauptman, K., & Jekl, V. (2016). Evaluation of mucoadhesive oral films containing nystatin. *Journal of Applied Biomedicine, 14*(4), 247-256.

Gan, Q., & Wang, T. (2007). Chitosan nanoparticle as protein delivery carrier - Systematic examination of fabrication conditions for efficient loading and release. *Colloids and Surfaces B-Biointerfaces, 59*(1), 24-34.

Gang, L., Dong-Hai, L., Xin-Xin, X., Li-Fang, Q., Jun-Teng, W., & Ke, L. (2013). Uptake and transport of furanodiene in Caco-2 cell monolayers: a comparison study between furanodiene and furanodiene loaded PLGA nanoparticles. *Chinese journal of natural medicines, 11*(1), 49-55.

García-Arieta, A. (2014). Interactions between active pharmaceutical ingredients and excipients affecting bioavailability: impact on bioequivalence. *European Journal of Pharmaceutical Sciences, 65*, 89-97.

Garcia-Fuentes, M., Torres, D., & Alonso, M. J. (2005). New surface-modified lipid nanoparticles as delivery vehicles for salmon calcitonin. *Int J Pharm, 296*(1-2), 122-132.

Garinot, M., Fievez, V., Pourcelle, V., Stoffelbach, F., des Rieux, A., Plapied, L., Theate, I., Freichels, H., Jerome, C., Marchand-Brynaert, J., Schneider, Y. J., & Preat, V. (2007). PEGylated PLGA-based nanoparticles targeting M cells for oral vaccination. *J Control Release, 120*(3), 195-204.

Garrigues, J. M., Bouhsain, Z., Garrigues, S., & de la Guardia, M. (2000). Fourier transform infrared determination of caffeine in roasted coffee samples. *Fresenius J. Anal. Chem., 366*(3), 319-322.

Gaspar, S., & Ramos, F. (2016). Caffeine: Consumption and Health Effects A2 - Caballero, Benjamin. In P. M. Finglas & F. Toldrá (Eds.). *Encyclopedia of Food and Health* (pp. 573-578). Oxford: Academic Press.

Gaumet, M., Gurny, R., & Delie, F. (2010). Interaction of biodegradable nanoparticles with intestinal cells: the effect of surface hydrophilicity. *Int J Pharm, 390*(1), 45-52.

Genina, N., Fors, D., Vakili, H., Ihalainen, P., Pohjala, L., Ehlers, H., Kassamakov, I., Haeggstrom, E., Vuorela, P., Peltonen, J., & Sandler, N. (2012). Tailoring controlled-release oral dosage forms by combining inkjet and flexographic printing techniques. *Eur J Pharm Sci, 47*(3), 615-623.

Genina, N., Janssen, E. M., Breitenbach, A., Breitkreutz, J., & Sandler, N. (2013). Evaluation of different substrates for inkjet printing of rasagiline mesylate. *Eur J Pharm Biopharm, 85*(3 Pt B), 1075-1083.

Giovinazzo, A. J., Hedden, D. B., de Somer, M. L., & Bryson, N. J. (2011). Sublingual apomorphine. Google Patents.

Giovino, C., Ayensu, I., Tetteh, J., & Boateng, J. S. (2012). Development and characterisation of chitosan films impregnated with insulin loaded PEG-b-PLA nanoparticles (NPs): a potential approach for buccal delivery of macromolecules. *Int J Pharm, 428*(1-2), 143-151.

Giovino, C., Ayensu, I., Tetteh, J., & Boateng, J. S. (2013). An integrated buccal delivery system combining chitosan films impregnated with peptide loaded PEG-b-PLA nanoparticles. *Colloids Surf B Biointerfaces, 112*, 9-15.

Giunchedi, P., Juliano, C., Gavini, E., Cossu, M., & Sorrenti, M. (2002). Formulation and in vivo evaluation of chlorhexidine buccal tablets prepared using drug-loaded chitosan microspheres. *European Journal of Pharmaceutics and Biopharmaceutics, 53*(2), 233-239.

Gombotz, W. R., Pankey, S. C., Phan, D., Drager, R., Donaldson, K., Antonsen, K. P., Hoffman, A. S., & Raff, H. V. (1994). The stabilization of a human IgM monoclonal antibody with poly(vinylpyrrolidone). *Pharm. Res., 11*(5), 624-632.

Gomes de Oliveira, M. E., Fernandes Garcia, E., Vasconcelos de Oliveira, C. E., Pereira Gomes, A. M., Esteves Pintado, M. M., Ferreira Madureira, A. R. M., da Conceicao, M. L., Ramos do EgyptoQueiroga, R. C., & de Souza, E. L. (2014). Addition of probiotic bacteria in a semi-hard goat cheese (coalho): Survival to simulated gastrointestinal conditions and inhibitory effect against pathogenic bacteria. *Food Research International, 64*, 241-247.

Goncalves, V. S., Gurikov, P., Poejo, J., Matias, A. A., Heinrich, S., Duarte, C. M., & Smirnova, I. (2016). Alginate-based hybrid aerogel microparticles for mucosal drug delivery. *Eur J Pharm Biopharm, 107*, 160-170.

Grasmeijer, N., Stankovic, M., de Waard, H., Frijlink, H. W., & Hinrichs, W. L. (2013). Unraveling protein stabilization mechanisms: vitrification and water replacement in a glass transition temperature controlled system. *Biochim Biophys Acta, 1834*(4), 763-769.

Gu, L., Gonzalez, F. J., Kalow, W., & Tang, B. K. (1992). Biotransformation of caffeine, paraxanthine, theobromine and theophylline by cDNA-expressed human CYP1A2 and CYP2E1. *Pharmacogenetics, 2*(2), 73-77.

Guideline, I. H. T. (2003). Stability testing of new drug substances and products. *Q1A (R2), current step, 4*, 1-24.

Guideline, I. H. T. (2005). Validation of analytical procedures: text and methodology Q2 (R1). *International Conference on Harmonization, Geneva, Switzerland* (pp. 11-12).

Gulzar, M., Bouhallab, S., Jardin, J., Briard-Bion, V., & Croguennec, T. (2013). Structural consequences of dry heating on alpha-lactalbumin and beta-lactoglobulin at pH 6.5. *Food Res. Int., 51*(2), 899-906.

Gunday Tureli, N., Torge, A., Juntke, J., Schwarz, B. C., Schneider-Daum, N., Tureli, A. E., Lehr, C. M., & Schneider, M. (2017). Ciprofloxacin-loaded PLGA nanoparticles against cystic fibrosis P. aeruginosa lung infections. *Eur J Pharm Biopharm, 117*, 363-371.

Hackett, M. J., Zaro, J. L., Shen, W. C., Guley, P. C., & Cho, M. J. (2013). Fatty acids as therapeutic auxiliaries for oral and parenteral formulations. *Advanced Drug Delivery Reviews, 65*(10), 1331-1339.

Hagens, W. I., Oomen, A. G., de Jong, W. H., Cassee, F. R., & Sips, A. J. (2007). What do we (need to) know about the kinetic properties of nanoparticles in the body? *Regul Toxicol Pharmacol, 49*(3), 217-229.

Hagesaether, E., Hiorth, M., & Sande, S. A. (2009). Mucoadhesion and drug permeability of free mixed films of pectin and chitosan: an in vitro and ex vivo study. *Eur J Pharm Biopharm, 71*(2), 325-331.

Harland, B. F. (2000). Caffeine and nutrition. *Nutrition (Burbank, Los Angeles County, Calif.), 16*(7), 522-526.

Harmonization, I. C. o. (2018). ICH. (Vol. 2018).

He, B., Lin, P., Jia, Z., Du, W., Qu, W., Yuan, L., Dai, W., Zhang, H., Wang, X., Wang, J., Zhang, X., & Zhang, Q. (2013). The transport mechanisms of polymer nanoparticles in Caco-2 epithelial cells. *Biomaterials, 34*(25), 6082-6098.

Hedoux, A., Willart, J. F., Paccou, L., Guinet, Y., Affouard, F., Lerbret, A., & Descamps, M. (2009). Thermostabilization mechanism of bovine serum albumin by trehalose. *J Phys Chem B, 113*(17), 6119-6126.

Höld, K. M., de Boer, D., Zuidema, J., & Maes, R. A. (1996). Saliva as an analytical tool in toxicology. *Int J Drug Test, 1*, 1-36.

Hoogstraate, A. J., Verhoef, J. C., Tuk, B., Pijpers, A., van Leengoed, L. A. M. G., Verheijden, J. H. M., Junginger, H. E., & Boddé, H. E. (1996). Buccal delivery of fluorescein isothiocyanate-dextran 4400 and the peptide drug buserelin with glycodeoxycholate as an absorption enhancer in pigs. *J. Control. Release, 41*(1–2), 77-84.

Ibrahim, H. R., Ahmed, A. S., & Miyata, T. (2017). Novel angiotensin-converting enzyme inhibitory peptides from caseins and whey proteins of goat milk. *J Adv Res, 8*(1), 63-71.

Iqbal, M., Zafar, N., Fessi, H., & Elaissari, A. (2015). Double emulsion solvent evaporation techniques used for drug encapsulation. *Int J Pharm, 496*(2), 173-190.

Izutsu, K., & Kojima, S. (2000). Freeze-concentration separates proteins and polymer excipients into different amorphous phases. *Pharm. Res., 17*(10), 1316-1322.

Jacobsen, J., Nielsen, E. B., Brøndum-Nielsen, K., Christensen, M. E., Olin, H. B. D., Tommerup, N., & Rassing, M. R. (1999). Filter-grown TR146 cells as an in vitro model of human buccal epithelial permeability. *European journal of oral sciences, 107*(2), 138-146.

Jacobsen, J., Pedersen, M., & Rassing, M. R. (1996). TR146 cells as a model for human buccal epithelium: II. Optimisation and use of a cellular sensitivity MTS/PMS assay. *Int J Pharm, 141*(1-2), 217-225.

Jacobsen, J., van Deurs, B., Pedersen, M., & Rassing, M. R. (1995). TR146 cells grown on filters as a model for human buccal epithelium: I. Morphology, growth, barrier properties, and permeability. *Int J Pharm, 125*(2), 165-184.

Jadallah, K. A., Kullab, S. M., & Sanders, D. S. (2014). Constipation-predominant irritable bowel syndrome: A review of current and emerging drug therapies. *World J. Gastroenterol., 20*(27), 8898-8909.

Jain, A., & Jain, S. K. (2016). In Vitro Release Kinetics Model Fitting of Liposomes: An Insight. *Chem Phys Lipids, 201*, 28-40.

Jana, S., Mandlekar, S., & Marathe, P. (2010). Prodrug design to improve pharmacokinetic and drug delivery properties: challenges to the discovery scientists. *Curr Med Chem, 17*(32), 3874-3908.

Janssen, E. M., Schliephacke, R., Breitenbach, A., & Breitkreutz, J. (2013). Drug-printing by flexographic printing technology--a new manufacturing process for orodispersible films. *Int J Pharm, 441*(1-2), 818-825.

Jin, L., Boyd, B. J., White, P. J., Pennington, M. W., Norton, R. S., & Nicolazzo, J. A. (2015). Buccal mucosal delivery of a potent peptide leads to therapeutically-relevant plasma concentrations for the treatment of autoimmune diseases. *J. Control. Release, 199*(0), 37-44.

Jorgensen, L., Hostrup, S., Moeller, E. H., & Grohganz, H. (2009). Recent trends in stabilising peptides and proteins in pharmaceutical formulation - considerations in the choice of excipients. *Expert Opin. Drug Deliv., 6*(11), 1219-1230.

Joshi, G., Kumar, A., & Sawant, K. (2016). Bioavailability enhancement, Caco-2 cells uptake and intestinal transport of orally administered lopinavir-loaded PLGA nanoparticles. *Drug Deliv, 23*(9), 3492-3504.

Kamerzell, T. J., Esfandiary, R., Joshi, S. B., Middaugh, C. R., & Volkin, D. B. (2011). Protein-excipient interactions: mechanisms and biophysical characterization applied to protein formulation development. *Adv Drug Deliv Rev, 63*(13), 1118-1159.

Kamimori, G. H., Karyekar, C. S., Otterstetter, R., Cox, D. S., Balkin, T. J., Belenky, G. L., & Eddington, N. D. (2002a). The rate of absorption and relative bioavailability of caffeine administered in chewing gum versus capsules to normal healthy volunteers. *Int. J. Pharm., 234*(1-2), 159-167.

Kamimori, G. H., Karyekar, C. S., Otterstetter, R., Cox, D. S., Balkin, T. J., Belenky, G. L., & Eddington, N. D. (2002b). The rate of absorption and relative bioavailability of caffeine administered in chewing gum versus capsules to normal healthy volunteers. *Int J Pharm, 234*(1-2), 159-167.

Khafagy, E. S., Kamei, N., Nielsen, E. J. B., Nishio, R., & Takeda-Morishita, M. (2013). One-month subchronic toxicity study of cell-penetrating peptides for insulin nasal delivery in rats. *European Journal of Pharmaceutics and Biopharmaceutics, 85*(3), 736-743.

Khafagy, E. S., & Morishita, M. (2012). Oral biodrug delivery using cell-penetrating peptide. *Advanced Drug Delivery Reviews, 64*(6), 531-539.

Khalil, N. M., do Nascimento, T. C., Casa, D. M., Dalmolin, L. F., de Mattos, A. C., Hoss, I., Romano, M. A., & Mainardes, R. M. (2013). Pharmacokinetics of curcumin-loaded

PLGA and PLGA-PEG blend nanoparticles after oral administration in rats. *Colloids Surf B Biointerfaces, 101*, 353-360.

Khan, S., Trivedi, V., & Boateng, J. (2016). Functional physico-chemical, ex vivo permeation and cell viability characterization of omeprazole loaded buccal films for paediatric drug delivery. *Int J Pharm, 500*(1-2), 217-226.

Kleiveland, C. R. (2015). Co-cultivation of Caco-2 and HT-29MTX. In K. Verhoeckx, P. Cotter, I. Lopez-Exposito, C. Kleiveland, T. Lea, A. Mackie, T. Requena, D. Swiatecka & H. Wichers (Eds.). *The Impact of Food Bioactives on Health: in vitro and ex vivo models* (pp. 135-140). Cham (CH): Springer.

Kulkarni, U., Mahalingam, R., Pather, I., Li, X., & Jasti, B. (2010). Porcine buccal mucosa as in vitro model: effect of biological and experimental variables. *J Pharm Sci, 99*(3), 1265-1277.

Kulkarni, U., Mahalingam, R., Pather, S. I., Li, X., & Jasti, B. (2009). Porcine buccal mucosa as an in vitro model: relative contribution of epithelium and connective tissue as permeability barriers. *J Pharm Sci, 98*(2), 471-483.

Kulkarni, U. D., Mahalingam, R., Li, X., Pather, I., & Jasti, B. (2011). Effect of experimental temperature on the permeation of model diffusants across porcine buccal mucosa. *AAPS PharmSciTech, 12*(2), 579-586.

Kumar, G. P., Phani, A. R., Prasad, R. G., Sanganal, J. S., Manali, N., Gupta, R., Rashmi, N., Prabhakara, G. S., Salins, C. P., Sandeep, K., & Raju, D. B. (2014a). Polyvinylpyrrolidone oral films of enrofloxacin: film characterization and drug release. *Int J Pharm, 471*(1-2), 146-152.

Kumar, G. P., Phani, A. R., Prasad, R. G., Sanganal, J. S., Manali, N., Gupta, R., Rashmi, N., Prabhakara, G. S., Salins, C. P., Sandeep, K., & Raju, D. B. (2014b). Polyvinylpyrrolidone oral films of enrofloxacin: film characterization and drug release. *Int. J. Pharm., 471*(1-2), 146-152.

Kumari, A., Yadav, S. K., & Yadav, S. C. (2010). Biodegradable polymeric nanoparticles based drug delivery systems. *Colloids Surf B Biointerfaces, 75*(1), 1-18.

Kwon, H. Y., Lee, J. Y., Choi, S. W., Jang, Y. S., & Kim, J. H. (2001). Preparation of PLGA nanoparticles containing estrogen by emulsification-diffusion method. *Colloids and Surfaces a-Physicochemical and Engineering Aspects, 182*(1-3), 123-130.

Lai, K. L., Fang, Y., Han, H., Li, Q., Zhang, S., Li, H. Y., Chow, S. F., Lam, T. N., & Lee, W. Y. T. (2018). Orally-dissolving film for sublingual and buccal delivery of ropinirole. *Colloids Surf B Biointerfaces, 163*, 9-18.

Landsberg, G., Milgram, B., Mougeot, I., Kelly, S., & de Rivera, C. (2017). Therapeutic effects of an alpha-casozepine and L-tryptophan supplemented diet on fear and anxiety in the cat. *J Feline Med Surg, 19*(6), 594-602.

Laurent, C., Besancon, P., & Caporiccio, B. (2007). Flavonoids from a grape seed extract interact with digestive secretions and intestinal cells as assessed in an in vitro digestion/Caco-2 cell culture model. *Food Chemistry, 100*(4), 1704-1712.

Lázaro Martínez, J. M., Leal Denis, M. F., Campo Dall'Orto, V., & Buldain, G. Y. (2008a). Synthesis, FTIR, solid-state NMR and SEM studies of novel polyampholytes or polyelectrolytes obtained from EGDE, MAA and imidazoles. *European Polymer Journal, 44*(2), 392-407.

Lázaro Martínez, J. M., Leal Denis, M. F., Campo Dall'Orto, V., & Buldain, G. Y. (2008b). Synthesis, FTIR, solid-state NMR and SEM studies of novel polyampholytes or polyelectrolytes obtained from EGDE, MAA and imidazoles. *Eur. Polym. J., 44*(2), 392-407.

Lee, J. C., & Timasheff, S. N. (1981). The stabilization of proteins by sucrose. *J Biol Chem, 256*(14), 7193-7201.

Lee, Y.-H., & Sinko, P. J. (2000). Oral delivery of salmon calcitonin. *Adv. Drug Deliv. Rev., 42*(3), 225-238.

Lehr, C. M. (1996a). From sticky stuff to sweet receptors - Achievements, limits and novel approaches to bioadhesion. *European journal of drug metabolism and pharmacokinetics, 21*(2), 139-148.

Lehr, C. M. (1996b). From sticky stuff to sweet receptors--achievements, limits and novel approaches to bioadhesion. *Eur. J. Drug Metab. Pharmacokinet., 21*(2), 139-148.

Li, J., Jiang, G., & Ding, F. (2008). The effect of pH on the polymer degradation and drug release from PLGA-mPEG microparticles. *Journal of applied polymer science, 109*(1), 475-482.

Li, L., Ni, R., Shao, Y., & Mao, S. (2014). Carrageenan and its applications in drug delivery. *Carbohydr. Polym., 103*(0), 1-11.

Li, S., Nguyen, T. H., Schoneich, C., & Borchardt, R. T. (1995). Aggregation and precipitation of human relaxin induced by metal-catalyzed oxidation. *Biochemistry, 34*(17), 5762-5772.

Li, S., Schoneich, C., & Borchardt, R. T. (1995). Chemical instability of protein pharmaceuticals: Mechanisms of oxidation and strategies for stabilization. *Biotechnol Bioeng, 48*(5), 490-500.

Lin, P. C., Lin, S., Wang, P. C., & Sridhar, R. (2014). Techniques for physicochemical characterization of nanomaterials. *Biotechnol Adv, 32*(4), 711-726.

Longer, M. A., Ch'Ng, H. S., & Robinson, J. R. (1985). Bioadhesive polymers as platforms for oral controlled drug delivery III: oral delivery of chlorothiazide using a bioadhesive polymer. *Journal of pharmaceutical sciences, 74*(4), 406-411.

Lozoya-Agullo, I., Araujo, F., Gonzalez-Alvarez, I., Merino-Sanjuan, M., Gonzalez-Alvarez, M., Bermejo, M., & Sarmento, B. (2017). Usefulness of Caco-2/HT29-MTX and Caco-2/HT29-MTX/Raji B Coculture Models To Predict Intestinal and Colonic Permeability Compared to Caco-2 Monoculture. *Mol Pharm, 14*(4), 1264-1270.

Lozoya-Agullo, I., Araujo, F., Gonzalez-Alvarez, I., Merino-Sanjuan, M., Gonzalez-Alvarez, M., Bermejo, M., & Sarmento, B. (2018). PLGA nanoparticles are effective to control the colonic release and absorption on ibuprofen. *Eur J Pharm Sci, 115*, 119-125.

Lundquist, P., & Artursson, P. (2016). Oral absorption of peptides and nanoparticles across the human intestine: Opportunities, limitations and studies in human tissues. *Adv Drug Deliv Rev, 106*(Pt B), 256-276.

Lv, R., Kong, Q., Mou, H., & Fu, X. (2017). Effect of guar gum on stability and physical properties of orange juice. *Int J Biol Macromol, 98*, 565-574.

Lynch, I., & Dawson, K. A. (2008). Protein-nanoparticle interactions. *Nano Today, 3*(1-2), 40-47.

Machado, A., Cunha-Reis, C., Araujo, F., Nunes, R., Seabra, V., Ferreira, D., das Neves, J., & Sarmento, B. (2016). Development and in vivo safety assessment of tenofovir-loaded nanoparticles-in-film as a novel vaginal microbicide delivery system. *Acta Biomater, 44*, 332-340.

Madureira, A. R., Amorim, M., Gomes, A. M., Pintado, M. E., & Malcata, F. X. (2011a). Protective effect of whey cheese matrix on probiotic strains exposed to simulated gastrointestinal conditions. *Food Res. Int., 44*(1), 465-470.

Madureira, A. R., Amorim, M., Gomes, A. M., Pintado, M. E., & Malcata, F. X. (2011b). Protective effect of whey cheese matrix on probiotic strains exposed to simulated gastrointestinal conditions. *Food Research International, 44*(1), 465-470.

Madureira, A. R., Tavares, T., Gomes, A. M., Pintado, M. E., & Malcata, F. X. (2010). Invited review: physiological properties of bioactive peptides obtained from whey proteins. *J. Dairy Sci., 93*(2), 437-455.

Maher, S., & Brayden, D. J. (2012). Overcoming poor permeability: translating permeation enhancers for oral peptide delivery. *Drug Discovery Today: Technologies, 9*(2), e113-e119.

Maitani, Y., & Hattori, Y. (2009). Oligoarginine-PEG-lipid particles for gene delivery. *Expert Opin Drug Deliv, 6*(10), 1065-1077.

Mansuri, S., Kesharwani, P., Jain, K., Tekade, R. K., & Jain, N. K. (2016). Mucoadhesion: A promising approach in drug delivery system. *Reactive & Functional Polymers, 100*, 151-172.

Martin, M. J., Calpena, A. C., Fernandez, F., Mallandrich, M., Galvez, P., & Clares, B. (2015). Development of alginate microspheres as nystatin carriers for oral mucosa drug delivery. *Carbohydr Polym, 117*, 140-149.

Martins, S., Sarmento, B., Souto, E. B., & Ferreira, D. C. (2007). Insulin-loaded alginate microspheres for oral delivery - Effect of polysaccharide reinforcement on physicochemical properties and release profile. *Carbohydrate Polymers, 69*(4), 725-731.

Maruthi, G., Smith, A. A., & Manavalan, R. (2011). Nanoparticles--A Review. *Journal of Advanced Scientific Research, 2*(4).

Mathiowitz, E. (1999). *Encyclopedia of controlled drug delivery*. Wiley-Interscience.

Mayr, L. M., & Schmid, F. X. (1993). Stabilization of a protein by guanidinium chloride. *Biochemistry, 32*(31), 7994-7998.

McLellan, T. M., Caldwell, J. A., & Lieberman, H. R. (2016). A review of caffeine's effects on cognitive, physical and occupational performance. *Neurosci Biobehav Rev, 71*, 294-312.

Merkle, H. P., & Wolany, G. (1992). Buccal Delivery for Peptide Drugs. *Journal of Controlled Release, 21*(1-3), 155-164.

Meyer, J. D., & Manning, M. C. (1998). Hydrophobic ion pairing: altering the solubility properties of biomolecules. *Pharm Res, 15*(2), 188-193.

Minton, A. P. (2005). Models for excluded volume interaction between an unfolded protein and rigid macromolecular cosolutes: Macromolecular crowding and protein stability revisited. *Biophysical journal, 88*(2), 971-985.

Mir, M., Ahmed, N., & Rehman, A. U. (2017). Recent applications of PLGA based nanostructures in drug delivery. *Colloids Surf B Biointerfaces, 159*, 217-231.

Mitoma, C., Lombrozo, L., LeValley, S. E., & Dehn, F. (1969). Nature of the effect of caffeine on the drug-metabolizing enzymes. *Archives of Biochemistry and Biophysics, 134*(2), 434-441.

Mohanraj, V., & Chen, Y. (2006). Nanoparticles–a review. *Trop J Pharm Res, 5*(1), 561-573.

Molinari, G., & Lata, G. F. (1962a). Interaction of Steroids with Some Pyrimidine and Purine Derivatives. *Archives of Biochemistry and Biophysics, 96*(3), 486-&.

Molinari, G., & Lata, G. F. (1962b). Interaction of steroids with some pyrimidine and purine derivatives. *Arch. Biochem. Biophys., 96*(3), 486-490.

Morales, J. O., & Brayden, D. J. (2017). Buccal delivery of small molecules and biologics: of mucoadhesive polymers, films, and nanoparticles. *Curr Opin Pharmacol, 36*, 22-28.

Morales, J. O., Ross, A. C., & McConville, J. T. (2013). Protein-coated nanoparticles embedded in films as delivery platforms. *Journal of pharmacy and pharmacology, 65*(6), 827-838.

Morck Nielsen, H., & Romer Rassing, M. (2000). TR146 cells grown on filters as a model of human buccal epithelium: V. Enzyme activity of the TR146 cell culture model, human buccal epithelium and porcine buccal epithelium, and permeability of leu-enkephalin. *Int J Pharm, 200*(2), 261-270.

Mosmann, T. (1983a). Rapid colorimetric assay for cellular growth and survival: application to proliferation and cytotoxicity assays. *Journal of Immunollogy Methods, 65*(1-2), 55-63.

Mosmann, T. (1983b). Rapid colorimetric assay for cellular growth and survival: application to proliferation and cytotoxicity assays. *J Immunol Methods, 65*(1-2), 55-63.

Mundargi, R. C., Babu, V. R., Rangaswamy, V., Patel, P., & Aminabhavi, T. M. (2008). Nano/micro technologies for delivering macromolecular therapeutics using poly(D,L-lactide-co-glycolide) and its derivatives. *J Control Release, 125*(3), 193-209.

Nafisi, S., Monajemi, M., & Ebrahimi, S. (2004). The effects of mono- and divalent metal cations on the solution structure of caffeine and theophylline. *J. Mol. Struct., 705*(1–3), 35-39.

Nagaraju, T., Gowthami, R., Rajashekar, M., Sandeep, S., Mallesham, M., Sathish, D., & Kumar, Y. S. (2013a). Comprehensive review on oral disintegrating films. *Curr. Drug Deliv., 10*(1), 96-108.

Nagaraju, T., Gowthami, R., Rajashekar, M., Sandeep, S., Mallesham, M., Sathish, D., & Kumar, Y. S. (2013b). Comprehensive review on oral disintegrating films. *Curr Drug Deliv, 10*(1), 96-108.

Nicolazzo, J. A., Reed, B. L., & Finnin, B. C. (2004). Assessment of the effects of sodium dodecyl sulfate on the buccal permeability of caffeine and estradiol. *J Pharm Sci, 93*(2), 431-440.

Nielsen, H. M., & Rassing, M. R. (1999). TR146 cells grown on filters as a model of human buccal epithelium: III. Permeability enhancement by different pH values, different osmolality values, and bile salts. *Int J Pharm, 185*(2), 215-225.

Nielsen, H. M., & Rassing, M. R. (2000a). TR146 cells grown on filters as a model of human buccal epithelium: IV. Permeability of water, mannitol, testosterone and β-adrenoceptor

antagonists. Comparison to human, monkey and porcine buccal mucosa. *Int J Pharm, 194*(2), 155-167.

Nielsen, H. M., & Rassing, M. R. (2000b). TR146 cells grown on filters as a model of human buccal epithelium: V. Enzyme activity of the TR146 cell culture model, human buccal epithelium and porcine buccal epithelium, and permeability of leu-enkephalin. *Int J Pharm, 200*(2), 261-270.

Nixon, A. E. (2014). *Therapeutic peptides*. Springer.

O'Hagan, D. T., McGee, J. P., Holmgren, J., Mowat, A. M., Donachie, A. M., Mills, K. H., Gaisford, W., Rahman, D., & Challacombe, S. J. (1993). Biodegradable microparticles for oral immunization. *Vaccine, 11*(2), 149-154.

OECD. (2014). Guidance on grouping of chemicals. *Series on testing and assessment* (Vol. 2016). Paris: OECD.

Ohtake, S., Kita, Y., & Arakawa, T. (2011). Interactions of formulation excipients with proteins in solution and in the dried state. *Adv Drug Deliv Rev, 63*(13), 1053-1073.

Olbrich, C., & Muller, R. H. (1999). Enzymatic degradation of SLN-effect of surfactant and surfactant mixtures. *Int J Pharm, 180*(1), 31-39.

Otte, J., Shalaby, S. M. A., Zakora, M., & Nielsen, M. S. (2007). Fractionation and identification of ACE-inhibitory peptides from α-lactalbumin and β-casein produced by thermolysin-catalysed hydrolysis. *INT. DAIRY J., 17*(12), 1460-1472.

Palestrini, C., Minero, M., Cannas, S., Berteselli, G., Scaglia, E., Barbieri, S., Cavallone, E., Puricelli, M., Servida, F., & Dall'Ara, P. (2010). Efficacy of a diet containing caseinate hydrolysate on signs of stress in dogs. *Journal of Veterinary Behavior-Clinical Applications and Research, 5*(6), 309-317.

Pan, F., Han, L., Zhang, Y., Yu, Y., & Liu, J. (2015). Optimization of Caco-2 and HT29 co-culture in vitro cell models for permeability studies. *Int J Food Sci Nutr, 66*(6), 680-685.

Parliament, E. (2011). Regulation (EU) 1169/2011 of the European Parliament and of the Council of 25 October 2011 on the provision of food information to consumers. *Off J Eur Communities. L, 304*, 18.

Patel, A., Cholkar, K., & Mitra, A. K. (2014). Recent developments in protein and peptide parenteral delivery approaches. *Ther Deliv, 5*(3), 337-365.

Patel, V. F., Liu, F., & Brown, M. B. (2012). Modeling the oral cavity: in vitro and in vivo evaluations of buccal drug delivery systems. *J Control Release, 161*(3), 746-756.

Pather, S. I., Rathbone, M. J., & Senel, S. (2008). Current status and the future of buccal drug delivery systems. *Expert Opin Drug Deliv, 5*(5), 531-542.

Pauletti, G. M., Gangwar, S., Siahaan, T. J., Aube, J., & Borchardt, R. T. (1997). Improvement of oral peptide bioavailability: Peptidomimetics and prodrug strategies. *Advanced Drug Delivery Reviews, 27*(2-3), 235-256.

Pawar, V. K., Meher, J. G., Singh, Y., Chaurasia, M., Surendar Reddy, B., & Chourasia, M. K. (2014). Targeting of gastrointestinal tract for amended delivery of protein/peptide therapeutics: strategies and industrial perspectives. *J Control Release, 196*, 168-183.

Peh, K. K., & Wong, C. F. (1999). Polymeric films as vehicle for buccal delivery: swelling, mechanical, and bioadhesive properties. *J. Pharm. Pharm. Sci., 2*(2), 53-61.

Peppas, N. A., & Sahlin, J. J. (1996). Hydrogels as mucoadhesive and bioadhesive materials: A review. *Biomaterials, 17*(16), 1553-1561.

Petropoulos, J. H., Papadokostaki, K. G., & Sanopoulou, M. (2012). Higuchi's equation and beyond: overview of the formulation and application of a generalized model of drug release from polymeric matrices. *Int J Pharm, 437*(1-2), 178-191.

Philip, A. K., & Philip, B. (2010). Colon targeted drug delivery systems: a review on primary and novel approaches. *Oman Med J, 25*(2), 79-87.

Platts, L., & Falconer, R. J. (2015). Controlling protein stability: Mechanisms revealed using formulations of arginine, glycine and guanidinium HCl with three globular proteins. *Int J Pharm, 486*(1-2), 131-135.

Pohler, H. (2010). Caffeine Intoxication and Addiction. *The Journal for Nurse Practitioners, 6*(1), 49-52.

Ponchel, G., & Irache, J. (1998). Specific and non-specific bioadhesive particulate systems for oral delivery to the gastrointestinal tract. *Adv Drug Deliv Rev, 34*(2-3), 191-219.

Popova, E. A., Nikolskaia, S. K., Gluzdikov, I. A., & Trifonov, R. E. (2014). An efficient synthesis of a novel analog of octreotide with an unnatural l-lysine-like tetrazolyl amino acid. *Tetrahedron Lett., 55*(36), 5041-5046.

Prabaharan, M. (2011). Prospective of guar gum and its derivatives as controlled drug delivery systems. *Int. J. Biol. Macromol., 49*(2), 117-124.

Preis, M., Woertz, C., Kleinebudde, P., & Breitkreutz, J. (2013). Oromucosal film preparations: classification and characterization methods. *Expert Opin Drug Deliv, 10*(9), 1303-1317.

Provenza, N., Calpena, A. C., Mallandrich, M., Sánchez, A., Egea, M. A., & Clares, B. (2014). Permeation studies through porcine small intestine of furosemide solutions for personalised paediatric administration. *Int. J. Pharm., 475*(1–2), 208-213.

Qiu, Y., Chen, Y., Zhang, G. G., Yu, L., & Mantri, R. V. (2016). *Developing solid oral dosage forms: pharmaceutical theory and practice*. Academic press.

Quintanar-Guerrero, D., Allemann, E., Fessi, H., & Doelker, E. (1997). Applications of the ion-pair concept to hydrophilic substances with special emphasis on peptides. *Pharm Res, 14*(2), 119-127.

Quirós, A., del Mar Contreras, M., Ramos, M., Amigo, L., & Recio, I. (2009). Stability to gastrointestinal enzymes and structure–activity relationship of β-casein-peptides with antihypertensive properties. *Peptides, 30*(10), 1848-1853.

Rang, H. (2007). Rang and Dale's Pharmacology, Churchill Livingstone. Elsevier.

Rathbone, M. J., Pather, I., & Şenel, S. (2015). Overview of Oral Mucosal Delivery. In Springer (Ed.). *Oral Mucosal Drug Delivery and Therapy* (pp. 17-29): Springer.

Rauck, R., North, J., Gever, L. N., Tagarro, I., & Finn, A. L. (2010). Fentanyl buccal soluble film (FBSF) for breakthrough pain in patients with cancer: a randomized, double-blind, placebo-controlled study. *Ann. Oncol., 21*(6), 1308-1314.

Ravi Kumar Reddy, J., Indira Muzib, Y., & Chowdary, K. P. R. (2013). Development and in-vivo characterization of novel trans buccal formulations of Amiloride hydrochloride. *Journal of Pharmacy Research, 6*(6), 647-652.

Rawat, M., Singh, D., Saraf, S., & Saraf, S. (2006). Nanocarriers: promising vehicle for bioactive drugs. *Biol Pharm Bull, 29*(9), 1790-1798.

Rehmani, S., & Dixon, J. E. (2018). Oral delivery of anti-diabetes therapeutics using cell penetrating and transcytosing peptide strategies. *Peptides, 100*, 24-35.

Reineke, J., Cho, D., Dingle, Y., Cheifetz, P., Laulicht, B., Lavin, D., Furtado, S., & Mathiowitz, E. (2013). Can bioadhesive nanoparticles allow for more effective particle uptake from the small intestine? *Journal of Controlled Release, 170*(3), 477-484.

Reix, N., Parat, A., Seyfritz, E., Van der Werf, R., Epure, V., Ebel, N., Danicher, L., Marchioni, E., Jeandidier, N., Pinget, M., Frere, Y., & Sigrist, S. (2012). In vitro uptake evaluation in Caco-2 cells and in vivo results in diabetic rats of insulin-loaded PLGA nanoparticles. *Int J Pharm, 437*(1-2), 213-220.

Rekha, M. R., & Sharma, C. P. (2013). Oral delivery of therapeutic protein/peptide for diabetes - Future perspectives. *Int J Pharm, 440*(1), 48-62.

Ripken, D., & Hendriks, H. F. J. (2015). Porcine Ex Vivo Intestinal Segment Model. In K. Verhoeckx, P. Cotter, I. Lopez-Exposito, C. Kleiveland, T. Lea, A. Mackie, T. Requena, D. Swiatecka & H. Wichers (Eds.). *The Impact of Food Bioactives on Health: in vitro and ex vivo models* (pp. 255-262). Cham (CH): Springer.

Rodopoulos, N., Hojvall, L., & Norman, A. (1996). Elimination of theobromine metabolites in healthy adults. *Scand J Clin Lab Invest, 56*(4), 373-383.

Rodopoulos, N., & Norman, A. (1996). Assessment of dimethylxanthine formation from caffeine in healthy adults: comparison between plasma and saliva concentrations and urinary excretion of metabolites. *Scand J Clin Lab Invest, 56*(3), 259-268.

Rodrigues de Azevedo, C., von Stosch, M., Costa, M. S., Ramos, A. M., Cardoso, M. M., Danhier, F., Preat, V., & Oliveira, R. (2017). Modeling of the burst release from PLGA micro- and nanoparticles as function of physicochemical parameters and formulation characteristics. *Int J Pharm, 532*(1), 229-240.

Rossi, S., Sandri, G., & Caramella, C. M. (2005). Buccal drug delivery: A challenge already won? *Drug Discov Today Technol, 2*(1), 59-65.

Rowe, R., Sheskey, P., & Owen, S. (2006). *Handbook of Pharmaceutical Excipients*. Pharmaceutical Press.

Ruiz-Henestrosa, V. M. P., Martinez, M. J., Sánchez, C. C., Patino, J. M. R., & Pilosof, A. M. R. (2014). Mixed soy globulins and β-lactoglobulin systems behaviour in aqueous solutions and at the air–water interface. *Food Hydrocolloids, 35*, 106-114.

Sahoo, N., Sahoo, R. K., Biswas, N., Guha, A., & Kuotsu, K. (2015). Recent advancement of gelatin nanoparticles in drug and vaccine delivery. *Int J Biol Macromol, 81*, 317-331.

Sander, C., Nielsen, H. M., & Jacobsen, J. (2013a). Buccal delivery of metformin: TR146 cell culture model evaluating the use of bioadhesive chitosan discs for drug permeability enhancement. *Int J Pharm, 458*(2), 254-261.

Sander, C., Nielsen, H. M., & Jacobsen, J. (2013b). Buccal delivery of metformin: TR146 cell culture model evaluating the use of bioadhesive chitosan discs for drug permeability enhancement. *International journal of pharmaceutics, 458*(2), 254-261.

Santos, C. I. A. V., Teijeiro, C., Ribeiro, A. C. F., Rodrigues, D. F. S. L., Romero, C. M., & Esteso, M. A. (2016). Drug delivery systems: Study of inclusion complex formation for ternary caffeine–β-cyclodextrin–water mixtures from apparent molar volume values at 298.15 K and 310.15 K. *Journal of Molecular Liquids, 223*, 209-216.

Santos, T. C. d., Hernández, R., Rescignano, N., Boff, L., Reginatto, F. H., Simões, C. M. O., de Campos, A. M., & Mijangos, C. (2018). Nanocomposite chitosan hydrogels based on PLGA nanoparticles as potential biomedical materials. *European Polymer Journal, 99*, 456-463.

Santos, T. C. D., Rescignano, N., Boff, L., Reginatto, F. H., Simoes, C. M. O., de Campos, A. M., & Mijangos, C. U. (2017). Manufacture and characterization of chitosan/PLGA nanoparticles nanocomposite buccal films. *Carbohydr Polym, 173*, 638-644.

Sarmento, B., Martins, S., Ferreira, D., & Souto, E. B. (2007). Oral insulin delivery by means of solid lipid nanoparticles. *Int J Nanomedicine, 2*(4), 743-749.

Sarmento, B., Ribeiro, A., Veiga, F., Ferreira, D., & Neufeld, R. (2007). Oral bioavailability of insulin contained in polysaccharide nanoparticles. *Biomacromolecules, 8*(10), 3054-3060.

Satarkar, N. S., & Hilt, J. Z. (2008). Magnetic hydrogel nanocomposites for remote controlled pulsatile drug release. *J Control Release, 130*(3), 246-251.

Schneider, C. P., & Trout, B. L. (2009). Investigation of Cosolute-Protein Preferential Interaction Coefficients: New Insight into the Mechanism by Which Arginine Inhibits Aggregation. *Journal of Physical Chemistry B, 113*(7), 2050-2058.

Schulz, J. D., Gauthier, M. A., & Leroux, J. C. (2015). Improving oral drug bioavailability with polycations? *Eur J Pharm Biopharm, 97*(Pt B), 427-437.

Senel, S., Kremer, M. J., Kas, S., Wertz, P. W., Hincal, A. A., & Squier, C. A. (2000). Enhancing effect of chitosan on peptide drug delivery across buccal mucosa. *Biomaterials, 21*(20), 2067-2071.

Shah, V., Bharatiya, B., Shukla, A. D., Mukherjee, T., & Shah, D. O. (2016). Adsorption of nonionic Brij and Tween surfactants at PTFE-water and air-water interfaces: Investigations on wetting, dispersion stability, foaming and drug solubilization. *Colloids and Surfaces a-Physicochemical and Engineering Aspects, 508*(Supplement C), 159-166.

Shailubhai, K., Comiskey, S., Foss, J. A., Feng, R., Barrow, L., Comer, G. M., & Jacob, G. S. (2013). Plecanatide, an oral guanylate cyclase C agonist acting locally in the gastrointestinal tract, is safe and well-tolerated in single doses. *Dig. Dis. Sci., 58*(9), 2580-2586.

Shaji, J., & Patole, V. (2008). Protein and Peptide drug delivery: oral approaches. *Indian J. Pharm. Sci., 70*(3), 269-277.

Sharma, S., Parmar, A., Kori, S., & Sandhir, R. (2016). PLGA-based nanoparticles: A new paradigm in biomedical applications. *Trac-Trends in Analytical Chemistry, 80*, 30-40.

Sharp, P., & Srai, S. K. (2007). Molecular mechanisms involved in intestinal iron absorption. *World J Gastroenterol, 13*(35), 4716-4724.

Shen, B. D., Shen, C. Y., Yuan, X. D., Bai, J. X., Lv, Q. Y., Xu, H., Dai, L., Yu, C., Han, J., & Yuan, H. L. (2013). Development and characterization of an orodispersible film containing drug nanoparticles. *Eur J Pharm Biopharm, 85*(3 Pt B), 1348-1356.

Shi, K., Cui, F., Yamamoto, H., & Kawashima, Y. (2008). Investigation of drug loading and in vitro release mechanisms of insulin-lauryl sulfate complex loaded PLGA nanoparticles. *Pharmazie, 63*(12), 866-871.

Shi, Y., Xue, J., Jia, L., Du, Q., Niu, J., & Zhang, D. (2018). Surface-modified PLGA nanoparticles with chitosan for oral delivery of tolbutamide. *Colloids Surf B Biointerfaces, 161*, 67-72.

Shtenberg, Y., Goldfeder, M., Prinz, H., Shainsky, J., Ghantous, Y., Abu El-Naaj, I., Schroeder, A., & Bianco-Peled, H. (2018). Mucoadhesive alginate pastes with embedded liposomes for local oral drug delivery. *Int J Biol Macromol, 111*, 62-69.

Sievens-Figueroa, L., Bhakay, A., Jerez-Rozo, J. I., Pandya, N., Romanach, R. J., Michniak-Kohn, B., Iqbal, Z., Bilgili, E., & Dave, R. N. (2012). Preparation and characterization of hydroxypropyl methyl cellulose films containing stable BCS Class II drug nanoparticles for pharmaceutical applications. *Int J Pharm, 423*(2), 496-508.

Sigurdsson, H. H., Kirch, J., & Lehr, C. M. (2013). Mucus as a barrier to lipophilic drugs. *Int J Pharm, 453*(1), 56-64.

Silva, D. S., Almeida, A., Prezotti, F., Cury, B., Campana-Filho, S. P., & Sarmento, B. (2017). Synthesis and characterization of 3,6-O,O'- dimyristoyl chitosan micelles for oral delivery of paclitaxel. *Colloids Surf B Biointerfaces, 152*, 220-228.

Singh, B. R., Wechter, M. A., Hu, Y. H., & Lafontaine, C. (1998). Determination of caffeine content in coffee using Fourier transform infra-red spectroscopy in combination with attenuated total reflectance technique: a bioanalytical chemistry experiment for biochemists. *Biochemical Education, 26*(3), 243-247.

Sionkowska, A., Wisniewski, M., Skopinska, J., Kennedy, C. J., & Wess, T. J. (2004). Molecular interactions in collagen and chitosan blends. *Biomaterials, 25*(5), 795-801.

Soares, S., Fonte, P., Costa, A., Andrade, J., Seabra, V., Ferreira, D., Reis, S., & Sarmento, B. (2013). Effect of freeze-drying, cryoprotectants and storage conditions on the stability of secondary structure of insulin-loaded solid lipid nanoparticles. *Int J Pharm, 456*(2), 370-381.

Sohi, H., Sultana, Y., & Khar, R. K. (2004). Taste masking technologies in oral pharmaceuticals: recent developments and approaches. *Drug Dev Ind Pharm, 30*(5), 429-448.

Song, H., Yu, W., Gao, M., Liu, X., & Ma, X. (2013). Microencapsulated probiotics using emulsification technique coupled with internal or external gelation process. *Carbohydr Polym, 96*(1), 181-189.

Sood, A., & Panchagnula, R. (2001). Peroral route: an opportunity for protein and peptide drug delivery. *Chem Rev, 101*(11), 3275-3303.

Soppimath, K. S., Aminabhavi, T. M., Kulkarni, A. R., & Rudzinski, W. E. (2001). Biodegradable polymeric nanoparticles as drug delivery devices. *Journal of controlled release, 70*(1-2), 1-20.

Sosnik, A., das Neves, J., & Sarmento, B. (2014). Mucoadhesive polymers in the design of nano-drug delivery systems for administration by non-parenteral routes: A review. *Progress in Polymer Science, 39*(12), 2030-2075.

Sousa, F., Castro, P., Fonte, P., & Sarmento, B. (2015a). How to overcome the limitations of current insulin administration with new non-invasive delivery systems. *Ther. Deliv., 6*(1), 83-94.

Sousa, F., Castro, P., Fonte, P., & Sarmento, B. (2015b). How to overcome the limitations of current insulin administration with new non-invasive delivery systems. *Therapeutic delivery, 6*(1), 83-94.

Spiller, G. A. (1997). *Caffeine*. CRC Press.

Staroszczyk, H., Sztuka, K., Wolska, J., Wojtasz-Pająk, A., & Kołodziejska, I. (2014). Interactions of fish gelatin and chitosan in uncrosslinked and crosslinked with EDC films: FT-IR study. *Spectrochim. Acta Mol. Biomol. Spectrosc., 117*(0), 707-712.

Sudhakar, Y., Kuotsu, K., & Bandyopadhyay, A. K. (2006). Buccal bioadhesive drug delivery--a promising option for orally less efficient drugs. *J Control Release, 114*(1), 15-40.

Suh, J. H., Cho, Y. H., & Lee, K. J. (1991). Macrocyclic Metal-Complexes Built on Polyethylenimine. *Journal of the American Chemical Society, 113*(11), 4198-4202.

Takahashi, Y., Takeda, C., Seto, I., Kawano, G., & Machida, Y. (2007). Formulation and evaluation of lactoferrin bioadhesive tablets. *Int J Pharm, 343*(1-2), 220-227.

Tan, J., Shah, S., Thomas, A., Ou-Yang, H. D., & Liu, Y. (2013). The influence of size, shape and vessel geometry on nanoparticle distribution. *Microfluid Nanofluidics, 14*(1-2), 77-87.

Tang, C., Guan, Y.-X., Yao, S.-J., & Zhu, Z.-Q. (2014a). Preparation of ibuprofen-loaded chitosan films for oral mucosal drug delivery using supercritical solution impregnation. *Int. J. Pharm., 473*(1–2), 434-441.

Tang, C., Guan, Y. X., Yao, S. J., & Zhu, Z. Q. (2014b). Preparation of ibuprofen-loaded chitosan films for oral mucosal drug delivery using supercritical solution impregnation. *Int J Pharm, 473*(1-2), 434-441.

Tang-Liu, D. D., Williams, R. L., & Riegelman, S. (1983). Disposition of caffeine and its metabolites in man. *J Pharmacol Exp Ther, 224*(1), 180-185.

Tavares, T., Contreras Mdel, M., Amorim, M., Pintado, M., Recio, I., & Malcata, F. X. (2011). Novel whey-derived peptides with inhibitory effect against angiotensin-converting enzyme: in vitro effect and stability to gastrointestinal enzymes. *Peptides, 32*(5), 1013-1019.

Tavares, T., Sevilla, M. Á., Montero, M. J., Carrón, R., & Malcata, F. X. (2012). Acute effect of whey peptides upon blood pressure of hypertensive rats, and relationship with their

angiotensin-converting enzyme inhibitory activity. *Molecular nutrition & food research, 56*(2), 316-324.

Teubl, B. J., Absenger, M., Frohlich, E., Leitinger, G., Zimmer, A., & Roblegg, E. (2013). The oral cavity as a biological barrier system: design of an advanced buccal in vitro permeability model. *Eur J Pharm Biopharm, 84*(2), 386-393.

Thakur, V. K., & Thakur, M. K. (2016). *Handbook of Sustainable Polymers: Structure and Chemistry*. CRC Press.

Tsai, A. M., van Zanten, J. H., & Betenbaugh, M. J. (1998). I. Study of protein aggregation due to heat denaturation: A structural approach using circular dichroism spectroscopy, nuclear magnetic resonance, and static light scattering. *Biotechnology and bioengineering, 59*(3), 273-280.

Tseng, Y. L., Liu, J. J., & Hong, R. L. (2002). Translocation of liposomes into cancer cells by cell-penetrating peptides penetratin and TAT: A kinetic and efficacy study. *Molecular pharmacology, 62*(4), 864-872.

Tyagi, P., Pechenov, S., & Anand Subramony, J. (2018). Oral peptide delivery: Translational challenges due to physiological effects. *J Control Release, 287*, 167-176.

Vaclavik, V. A., & Christian, E. W. (2014). Pectins and Gums. *Essentials of Food Science* (pp. 53-61): Springer.

Vadlapudi, A. D., Vadlapatla, R. K., Kwatra, D., Earla, R., Samanta, S. K., Pal, D., & Mitra, A. K. (2012). Targeted lipid based drug conjugates: a novel strategy for drug delivery. *Int J Pharm, 434*(1-2), 315-324.

Veuillez, F., Kalia, Y. N., Jacques, Y., Deshusses, J., & Buri, P. (2001). Factors and strategies for improving buccal absorption of peptides. *Eur. J. Pharm. Biopharm., 51*(2), 93-109.

Vidal, B. d. C. (2014). Fluorescence, aggregation properties and FT-IR microspectroscopy of elastin and collagen fibers. *Acta Histochem., 116*(8), 1359-1366.

Vilhardt, H., & Lundin, S. (1986). In vitro intestinal transport of vasopressin and its analogues. *Acta Physiol Scand, 126*(4), 601-607.

Wang, W. (1999). Instability, stabilization, and formulation of liquid protein pharmaceuticals. *Int J Pharm, 185*(2), 129-188.

Wang, W. T., Liu, J. G., Sun, W. H., Wang, W. Y., Wang, S. L., & Zhu, N. H. (2014). Widely tunable single bandpass microwave photonic filter based on Brillouin-assisted optical carrier recovery. *Opt Express, 22*(24), 29304-29313.

Washington, N., Washington, C., & Wilson, C. (2000). *Physiological pharmaceutics: barriers to drug absorption*. CRC Press.

Watanabe, S., & Dawes, C. (1988a). The effects of different foods and concentrations of citric acid on the flow rate of whole saliva in man. *Arch Oral Biol, 33*(1), 1-5.

Watanabe, S., & Dawes, C. (1988b). The effects of different foods and concentrations of citric acid on the flow rate of whole saliva in man. *Archives of oral biology, 33*(1), 1-5.

Wehling, F., Schuehle, S., & Madamala, N. (1993). Effervescent dosage form with microparticles. Google Patents.

Westerhout, J., Steeg, E. v. d., Grossouw, D., Zeijdner, E. E., Krul, C. A. M., Verwei, M., & Wortelboer, H. M. (2014). A new approach to predict human intestinal absorption using porcine intestinal tissue and biorelevant matrices. *Eur. J. Pharm. Sci., 63*, 167-177.

Win, K. Y., & Feng, S. S. (2005). Effects of particle size and surface coating on cellular uptake of polymeric nanoparticles for oral delivery of anticancer drugs. *Biomaterials, 26*(15), 2713-2722.

Xiong, M. H., Bao, Y., Yang, X. Z., Zhu, Y. H., & Wang, J. (2014). Delivery of antibiotics with polymeric particles. *Adv Drug Deliv Rev, 78*, 63-76.

Yalkowski, S. H., He, Y., & Jain, P. (2010). Handbook of aqueous solubility data second edition. New York: CRC Press.

Yoshikawa, M. (2015). Bioactive peptides derived from natural proteins with respect to diversity of their receptors and physiological effects. *Peptides, 72*, 208-225.

Zeng, N., Mignet, N., Dumortier, G., Olivier, E., Seguin, J., Maury, M., Scherman, D., Rat, P., & Boudy, V. (2015a). Poloxamer bioadhesive hydrogel for buccal drug delivery: Cytotoxicity and trans-epithelial permeability evaluations using TR146 human buccal epithelial cell line. *Int J Pharm, 495*(2), 1028-1037.

Zeng, N., Mignet, N., Dumortier, G., Olivier, E., Seguin, J., Maury, M., Scherman, D., Rat, P., & Boudy, V. (2015b). Poloxamer bioadhesive hydrogel for buccal drug delivery: Cytotoxicity and trans-epithelial permeability evaluations using TR146 human buccal epithelial cell line. *International Journal of Pharmaceutics, 495*(2), 1028-1037.

Zhang, L., & Bulaj, G. (2012). Converting Peptides into Drug Leads by Lipidation. *Current medicinal chemistry, 19*(11), 1602-1618.

Zhang, S., Kim, N., Yokoyama, W., & Kim, Y. (2018). Effects of moisture content on mechanical properties, transparency, and thermal stability of yuba film. *Food Chemistry, 243*, 202-207.

Zhang, S., Zhang, Z., & Vardhanabhuti, B. (2014). Effect of charge density of polysaccharides on self-assembled intragastric gelation of whey protein/polysaccharide under simulated gastric conditions. *Food Funct., 5*(8), 1829-1838.

Zhang, Y., & Cremer, P. S. (2010). Chemistry of Hofmeister anions and osmolytes. *Annu Rev Phys Chem, 61*, 63-83.

Zhao, Y., Quan, P., & Fang, L. (2015). Preparation of an oral thin film containing meclizine hydrochloride: In vitro and in vivo evaluation. *Int J Pharm, 496*(2), 314-322.

Zolnik, B. S., & Burgess, D. J. (2007). Effect of acidic pH on PLGA microsphere degradation and release. *J Control Release, 122*(3), 338-344.